Altered Biological Responsiveness of Cells Regulating Intramembranous Bone Repair Associated with Type 2 Diabetes Mellitus

A thesis submitted to Cardiff University in partial fulfilment
of the requirements for the Degree of

Doctor of Philosophy (PhD)

February 2015

Norhayati Yusop, BSc. (Hons), MSc,
Tissue Engineering and Reparative Dentistry,
School of Dentistry,
Cardiff University,
Wales,
United Kingdom.

Acknowledgements

First and above all, I praise The God, the Almighty, for providing me this opportunity and granting me the capability to proceed successfully. I would like to express my sincere gratitude to my supervisor, Professor Rachel Waddington, for her patience, encouragement, and endless knowledge. Furthermore, without Dr Ryan Moseley's leadership, enthusiasm, and immense advice, as well as Professor Alastair Sloan's invaluable insight, it would have been impossible to complete this study in time.

I would also like to express my gratitude to all those who in some way or other contributed to this research. In particular, I am indebted to Professor Joji Okazaki, from the Osaka Dental Institute in Japan for the collaboration and assistance provided pertaining to implant procedures with animal model. I would like to thank Dr Jan Hobot from the Medical Microscopy Department Cardiff University, Mrs Wendy Rowe for the unwavering support provided on the TEM work, Kath Allsop from the Histology Unit School of Dentistry for offering me the invaluable expertise on histological analysis, and Professor Bruce Caterson from School of Biosciences Cardiff University for the generous aids of proteoglycans antibodies. I would also like to thank the Malaysian Ministry of Higher Education and Universiti Sains Malaysia for funding this PhD.

In addition, I would like to acknowledge the contributions made by the respective MTG members in making my research endeavour possible. For offering me invaluable advice and experience on both research and PhD journey, I would like to thank Dr Jodie Harrington, Dr John Colombo, Dr Amr Alraies, and Dr Fraser Young. For the supportive criticism and endless support, I am grateful to Dr Abeer and Dr Jess Roberts.

My family and friends too deserve a special mention. For my father and mother, who taught me the values of integrity, perseverance, and gratitude, besides for being always there when I needed them. Not forgetting my family as well, who provided me with understanding and encouragement. Nevertheless, it is to my husband, Dr Muhamad Kamil, who I dedicate this work to, for his unconditional support and loving companionship throughout this long journey. Last but not least, for Haris and Hanaa, for being the source of strength and inspiration.

“Verily, with every hardship, there is ease.” (The Quran, 94:5-6)

Abstract

The successful outcome from implant procedure relies heavily on the integration between the implant and the surrounding bone tissues. Besides, Type 2 Diabetes Mellitus (T2DM), which is linked with delay of osseointegration and reduction of bone-implant interface, further compromises the success rate of implant in diabetic patients. Apart from hyperglycaemia, the precise mechanism of diabetes influence on bone repair associated with dental implants is not completely understood. Nevertheless, the transforming growth factor-β_1 (TGF-β_1) has been indicated to increase healing processes, by exerting the stimulatory role on mesenchymal stem cells (MSCs) and macrophage populations during the inflammatory stage of bone repair. Moreover, the bioavailability of growth factors has been associated with the functional role of SLRPs, particularly biglycan and decorin. However, the responsiveness of each relevant bone-repair cell and biomolecule during bone repair in a diabetic environment has not been fully evaluated.

On the other hand, the *in vivo* osseointegration of implant in T2DM animal models, investigated in respect to the expression of TGF-β_1 by MSCs, demonstrated statistically significant differences in TGF-β_1 labelled between the young diabetic and the control groups. Besides, the *in vitro* assessment demonstrated alterations for TGF-β_1 expression and synthesis by osteoprogenitor cells, macrophages populations, between cells with different proliferative states, and prior hyperglycaemic-induction. Moreover, hyperglycaemia altered osteogenic and adipogenic differentiation capacities in MSCs. The data also suggested that hyperglycaemia induced lower proliferative capacity in MSCs, which led to significant changes in growth factor and proteoglycans bioactivity in bone repair. Hence, the data gathered from both *in vivo* and *in vitro* experiments suggested the potential association of MSCs proliferative stage with bioavailability of TGF-β_1 and proteoglycans sequestration in the extracellular matrix compartment. Apart from that, the inter-dependent relationship observed between the osseointegration biomolecules directly exerted a synergical impact on the capability of MSCs to form osteoblast and further stimulate bone formation in order to induce bone-healing processes. Thus, the original contribution of this study to the field of reparative medicine is the novel identification and the characterisation of key biological components in both cellular and molecular bone repairs; the osteoprogenitor cell populations, as well as the macrophages, in relation to hyperglycaemia that directly influences growth factors, signalling the role of proteoglycans during the bone repair processes in T2DM. Collectively, the evidence gathered within this study is highly valuable to assist in elucidating the relevant therapeutic target to accelerate bone repair processes in T2DM patients.

Keywords: diabetes, osseointegration, hyperglycaemia, bone, growth factors.

Abbreviations

AGE	Advanced glycosylation end-products
Arg1	Arginase 1
ALP	Alkaline phosphatase
AP	Activator protein
ASC	Adipose tissue stem cells
BCA	Bicinchoninic Acid
bFGF	Basic fibroblast growth factor
BCE	Bone chips explant
BMP	Bone morphogenetic protein
BMSC	Bone marrow stem cell
CBFa1	Core binding factor alpha subunit protein
CCM	Complete culture medium
C/EBPα	CCAAT/enhancer binding protein alpha
CFE	Colony forming efficiency
CD163	Cluster of differentiation 163
cDNA	Complementary DNA
Ct	Cross threshold
DAPI	4’6-Diamidino-2-Phenylindole
DNA	Deoxyribonucleic acid
dNTP	Deoxyribonucleotide triphosphate
ECM	Extracellular matrix
EGF	Epidermal growth factor
eNOS	Endothelial nitric-oxide synthase
EPC	Endothelial progenitor cells
ESC	Embryonic stem cell
FABP4	Fatty acid binding protein 4
FGF	Fibroblast growth factor
FITC	Fluorescein Isothiocyanate
FDA	Food Drug Administration
FFA	Free fatty acids
GAG	Glycosaminoglycan
GK	Goto-Kakizaki
HGCM	High glucose culture medium

H&E	Haematoxylin and eosin
HRP	Horseradish peroxidase
IDF	International Diabetes federation
IBMX	3-isobutyl-1-methylxanthine
IFNϒ	Interferon gamma
IGF	Insulin-like growth factor
INOS	Inducible nitric oxide synthase
IR	Insulin receptor
IRS	Insulin receptor substrate
JNK/SAPK	Jun kinases/stress activated protein kinases
LPL	Lipoprotein lipase
MSCs	Mesenchymal stem cells
MMP	Metalloproteinase
MRC1	Macrophages mannose receptor 1
MSC	Mesenchymal stem cell
NFκB	Nuclear factor-κB
OCN	Osteocalcin
OPN	Osteopontin
OSX	Osterix
PBS	Phosphate buffer saline
PCR	Polymerase chain reaction
PD	Population doubling
PDGF	Platelet-derived growth factor
PG	Proteoglycan
PI3K	Phosphatidylinositol 3-kinase
PKC	Protein kinase C
PPARγ	Peroxisomal proliferator-activated receptor gamma
qRT-PCR	Quantitative real-time polymerase chain reaction
RAGE	Receptor for AGE
RNA	Ribonucleic acid
RNS	Reactive nitrogen species
ROS	Reactive oxygen species
RT	Reverse transciptase
Runx2	Runt-related transcription factor 2 (aka Cbfa1)

SEM	Scanning electron microscopy
SDS	Sodium dodecyl sulphate
SOD2	Manganese superoxide dismutase
STZ	Streptozocin
SLRP	Small leucine rich protein
TA	Transit amplifying
TBS	Tris buffered saline
T1DM	Type 1 diabetes mellitus
T2DM	Type 2 diabetes mellitus
TMB	3,3',5,5'-tetramethylbenzidine
TNF	Tumour necrosis factor
TEM	Transmission electron microscopy
TGF-β	Transforming growth factor-β
µCT	Micro-computed tomography
UCP	Uncoupling protein
UV	Ultraviolet
VEGF	Vascular endothelial growth factor

Unit of measurement

%	percentage
bp	base pairs
^{o}C	degree celcius
cm	centimetre
cm^{2}	centimetres squared
g	gravitional acceleration
M	mole
mA	milliampere
mg	milligram
ml	millilitre
mm	millimetre
mM	millimole
nm	nanometre
µg	microgram
µl	microlitre
µm	micrometre
rpm	revolutions per minute

Table of Contents

Table of Tables

Table of Figures

Chapter 1

General Background

1.0 Introduction

Implant technologies have significantly improved the rates of success and survival in treated subjects, besides making various improvements in treatment for bone loss and repair. Besides, studies on both animal and human have provided useful insights towards assisting in better post-implant recoveries. Approximately 188,000 hips and knees replacements are performed each year in England and Wales (National Joint Registry, 2014). Replacement surgeries are critical to replace the damaged tissues, as well as to restore the initial function and the structural features of the skeletal area, by replacing the joints with prosthetic implant. Nonetheless, in clinical dentistry, implants are preferred in comparison to removable prosthetic appliances, as they provide long-term stability and comfort with excellent post-surgical performance. However, the successful outcomes from implantology rely heavily on the osseointegration process between the implant and the surrounding tissues, which is variously influenced by a number of biological and pathophysiological factors. For that reason, implant treatment has been restricted to certain groups of individuals where high risk of failure is minimal or low.

Furthermore, rigorous pre-clinical guidelines have been introduced to increase the efficacy and the long-term benefit of implant procedure, by eliminating the risk factors that may impair the implant success. In fact, the presence of an underlying disease is identified as a possible risk in implant treatment (Soballe 1993). Therefore, patients with chronic conditions of metabolic bone diseases, such as hyperparathyroidism, osteoporosis, and diabetes mellitus, with altered physiological activities to compromise healing are likely to be excluded from implant treatment. Moreover, epidemiological studies suggested an increase in the incidences of hip fracture and periodontal diseases in Type 2 Diabetes Mellitus (T2DM), in comparison to non-diabetic group (Lipscombe et al. 2007). These directly indicate the extreme necessities of this group to undergo implant treatment. In view of these important factors, the exclusion criteria are likely to bring a substantial negative impact on the present society, due to the epidemic prevalence of T2DM. As of 2013, at least 382 million people worldwide were diagnosed with diabetes; and the number is estimated to increase up to 592 million by 2035 (International Diabetes Federation, 2014). Nevertheless, there is no clear-cut boundary in epidemics of T2DM, as the

emergence of this disease is obviously not limited by geographical locations, ages, gender, ethnic origins or even family medical history. On 14th December 2006, the United Nations General Assembly had unanimously agreed to pass Resolution 61/225, proclaiming and recognizing diabetes as the world's major health crisis to combat. The emerging threat of T2DM epidemic on paediatric groups implies the crucial needs for finding therapeutic option in dealing with future diabetic burdens in world population (Kitagawa et al. 1998; Zimmet et al. 2001).

Diabetes compromises wound or bone healing progress, and consequently, affects the osseointegration of implants. Hence, the evaluation of implant survival via *in vivo* demonstrated a delay and reduction of new bone formation in diabetic models (McCracken et al. 2006; Kwon et al. 2008; Colombo et al. 2011). Besides, histological and histomorphometric analyses confirmed reduced formation of bone in diabetic conditions, following implant placement. On top of that, impaired bone healing processes may often lead to other post-surgical complications, such as microbial infections (Goodson and Hunt 1979; Tonetti et al. 1994). Thus, the success rates of titanium implants being placed in healthy individuals are higher, compared to patients with T2DM (Morris et al. 2000). Sustaining elevated cycles of bone remodelling processes at the healing site is vital to maintain the progress of osseointegration (Garetto et al. 1995). Although a considerable amount of researches has been devoted to improving the rate of osseointegration, less attention has been paid to investigate the prolonged effects of high glucose on bone healing tissue. Hyperglycaemia plays a role in the pathophysiological progress of diabetic complications. These hyperglycaemic-induced mechanisms consist of a combination of oxidative stress, impaired inflammatory cytokines activation, as well as altered activation of NF-κB, JNK/SAPK, and p38 MAPK pathways (Evans et al. 2002). Understanding the fundamental mechanisms may provide strong evidence to formulate key therapeutic compounds, in order to promote bone healing among the diabetic group.

The current strategies employed in regenerative therapies include manipulation of the growth factor level in the systemic environment, along with pharmacological drug administration, to keep the glucose level. Although the topical and gene therapy

delivery of growth factor seems promising in promoting tissue healing, the conclusive role of growth factor within hyperglycaemic environment, particularly during bone repair in T2DM, has not been fully elucidated. The different mechanisms of insulin actions in Type 1 Diabetes Mellitus (T1DM) seem unlikely to be applicable for T2DM, where insulin resistance is a known pathogenic mechanism. Besides, it would seem that further studies might provide more reliable and valuable evidence in supporting the clinical management of T2DM patients who undergo implant treatment. Until then, effective strategies to improve the osseointegration ability within hyperglycaemic environment are still far from becoming available to T2DM patients.

Against this background, this study investigated and characterized the cellular activity in bone progenitor cells during culture in a hyperglycaemic environment, similar to T2DM. With *in vivo* and *in vitro* applied on animal models, focus was given to the growth factor bioavailability within the healing situation. Moreover, it further elucidated the potential of mesenchymal stem cells (MSCs) to migrate to bone repair sites, to form osteoblasts and further regenerate new bone tissue formation. The study also looked into potential small matrix proteins and biomolecules, which might be relevant in regulating the inflammatory response during diabetic bone healing, by indirectly causing alterations in growth factors signalling. Therefore, detailed analysis and information derived from this study should shed some light on the current knowledge of reparative strategies. The data obtained could also assist in any future work to design a specific therapeutic agent to reverse the altered hyperglycaemic-induced responses, as well as to improve rates of successful clinical outcomes.

1.1 Bone biology

Bone is a dynamic structure in the body that is comprised of various active cell types and organic matrix components. The bone structure is strengthened by calcium and inorganic mineral deposition that mainly exist in the form of hydroxyapatite. Bone plays an important role in regulating metabolic reservoir, providing mechanical support, and also protecting vital organs. The unique composition and properties of bone are mainly controlled by multiple actions; regulated between cellular material, matrix composition, and mineral contents. The bone structure and its biological functions are maintained through a series of synchronized events that takes place in parallel to physiological and biochemical changes in the body.

1.1.1 Bone structure

Bone structure comprises of two important features; the cortical bone and the trabecular bone. Cortical or compact bone is the hard, dense, and rigid form of bone tissue, which forms the outer layer of bone surrounding the marrow space. Enclosed within these layers is the trabecular bone, a network of plate-like and rod-like trabecular microstructures, which create sponge-like features within the bone marrow compartment. The outermost layer of cortical bone, the periosteal, is a thin and tough membrane of fibrous connective tissue, which contains nerve fibres, blood vessels, osteoblasts, and osteoclasts (Kini and Nandeesh 2012). It provides support for tendon and muscles, as well as assist in bone formation during skeletal growth and reparative processes. Lying beneath the trabecular sheath is an endosteum layer, a membranous structure that contains osteoprogenitor cells, osteoblasts, and osteoclasts (Garg, 2004). Meanwhile, the innermost portion of the bone is a hollow space filled with marrow.

In addition, microscopic analysis of bone differentiation has identified two types of bone formation, which differ in their patterns of the collagen fibres forming the osteoid. First, the woven bone encompass a rapid formation of osteoid from osteoblasts, which leads to random distribution of collagen fibres, leaving a weakly structured woven-like appearance of fibrous matrix. Second is the lamellar bone that is characterised by uniform alignment of highly organized collagen sheets, which form the mechanically strong lamella structure (Eriksen 1994).

1.1.2 Bone formation

Formation of bone tissues starts during embryonic development and remains until the period of postnatal bone growth. Bone formation is vital, in order to maintain biological homeostasis and to support skeletal growth. Different mechanisms of bone formation take place within the skeletal organ, depending on the site and the shape of the bone involved, classified as intramembranous ossification and endochondral ossification (Pfeilschifter et al. 1992). In intramembranous ossification, the process is directed to develop bones within a collagenous mesenchymal matrix. This process utilises osteoprogenitor cells or undifferentiated MSCs, which mature into bone-forming cells, such as osteoblasts; and further develop into osteoid. The bone growth then continues to form a network of immature bone structures, referred to as woven bone. The immature woven bone structure, which consists of randomly distributed collagen fibres, will eventually be replaced by lamellar bone formation. Intramembranous ossification takes place in flat bones, such as the skull, sternum, mandible, and clavicle, and the major ossification mechanism is associated with osseointegration.

Endochondral ossification regulates the replacement of a cartilage matrix by bone, following the recruitment, the proliferation, and the differentiation of MSCs to the site. Besides, the development and the growth of cartilage model play an important role in the formation of the ossification centre for osteoblast migration and maturation. Thereafter, the mineralization of cartilage takes place (Poole et al. 1982). Each process in endochondral ossification occurs in multiple stages of temporal characteristics, whereby in the end, calcified cartilage is replaced by compact bone.

1.1.3 Bone remodelling

Bone undergoes a sequence of remodelling or turnover processes throughout life. The remodelling process involves changes in the structure, the size, the shape, and the quality of bone that is being produced in the skeletal system. During bone remodelling, a cascade of events will take place simultaneously within the bone to remove the old osseous tissues, and immediately followed by the formation of new tissue to replace the existing bone. Remodelling of bone is important for bone growth and development to regulate calcium homeostasis, and also to provide a reparative

mechanism in response to injury or fracture damage. Bone remodelling frequency in growing tissue is controlled by both mechanical and metabolic factors. Besides, the evidence of tight coupling behaviour between bone resorption and bone formation validates the impairment of bone remodelling in patients with osteoporosis and metabolic bone disorders. The delayed resorption activity is postulated to impair bone formation and remodelling system, which leads to alteration of net change in bone mass and quality after the remodelling cycle (He et al. 2004). Meanwhile, bone morphogenetic proteins (BMPs) are a type of growth factor in the TGF-β superfamily that integrates interactions between bone resorption and bone formation to maintain the cues for bone turnover in biological systems (Marx and Garg 1998). It is believed, however, that during osteoblast deposition on the bone surface, they also secrete BMPs into the mineralising matrix. The insoluble properties of BMPs at pH1.0 explain the release of this protein from the bone matrix as soon as osteoclasts initiate the resorption activity (Urist 1997). The release of BMPs subsequently induces differentiation of osteoblastic cells, which stimulates bone formation.

1.1.4 Bone cellular components

Four different types of bone cells are closely related to bone metabolism and physiology; osteoblasts, osteoclasts, osteocytes, and osteoprogenitor cell populations. These bone cells mainly develop from mesenchymal progenitor cells and are commonly associated with important roles in skeletal development. MSCs originate from multipotent stromal cells and display great capability to differentiate and form various types of cells; including the major bone-forming cells, osteoblasts, and other mesenchyme lineages cells, such as chondrocytes and adipocytes. The whole mechanism of MSC differentiation into osteoblasts has been documented using *in vitro* cell culture. Hence, the evidence has further pointed out the importance of MSCs as the major type of cells involved in bone remodelling and repair process.

Osteoblasts actively produces bone matrix, which largely consists of Type I collagen and a variety of non-collagenous proteins. The inorganic matrix component is subsequently mineralised and becomes new bone, providing rigidity and strength to skeletal composition. However, in later stages of bone formation, osteoblasts eventually become embedded in the bone matrix, and these cells are transformed to

form part of bone components called osteocytes. Osteocytes cells have a basophilic cytoplasm that contributes to the formation of a canaliculi network system; which serves as a platform for metabolic and biochemical exchanges between the bloodstream and the bone cells (Marx and Garg 1998). Another group of bone cells that play an important role in bone development is osteoclasts. Osteoclasts are a group of bone cells that originally develop from the haematopoietic lineage. During the activation of bone remodelling, osteoclasts adhere to the bone matrix and secrete a combination of acid and lytic enzymes that degrade the existing bone cell structure. The interaction between osteoblasts and osteoclasts commonly takes place in active bone turnover sites, which occur in periosteal, endosteal, trabecular, and cortical bones (Hughes and Boyce 1997). Besides, the imbalanced actions in the bone area can lead to perturbation of bone quality, growth, and structure.

1.1.5 Bone progenitor cells

Both regeneration and repair of bone are commonly associated with osteoprogenitor cells and their precursors, the MSCs. MSCs are a group of progenitor cells, derived from the subset identified in non-hematopoietic, a bone marrow component. MSCs were first introduced by Friedstein (Friedenstein et al. 1976). MSCs have demonstrated sustained proliferation capacity and differentiation capacity to be developed into various stroma-supporting cells, including bone precursor cells. The success of osteoprogenitor cells and MSCs application in accelerating endosseous healing is determined by coordinated interactions between the participating cells, the growth factors, and the extracellular matrix components, which provide the local biochemical and mechanical support for cell proliferation and differentiation. Hence, *in vitro* cell culture models have often been utilised to study the microenvironment of cellular and molecular activities of bone cells within the healing interface to further investigate the potential role of bone precursor cells and MSCs in the reparative processes. At present, the isolation of mesenchymal progenitor cells is performed actively from bone marrow and other additional mesenchymal sources, such as adipose, skeletal, and muscles (Zuk et al. 2001; Qu-Petersen et al. 2002; Lee et al. 2004; Nakamura et al. 2010).

MSCs have long been utilised in orthopaedic medicine, whereby the administration of these skeletal progenitor cells typically involves their local delivery to the targeted area. For example, MSC application has been demonstrated in treatments of spine injury (Muschler et al. 2003), fracture repair (Granero-Moltó et al. 2009), craniotomy defect (Krebsbach et al. 2003), and segmented bone defects (Quarto et al. 2001). Apart from that, a recent study demonstrated that bone marrow-derived MSCs (BM-MSCs) application significantly improved wound healing in normal and diabetic mice. The medium of BM-MSCs has been found to increase angiogenesis and consists of high levels of vascular endothelial growth factor (VEGF) and angiopoietin-1, which further explain the improvement of wound healing in BM-MSC treated areas (Wu et al. 2007). Several other studies also indicate the potential benefits of BM-MSCs in promoting rapid bone healing in both normal and diabetic groups (Bruder et al. 1998; Kwon et al. 2008; Fiorina et al. 2010; Albiero et al. 2011). Apart from mainly relying on MSCs derived from bone marrow to provide bone progenitor cells, more experimental work has been dedicated to assessing into other potential sources of progenitor stem cells, which provide less invasive methods of extraction. Therefore, hair follicles, dental pulp, and oral mucosa lamina propia (OMLP)-derived stem cells have been explored for this purpose (Gronthos et al. 2000; Oshima et al. 2001; Davies et al. 2010). Previous studies also revealed that dental pulp stem cells (DPSCs) differentiate into osteoblasts and further stimulate secretion of ECM component to support *in vitro* bone formation (Laino et al. 2005; Laino et al. 2006). DPSCs also revealed positive results for *in vitro* and *in vivo* experiments to induce bone formation in damaged or injured tissues (D'Aquino et al. 2008; D'Aquino et al. 2009). These extensive studies provide much promising evidence for the future application of MSCs in facilitating rapid recovery process, following implant placement.

The main rationale for MSC applications in bone repair is based on their ability to differentiate into osteoprogenitor cells and osteoblasts. Besides, the differentiation capacity of MSCs can be manipulated by controlling the stem cells niche and microenvironment. Moreover, different signalling molecules have been identified to have a modulatory effect on MSCs differentiation into various types of progenitor cells, such as osteoblasts, adipocytes, chondrocytes, and tenocytes. Experimental

studies also have demonstrated the differentiation capacity of MSCs to form osteoblasts with the application of metabolic hormone, such as 1,25-dihydroxyvitamin D3, growth hormone, leptin, and prostaglandin E2 (Kröger et al. 1997; Kelly and Gimble 1998; Thomas et al. 1999; Keila et al. 2001); cytokine, such as interleukin-6 (IL-6) (Taguchi et al. 1998); and growth factors, such as bone morphogenetic protein-4 (BMP-4), and transforming growth factor- β_3 (TGF-β_3) (Ahrens et al. 1993; Pittenger et al. 1999).

1.1.6 Bone signalling pathways

The study of bone signalling pathways has enhanced our comprehension on bone cell differentiation, migration, and activation. Biochemical challenge and stress activate different bone signalling pathways. Systematic regulations of osteoblasts and osteoclast functions are important to maintain normal bone remodelling process. Few of the known major transcription factors in osteogenesis are Runx2, Taz, Osterix (OSX), and Dlx5. These transcription factors are mainly important in inducing progressive differentiation of multipotent MSCs into osteoblasts, osteocytes, and other types of cells from multiple lineages, in supporting osteogenesis (Abbas et al. 2003; Lee et al. 2003). Runx2 is a major gene of core-binding factor A1 (Cbfa1), which regulates osteogenesis by binding to OSE2 promoter region of major osteoblast genes. Runx2 also regulates the expression of osteocalcin (OCN), bone sialoprotein (BSP), osteopontin (OPN), type I collagen, and others (Ducy et al. 1997; Javed et al. 2001). Besides, Runx2 has been proven as the major transcription factor for osteoblast differentiation. However, their action on osteoblast differentiation is inhibited by tumour necrosis factor-α (TNF-α), via TNF type-1 receptor activation (Abbas et al. 2003). Meanwhile, Taz is a transcriptional co-activator with PDZ-binding motive, which activates Runx2 expression via FGF2 signalling to stimulate osteoblast differentiation (Cui et al. 2003; Byun et al. 2013). Taz also plays an important role in modulating the switch between osteogenesis and adipogenesis, by inhibiting PPARγ gene transcription (Hong et al. 2005). Next, OSX is a zinc-finger containing transcription factor, which is specifically expressed in all developing bones and plays an important role in bone mineralization. OSX transcription factor is located downstream to Runx2, as no OSX expression was observed in Runx2-knocked out mice (Nakashima et al. 2002a). While Runx2 had been postulated to be

responsible for mediating the differentiation of osteoblast to chondro-progenitor cells, OSX activation predominantly effects terminal differentiation of osteoblasts, whereby they act to distinguish the osteogenic pathway from the chondrogenic one. Another major bone-inducing transcription factor expressed in differentiating osteoblasts is known as distal-less homeobox-5 (Dlx5) (Ryoo et al. 1997). Dlx5 plays a pivotal role in BMP-2-induced osteoblast differentiation by stimulating downstream of transcription factor Runx2. Furthermore, another study indicated that Dlx5, instead of Runx2, which is located upstream, mediated BMP-2-induced Osx expression (Lee et al. 2003). Forced expression of Dlx5 demonstrated an increase in osteocalcin expression and the formation of a mineralized matrix in cell culture, which indicate the functional importance of Dlx5 in osteoblast differentiation (Tadic et al. 2002).

Several different identified pathways and components control the regulation and the differentiation of osteoclasts, including macrophage colony-stimulating factor (MCSF) (Asagiri and Takayanagi 2007); osteoprotegerin (OPG); TNF receptor activator of nuclear factor-κB (RANK); and receptor activator of nuclear factor-κB ligand (RANKL) (as reviewed by Boyle et al. 2003). These identified pathways lead to the differentiation of osteoclasts from hematopoietic progenitor cells, thus controlling osteoclastogenesis, bone remodelling, as well as regulation of bone mass and density. On the other hand, OPG is a soluble and secreted TNFR-related protein that blocks osteoclast formation *in vitro* and bone resorption *in vivo*. OPG-knocked out mice demonstrated osteopenia and OPG-overexpressed transgenic mouse exhibited major increment in bone mass. These indicate the critical role of the OPG pathway in mediating osteoclastogenesis and bone remodelling (Simonet et al. 1997; Bucay et al. 1998). Meanwhile, RANKL is a soluble transmembrane protein found on the surface of expressing osteogenic cells (Anderson et al. 1997; Wong et al. 1997). The expression of RANKL is important to co-ordinate bone remodelling, by inducing bone resorption in local osteoclasts that consecutively stimulate bone synthesis from the adjacent osteoblasts through a process called ‘coupling’ (Udagawa et al. 2000). Therefore, knocked out mice lacking in RANK and RANKL were found to develop osteopetrosis, which resulted from impaired osteoclasts functions and bone resorption (Dougall et al. 1999). The RANK:OPG ratio

represents an interdependent relationship with osteoclasts activities, which relatively include overall changes in bone microenvironment and remodelling; such as alterations in local growth factors and calcium release from bone matrix (Dougall 2011). Together, these identified bone signalling pathways act as key regulatory factors in formation and function of osteogenic cells to maintain normal physiological bone remodelling activities (Figure 1.1). Hence, any alteration or disruption of these signalling pathways may potentially suppress or delay bone development and repair process.

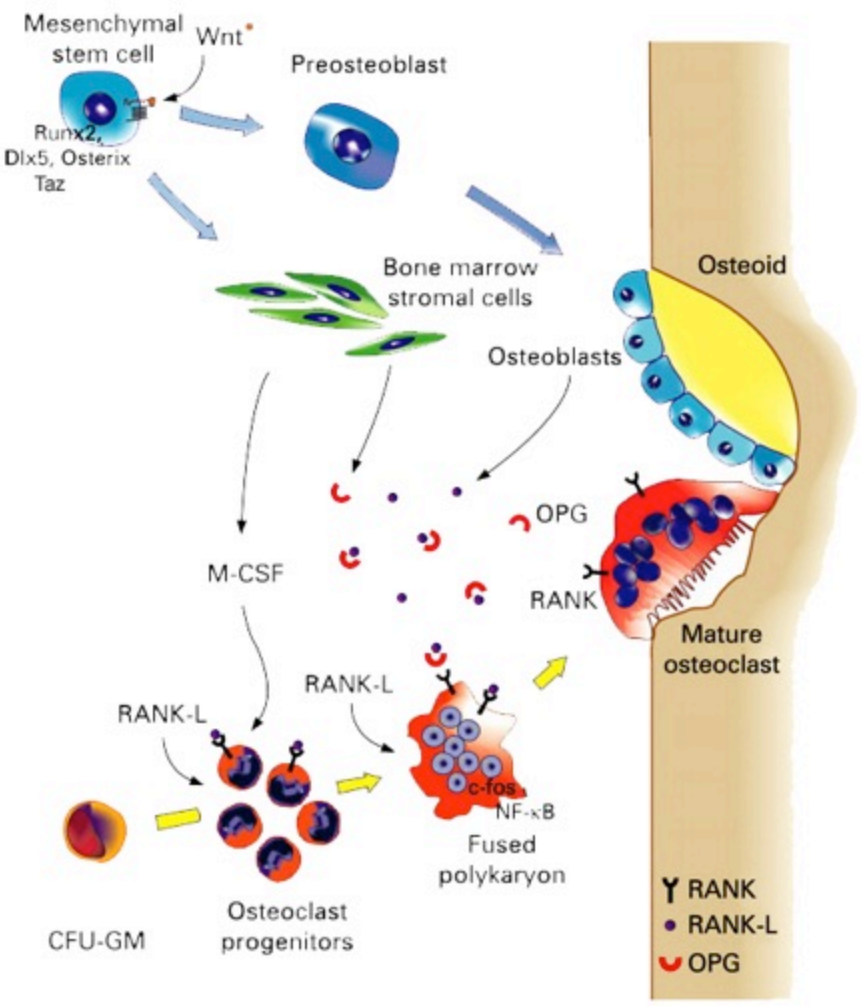

Figure 1.1 Bone remodelling pathways involves several cell types; including osteoblasts, bone marrow stromal cells and osteoclasts. Osteoblasts are derived from mesenchymal stem cells, via induction of the osteoblastogenic transcription factors Runx2, Dlx5, Taz and osterix. Osteoclasts on the other hand are derived from myeloid precursors under the permissive influence of receptor activator of nuclear factor-κB (RANK), which is activated by RANK ligand (RANKL). The balance of RANKL:OPG ratio regulates bone homeostasis. Adapted from Tilg et al. (2008).

1.2 Bone healing associated with osseointegration

Bone holds substantial capacity to repair and regenerate in response towards injury and surgical procedures, comprising of a series of processes and simultaneous reparative functions, besides being triggered in response to damage. Following an implant placement, the repair processes involve integration between the metal implant and the surrounding bone tissues, which is known as osseointegration. Contact osteogenesis and distance osteogenesis are two suggested terms, which refer to the location of osseointegration. Contact osteogenesis is bone formation on the implant surface, whereas distance osteogenesis is bone formation by recruitment of osteoblasts cells deposition on bone surfaces (Davies 2003). The activity of osseointegration correlates with the success rate and survival of implants in treated patients because prolongation of the osseointegration process may increase the susceptibility of bone-implant interface towards infections and other post-surgical complications.

1.2.1 Osseointegration: The healing phases

Repair and regeneration of bone tissue at the healing site is a constant process, which primarily involves restoration of the injured tissue, as a consequence of differentiation of bone progenitor cells to form new bone tissue. Nevertheless, due to the complexity of the *in-vivo* environment, it is relatively challenging to fully characterize the complexity of bone-implant contact during the healing process. Although several biomolecules have been identified at the bone-implant interface, the possibility of many other essential biomolecules involved in the process might still be unknown (Puleo and Nanci 1999). The osseointegration of implants and surrounding bone tissues consist of three different stages, which are generally described as the initial inflammatory phase, restorative phase; and the late remodelling phase. Controlling the bone-implant interface to induce osseointegration is likely to be possible, if the fundamental factors, such as biomaterial, biomechanics, and biological events, which effect the healing phase, are precisely manipulated. Expression of osteocalcin (OCN) indicate differentiation lineage of mesenchymal cells during the early stage of healing. The molecular and the cellular events near the bone-implant contact mainly involve intramembranous ossification, as very small

amount of ColIIa expression was detected in the stabilized fractures, indicating that healing occurs mainly through intramembranous ossification (Thompson et al. 2002).

1.2.1.1 Phase 1: Inflammatory phase

The healing mechanisms, which consist of multiple important events, are immediately generated following injury and damage to the bone microenvironment. The damage to tissue structure triggers the formation and the migration of clotting factor to the site of the injury. Clot formation induces homeostasis and provides a matrix for the recruitment of inflammatory cells, such as macrophages, monocytes, lymphocytes, and polymorphonuclear cells, to the injury site (Barrientos et al. 2008). Collectively, the existence of inflammatory cells at the bone-implant interface provides the source of various active signalling molecules, such as growth factors, cytokines, and chemokines, to the site of injury; and further activates signalling pathways for coordinating cellular repair. Besides, complex integration of signalling molecules is critical to induce the migration of undifferentiated mesenchymal progenitor cells from the inner layer of the cortex to the healing site. These precursor cells are essential to repair processes as they represent the key components in regeneration of new bone tissue.

1.2.1.2 Phase 2: Restorative phase

Usually, when an implant is placed into the cancellous marrow space of a mandible or maxilla, only a small amount of bone cells remains in the insertion site to form interactions with the surface area of the implant (Marx and Garg 1998). Following the inflammatory phase, the initial bone-implant interface becomes occupied with bone precursor cells. At this restorative phase, mesenchymal progenitor cells may be evenly distributed along the surface of the implant or along the surface of the old bone. The different locations in the lining depositions of these osteoprogenitor cells are commonly associated with the terms ‘contact osteogenesis’ and ‘distance osteogenesis’. Contact osteogenesis refers to the formation of a thin layer of progenitor cell localised along the implant surface to induce osteogenesis, while the latter involves the formation of lining cells on the surface of the old bone (Davies 2003). The progenitor cells form an interaction with extracellular matrix

components; and further proliferate and differentiate at the healing site to form granulation tissue, as well as induce *de novo* bone formation. In the *de novo* bone formation, the osteogenic cells secrete a non-collagenous layer of organic matrix between the osteoprogenitor cells and the adjacent bone or the implant surface. Bone proteins, such as OPN, BSP, and proteoglycans, have been found among this non-collagenous organic phase (Berglundh et al. 2003). The theory of contact osteogenesis is important in *de novo* bone formation, as the non-collagenous matrix provides a template for calcium phosphate mineralization, followed by formation of bone collagenous matrix components, which further embed a large number of MSCs in the woven matrix, and stimulates calcification by bone cells (Cardaropoli et al. 2003). The primary bone consists of immature woven bone structures, which later on, are replaced with more mature bone tissue that consists of plate-like trabeculae, fibre lamellar bone, and marrow space (Berglundh et al. 2003). Furthermore, induction of angiogenesis during this repair phase is also as important as osteogenesis, to maintain the osseointegration process.

1.2.1.3 Phase 3: Remodelling phase

Osseointegration consists of a dynamic process, both during its establishment of inflammatory and restorative phases, as well as its maintenance in the remodelling phase. As remodelling begins in the healing interface, it often indicates the last stage of healing progress, also known as osteoadaptation, as in this phase, the bone cells begin to adapt to a new matrix environment and continue to grow in parallel to the implant. Bone remodelling at the healing sites consists of both osteoblasts and osteoclasts, which facilitate in restoration of original structure, shape, and mechanical strength of bone. As the healing bone learns to adapt to loading forces, the mechanisms of bone resorption and bone formation simultaneously take place in order to continuously reconstruct the bone according to its function. Therefore, the late remodelling phase in healing site is important to secure and to maintain the osseointegration process, prior to adaptation and function (Berglundh et al. 2003).

1.2.2 Signalling pathways in osseointegration

Initial bone healing responses involve activation of fibroblast, endothelial cells, macrophages, and platelets (Brem and Tomic-Canic 2007). Activation of these cells is triggered by the release of important cytokines, such as IL-1, IL-6, and TNF-α, as well as growth factors, such as TGF-β_1, BMPs, and VEGF, which are essential to enhance and maintain healing processes (Al-Aql et al. 2008). The expressions of these biomolecules are regulated by the activation of multiple signalling-induced pathways. The two important signalling pathways that have been identified to play an important role in mediating the activation of cellular response to facilitate healing and osseointegration are p38 MAPK and ERKs. The p38 MAPK and the ERKs are members of the complex superfamily of MAP serine/threonine protein kinases. The ERKs are typically activated by mitogens, but the p38 MAPK pathway is often associated with stress-activated kinases (Evans et al. 2002). Moreover, it is believed that the activation of MAPK pathway in osseous healing is mainly stimulated by the presence of pro-inflammatory cytokines, such as IL-1β and TNF-α (Eda et al. 2011).

Furthermore, the activation of the MAPK signalling cascade is known to stimulate a variety of cellular changes during gene transcription, including initiation of angiogenesis, which is important in the development of a vascular supply in stages of wound and bone repair (Sharma et al. 2003). Meanwhile, the cross-talk activation of p38 MPKs and/or ERK1/2 pathways are accountable for sheer stress-dependant angiogenesis, endothelial cell migration, and vasculature formation, leading to overall tissue-repair responses (Bajpai et al. 2007; Huang and Sheibani 2008; Gee et al. 2010). However, few experimental studies have characterised the potential role of p38 and/or ERK1/2 pathways in directing VEGF expression from endothelial cells and MSCs (Mezentsev et al. 2002; Kim and Wong 2009), which plays a critical role in angiogenesis. Recent experimental data also suggested that administration of exogenous biomolecules, such as 14S,21R-diHDHA, to activate the p38 MAPK signalling pathway in endothelial cells and MSCs, were found to have a positive effect in accelerating diabetic wound healing and MSC functions (Tian et al. 2010).

1.3 Growth factors in bone metabolism

Growth factors are a group of soluble proteins produced by cells, which are capable of carrying out multiple cellular actions on targeted cells. Growth factor actions in the cellular environment are divided into three types; autocrine, paracrine, and endocrine. In autocrine actions, growth factor acts on targeted cells with the same phenotype as those cells that secreted them. For example, growth factor secreted by osteoblast will have effect on osteoblast functions. Meanwhile, in paracrine actions, the growth factor acts on cells that reside near the secretory cells; and endocrine actions refer to the ability of growth factor to act on target cells that are located remotely from the cell of origin. Growth factor secretion exerts a wide range of effects on cellular behaviour as they take part in a series of molecular signalling events, which control cell growth and division, tissue differentiation, and matrix synthesis. For example, insulin-like growth factor-I (IGF-I), basic fibroblast growth factor (bFGF), and platelet-derived growth factor (PDGF) are known to have a profound mitogenicity effect on cellular functions, whereas bone morphogenetic proteins (BMPs) enhances collagen synthesis through osteoinduction (Mohan and Baylink 1991; Lind 1998).

In addition, growth factors serve a clinical role in bone development through phases of endochondral and intramembranous ossifications; as well as participation in bone remodelling from embryonic life to postnatal period. Besides, growth factor regulations are known to have significant effects on the induction of bone and cartilage formation, which correlate with their substantial role in bone or fracture healing progress (Hughes et al. 2006). Abundant amounts of growth factors, such as PDGF, TGF-β_1, and BMP-2, are secreted during the healing phase, following bone fracture or wound injury, to promote the release of inflammatory cytokines (as reviewed by Dimitriou et. al, 2005); and further initiate migration of progenitor cells to the injury site. This understanding has become the basis of attempts to manipulate growth factors for therapeutic use in inducing bone repair process. Therefore, various types of growth factors have been manipulated via cloning techniques and are recombinantly produced in order to serve their therapeutic roles in bone growth and remodelling, such as rhIGF-1, rhFGF, and rhTGF-β_1 (Marcelli et al. 1990; Ebeling et al. 1993; Nakamura et al. 1995). Delivery of these molecules, which normally plays

essential roles in osteogenesis, is believed to accelerate osseointegration capacity at the tissue-implant interface, particularly following placement of implant in compromised patients.

1.3.1 Origins of growth factors in bone

Most of the growth factors involved in bone and cartilage regulations originate from osteoblast and extracellular matrix components (Hughes et al. 2006; Discher et al. 2009). Osteoblasts and osteoclasts are known to secrete several types of pro-inflammatory cytokines and growth factors, such as BMPs, FGF, IGF, and PDGF, which are subsequently located within the bone matrix (Hughes et al. 2006). Growth factors in bone development may also be derived from various other cells, such as osteoprogenitor cells (BMPs), macrophages (FGF), platelets (PDGF, TGF-β), and chondrocytes (FGF, IGF) (Lieberman et al. 2002). It has long been recognised that the synthesis and the deposition of extracellular matrix are determined by growth factor actions, cytokine expression, and mechanical signals generated through cell surface receptors. As a consequence, extracellular matrix also serves as a reservoir for the deposition of growth factors and secretory proteins following a wound or injury to the bone area. In fact, several growth factors have been identified residing within the bone matrix and extracellular components, such as BMPs, IGF, and TGF-β1, which modulate and coordinate the cues for the bone remodelling process. In this way, the extracellular matrix does not only mediate cell attachment, but also facilitates in retaining the growth factor functions within its short lifespan by limiting the diffusion (Discher et al. 2009). Hence, this explains the association of appropriate distribution and release of growth factors by extracellular matrix, with several impacts on cellular activity, including prolongation of growth factor action, localisation of growth factor activity to the immediate environment, and alterations in growth factor activity (Flaumenhaft and Rifkin 1992).

1.3.2 Receptors for growth factors in bone

Effects of growth factors on bone metabolism are mediated through specific receptor on osteoblasts and neighbouring cells. Cell surface receptors act as attachment sites for growth factors and other proteins, so that they can trigger the mechanical signal for coordination of a functional deposited matrix. Following binding, the receptor

will activate an intracellular signal transduction response directed to the nucleus and induce biological responses in the target cells. The binding of growth factors to its receptors is known as ligand-receptor interaction (Lieberman et al. 2002). Theoretically, each type of receptor is assigned to bind to a single specific type of growth factor, corresponding to its unique protein structure. However, ligand-receptor interactions in growth factor activation are more complex with one or more ligands binding to one single receptor, or a single type of ligand is able to bind to several types of growth factor receptors (Trippel et al. 1996; Barnes et al. 1999). These unique and complex ligand-binding interactions indicate that growth factors action is taking place in a coordinated cascade of events, which involves a definitive combination of growth factors to completely exert its overall effect on bone restoration (Lee et al. 2011). This has been proven in experimental studies, as treatment with a combination of growth factors showed various responses in stimulatory and inhibitory effects towards bone formation. For instance, the application of IGF-I and TGF-β_1 in a rat tibia fracture model demonstrated improved healing responses (Schmidmaier et al. 2003), whereby local deliveries of TGF-β and IGF-1 in a biodegradable polymer or hydroxyapatite (HA) coating markedly increased the fixation and the osseointegration rates of titanium implants in animal models (Lamberg et al. 2006; Lamberg et al. 2009). However, a combination of BMP-2 and bFGF in rabbit tibia fracture model resulted in decreased bone formation (Vonau et al. 2001). Therefore, an optimal combination of growth factors for delivery, together with adequate release kinetics based on identified temporal characteristics, may provide a substantial formulation of successful bone and wound healing in treated subjects.

1.3.3 Growth factors in bone formation

Since growth factors play an important role in the modulation of tissue growth and repair, evaluation of their precise roles in the healing process is extremely beneficial. Following injury, the expression of growth factors in cells is elevated, due to its association with cell degranulation and inflammatory processes. However, at later stages, when bone remodelling processes and reorganization of extracellular matrix become more active, growth factor levels return to normal or become undetectable. Owing to this evidence, temporal expression of growth factors in the healing process

had been proposed (Würgler-Hauri et al. 2007). Experimental studies have demonstrated the role, the expression, and the application of different growth factors in facilitating bone healing, either in animal models or human subjects (Katagiri and Takahashi 2002; Baker et al. 2009; Ehnert et al. 2010). Growth factors play an important role in the stimulation of molecular mechanism for controlling osteoblasts proliferation and differentiation, which results in coordinated bone formation during fracture healing and distraction osteogenesis (Al-Aql et al. 2008). Among the abundant growth factor available, a number of them have been identified to be relatively significant in bone healing and repair.

1.3.3.1 Transforming growth factor-β

Transforming Growth Factor-β (TGF-β) predominantly exists within the bone matrix. The TGF-β superfamily consists of five isoforms that range from TGF-β_1 to TGF-β5, the BMPs, growth differentiation factor (GDFs), activins, inhibins, and anti-Mullerian hormones (Linkhart et al. 1996; Rosier et al. 1998; Massagué and Wotton 2000). This family of proteins participate in system regulation and cellular functions, such as proliferation, differentiation, and extracellular matrix synthesis. These isoforms exert their effect on cell development by interactions with specific heterodimer receptor complexes, which consist of two distinct transmembrane proteins, known as TGFβ-receptor I (TGF-β1R) and TGFβ-receptor II (TGF-β2R). These two transmembrane proteins belong to the serine-threonine kinase receptor family (Hu et al. 1998). Meanwhile, the type III receptor, known as betaglycans, has not been directly associated with TGFβ signalling, but may have a profound effect on binding of TGF-β to receptor II (Pfeilschifter et al. 1998). Besides, most of the TGF-β receptors are found in osteoblastic cells from various origins (Robey et al. 1987). TGF-β has a positive effect on bone healing progression, as it has been proven to induce in vitro cell growth via activation of IGF-I and significantly increase the osteogenic capacity of primary human osteoblasts (Viereck et al. 2002). Their role in proliferation of MSCs is controlled by other factors, such as the extracellular environment, the ligand-receptors interactions with other growth factors, and the total concentration at the healing site. Therefore, TGF-β is known to exert their effect on bone metabolism more as a modulator instead of a stimulator, as it coordinates local growth factors that reside within the bone extracellular matrix, such as IGF-I

and PDGF, for a wide range of effects in the resorption and formation of bone (Pfeilschifter et al. 1998). On top of that, TGF-β_1 has been reported to have long-term positive effects on bone matrix turnover by taking part in the differentiation osteoblast precursor cells to become mature osteoblast. TGF-β_1 also participates in suppression of bone resorption by inhibiting osteoclast activity and inducing the apoptosis of osteoclasts (Ehnert et al. 2010). Therefore, TGF-β_1 plays an important role in bone remodelling, as it induces osteoid formation and increases the number of osteoblasts. Moreover, TGF-β_1 is suggested to modulate collagen and fibronectin production, as well as induce angiogenesis by increasing adherence capacity of TGF-β_1 to the extracellular matrix compartment (Ignotz and Massagué 1986).

TGF-β_1 expression has been demonstrated to increase in early inflammatory phase and later stage of healing (Cho et al. 2006; Würgler-Hauri et al. 2007). Localization of TGF-β1 in healing tissue also has shown that this growth factor is sequestrated within the newly formed tissues, around the insertion site and the articular surface. In fact, their concentration was found to be the highest in healing sites; at around 10 days post-surgical period, but after 16 weeks, TGF-β_1 was no longer detectable (Galatz et al. 2006; Würgler-Hauri et al. 2007). However, higher expression of TGF-β_1 in the early process of healing has been associated with the excessive formation of scars in the healing tissues (Tsubone et al. 2006). A recent study has also depicted that TGF-β_1 is able to stimulate the migration of diabetic monocytes through the stimulation of ALK5 kinase activity, as well as signalling via phosphoinositide 3-kinase (PI3K) and p38 pathways (Olieslagers et al. 2011). These evidences support the potential application of TGF-β_1 in stimulating collateral growth in diabetic environment.

1.3.3.2 Bone morphogenetic proteins (BMPs)

BMPs belong to the large TGF-β superfamily. The BMPs are mostly present in the bone matrix and have effects on stimulating ectopic bone formation *in vivo* (as reviewed by Mundy et al. 1995). BMP-12, a member of the BMPs' large family, is also found in active fibroblasts. Application of human recombinant-BMPs (rhBMPs) has been reported to be significantly relevant in facilitating the healing process in acute diaphyseal, open tibial fracture, and reducing the risk of secondary intervention

(Govender et al. 2002; Lyon et al. 2013). BMPs are expressed by osteoblastic cells during the differentiation process and later exert their effects on bone formation via autocrine actions (Harris et al. 1994). Three osteogenic master transcription factors; Dlx5, Runx2, and OSX, are controlled by the BMP-2 expression (Lee et al. 1999; Miyama et al. 1999; Nakashima et al. 2002b). Besides, a study of fracture healing reported an increase in the expression of potent osteogenic factor, BMP-2, at the fracture site, where it exerted an osteogenic role via direct stimulation of osteoblasts (Bouletreau et al. 2002).

1.3.3.3 Basic fibroblast growth factor (bFGF)

bFGF is known as a modulator of cartilage and bone growth. These growth factors are localised in the extracellular matrix and are mainly expressed and regulated in osteoblastic cells (Hurley and Florkiewicz, 1996). However, in other *in vitro* work, bFGF had shown to suppress collagen synthesis (Katagiri and Takahashi 2002). Therefore, temporal profiles of these growth factors are important to facilitate in the application of bFGF as an effective therapeutic agent. Mice with defects in bFGF expression were found to have reduced plate-like trabeculae structures, indicating a significant decrease in bone quality, which directly represent lower bone volume, less mineral apposition, and impaired bone formation (Montero et al. 2000). In addition, bFGF treatment had been found to demonstrate increased cancellous bone formation, suggesting that osteoblast precursors in the marrow cavity act as an important source for bFGF activity (Mayahara et al. 1993). Thus, these studies indicate the important role of bFGF in fracture and bone repair.

1.3.3.4 Vascular Endothelial Growth Factor (VEGF)

VEGF has been reported to increase the rate of bone metabolism by stimulating vascularisation (Ferrara et al. 1998). VEGF is produced by osteoblasts to stimulate angiogenesis and to increase osteogenesis in response to BMP expression (Deckers et al. 2002). More studies in recent years have also indicated the participation of VEGF in ossification, where the expression of VEGF was observed in hypertrophic chondrocytes, woven bone, and fibroblastic cells close to new bone formation (Ferguson et al. 1999; Gerber et al. 1999; Street et al. 2002). Moreover, VEGF has

been identified as a potent stimulator of endothelial cell proliferation, often expressed during endochondral ossification and bone formation. Hence, the topical application of VEGF has been found to induce wound healing in diabetic patients by inducing angiogenesis and the mobilization of bone marrow progenitor cells to the healing site (Galiano et al. 2004). Additionally, VEGF and angiopoietin-1 are significantly present in higher concentrations in BM-MSCs, thus indicating the potential role of BM-MSCs application in promoting wound healing (Wu et al. 2007). The expression of VEGF, BMP-2, and BMP-4 in rat models also suggested that angiogenesis occur before osteogenesis in distraction osteogenesis (Sojo et al. 2005).

1.3.3.5 Insulin-like Growth Factor (IGF)

IGF is one of the major anabolic growth factors, with effects on inducing bone matrix apposition by stimulating osteoblast proliferations, differentiation, and matrix synthesis. IGF and PDGF are stimulator of cells of the osteoblastic lineage, as their application has been demonstrated to induce cell proliferation in osteoblasts culture (Katz et al. 1995; Zhang et al. 2002; Aberg et al. 2003). Two types of IGF receptors have been identified in bone cells, IGF Type I and Type II receptors. Activity of IGF-I is mediated by IGF Type I receptor (IGF-1R), which is a ligand-dependant tyrosine kinase receptor. Following ligand-receptor interactions, IGF-1R activates phosphorylation and triggers downstream signalling of MAPK and P13/AKT pathways, which play an important role in osteoblast differentiation and bone growth. Hence, experimental study using mice that lacked IGF and IGF-1R demonstrated impaired skeletal growth and development (Linkhart et al. 1996). Another study postulated that IGF-1R is likely to share the same homological structure with insulin receptors, giving the possibility for IGF-I to have the affinity to bind to the insulin receptor (Taniguchi et al. 2006). Application of insulin therapy in experimental studies exhibited an elevation in osteoblasts activity, increased cell proliferation, and higher alkaline phosphatase (ALP) activity. Based on these results, there is a possibility that administrated insulin is bound to IGF receptor and activates the signalling pathway for cell proliferation, leading to stimulation of certain growth factor receptors (Gandhi et al. 2005). However, the result is expected to differ in

T2DM cases, due to distinct physiological evidence of insulin resistance, which is probably non-susceptible to IGF stimulation.

1.3.4 The role of extracellular matrix (ECM) in growth factor regulation

The ECM is composed of different biomolecules that are produced and deposited outside the cell. ECM and growth factors have been proposed to have an interdependent relationship. For instance, TGF-β1 demonstrated the ability to inhibit proteolytic degradation of ECM, but at the same time, relying on ECM components, such as proteoglycans, to assist with sequestration and bioactivity of TGF-β_1 within ECM (Schultz and Wysocki 2009). Besides, the rate of bone formation is highly associated with the number and the activity of available precursor cells to participate in the healing process, together with appropriate interaction with the ECM. The dynamic interactions between growth factor and extracellular matrix can be either direct or indirect, whereas the target cells do not necessarily bind to extracellular matrix in order to response to growth factor signalling (Schultz and Wysocki 2009). It is also postulated that cell-to-cell interaction is developmentally crucial to mediate the unfolding force of conserved membrane signalling system (Discher et al. 2009). However, growth factor regulation of the bone matrix has not been fully characterised in terms of stem cell behaviour and function. Since there is limited evidence, more *in vitro* studies have been required to look into the regulatory mechanisms of the ECM components and growth factors, to identify the exact roles of participating molecules in the regulation of healing processes.

1.3.5 The role of small leucine-rich proteoglycans (SLRPs) in bone repair

The regulation of growth factor activities within bone repair sites are mainly coordinated through complex interactions with many types of biologically active ECM components, known as proteoglycans. Small leucine-rich proteoglycans (SLRPs) is a unique sub-group in a bigger class of proteoglycans, identified by the presence of a core protein and tandem leucine-rich repeats (LRRs) in the primary structure, which is covalently linked to either chondroitin- or dermatan-sulphate glycosaminoglycan (GAG) side chains at the N-terminus of the core protein (Frey et al. 2013). Apart from the structural function in maintaining the ECM assembly,

emerging evidence has revealed the importance of SLRPs in modulating cell-matrix crosstalk and signalling processes by controlling growth factors sequestration and activation. Two of the widely characterized SLRPs, decorin and biglycan, exhibit their vital role as endogenous ligands of Toll-Like Receptors (TLRs) 2 and 4, with the capability to modify the signalling events that directly influence the innate immune-inflammatory response. Taken together, better understanding of the molecular mechanisms underlying interactions between SLRPs and these innate immunity receptors is highly important, to gather significant knowledge of their functional roles in the inflammatory phase, exclusively in correlation with tissue repair and regeneration.

1.3.5.1 Biglycan

Biglycan is a class I SLRP, which consists of 42kDa core protein, and accompanied by two GAG side chains on the N-terminus. Biglycan also exists in non-intact forms, particularly in aging articular cartilage and invertebral disc (Roughley et al. 1993). Upon tissue damage and stress, proteolysis on the ECM releases abundant amount of biglycan, either as the cleaved core protein or as various fragments of biglycan (Moreth et al. 2012). The released bioactive molecules of biglycan interact with TLR2/4 to stimulate major signalling pathways to generate rapid inflammatory responses (Moreth et al. 2014). Besides, previous studies have indicated the importance of biglycan in the proper sequestration of TGF-β within the ECM (Young et al. 2002). Furthermore, viral transduction of biglycan in MSCs has been found to stimulate the proliferative capacity and the osteogenic potential of MSCs, through activation of TGF-β_1, Smad2, and Smad3 signalling pathways (Wu et al. 2013). In fact, a study on biglycan-deficient cell line reported that marked elevation in TGFβ levels resulted in apoptosis and growth retardation (Yang et al. 2009). Moreover, biglycan-deficient mice exhibited collagen fibrils abnormality and increased bone fragility (Bi et al. 2005). Interestingly, the inverse relationship between biglycan and TGF-β expression diminished in the diabetic environment as the diabetic mice displayed the overexpression of biglycan, accompanied by an elevation in TGFβ, and renal lipid retention (Thompson et al. 2011). Moreover, it has been postulated that hyperglycaemia induces abnormal synthesis of biglycan, with elongated GAG chains, in response to the abundance of TGF-β_1 (Yang et al. 2009). However, longer

GAG chains were shown to have higher affinity towards low-density lipoprotein (LDL), leading to alterations in cellular activity (Tannock 2006).

1.3.5.2 Decorin

Decorin consists of 36-40kDa core protein, 12 LLRs, and one GAG chain, which is found uniformly expressed all over the osteogenic and the non-osteogenic layers of periosteum (Bianco et al. 1990). The matrix-bound form of decorin is predominantly expressed in articular cartilage and bone matrix to provide the proper assembly of collagen fibrils in building the structure of the ECM. Hence, studies with decorin-null mice had shown collagen malformation and increased skin fragility (Reed and Iozzo 2002). Decorin also exhibits a significant interaction with members of TGF-β family to stimulate osteoprogenitor cells recruitment and proliferation (Alliston et al. 2001), but at the same time, inhibiting TGF-β_1 activation, leading to anti-fibrotic effect in the targeting organ (Schaefer 2011). On top of that, the soluble form of decorin is associated with perturbations in bone and ECM synthesis as decorin-deficient mice model exhibited severe osteopenia and increased skin fragility, owing to the capability of intact decorin to act as a pro-inflammatory agent by signalling through TLR2/4 (Young et al. 2002). Apart from the angiogenic role of decorin in aiding vascularization during bone repair (Waddington et al. 2003), decorin also plays a role in down-regulating TLR-regulated pro-inflammatory genes, indicating a competitive binding to endogenous ligands of TLR2/4 and further representing a complex mechanism of the role of SLPRs in immunity response (Buraschi et al. 2012).

1.4 Diabetes Mellitus: Type I and Type II

Diabetes is a medical condition that is associated with hyperglycaemia, with defects in insulin secretion or insulin resistance, or a combination of both. The progression of diabetes in individuals tends to develop through both pathological and physiological factors. The most striking feature of diabetes mellitus is an abnormally high level of glucose in blood. Therefore, diagnosis of diabetes is indicated when fasting plasma glucose exceeds 126mg/dL. Diabetes mellitus can be divided into two different categories because of variations in the etiology of the disease. Therefore,

diabetes mellitus in human populations is commonly known either as type 1 (T1DM) or type 2 (T2DM) diabetes mellitus. Of note, this study only looked into T2DM pathological perturbations in regards to bone reparative capacity.

T1DM is a chronic autoimmune disease, which is mainly associated with pathogenic action of T lymphocytes on insulin-producing β cells, resulting in defects of insulin secretion from the β-islet cells of pancreas. The exact reason behind the etiology of impaired insulin secretion in this type of diabetes has not been fully elucidated. However, it is believed that the abnormal reaction, which leads to impairment of β cells, is mainly triggered by viral or external pathogen (Jun and Yoon 2001). This type of diabetes is mostly present in younger populations, but can also be diagnosed in adults. The general characteristic of T1DM is hyperglycaemia with non-obese characteristics, which mainly lead to ketoacidosis condition if the insulin treatment is withdrawn. Therefore, exogenous insulin administration is commonly employed in the treatment of this disease.

Meanwhile, T2DM is a physiological disorder, which occurs as a result of one or a combination of both insulin deficiency and insulin resistance in liver and peripheral tissues. Most T2DM cases in the modern world comprise of a combination of both defects, as insulin resistance is highly associated with obesity; and peripheral fat deposition is closely linked to induce insulin desensitization (Hotamisligil et al. 1994). The most striking features of T2DM are abnormal insulin secretion in response to glucose (hyperinsulinaemia), dyslipidaemia, hypertension, insulin resistance in association obesity, hyperphagia, and excessive hepatic gluconeogenesis (Šedová et al. 2007). Apart from genetic predisposition, the risk of developing T2DM in humans also increases with age, obesity, underlying cardiovascular disease, and lifestyle factors, such as diet and physical activity. Therefore, it is often complicated to outline the underlying factors in the diagnosis of T2DM, as there is no clear evidence of each contributing factor in the development of disease.

Moreover, the current treatment for diabetes mellitus involves a combination of administered insulin to control the glycaemic index; and the utilisation of oral anti-diabetic agents, such as sulfonylureas, to stimulate pancreatic insulin secretion or to

reduce hepatic glucose production (Srinivasan and Ramarao 2007). However, more information of the molecular and cellular roles in diabetic progress is needed to provide further information in assisting formulation of new drugs or therapeutic agent to manage T2DM complications.

1.4.1 Epidemiology and prevalence of Type 2 Diabetes Mellitus

The growing pandemics of T2DM in the modern world are strongly associated with human lifestyle and behaviour changes over the last few decades. Until now, there is no clear evidence of genetic predisposition influencing the etiology of diabetes, as the epidemics of diabetes in global populations are more likely to develop from multiple environmental factors, such as unhealthy diet, obesity, and sedentary lifestyle. Increasing number of diabetes cases in children groups are overwhelmingly disturbing, which leads to another hypothetical role of epigenetics to influence the maternal environment and in-utero development of diabetes (Kitagawa et al. 1998). Theoretically, the expected number of diabetes patients worldwide, as published by the International Diabetes Federation (IDF), merely account for patients who are being treated and diagnosed with this condition. Conversely, many cases of diabetes will remain undiagnosed and indeed untreated, particularly in developing countries; which indicate a substantial epidemic and burden of diabetes to worldwide populations.

Diabetes has long been given extra attention in well-developed countries, such as US, UK, and Japan, due to the economic burden of managing the treatment of patients and complications resulted from this metabolic disease. Diabetes imposes a large economic burden on national healthcare systems, as the expenditure for diabetes alone was reported to account for almost 11.6% of the total healthcare expenses in the world in 2010. By 2030, the global expenses or the prevention, management and treatment of diabetes, as well as its complications are estimated to reach at least $449 billion, which roughly cost an average of $703 per person (Zhang et al. 2010). In recent years, T2DM has shown a dramatic epidemic proportions in many developing countries, as reported in Middle-Eastern nations, China, India, Korea, Australia, as well as minority groups in developed countries (Saadi et al. 2007; Magliano et al. 2008; Ramachandran et al. 2010). Massive increases in the number of diabetes cases in developing nations are a reflective of indirect influence

of modernisation, industrialization, and economic forces, which are drastically changing their lifestyles, including dietary and physical activity, that substantially compromise health status. For example, a retrospective study conducted to investigate the prevalence of diabetes in selected Asian nation showed a minimum of 1.5 and maximum of 5.1 multiplicative increases during the period of study (Yoon et al. 2006). This evidence indicates that diabetes has become a major threat to public health globally, and hence, extensive strategies aimed at the prevention, the management, and the treatment of diabetes, are strongly required.

1.4.2 Complication of diabetes

1.4.2.1 General health

T2DM is known to have detrimental effects on the human biological system, which compromises the molecular signalling and biochemical synthesis pathway; besides leading to cellular damage. Until recently, many experimental studies have demonstrated diabetes with complications of microvascular and macrovascular diseases, such as microangiopathy and arteriosclerosis (Jennings et al. 1987; Creager et al. 2003), which further increase the risk of developing cardiovascular disease and chronic complications of retinopathy, nephropathy, and neuropathy (Kannel and McGee 1979; Fowler 2008). Furthermore, diabetes pathogenesis has also been associated with various disorders of calcium metabolism, which result in impairment of calcium absorption in the intestine, and increased urinary loss of calcium, which consequently lead to increased risk of secondary thyroid disease and other hormone imbalances complications (Brenta 2010). It has been postulated that the metabolic alterations in diabetes significantly affect the rate of osteogenesis and angiogenesis at a cellular level, by suppressing the production of endothelial progenitor cells (EPCs). Moreover, more studies have reported that diabetic animals are found to have altered bone strength and mechanical properties, owing to lower overall bone mineral density (Lu et al. 2003; He et al. 2004; Prisby et al. 2008). Diabetic patients are also found to have a higher tendency in developing periodontal disease and osteogenic disorders (Shlossman et al. 1990; Katz et al. 1991). From these experimental studies, it is clear that diabetes mellitus is accountable for multiple negative impacts on

human biology, although the specific mechanisms by which this occurs are not fully understood.

1.4.2.2 Direct impact on wound and bone repair

Diabetic environments are often associated with systemic adverse effects, which result in the impairment of wound and bone healing. This correlates with the findings of many experimental studies that reported a reduction in bone and matrix formation in diabetic models (Hou et al. 1993; Suzuki et al. 2005; Kwon et al. 2008). Moreover, from genetic to biochemical analyses, *in vivo* to *in vitro* animal models, and clinical data evaluations; various strategies and approaches have been employed in order to prove the underlying mechanism, which leads to the impairment of healing in diabetic subjects. Theoretically, the cumulative findings have summarized that the healing process in T2DM is impaired because of possible alterations to one or more processes in the healing event (Evans et al. 2002). It begins with a delay in the influx of progenitor cells to the wound site, which leads to a decrease in both angiogenesis and osteogenesis (Fiorina et al. 2010). For example, bone marrow-derived endothelial progenitor cells (EPCs) are known to promote tissue healing and angiogenesis. However, diabetes is found to have negative effects on BM-EPC biology at the sites of wound healing by reducing EPC proliferation, recruitment, and differentiation capability, thus, it directly impairs their contribution to healing event (Albiero et al. 2011). In fact, eNOS (endothelial nitric-oxide synthase) activation in peripheral blood was demonstrated to inhibit the migration of EPCs to the healing site, which further supports these altered mechanisms (Gallagher et al. 2007). Hyperglycaemia is also well-recognised as one of the factors, which lead to altered mechanism of healing in diabetic groups. Experimental evidence reported an increase in crestal bone loss among diabetic patients during the first year of implant function, indicating the role of hyperglycaemia in impaired osseointegration (Kotsovilis et al. 2006).

An alternative mechanism that impairs diabetic tissue healing includes the reduction in migration of pro-inflammatory cells or cytokines to the injury site. Wound healing responses involve activation of keratinocytes, fibroblast, endothelial cells, macrophages, and platelets (Brem and Tomic-Canic 2007). Activation of these cells

will trigger the release of important cytokines and growth factors, which are needed to enhance and to maintain the healing process. Therefore, it had been proposed that diabetic wounds have a lower chemotactic ability to recruit inflammatory cells to the damage tissue site, which subsequently reduces angiogenesis and osteogenesis (Medina et al. 2005). Moreover, the whole combination of impaired cellular immune responses, altered inflammatory cytokine profiles, and microcirculation during the healing process would lead to higher rate of infectious complications in uncontrolled diabetic in animals (Blondet and Beilman 2007). Diabetes is also well associated with alterations in growth factor production and expression within the bone matrix (Al-Zube et al. 2009). It is believed that high glucose concentrations within the system have a direct detrimental effect on growth factor regulation, which results in impaired neovascularization and reduced oxygen supply. However, a recent hypothetical analysis tended to correlate hyperglycaemia with increased interaction of AGE and AGE receptor (RAGE), which stimulated the expression of TNF-α and matrix metalloproteinases (MMPs), and thus, indirectly resulted in a lower deposition of collagen within the ECM. The reduction in matrix collagen synthesis, coupled with chronic inflammation, minimized the capacity of ECM to support growth factors expression, and subsequently, delays tissue healing. Undeniably, growth factors expression is also influenced by macrophage production following the pro-inflammatory cytokines release. However, diabetic conditions were found to suppress macrophage production and activation, which resulted in reduced lymphatic vessel formation and led to impair wound and bone healing (Maruyama et al. 2007). Meanwhile, as for molecular analysis of diabetic in animal models, diabetes had been found to induce 71 genes that correlated with apoptosis and enhanced caspase-8, -9, and -3 activities. Alterations in pan-caspase gene activity were proven to decrease healing capacity, owing to reduction in fibroblast density and collagen synthesis, which led to lower matrix formation (Al-Mashat et al. 2006).

1.4.2.3 Current management of healing problem in diabetes

Typically, the presence of uncontrolled diabetes has been associated with higher outcome variability and increased rates of infectious complications. For that reason, monitoring glycaemic index is extremely crucial in the assurance of positive and successful outcomes among diabetes patients who wish to undergo implant

treatment. Current requirements for optimal glycaemic level control were found to reduce the variability of the outcome, thus improving the consistency and the predictability of the guided bone regeneration treatment in experimentally-induced diabetes (Retzepi et al. 2010). However, in reality, glycaemic control has remained poor in the majority of diabetes patients, although many drugs are available to facilitate in controlling the diabetic complications.

To date, the FDA-approved evidence-based medicines that are relevant in the treatment of diabetic osseous healing include recombinant human-fibroblast graft application and keratinocytes delivery via type I collagen (Brem et al. 2000; Marston et al. 2003). Current evidence suggested the potential use of demineralised dentin matrix in stimulating bone defect healing in a T2DM rabbit model (Gomez-Moreno et al. 2014). Besides, advances in growth factor treatment include the application of human recombinant PDGF-BB (becaplermin) on diabetic ulcers, also BMP-2 and BMP-7 application in treating open tibia, non-union fractures, and spine injuries (Friedlaender et al. 2001; Embil and Nagai 2002; Poynton and Lane ; Carragee et al. 2011). However, the number of FDA-approved growth factors and cell therapies in the treatment of bone healing is still considerably very limited due to insufficient pre-clinical data and clinical evaluations. Furthermore, studies that reported the association of rhBMP-2 and PDGF-becaplermin application with increased rate of developing cancer have raised the issue of safety and concern among treated patients (Schafer and Werner 2008; Cheng et al. 2011). In view of this evidence, more randomized clinical trials are required in looking for other potential growth factors, which are often associated with efficacy in stimulating the healing process. In a way, further information may provide useful insights into its potential application for the treatment of skeletal wounds and defects, as well as further enable the professionals to apply evidence-based medicine into clinical practice.

Apart from that, the total number of active EPCs has been known to be lower in diabetic animals, thus indicating the need to increase the number of EPCs in the bloodstream; and directing these to the healing site in order to promote rapid healing. Hyperbaric oxygen therapy (HBO) is another FDA-approved protocol to enhance healing in problem wounds, which is often associated with diabetes complications (Löndahl et al. 2010; Tiaka et al. 2012). However, the application of HBO has

reported inconsistency in treatment outcome. Gallagher et al., (2007) demonstrated that a combination of hyperoxia and stromal cell-derived factor 1α (SFD-1α) positively enhanced wound healing in diabetic animals. Hyperoxia acts to stimulate eNOS activation in the bone marrow to produce a higher number of EPCs in the bloodstream; and SFD-1α is responsible to enhance the mobilization of bone marrow-derived progenitor cells to the injury site, resulting in faster healing process. Therefore, simultaneous administration of both HBO and stromal cell-derived factor-1α (SFD-1α) at the wound site was suggested to be of a combination to provide a better prognosis in patients with diabetes, in comparison to current HBO application protocol.

1.4.3 Animal models in the study of Type 2 Diabetes Mellitus

Different types of animal models have been developed and proposed for *in vivo* and *in vitro* analyses of diabetes progression in living organisms. The utilisation of animal models to study diabetes is relatively advantageous in biomedical fields, as it facilitates better understanding of diabetes pathological and physiological progress, as these animal models were found to exhibit diabetes characteristics by induction of multiple factors, such as genetic predisposition, controlled environmental factor or drug stimulation. Hence, it further provides evidence to support the various hypotheses of diabetic progression in humans. Several animal models have been developed for the study of T2DM. Despite more experimental work being inclined towards manipulating chemically-induced diabetes animals, such as by low dose alloxan to study non-obese T2DM, the stimulation effect from chemical-induced diabetes are often unfavourable, in agreement with human T2DM. For instance, the direct toxicity induced in animal models tends to enhance insulin deficiency, rather than insulin resistance. Additionally, chemically-induced diabetes is also found to be reversible, unstable, and causing toxicity to other systemic components (as reviewed by Srinivasan and Ramarao in 2007). Therefore, more experimental work has now begun to make use of spontaneous or single-gene defects in T2DM models, such as the leptin-deficient (ob/ob) mouse, the leptin receptor-deficient (db/db) mouse, Zucker diabetic fatty (ZDF) rat, and Otsuka Long Evans Tokushima Fatty (OLETF) rat, which majorly represent the obese type of human T2DM. Although a large number of genes can either be knocked out or overexpressed to produce the insulin-

resistant phenotype, the development and the availability of polygenic non-obese T2DM animal models are still very limited and expensive for experimental studies (Almon et al. 2009).

In this study, GK (Goto-Kakizaki) rats were chosen as the experimental animal model. GK rat is a commercially available non-obese polygenic model of T2DM. The diabetic strain in animal models was established in Japan by Goto and his collaborators, through selective inbreeding of Wistar rats with abnormal glucose tolerance rats, repeated over several generations in 1973 (Goto and Kakizaki 1981). The progression of diabetes in GK rats had been reported to start as early as 4 weeks and continued to progress up to 12 weeks of life. After that, the hyperglycaemia stage was found to be constant throughout their lives. Plasma insulin demonstrated a steep increase between 4 and 8 weeks and after that period, the decline of insulin in GK suggested β-cell failure. A functional analysis of these genes indicated that disruption of lipid metabolism in the liver is a major consequence of the chronic hyperglycaemia in the GK strain. In addition, the results suggested that chronic inflammation contributed significantly to the development of diabetes in the GK rats (Almon et al. 2009). GK rats also exhibited mild hyperglycaemia as early as 1 week of age, indicating that these animals had pancreatic abnormalities in embryonic stages, which seemed likely comparable to T2DM cases in recent cases of maternal and paediatric human population (Fujii et al. 2008). Even though the pathology of T2DM in GK rats are not entirely analogous to human T2DM, these present the main characteristics that exhibit similar metabolic, hormonal, and vascular disorders to human diabetes, demonstrating fasting hyperglycaemia, impaired secretion of insulin in response to glucose, as well as hepatic and peripheral insulin resistance at early stage of life, which are likely to make these a valid model for the T2DM in human population.

1.5 Alterations of osseous healing in Type 2 Diabetes Mellitus

T2DM has been acknowledged to impair the bone remodelling and osseointegration processes (Lu et al. 2003; Valero et al. 2007; Prisby et al. 2008; Colombo et al. 2011; Graves et al. 2011). Therefore, T2DM is often associated with increased risk of implant failure, owing to compromise healing progress and higher occurrence of

post-surgical complications. For example, clinical studies addressing the survival rates of titanium dental implants reported that diabetes patients had a significantly higher risk of implant failure in comparison to healthy controls, as 85.7% of survival rate had been reported in diabetic subjects over 6.5 years of functional use, as opposed to 99.9% of success rate documented in healthy individuals (Fiorellini et al. 2000).

Hence, alterations in cellular microenvironments and molecular signalling pathways have been suggested as the major cause of physiological and pathological perturbations in T2DM. Despite extensive studies dedicated to characterise the roles of hyperglycaemia and hyperinsulinaemia on impairment of osseous healing status in T2DM, the exact mechanisms involved in perturbation of diabetic bone healing are still under investigation. Overall, understanding the alteration mechanisms of diabetic bone healing is considerably essential in providing further knowledge to assist in the formulation of therapeutic strategies to promote rapid healing in diabetic environment.

1.5.1 Unifying hypothesis in diabetic alterations

There are various hypothesized mechanisms to explain hyperglycaemia, insulin resistance, and islet β-cell dysfunction roles in etiology of T2DM. However, it is rather difficult to determine the most relevant and important mechanism in each tissue, in different model or individual with T2DM. The general hypotheses proposed to explain T2DM pathogenesis include oxidative stress and generation of reactive oxygen species (ROS); activation of stress activated pathways; endoplasmic reticulum stress; lipotoxicity and glucotoxicity; dysfunction of endothelial progenitor cells; and inflammatory role by alterations in cytokines release (Baynes 1991; Evans et al. 2003; Forbes et al. 2003; Eizirik et al. 2008; Donath and Shoelson 2011). Hence, a unified hypothesis was proposed to combine all the important factors in regard of diabetes-induced alterations within the biological system (Evans et al. 2002). By linking all these key mechanisms, it may further assist researchers to understand the precise roles of hyperglycaemia and hyperinsulinaemia in the stimulation of complex pathophysiological events during T2DM.

1.5.1.1 Hyperglycaemia-induced cell and tissue damage

In addition, many experimental work has indicated that hyperglycaemia is known to activate several major signalling pathways that are significant in etiology of diabetic complications. Four major signalling pathways that have been implicated in hyperglycaemia-induced tissue damage include, advance glycation end products (AGEs), protein kinase C (PKC), hexosamine, and polyol pathway flux (Figure 1.2). Besides, it has been postulated that hyperglycaemia participates in activation of these major pathways by inhibiting glyceraldehyde 3-phosphate dehydrogenase (GAPDH), which is mediated through the activation of poly-ADP ribose polymerase (PARP) (Brownlee 2005).

Moreover, hyperglycaemia is often associated with the generation of ROS, which leads to induction of oxidative stress in a variety of tissues (Baynes 1991; Rolo and Palmeira 2006; Feng et al. 2013). Oxidative stress is a state in which the presence of ROS exceeds the endogenous antioxidant production. ROS will induce oxidant production, which is harmful to cell environments. The detrimental effect of ROS and oxidative stress in cells and tissue are worsened by further absence of response and regulation of endogenous antioxidant in the system. A recent study claimed that free fatty acids (FFA) also play an important role in activating the oxidative stress, as proven in culture of human hepatocytes (Soardo et al. 2011). Hence, protein carbonyl content has been suggested as a biomarker for the development of oxidative stress status in diabetic tissues (Dalle-Donne et al. 2003). Up to now, the excessive level of ROS has often led to the damage of proteins, lipid, and DNA (Waddington et al. 2000; Moseley et al. 2004).

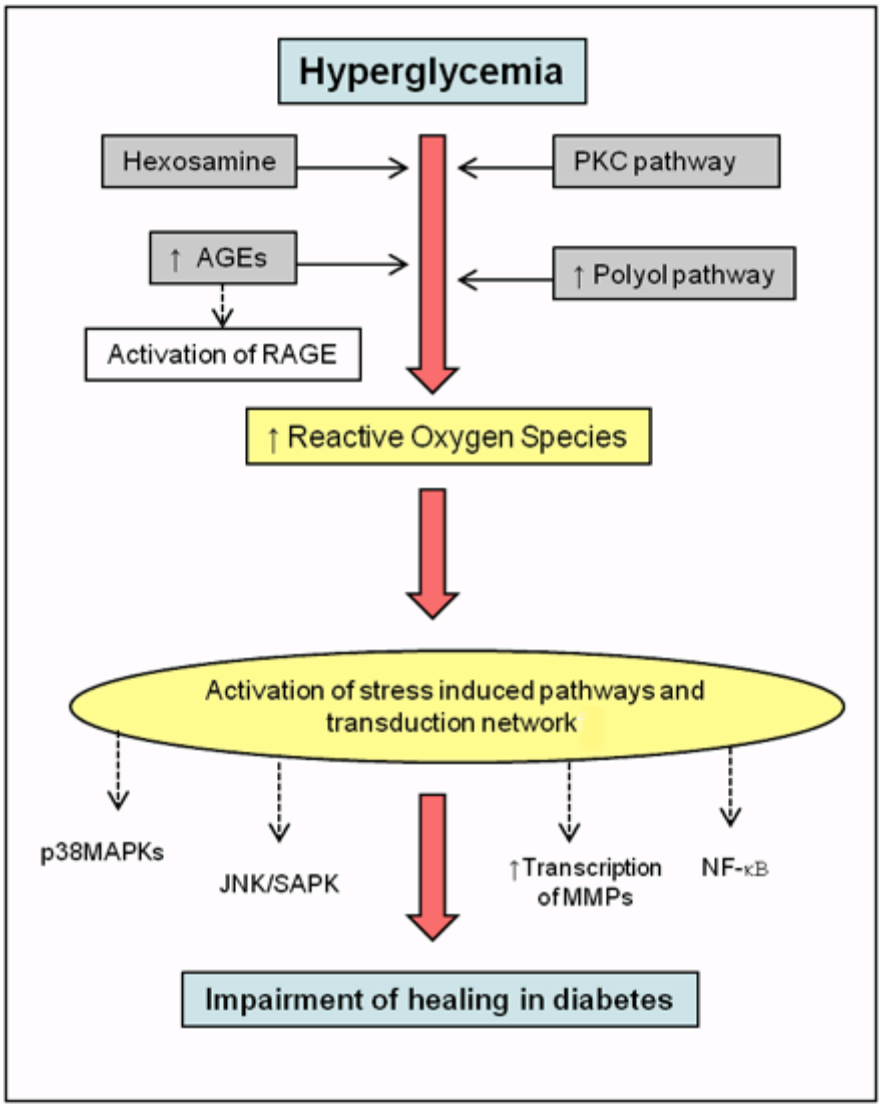

Figure 1.2 Interrelations between hyperglycaemia, reactive oxygen species (ROS), and impairment of healing in diabetes. Adapted from Elmarakby et al. (2010).

In normal physiology, glucose is metabolised via tricarboxylic acid cycle (TCA cycle), which activates electron pump channels to transfer electrons across the mitochondrial membrane and to create a certain amount of energy within the cells. However, higher concentrations of glucose in the system result in an increase of voltage across the mitochondrial membrane, which results in the formation of superoxide ($O_2^{\bullet-}$), mediated by NADPH oxidases. This mechanism was established when no significant changes to ROS level was observed, following suppression of the mitochondrial voltage gradient by mitochondrial uncoupling proteins (UCP) overexpression (Brownlee 2005).

$O_2^{\bullet-}$, one of the most important ROS in the vasculature, is formed by the univalent reduction of oxygen. Later on, dismutation of $O_2^{\bullet-}$ by superoxide dismutase (SOD) generates more stable ROS, hydrogen peroxide (H_2O_2), which is then converted enzymatically into H_2O by catalase and glutathione peroxidase (GPx) (Taniyama and Griendling 2003). Significantly, reduction and absence of catalase have been reported in diabetic tissues (Goth 2008; Waddington et al. 2011b). Both $O_2^{\bullet-}$ and H_2O_2 are essential for the formation of more reactive ROS, ·OH (Ahmad 1995). Besides, the imbalances of cellular antioxidants and ·OH levels accelerate the detrimental mechanisms on cellular damage (Waddington et al. 2000).

Furthermore, bioavailability of nitric oxide ($^{\bullet}NO$) is significantly lower in T2DM patients, which results in a decrease in number and functionality of endothelial progenitor cells that can cause impaired vascularisation in healing tissue of bone healing (Hamed et al. 2010). Osteoclasts have been demonstrated to contain $^{\bullet}NO$ and actively produce $O_2^{\bullet-}$ during the bone resorption process (Steinbeck et al. 1994) and both are found to increase in the study pertaining to impaired fracture healing (Kayal et al. 2007).

1.5.1.2 AGE/RAGE pathway

Advance glycation end (AGE) product formation leads to increased cellular apoptosis (Bierhaus et al. 1997). AGE is chemical modification of long-lived proteins. The formation of AGE products within the biological system involves the formation of covalent bond between reducing sugars and free amino groups in proteins (as reviewed by Singh et al. in 2001). Besides, AGE binds to cognate cell-surface receptor, RAGE, in order to activate signalling and generation of intracellular ROS, induces activation of gene expression (Schmidt et al. 1994; Bierhaus et al. 1997). AGE products are claimed to be responsible for their detrimental effects on bone modelling by inhibiting the proliferation and differentiation of osteoblast cells. $O^{\bullet}_{2}{}^{-}$ is postulated to activate the AGE pathway when glucose-3-phosphate is converted to methylglyoxal (Kanwar and Kowluru 2009; Madsen-Bouterse et al. 2010).

1.5.1.3 Protein kinase C (PKC) pathway

Chronic hyperglycaemia is known to increase PKC expression in cellular environments. Activation of PKC pathways are associated with many micro- and macro-vascular complications of diabetes mellitus (Koya and King 1998; Igarashi et al. 1999). Activation of PKC isoforms is generated by *de novo* synthesis of the lipid second messenger; diacylglycerol (DAG) (Xia et al. 1994; Meier and King 2000). Moreover, a recent experimental work demonstrated bFGF stimulation increased membrane translocation of various PKC isoforms, including α, β, €, and δ in primary osteoblastic cultures, which indicated the role of β1 in bone formation through PKC-dependent pathway (Tang et al. 2004). Both high glucose level and palmitate are suggested to stimulate ROS production through PKC-dependent activation of NADPH oxidase in both vascular MSCs and endothelial cell. This finding may involve the excessive acceleration of atherosclerosis in patients with diabetes and insulin resistance syndrome (Inoguchi et al. 2000).

1.5.1.4 Polyol pathway

The aldose reductase (AR) polyol pathway contributes to diabetic microvascular complications, but how it mediates vascular damage in response to hyperglycaemia is less understood. Aldose reductase activity is stimulated in chronic hyperglycaemia environment, which particularly is associated with the existence of insulin resistance, such as in T2DM (Kador 1988). Besides, sorbitol accumulation within the cells has been validated to cause cellular damage. Moreover, a recent study suggested that Runx2 activation and cellular wound healing in diabetic tissue had been regulated through the AR polyol pathway (D'Souza et al. 2009).

1.5.1.5 Hexosamine bisynthesis pathway

Activation of the hexosamine biosynthesis pathways (HBP) is triggered by hyperglycaemia and produces excessive flux of FFA and UDP-GlcNAc (Uridine 5-diphospho N-acetylglucosamine) in circulation, and consequently, develops progression of insulin resistance (Hebert et al. 1996; McClain and Crook 1996; Buse 2006). *N*-acetyl glucosamine is converted from the fructose-6 phosphate by an enzyme, glutamine fructose-6-phosphate amidotransferase (GFAT). Post-translational modification, known as O-GlcNAc glycosylation (O-GlcNAcylation), consists of addition of N-acetylglucosamine on serine and threonine residues of transcription factors. This reversible O-GlcNAcylation often results in pathologic changes in gene expression, with capability of modifying protein based on glucose availability (Issad and Kuo 2008). Therefore, the activation of HBP and GFAT expressions in animal model, along with O-GlcNAcylation, has demonstrated various pathological perturbations, which directly participate in several micro- and macro-vascular complications, such as insulin resistance (Buse 2006); development of hyperlipidaemia and obesity (Veerababu et al. 2000); as well as increased NF-κB - dependent promoter activation (James et al. 2002).

1.5.1.6 Lipotoxicity and glucotoxicity

Several years ago, some studies revealed the role of endocrine organs, such as bone and adipose tissues, in regulating hormones and growth of cells (Kershaw and Flier 2004; Lee et al. 2007). The interaction between bone and adipose tissues is

significant as bone marrow stem cells can give rise to osteoblasts and adipocytes. Leptin and adiponectin, two adipokines secreted by fat tissues, have been identified to have complex actions on the skeleton and indirectly effect bone remodelling by modulation of adipose cell sensitivity and insulin secretion (Das et al. 2009; de Paula et al. 2010). High glucose concentrations have long been known to induce toxicity in osteoblasts by decreasing cells activity and suppressing proliferation. *In vitro* osteoblast cell culture in diabetic glucose concentrations demonstrated a slight decrease in expression of proteins associated with the stem cell state, in comparison to culture in normal physiological glucose, suggesting an impairment in osteoblasts and osteoclasts differentiation (Dienelt and zur Nieden 2011). In addition, hyperglycaemia stimulates changes in circulating calciotropic hormones and growth factors, alters regulation of biochemical processes, and subsequently, results in impaired bone quality.

1.5.1.7 Activation of stress-induced pathways

Hyperglycaemia and an abundance of ROS create imbalance within the cellular compartment and activate the stress-induced pathways responsible for the late complications of diabetes. These mechanisms lead to activation of other signalling pathways that mediate insulin resistance and impaired insulin secretion (Evans et al. 2002). The stress sensitive signalling systems and transduction mechanisms that are potentially activated include JNK/SAPK pathway, P38 MAPK pathway, NF-κB pathway, and matrix metalloproteinases (MMPs). Recently, it has been proven that MMPs play an important role in vascularisations, which potentially indicate the activation of this transcription factor during bone healing (Rogowicz et al. 2007). Expression of MMPs is stimulated by signalling biomolecules, including proinflammatory cytokines, such as IL-1, IL-6, and TNF-α, as well as hormones and growth factors, including TGF-β, EGF, PDGF, and bFGF. Meanwhile, the regulation of MMPs is suppressed by corticosteroids, retinoic acid, heparin, and IL-4 (Murphy et al. 1994).

1.5.1.8 Inflammatory role: altered cytokines response

Several experimental studies were carried out to investigate the pathological mechanisms in T2DM, including the association of insulin resistance and islet β-cell failure in correlation with tissue inflammation. Pro-inflammatory cytokines cascade, which comprises of various signalling biomolecules, such as IL-I α, IL-Iβ, TNFα, IL-6, and IL-8; is mainly activated in response to infection, immunological stress or tissue injury. Apart from immunological effects, these cytokines have inhibitory and stimulatory effect on bone formation. For example, IL-I is closely linked with osteocalcin, the non-collagenous protein that has an important role in bone formation (Li and Stashenko 1992). Moreover, TNF-α and other cytokines are found to alter glucose metabolism in adipose, skeletal muscle cells, and liver. TNF-α is a key mediator of insulin resistance in animal models of non-insulin-dependent diabetes mellitus. TNF-α interferes with insulin action and induced insulin resistance through down-regulation of the insulin-regulated glucose transporter, (GLUT4) mRNA, and protein (Hotamisligil et al. 1994).

1.5.1.9 Endoplasmic reticulum (ER) stress

Despite the increasing number of experimental work dedicated to elucidating the underlying pathogenesis of β-cell failure, the exact mechanism of the disorder has remained unknown. In T2DM, β-cells demonstrate an inability to recognize insulin, which results in a condition known as insulin resistance. It causes a flux of protein across endoplasmic reticulum and leads to imbalances of energy in cellular compartment, leading to ER stress (Harding and Ron 2002). Besides, recent evidence in genetic, experimental, and clinical data had proposed the role of ER stress in inducing β-cell dysfunction and apoptosis (Eizirik et al. 2008). Furthermore, hyperactivation of the unfolded protein response (UPR) to counteract metabolic stress was identified as the major mechanism associated with β-cell dysfunction and apoptosis (Back et al. 2012).

1.5.2 Alterations of bone cellular activity in diabetic environments

Hyperglycaemia condition in diabetes is strongly correlated with the decreased rate of bone formation, resulting in the production of bone with reduced bone density and

quality (Okazaki 2013). Moreover, numerous studies have demonstrated that hyperglycaemia significantly increases the generation of ROS in both mitochondrial and cytoplasm (Rolo and Palmeira 2006; Giacco and Brownlee 2010). Diabetic-induced mitochondrial dysfunction leads to overproduction of ROS levels, which further attenuates osteoblast apoptosis (Zhen et al. 2010), osteoblast dysfunction, and inhibition of cell proliferative capacity (Nishikawa and Araki 2007; Cunha et al. 2014). Elevation of ROS was identified to induce cellular dysfunction of most bone cellular components, including osteoprogenitor cells, osteoblasts, and osteoclasts, which negatively influence bone formation processes, and thereby compromises *in vivo* osseointegration of titanium implant in animals (Feng et al. 2013). Similarly, diabetes is associated with higher outcome variability and increased rate of infectious complications during *de novo* bone formation, which compromise implant osseointegration processes (Retzepi et al. 2010). Furthermore, the oxidative stress marker was markedly increased in T2DM group, accompanied with less osteoid, osteoblast, and osteoclast deposition on the bone surface; lower mineral apposition; and decreased rate of bone formation, significantly indicating an impaired bone turnover in diabetic animal (Fujii et al. 2008). Diabetic animals also exhibit decreased number of osteoprogenitor cells, which lead to reduced osteoblastogenesis and bone formation (Weinberg et al. 2014). Significantly, co-culture MSCs with osteoblast in hyperglycaemic levels exhibit diminished interactions between these bone cellular components, along with reduced MSCs viability and clonogenicity (Rinker et al. 2014). In fact, glucose levels and extracellular matrix during culture significantly induce a different metabolic state in osteoprogenitor cells, which affects the viability and the terminal differentiation of the MSCs (Deorosan and Nauman 2011).

1.6 Macrophages in high glucose environments

The primary issue of macrophages plasticity remains controversial, although more evidence and experimental approaches have now become widely available to potentially differentiate between classical activated macrophages (CAM) and alternatively activated macrophages (AAM). These two terms were introduced to identify two phenotypic subtypes of macrophages, based on gene expression induced in response to cytokine and pathogen-derived stimulation. Besides, high glucose has

been known to alter inflammatory responses in bone healing (Brown et al. 2012). To date, animal studies have demonstrated that diabetes-induced hyperglycaemia causes polarisation in macrophages phenotype and function, inducing the production of CAMs with pro-inflammatory phenotype (M1 macrophages), rather than the reparative/proliferative phenotype of AAMs (M2 macrophages), indirectly suggesting that alterations in macrophages profiles represent cellular mechanism, are partly responsible for delayed bone healing (Schmidt-Bleek et al. 2012). However, only a few studies have examined the specific effects of macrophage polarization through insertion of implant in compromised patients, such as T2DM; restricting our understanding on the mechanisms of controlling macrophage polarization; and our subsequent manipulation of any effectors with advantageous effects upon improving the tissue remodelling outcome.

1.7 Aims of the thesis

Prolonged inflammatory signalling cascade, altered cytokine growth factor activation, and delayed bone healing responses in the hyperglycaemic environment are some of the major consequences of diabetic perturbations, compromising the long-term comfort and stability following implant surgical procedures. Although many investigations have greatly contributed towards better understanding of the mechanisms in regulating growth factors-mediated osseointegration, many questions have remained unanswered about the regulation and the responsiveness of these growth factors in high glucose environments. It is still not clear if one type of growth factor is directly or indirectly affected in diabetic bone mineralisation, or if more types of growth factors are involved. Hyperglycaemia might possibly trigger different responses of growth factors between different tissues. Therefore, the aim of this study is to gain a greater insight into the processes that take place during the initiation of cell-mediated mineralisation during diabetic bone repairs and the role of relevant effectors involved in these processes.

Chapter 2 is dedicated to the isolation, the expansion, and the characterisation of MSCs from rat adult tissues. Hence, comparative analysis performed on rat MSCs population derived from different tissue niches assisted in the selection of suitable progenitor cell types for *in vitro* disease model application in this study.

Chapter 3 assesses the effect of hyperglycaemia on bone-derived MSCs proliferative and differentiation capacity. Besides, the exposure of MSCs to long-term and short-term high glucose concentrations revealed a significant change in cells; doubling time and gene expression of both osteogenic and adipogenic markers.

Chapter 4 depicts the investigation on the availability of the growth factor, TGF-β_1; and proteoglycans response to high glucose exposure. The results from *in vivo* osseointegration model demonstrated a significant increase of TGF-β_1 in the young-diabetic group, in comparison to the control group. Further *in vitro* study within hyperglycaemic environment revealed a significant alteration of TGF-β_1, decorin, and biglycans. Therefore, a combination of *in vivo* and *in vitro* osseointegration analyses facilitated in further elucidating the synergistic role of the above biomolecules during bone repair.

Apart from MSCs, macrophages have also been identified as another potential source of TGF-β_1 expression within the bone healing area. Hence, Chapter 5 demonstrates subsequent investigations concerning the effects of high glucose on macrophage polarisation, which potentially altered TGF-β_1 expression during the inflammatory stages of bone repair. Detailed analysis of macrophage cytokine expression in diabetic environments excluded their associated role in supporting elevation of TGF-β_1 expression. It further led to fundamental changes in our understanding on the plasticity of macrophage phenotype and their actual involvement in diabetic pathologies. Finally, Chapter 6 summarises the main conclusions of this thesis.

Chapter 2

Isolation and Characterisation of Bone-Derived Rat Mesenchymal Progenitor Cells Populations

2.0 Introduction

Mesenchymal stem cells (MSCs) are a distinct type of progenitor cells with unique capabilities for programmed self-renewal and differentiation into broad lineages of mesenchymal origins, such as bone, fat, and cartilage (Bruder et al. 1997; Krebsbach et al. 1999; Pittenger et al. 1999). Adult multipotent MSCs can be found in nearly all tissues, but are often associated or limited within the perivascular niches (Shi and Gronthos 2003; Tropel et al. 2004). Apart from the migratory abilities of MSCs to re-populate the repair site, they were also found to secrete protective factors for tissue regeneration during inflammation, tissue injury, and certain cancers; suggesting the huge potential benefit to study these cells types further (Batouli et al. 2003; Abraham et al. 2008; Chatterjee et al. 2010).

Due to these outstanding features, MSCs offer great potential for application in stem cell repair and regenerative therapies; involvement in developing *in vitro* models of disease progress; and also in monitoring prognosis of drug or therapeutic components in accelerating a wide variety of clinical outcomes (Dimitriou et al. 2005; Chatterjee et al. 2010; Fiorina et al. 2010; Scotti et al. 2010). The improvement of bone repair and regeneration through cell engineering, modification of implant surface, gene therapy, and the optimisation of pro-lineages inducing medium have been extensively studied in recent years (Brown et al. 1989; Franceschi et al. 2000; Krebsbach et al. 2000; Franceschi et al. 2004; Koh et al. 2008). However, to achieve the desired objectives for the application of MSCs and in accelerating bone repair, it is undeniably crucial for researchers to optimise and fully characterise every detail of these MSCs, starting from their isolation techniques until their senescence stage to assist a smooth transfer of knowledge from laboratory-based technology to clinical practice. Furthermore, the successful application of stem cells for bone reparative care relies heavily on the efficiency of the isolated MSCs to maintain their proliferative capacity, pluripotency, and differentiation ability over prolonged *in vitro* culture.

The universally accepted characteristic of MSCs and the proposed biological properties have only been provided after years of studying *in vitro* expanded cells, primarily analysing the behaviour of MSCs out of their native context. *In vivo*, the

cellular identification of MSCs, along with their exact localisation and biological functions in co-ordinating tissue homeostasis, have been partly understood (Nombela-Arrieta et al. 2011). However, compared to other tissue-derived stem cells, bone marrow MSCs has been well characterised in terms of their biological function *in vivo*, particularly in maintaining tissue homeostasis and skeletal repair in the bone marrow environment.

Moreover, bone stromal niches are richly populated by various important cell types, which represent the heterogeneous marrow stroma. The complexity of cells residing within the stromal niche provides a microenvironment for haematopoiesis and contributes to the maintenance, as well as regeneration of skeletal tissues. Bone marrow is considered as one of the most feasible sources of MSCs due to the straightforward approach in isolating, expanding, and manipulating the cells in culture (Silva et al. 2001). However, the use of bone marrow-derived cells is not always acceptable due to high risk of contamination with macrophages and monocytes, with high susceptibility of viral infection and inconsistency in proliferative, plus differentiation capacity over cultivation time (Minguell et al. 2001; Barry and Murphy 2004; Choudhery et al. 2012). Reports have also highlighted the variations in BM-MSCs behaviour, as clonal populations demonstrated inconsistent proliferative capacity and differentiation potential in comparison to heterogeneous BM-MSCs culture (Phinney et al. 1999; Pittenger et al. 1999; Muraglia et al. 2000; Peister et al. 2004). For these reasons, more researches are looking at possible alternatives for MSCs source other than bone marrow, which is considerably valuable.

Classically, MSCs were isolated from bone marrow of human and rodent species by manipulating their distinct ability to expand in culture following adherence to plastic culture surfaces, as the techniques have shown a potential in reducing the co-culture of haematopoietic cells (Friedenstein et al. 1976). However, the property of plastic adherence itself is not sufficient for isolation of MSCs due to the abundant existence of unwanted hematopoietic cells, endothelial cells, and granulo-monocytic cells, reported in early and later stages of passage culture (Pittenger et al. 1999; Deans and Moseley 2000). Frequently, bone marrow stromal cells are subjected to fractionation

on a density gradient solution, such as Ficoll^{TM}, to improve the purification strategies; followed by low density plating method (Phinney et al. 1999; Pittenger et al. 1999; Neuhuber et al. 2008). However, recent evidence demonstrated growing interest in using fibronectin-coated plates for MSCs isolation, from both human and animal species, manipulating the binding capacity of fibronectin receptors and surface $\alpha_5\beta_1$ integrin to promote rapid adhesion of multipotent primitive cells (Jones and Watt 1993; Pimton et al. 2011).

Despite the growing interest in the application of MSCs for repair strategies, there is no well-defined protocol for the isolation of prospective MSC populations in order to accurately study the cells biological properties prior to regenerative treatment. Optimisation of MSCs isolation protocols by manipulating cell behaviour and responses in growth culture conditions will not only ensure a high yield number of MSCs with the desired characteristics, but also maximise the potential use of MSCs, indirectly expanding the beneficial effects of these cells in future medical applications. For example, apart from the common idea of cell-driven technology involving tissue engraftment and wound healing, studies are now looking into the potential applications of MSCs as growth factor delivery and release, insulin, as well as other hormonal-producing supply.

As of now, inconsistency does exist, in general, for the identification of MSCs, as no specific marker has been universally accepted to confirm the definitive MSCs phenotype. However, the vast majority of stem cells studies have identified MSCs populations by fulfilling these minimum three criteria; 1) the ability to proliferate by adherence to tissue culture plastic; 2) positive expression of at least three pro-mesenchymal stem cells markers, such as CD90/Thy1, CD105/endoglin, and CD73/ecto-5'-nucleotidase; and 3) the ability to differentiate mesenchyme lineages cells, through osteogenic, adipogenic or chondrogenic induction (Horwitz et al. 2005; Dominici et al. 2006; Le Blanc 2006). Extensive studies of MSCs from various species and tissue sources, together with variations in isolation techniques, will generate comprehensive data and provide in depth analysis to further comprehend the behaviour of MSCs, prior to their application in bone repair therapies.

For over four decades, several different protocols had been evaluated for the isolation of MSCs populations of rats, whereby most of the work had focused on extraction from bone marrow, in addition to other tissues, such as dental pulp, fat, muscle, cartilage, and synovial fluid (Jones et al. 2002; Tropel et al. 2004; Sung et al. 2008; Nakamura et al. 2010b; Zhu et al. 2010). With the growing development and technologies in bone engraftment and skeletal tissue repair, the search for potential MSCs candidate with specific pro-osteoinductive and osteoconductive capacities directly derived from endosteal niches seems promising for application in bone repair treatments. Interestingly, recent studies have successfully performed the isolation of MSCs from mouse compact bone explants, suggesting the potential application of this method as an alternative in providing MSCs for bone repair therapies and for *in vitro* models of cellular behaviour (Sung et al. 2008; Nakamura et al. 2010b; Zhu et al. 2010).

This Chapter presents the data comprising of isolation, expansion, and characterisation of purified homogenous and heterogeneous rat MSCs from bone marrow and compact bone explants. Briefly, these MSC populations were isolated using three different protocols, which were adopted by technically manipulating the known classical biological components of the cells. Much attention was given to compare the efficiency of each purification method by analysing cells proliferative capacity and differentiation potential towards osteogenic and adipogenic lineages, following a long-term *in vitro* culture. The successful isolation and characterisation of these MSCs revealed that both bone marrow and compact bone offered a promising suitable source of MSCs for the development of a rat MSC model.

2.1 Materials and Methods

2.1.1 Animals

28 days old, male Wistar rats were obtained from the colony maintained by Charles River European Suppliers (Charles River UK Ltd., Margate, UK). The animals were

each well of fibronectin-coated plates, immediately after removing PBS. Cells were then incubated for 20min at 37°C, to select the α-5/β-1 integrin positive immature mesenchymal cells population that adhered to fibronectin. After 20min incubation, non-adherent cells were removed by washing with PBS. Adherent cells were incubated in complete culture medium (CCM) consisting of alpha modification Minimum Essential Medium (αMEM), with ribonucleosides and deoxyribonuclosides (Invitrogen, Renfrewshire, UK), supplemented with 20% heat-inactivated fetal bovine serum (FBS) (Invitrogen), 1% antibiotic-antimycotic (Sigma) and 100μm L-ascorbic acid 2-phosphate (Sigma) at 37°C in a humidified atmosphere containing 5% CO_2 to allow colony formation. The colony formation (>32 cells) within each wells were counted on days 3, 6, 10 and 12 and each colony was marked and allowed to expand in culture. On day 14, colonies were isolated using StemPro® Accutase® enzyme (Invitrogen), to dissociate the cells colonies from the plastic surface of culture flask and forming a population of single cells. The 6-well plate was washed three times with PBS before 150μl StemPro® Accutase® was added and incubated at 37°C for 8min. Cells were recovered and collected together, prior to cell counting and seeding in a new 96-well plate at 10,000 cells/cm^2 for expansion. Cells were maintained in CCM and the medium was changed every two or three days until the cell culture reach approximately 70% confluence. Cells were then passaged with StemPro® Accutase® and cell counts were conducted accordingly.

2.1.1.2 Isolation of bone marrow heterogeneous population by plastic adherence and fibronectin selection

Bone marrow was isolated from the long bones of Wistar rats using the method previously described in Section 2.1.1.1 and passed through a 70μm cell strainer. Bone marrow from each femur and humerus was flushed into one T-75 tissue culture flask. After 24h, non-adherent cells were removed by washing twice with PBS and adherent cells were further cultured in CCM for 2 supplementary days. On day 3, the adherent cells were retrieved using StemPro® Accutase® and cell count was conducted accordingly. The cells were seeded at 4,000 cells/cm^2 in 1ml working medium, into each well of fibronectin-coated plates. After 20min incubation, non-adherent cells were removed by washing with PBS. Heterogeneous adherent cells

population were then supplemented with CCM and incubated at 37°C in a 5% CO_2 atmosphere. Culture medium was changed every two or three days.

2.1.1.3 Isolation of heterogeneous populations from rat bone chip explant culture by collagenase digestion and plastic adherence

The femur and humerus were aseptically removed, cleaned of all connective tissue and placed on ice in 10ml in isolation medium (IM). IM consisted of αMEM with 10% antibiotic-antimycotic. Bone marrow cells were removed by strong flushing of each femur and humerus with 10ml of IM through a 21-G needle. After the bone marrow was flushed, the femur and humerus were scraped to remove any remaining soft tissue. The diaphysis were then cut into 1-3mm^2 bone chips and digested under agitation in 3mg/ml collagenase II (Sigma) in αMEM for 2h at 37°C. After 2h, the digestion medium and released cells were removed and the bone chips washed three times with 5ml complete culture medium (CCM, as described in Section 2.1.2). The digested bone chips were then supplemented further with CCM and incubated at 37°C in a 5% CO_2 atmosphere. On day 3, the bone chips and non-adherent cells were removed and remaining adherent cells were cultured to allow for colony formation and expansion. After 12 days from initial plating, the adherent cells were harvested using StemPro® Accutase® for 7min at 37°C (Passage 0), counted on a haemocytometer, and re-plated at 4,000 cells/cm^2 in T25 culture flask for further expansion. Culture medium was changed every two or three days. Once the cells have reached 70% confluence, they were further passaged and counted on a haemocytometer to determine the fold increases in expansion.

2.1.1.4 Assessment of population doubling levels

Each of the isolated MSC populations was assessed for their population doubling levels (PDs) to monitor their proliferation potential during the expansion period. Cell counts were performed at each passage and population doubling values were assessed as a proportion of the original number of cells seeded using the formula:

$$\text{Population doubling levels} = \frac{\log \text{final cell number} - \log \text{seeding cell number}}{\log_2 \times \text{days in culture}}$$

where the final cell number represents the cell number at 70% confluence, divided by the initial number of cells seeded. The final population doublings value for each colony was represented as the sum of population doubling values obtained at each passage. Each type of isolation protocol was repeated at least twice to ascertain the reproducibility of each protocol and provide reliable definitive characteristics for each established MSC population.

2.1.1.5 Mycoplasma testing of primary cultures

Mycoplasma testing was conducted using VenorGeM Mycoplasma Detection Kit for Conventional PCR standard protocol (Cambio, Cambridge, UK). Briefly, 100µl of supernatant sample was used from cell cultures at approximately 90% confluency. The sample was incubated at 95^{o}C for 5min, centrifuged to pellet cellular debris; and 2µl of supernatant used for PCR in a final volume of 25µl containing master-mix kit. PCR cycling condition used is as following: 1 cycle at 94°C for 2min, 94°C for 30s, 55°C for 30s, 72°C for 3s, and hold at 4°C. Products were separated using 2% agarose/safeview gels and captured using UV light. Bands were seen at 191bp for negative sample and 270bp for positive sample. RNA free water was used as a negative control and DNA template used as positive control. Mycoplasma testing was routinely conducted every 2 weeks for each culture. If found positive, cell cultures were treated with 10µg/ml BM cyclin 1 and 5µg/ml BM Cyclin 2 (Roche, Burgess Hill, UK) for 2 weeks until tested negative.

2.1.1.6 Cryopreservation of cells

Cryopreservation of cultured cells was conducted by resuspending the cells in sterile FBS with 10% v/v dimethylsulfoxide (DMSO), at a concentration of 1x10^{6} cells/ml. The vials were then transferred into Mr. Frosty containers, with isopropanol; and maintained at -80°C overnight before being transferred into liquid nitrogen for long-term storage.

2.1.2 Characterisation of MSC populations at early-, mid- and late-population doubling levels

2.1.2.1 Cell morphological analysis by light microscopy

Cellular morphology was compared in the various isolated populations, from early-(PD15), mid-(PD50) and late-(PD100) population doubling level, by using light microscopy with serial images captured on digital cameras Canon PC1234 (Canon UK Ltd., Surrey, UK).

2.1.2.2 Phalloidin-FITC staining and fluorescence microscopy

The actin cytoskeleton of cells was stained with phalloidin-FITC (Sigma) to further examine cellular morphology. The cells cultured in BD Falcon™ glass chamber slides (BD Biosciences, Oxford, UK) were washed with PBS and fixed with 200µl/well 4% paraformaldehyde (PFA, Santa Cruz Biotechnology Inc., California, USA), for 10min at room temperature The PFA was then aspirated and cells washed twice with 200 µl/well PBS at 5min interval. The PBS was then replaced with 200 µl/well 0.1% Triton-X100 (Sigma) for 30min, with gentle shaking at room temperature. The Triton-X100 was aspirated and the cells were washed twice with Tris buffered saline (TBS, pH 7.5). The cells were blocked with 200µl/well 1% bovine serum albumin (BSA, Fisher Scientific, Loughborough, UK) in TBS (1% BSA-TBS), for 1h at room temperature with gentle shaking. The blocking buffer was then removed before the addition of 100 µl/well phalloidin-FITC (20µg/ml, Sigma), in 1% BSA-TBS; and incubated for 1h under darkness at 4°C with gentle shaking. The stains were aspirated and cells were washed twice with 200 µl/well TBS at 5min intervals. The cells chamber was removed and the cells were stained with Vectashield® mounting medium with DAPI (Vector Laboratories Ltd, Peterborough, UK) prior to attachment of cover slips. Images were captured using an ultraviolet (UV) microscope (Olympus AX70 with Digital Eclipse DXM1200 digital camera attachment, Olympus Optical Co. Ltd., Tokyo, Japan). The images were captured using Automatic Camera Tamer (ACT-1) control software (Nikon Instruments UK, Surrey, United Kingdom) at 373nm/456nm (FITC).

2.1.2.3 Total RNA isolation from MSCs and quantification

For RNA extraction, cells were seeded at 4,000 cells/cm^2 in 3 wells of 6 well-plate. Once the culture reached 70% confluence, total RNA was extracted using the RNeasy® Mini kit and QIAShredder (Qiagen Ltd., Crawley, UK). Cells were washed twice with PBS before addition of lysis buffer and centrifuged at 13,300rpm for 2min at room temperature. The lysis buffer consists of RLT buffer (Qiagen) supplemented with 10µl/ml of β-mercaptoethanol. RNA pellets in the column were washed with 600µL of 70% ethanol, followed by centrifugation for 15s at 13,300rpm. RNA solutions were treated with DNase to remove genomic DNA using the DNA-free kit (Qiagen), according to manufacturer's instructions. RNA was eluted from the column in a final volume of 30µl elution buffer. The RNA template was quantified using NanoVue™ (GE Healthcare, Chalfont St Giles, UK) spectrophotometry, using A260/A280 absorbance. The RNA products were stored at -80°C for use in reverse transcription reactions.

RNA from the isolated MSCs was analysed at three different time-points during cultivation time, early-(PD15), mid-(PD50) and late-(PD100). At each selected population doublings level, the cells were analysed for the expression of selected mesenchymal progenitor cells surface antigens; CD90 (Thy-1); CD105 (endoglin) and CD73 (ecto-5-nucleotidase), hematopoietic surface antigens; CD45 and CD34; and embryonic stem cells surface markers; Oct4, Sox-2 and Nanog. The cells were also assessed for transcription markers of osteogenesis and adipogenesis, to further investigate the potential existence of mesenchymal lineages progenitor cells within the isolated cells population derived from each bone microenvironment.

2.1.2.4 Reverse transcription of MSC RNA

cDNA was synthesized from 500ng of total RNA using 1µl random primer (Promega, Southampton, UK), added to RNA-free water to a final volume of 15µl. The sample was run at 70^{o}C for 5 min. RT reaction mix was prepared, containing 5µl 5X Moloney Murine Leukemia Virus Reverse Transcriptase (MMLV) reaction buffer, 3.4µl 10mM deoxynucleotide triphosphates (dNTPs), 0.6µl RNasin and 1µl MMLV enzyme, added to RNA-free water to give a volume of 10µl. Next, 15µl of

random primer/RNA mix was added to the RT reagents to produce a final volume of 25µl cDNA. The 25µl final volume was run at 37°C for 1h. All reactions were run on a G-Storm™ GSI thermal cycler Software 45 V3.3.0.0 (Genetic Research Instrumentation Ltd., Braintree, UK). For each cDNA preparation, a negative control was produced, where primers and RT enzyme were subject to the same synthesis conditions, minus mRNA. All resulting cDNA was stored at -20°C for use in PCR reactions.

2.1.2.5 Polymerase chain reaction (PCR) and product visualisation

PCR was carried out using PCR reagents (Promega) and 1µl cDNA. The PCR reagents used for each reaction contain 5µl 5x buffer, 0.5µl 10mM dNTP, 1.25µl 10µm forward and reverse primer (as shown in Table 2.1), 1µl 25mM magnesium chloride, 0.25µl Taq polymerase; and reconstituted with RNA-free water to a total volume of 25µl per reaction. For each PCR preparation, a negative control was produced, where primers and enzyme were subject to the same synthesis conditions, minus cDNA sample. Primers sequences were obtained from various related studies that fulfil the corresponding PCR criteria and a basic local alignment tools (BLAST) search was run on each primer, to ensure specificity for the intended amplification target (Altschul S.F. 1990). β-actin was used as a housekeeping gene. Reactions were performed in G-Storm™ GSI Thermal Cycler, with an initial denaturing step of 94°C for 5min, followed by 35 cycles of 1min 94°C denaturing step, 30s 55°C annealing step and 30s 72°C extension step, with final run of 72°C extension step for 7min. The same condition was applied to all primers with exception for Nanog, Oct4, CD73, CD105 and osteocalcin. RT-negatives and PCR-negatives were used as the experimental controls and β-actin was used as the housekeeping gene. PCR products were kept at -20°C until visualisation. Products were separated using 2% agarose (Geneflow, Staffordshire, UK)/0.5X TBE (Sigma) with 1% Safeview (NBS Biological Ltd., Cambridge, UK). 10µl of PCR product were loaded and run in 0.5X TBE buffer at 90V for 1h. Gel was viewed on a GelDoc™ Scanner (Bio-Rad Laboratories Ltd., Hemel Hempstead, UK), using UV light. Images were captured using Quantity One Image Analysis Software (Bio-Rad)

Table 2.1 Primer sequences and product sizes of selected mesenchymal stem cell markers and differentiation negative control for PCR analysis

Gene	cDNA sequence (5'-3') F, Forward; R, Reverse	Length (bp)	References
Nanog	F:GGGGATTCCTCGCCGATGCCTGCCGTT R:GGGATACTCCACCGGCGCTGAGCCCTT	477	Nozaki and Ohura, 2011
Oct4	F:GCCCACCTTCCCCATGGCTGGACACCT R:GCAGGGCCTCGAAGCGGCAGATGGTTG	563	Gonzalez et al. 2009
CD73	F:TCCCGCGGCTGCTACGGCACCCAAGTG R:ACCTTGGTGAAGAGCCGGGCCACGCCG	204	Scherer et al. 2012
CD90	F:CCTGACCCGAGAGAAGAA R:TGAAGTTGGCTAGAGTAAGGA	125	Nakamura et al. 2010
CD105	F:ACATGGTGCCCACACCCGCAGCTGGCA R:CACTGCCACCACGGGCTCCCGCTTGCT	263	Meurer et al. 2005
CD34	F:GTCACACTGCCTACTACTTC R:TCCTCGGATTCCTGAACAT	210	Shyu et al. 2006
CD45	F:AGCAATACCAGTTCCTCTATGA R:TCCGTCCACTTCGTTATGA	113	Wang et al. 2010b
Runx2	F:CCAGATGGGACTGTGGTTACC R: ACTTGGTGCAGAGTTCAGGG	381	Gilbert et al. 2002
OCN	F:ACAGACAAGTCCCACACAGCAACT R:CCTGCTTGGACATGAAGGCTTTGT	161	Hak Auth, 2008
PPARγ	F:GGAAAGACAACAGACAAATCAC R:GAACTTCACAGCAAACTCAAAC	408	Tholpady et al. 2003
Sox-9	F:CCCTTCAACCTCCCACACTACAGC R:TGTGTAGACGGGTTGTTCCCAGTG	249	Schumacher et al. 2008
β-actin	F:TGAAGATCAAGATCATTGCTCCTCC R:CTAGAAGCATTTGCGGTGGACGATG	155	Gatto et al. 2008

2.1.2.6 β-galactosidase stain for cell senescence

Cell senescence was analysed by the presence of β-galactosidase staining using a Senescence Cells Histochemical Staining Kit (Sigma), according to manufacturer's instruction. Briefly, the cells were seeded in 3 well of 6-well plate at density of 2,000 cells/cm^2. At 24h, the culture medium was removed from the cells and washed twice with 1X PBS per well/plate. 1X fixation buffer was added and incubated for 6-7 minutes at room temperature. Cells were rinsed thrice with 1X PBS. Staining mixture was added and left overnight at 37°C without CO_2. The number of blue-stained positive cells out of 100 was counted from at least 5 five random fields of 30μm^2 of view, to give an average percentage.

2.1.3 Differentiation of MSCs into osteogenic and adipogenic lineages

In order to assess the bi-potential differentiation capacity of the isolated MSCs, the expression of stem cell specific differentiation markers and transcription factors were examined, both at gene and protein level.

2.1.3.1 Cell source

MSCs taken at 50PDs of each cell population were selected for osteogenic and adipogenic induction. Protocol was carried out to confirm the ability of isolated cells to differentiate along the chosen mesenchymal lineages.

2.1.3.2 Osteogenic differentiation

Osteogenic medium consisted of αMEM with ribonucleosides and deoxyribonuclosides, supplemented with 10% FBS, 1% antibiotics-antimycotics, 100μm L-ascorbic acid 2-phosphate, 10nM dexamethasone and 100uM β-glycerophosphate (all from Sigma).

For osteogenesis, the cells were plated in duplicate at 4,000 cells/cm^2, in 3 wells of 6-well plates for total RNA extraction; and 8-well chamber slides for histological staining. Cells were cultured in CCM for 24h, before the medium was removed and replaced with osteogenic mineralising medium and further incubated in 37°C, 5% CO_2 for 28 days, with medium changes every 2 or 3 days. As a control for

mineralisation, the cells were also cultured in non-conditioned medium (NCM), consisted of αMEM with 10% FBS, 1% antibiotics-antimycotics and 100μm L-ascorbic acid 2-phosphate only.

2.1.3.3 Adipogenic differentiation

The adipogenic medium was formulated based on supplementation used in Davies et al. 2010, which consisted of adipogenic induction medium (AIM) and adipogenic maintenance medium (AMM). AIM consist of αMEM with ribonucleosides and deoxyribonuclosides, supplemented with 10% FBS, 1% antibiotics-antimycotics, 100μm L-ascorbic acid 2-phosphate, 1μM dexamethasone, 100uM indomethacin and 100uM 3-isobutyl-1-methylxanthine (all from Sigma). AMM consist of αMEM with ribonucleosides and deoxyribonuclosides, supplemented with 10% FBS, 1% antibiotics-antimycotics, 100μm L-ascorbic acid 2-phosphate and 10μg/ml insulin (all from Sigma).

For adipogenesis, the cells were plated in duplicate at 10,000 cells/cm^2, in wells of 6-well plates for total RNA extraction, and 8-well chamber slides for histological staining with LipidTOX™ (Life Technologies, Paisley, UK). The cells were cultured in CCM (as described in Section 2.1.1.2), until the culture reached 90% confluence, before the medium was removed and replaced with AIM and cultured in 37°C and 5% CO_2 for 14 days. Medium was changed every 72h. At day 6, cultures were supplemented with AMM for 48h to replace the AIM. Each of the adipogenic media was freshly prepared, prior to use. As a control for adipogenesis, the cells were also cultured in non-conditioned medium (NCM), consisted of αMEM with 10% FBS, 1% antibiotics-antimycotics and 100μm L-ascorbic acid 2-phosphate only.

2.1.4 Cellular imaging and gene expression analysis of differentiated cultures

2.1.4.1 Alizarin red S staining

The alizarin red S solution was prepared prior to staining, by dissolving 20g/L alizarin red S in double-distilled water, pH 4.2. On day 14, samples were washed twice with PBS, followed by 10min fixation with 4% paraformaldehyde (PFA) at room temperature. The PFA was then removed and the fixed cells were washed twice

with PBS, before 100uL alizarin red S solution added and gently agitated for 2-5min. The excess staining solution was then removed and washed with distilled water. Slides were left to dry at room temperature, before viewing under light microscopy with serial images captured on digital cameras Canon PC1234 (Canon UK Ltd., Surrey, UK).

2.1.4.2 Oil Red O staining

The Oil red O staining solution was freshly prepared prior to staining, by mixing oil red O stock (3.5 g/L oil red O dissolved in propanol) and double-distilled water in a 4:6 ratio. The staining mixture was agitated for 10min at room temperature, before being filtered through Whatman™ grade 42 (2.5uM) filter paper (Sigma). The adipogenic and control cultures were gently washed with 60% isopropanol for 5min, followed by addition of 100uL oil red O working solution into each chamber well. After 10min, the excess staining solution was removed by gentle washing steps with double-distilled water and immediately followed by staining with haematoxylin (Sigma) for 2min at room temperature before final rinsing with double-distilled water. The samples were then immersed in 70% glycerol and before viewing under light microscopy with serial images captured on digital cameras Canon PC1234 (Canon UK Ltd).

2.1.4.3 Immunofluorescent detection of lipid vesicles in differentiated cultures using LipidTOX™

1000X LipidTOX™ neutral lipid stain was diluted 1:1000 in buffer to make 1X solution. After removal of second PBS wash, the cells in each chamber were incubated with 200µl LipidTOX™ for 30min. Following 3 final washes with PBS, the chamber was removed and the cells were stained with Vectashield® mounting medium with DAPI (Vector Laboratories Ltd.) prior to attachment of cover slips. Images were viewed under ultraviolet (UV) microscope Olympus AX70. The images were captured using Automatic Camera Tamer (ACT-1) v.2.63 software (Nikon Digital, Tokyo, Japan) at 373nm/456nm.

2.1.4.4 PCR of differentiated cultures

PCR analysis was conducted on osteogenic, adipogenic and control-treated cultures, by collecting the RNA on day 14 and day 28, following the respective induction processes. Control-treated cultures, supplemented with NCM were used as pre-differentiation negative control. RNA was collected once the culture reaches confluence. Meanwhile, another control culture was carried out alongside the differentiation culture to act as a negative control culture, supplemented with NCM for 14 and 28 days accordingly. PCR reactions were carried out using the same cycling condition as stated in Section 2.1.2.5, with exception to osteocalcin as the annealing temperature was set at 62°C. Details of the selected differentiation markers are summarised in Table 2.2.

Table 2.2 Primer sequences and product sizes of selected osteogenic and adipogenic differential markers for qRT-PCR analysis.

Gene	cDNA sequence (5'-3') F, Forward; R, Reverse	Length (bp)	References
Osteocalcin	F: ACAGACAAGTCCCACACAGCAACT R: CCTGCTTGGACATGAAGGCTTTGT	161	Owen et al. 2012
Osteopontin	F:TCCAAGGAGTATAAGCAGAGGGCCA R: CTCTTAGGGTCTAGGACTAGCTTGT	200	Singh et al. 1992
Osterix	F: GCTTTTCTGTGGCAAGAGGTTC R: CTGATGTTTGCTCAAGTGGTCG	136	Georgiou et al. 2012
Lipoprotein Lipase	F: AGGTCAGAGCCAAGAGAAGCA R: GGAGTAGGTTTTATTTGTGGCG	215	Levak-Frank et al. 1995
FABP4	F: GGAATTCGATGAAATCACCCC R: TGGTCGACTTTCCATCCCACT	104	Minoura et al. 2007
C/EBPα	F: GGGAGAACTCTAACTCCCCCAT R: CTCTGGAGGTGGCTGCTCATC	82	Calkhoven et al. 2000
Adiponectin	F: GAATCATTATGACGGCAGCAC R: CTTGGAGCCAGACTTGGTCTC	224	Puerta et al. 2002
β-actin	F: GGGTCGAGTCCGCGTCCAC R: CGACGAGCGCAGCGATATC	108	Park et al. 1997

2.1.4.5 Time-based quantitative real-time PCR (qRT-PCR) analysis of osteogenic and adipogenic differentiation markers

For osteogenic induction, mRNA sample of 50PDs cells was collected on day 2, 7, 14 and 28 following the differentiation protocol, whereas mRNA sample from adipogenic induction was collected on day 2, 7 and 14. RNA isolations and reverse transcription reactions were performed as described in Section 2.1.2.2 and section 2.1.2.3. cDNA was pre-diluted 1:5 with RNA-free water prior to analysis. Each qRT-PCR reaction was performed using 2.5µl 3µm primers (forward and reverse), 5µl diluted cDNA sample and 10µl SYBR Green Precision qRT-PCR Master Mix (Primerdesign Ltd., Southampton, UK). All samples were analysed in triplicate in Bright White 96-well plates (Primer Design Ltd), using ABI Prism 7000 Sequence Detection System and ABI Prism 7000 SDS Software V1.0 (Life Technologies Ltd., Paisley, UK). Reactions conditions were: 1 cycle of 95°C for 10min, 40 cycles of 95°C for 15s, 55°C for 30s and 72°C for 30s for all primers except for osteocalcin, as the annealing temperature was set at 62°C. Primers sequences were obtained from various related studies that fulfil the corresponding qRT-PCR criteria (see Table 2.2). For quantitative analysis, the gene expression profile were normalised to expression of β-actin as the housekeeping gene, using the $2^{-\Delta\Delta Ct}$ method (Livak and Schmittgen 2001). Gene expression in 28 days osteogenic medium and 14 days adipogenic medium were presented as the fold increase or decrease of that in basal, non-differentiating medium at day 0, prior to induction in osteogenic or adipogenic medium. Error bars represent SD. Products were separated by electrophoresis using 2% agarose/Safeview gels and captured using UV light to confirm the amplified product band.

2.1.5 Protein expression profile of osteogenic cultures

Western Blot was performed to determine if osteogenic gene expression in the conditioned medium led to the expression of bone specific proteins (osteocalcin and osteopontin) by MSCs.

2.1.5.1 Protein extraction

For protein analysis, MSCs were seeded at density of 4,000 cells/cm^2 in T25 tissue culture flask. Protein was extracted from MSCs grown in the osteogenic medium at day 28. Cultured cells were washed twice in ice-cold PBS and scraped into ice-cold RIPA extraction buffer 1X (Fisher Scientific UK Ltd., Loughborough, UK), supplemented with protease inhibitors Complete™ Protease Inhibitor Cocktail (Roche). Cells suspensions were sonicated using Digital SLPe Cell Disruptor (Branson Ultrasonics Corp., Danbury, USA) and debris collected by centrifugation at 8,000rpm for 5min. The protein concentration of cell supernatant was analysed using a BCA Protein Assay Kit (Fisher Scientific), according to manufacturer's instructions.

2.1.5.2 Western Blot

20µg of proteins samples were diluted 1:1 with 1X Laemmi buffer (62.5mM Tris-HCl buffer, pH 6.8, 2% (v/v) SDS in distilled water, 10% (v/v) glycerol, 0.5% (w/v) bromophenol blue in distilled water and 2.5% (v/v) β-mercaptoethanol), before being loaded on 4-15% Mini-Protean® TGX™ Precast Gels (Bio-Rad) along with 10µl Kaleidoscope™ Prestained Standard Markers (Bio-Rad). Protein samples were separated under reducing conditions by sodium dodecyl sulphate-polyacrylamide gel electrophoresis (SDS-PAGE) at 200V, for 35min (Mini-Protean® Tetra Cell System, BioRad). Proteins were electrotransferred onto Hybond™-ECL extra nitrocellulose membrane (GE Healthcare, Little Chalfont, UK) at 15V for 30min, using Semi-Dry Trans-Blot System (Bio-Rad). Membranes were blocked with 5% semi-skimmed milk with TBS-T (Tris-buffered saline and 1% Tween 20), at 4^{o}C overnight.

2.1.5.3 Protein detection

Following the blocking procedure, membranes were immuno-probed with polyclonal anti-goat osteocalcin (1:100) and polyclonal anti-rabbit osteopontin (1:100) (Insight Biotechnology, Wembley, UK), in 5% semi-skimmed milk with TBS-T, at room temperature for 1h. Membranes were rinsed 3 times with TBS-T and incubated with rabbit anti-goat horseradish peroxidase (HRP)-conjugated secondary antibody (1:3000, Insight Biotechnology) in 5% semi-skimmed milk in TBS-T at room

temperature for 1h. In parallel, β-actin control samples were incubated in polyclonal swine anti-rabbit HRP-conjugated secondary antibody (1:3000, Dako UK Ltd., Cambridge, UK) in 5% semi-skimmed milk in TBS-T at room temperature for 1h. Normalised protein loading was confirmed by β-actin Loading Control immuno-probing (1:1000, Abcam, Cambridge, UK). Membranes were washed three times and incubated in ECL™ Plus Detection Reagent (GE Healthcare) for 2min. Chemiluminescence was detected by exposing the membrane to Hyperfilm™ (Fisher Scientific UK Ltd.) and developed using a Curix 60 Auto-developer (AGFA, Mortsel, Belgium), according to manufacturer's instructions.

2.1.6 Statistical analysis

Unless otherwise stated, data was expressed as mean±standard deviation (SD). All statistical analyses were performed using SPSS version 20.0 (IBM, NY, USA). Data were analysed by two-way Analysis of Variance (ANOVA), followed with a Tukey's post-hoc test, with a significance level accepted at $*p<0.05$ and $**p<0.01$.

2.2 Results

2.2.1 Establishment of rat MSC populations from bone explants and bone marrow

2.2.1.1 MSCs morphological analysis

MSCs were successfully isolated from rats bone chip explants and bone marrow, using different selection methods; 1) collagenase digested bone chips explants culture followed by plastic adherence selection (BCE), 2) Plastic adherence selection of bone marrow stromal cells, followed by fibronectin preferential adherence (PFNA), 3) Histopaque® gradient separation of bone marrow cells, followed by fibronectin adherence selection (FNA). Adherent cells were observed in the heterogeneous samples; BCE and PFNA as early as 1-5 days in culture. BCE and PFNA at 15PDs rapidly generated a confluent layer of monolayer cell, mainly consist of stellate-shaped cells, with large flattened and nucleated spread body, mixed with smaller amount of spindle-shaped, fibroblastic-like morphology cells (Figure 2.1a-b).

The actin staining of heterogeneous cells population taken from early PDs, revealed clear observation of wide spread actin filaments, located within the periphery of the cells (Figure 2.2a-b). However, after 60 to 70 days post-isolation, a new cell population appeared within the heterogeneous culture and rapidly became the most predominant cell type present in the culture, replacing the former widespread and stellate shaped cells (Figure 2.1d and 2.1e). Similarly, this can be seen in Figure 2.2d and 2.2e, as the cells from mid PDs showed an organised pattern of actin cytoskeleton, formed centrally within a spindle-shaped cells.

Adherent cells from clonal bone marrow (FNA) were observed only after a minimum of 12 days following the initial seeding date. The cells demonstrating uniform spindle-shaped cells morphology from early to late PDs with only slight increase in nucleus size (Figure 2.1c, 2.1f and 2.1i). The homogenous appearances of FNA cells were also consistently observed from 15PDs, 50PDs and 100PDs with an actin filaments staining (Figure 2.2c, 2.2f and 2.2i). In contrast, BCE and PFNA

populations demonstrated short stellate-like processes and a more polygonal morphology with flattened body over expansion time, from 50PDs to 100PDs (Figure 2.1g-h and 2.2g-h). Comparison made between all MSCs groups at 50PDs demonstrated similar predominant pattern of fibroblastic-like appearances despite different tissue source and separation methods applied in isolation steps.

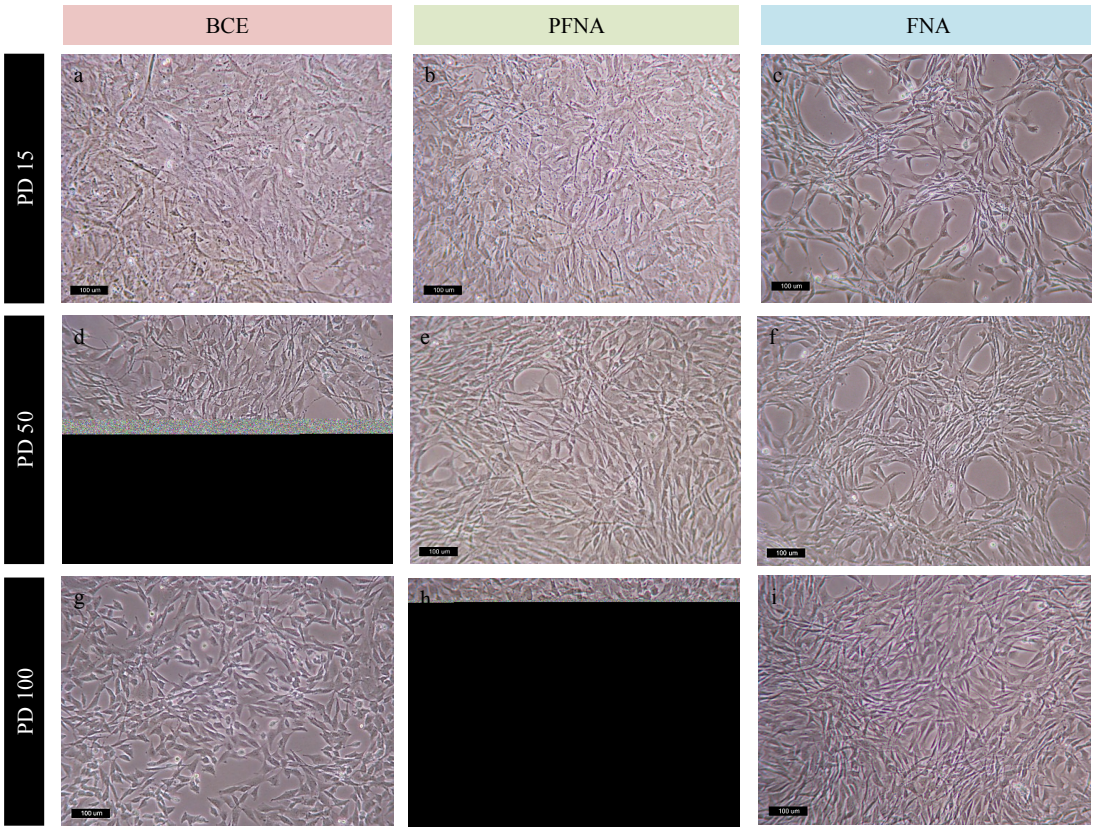

Figure 2.1 Phenotype and morphology of isolated MSCs viewed under light microscopy. Both heterogenous MSCs population, BCE and PFNA showed alteration of cells morphologies with increase level of cells doubling time, whereas clonal MSCs (FNA) demonstrated more uniform cells shape along the expansion period. Scale bar= 100µm. BCE, bone chips explant MSCs; PFNA, plastic and fibronectin adherence BMMSCs; FNA, Histopaque® and fibronectin adherence clonal BMMSCs; PD, population doubling level.

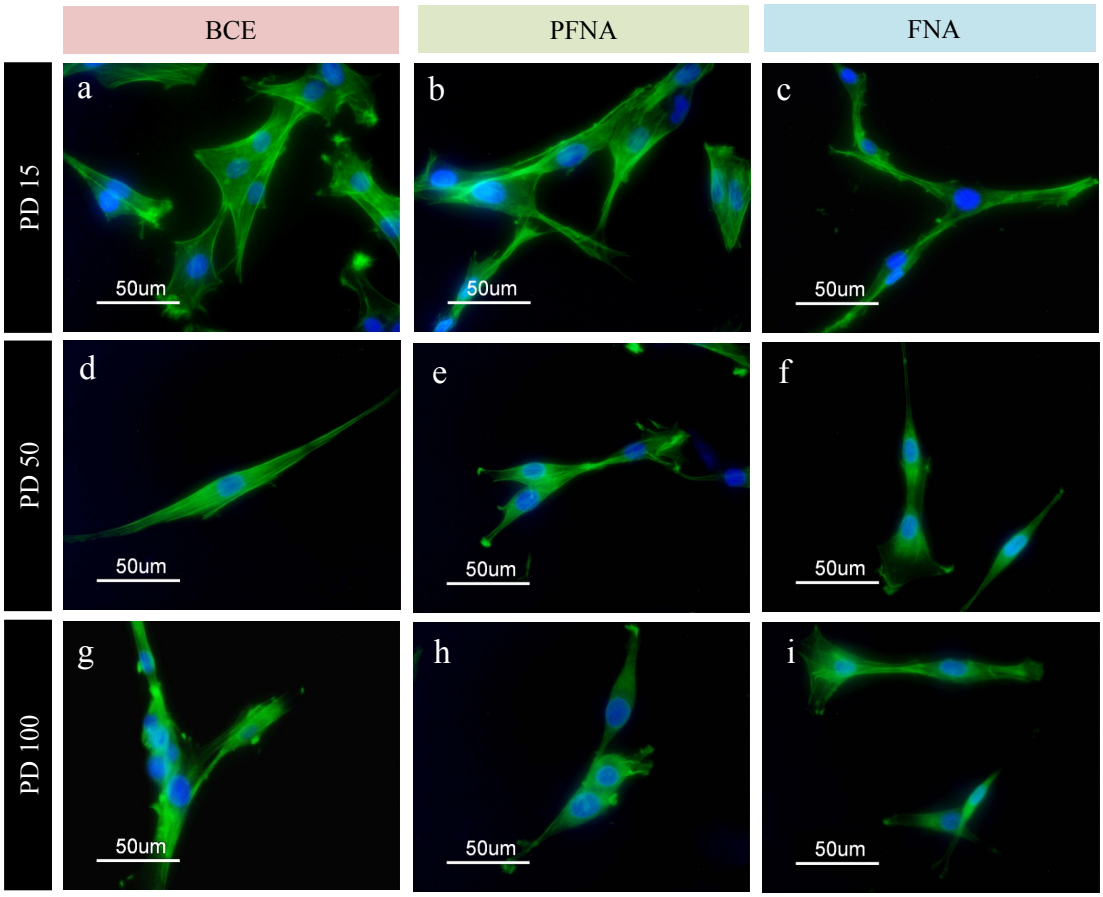

Figure 2.2 Phenotype and morphology of isolated rats MSCs following the Phalloidin-FITC staining. BCE= bone chips explant MSCs, PFNA=plastic and fibronectin adherence BMMSCs, FNA= Histopaque® and fibronectin adherence clonal BMMSCs. Different actin filament distribution was observed in intact MSCs, from early-PD and late-PD culture, particularly in between cells with different homogeneity. Scale bar= 50µm. PD, population doubling level.

2.2.1.2 Proliferative capacity of isolated MSCs

Consistent numbers of cells with an average number of 4.18x106 progenitor cells/ml per raw bone marrow were collected from both femurs and humerus of 2 combined animals, as well as $2.43x10^6$ progenitor cells/ml from the mononuclear fraction. Meanwhile, an average of $5.4X10^5$ progenitor cells/ml was recovered from the bone chip explants, growing outward and adhering to the plastic surfaces after 5 days in culture.

In order to compare the effects of the 3 different separation methods and different tissue source on the proliferative capacity of MSCs, the cumulative population doubling level (PDs) was evaluated for all isolated MSC populations, as shown in Figure 2.3. After 60 days of an initial lag phase, both heterogeneous BCE and PFNA MSCs began to demonstrate a consistent proliferation pattern, with rapid exponential growth until 100PDs were reached. The variability in MSCs PD profiles amongst the different BCE and PFNA cell populations was less apparent. In contrast, the clonal MSCs (FNA) demonstrated inconsistent proliferative capacity with huge variation during plateau stages between the same isolation techniques. FNA2 exhibit twice much longer lag phase of 120 days before the rapid proliferative stage began to take place, in comparison to FNA1, which demonstrate 60 days of lag phase, in equivalence with other isolated cell populations. In addition, starting from 15PDs, the isolated MSCs reach 70%-80% confluence every 2 to 3 days and the average PDs recorded per week was 5.42 for BCE, 5.2 for PFNA and 5.194 for FNA. The isolated MSCs were maintained for a minimum of 100PDs in culture, without any signs of cellular aging, which were confirmed by assessing the doubling rate, showed consistent at >4.9 PD/week and β-galactosidase staining (Figure 2.4), which demonstrated an average of <2% blue-stained cells in every $30\mu m^2$ random selected field, indicating good cells viability and the absence of cellular senescence.

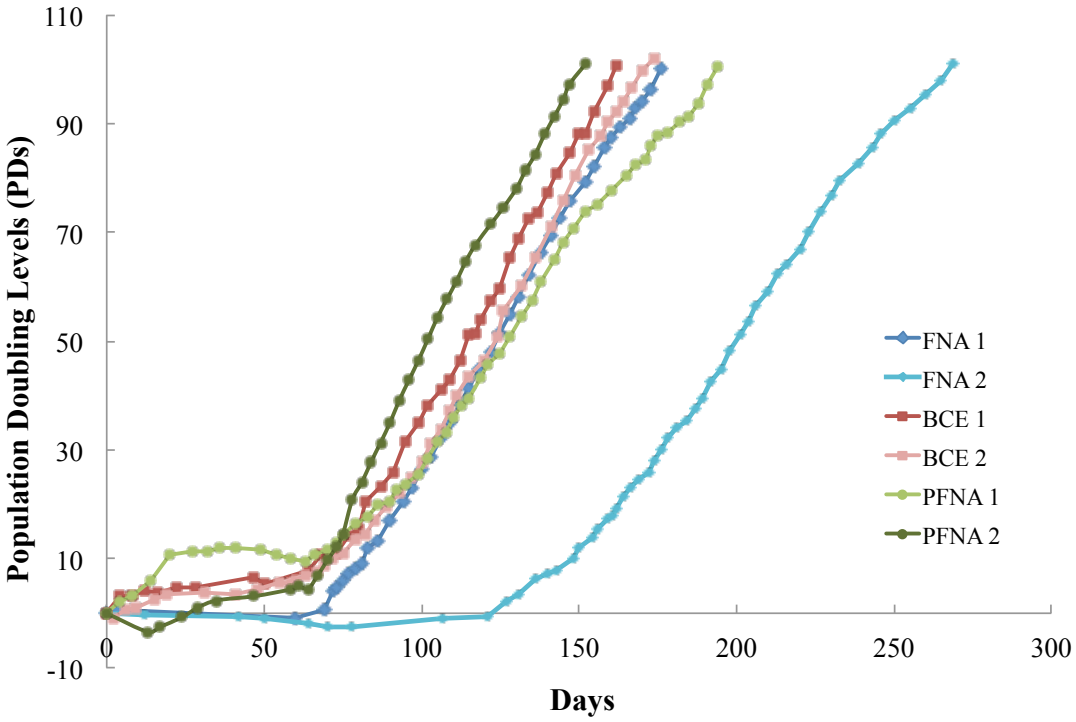

Figure 2.3 Cumulative population doubling levels (PDs) of MSCs for each clonal and non-clonal population. All of the MSCs were plated at 10,000 cells/cm^2 and cultured until reaching 70% confluence, before further expansion. BCE, bone chips explant MSCs; PFNA, plastic and fibronectin adherence BMMSCs; FNA, Histopaque® and fibronectin adherence clonal BMMSCs. Each isolation protocols were repeated twice, n=2. Both replicate of heterogenous cells populations (BCE and PFNA) showed uniform proliferative capacity, whereas the homogenous populations (FNA), demonstrated inconsistent pattern of proliferative potential between each clonal expansion.

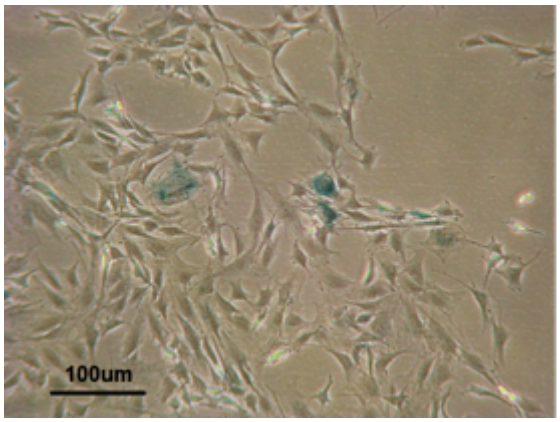

Figure 2.4 β-galactosidase expressions in MSCs at late PDs (100PDs) from PFNA cells. X-gal staining was performed two days after seeding. Scale bar= 100µm.

2.2.1.3 MSCs gene expression profiles

The complete analysis of expressed surface antigens by MSCs isolated using all three different methods, are summarised in Figure 2.5. MSCs from the heterogeneous populations, BCE and PFNA consisted of a mixture of cell types, with variant phenotypes at selected PD time-points. Cells from BCE and PFNA positively expressed the mesenchymal stem cells markers, CD73, CD90 and CD105; and were found to be negative for the expression of leukocyte common antigen CD45. However, cells from both BCE and PFNA demonstrated low expression of the lipopolysaccharide receptor, CD34, at 15PDs, which was eventually lost over cultivation time. The expression of adipogenic differentiation markers, PPARγ, was negative in MSCs from BCE and PFNA groups. Findings also demonstrated positive expression of Runx2, along with detectable low expression of osteocalcin and Sox9 in BCE and PFNA cells from all tested PDs.

In contrast, the cultured clonal FNA cells comprised of a single phenotypic population at all tested PDs, as these attached cells were found uniformly positive for CD73, CD90, CD105, Nanog and Runx2; as well as consistently negative for expression of hematopoietic lineage marker, CD34, embryonic marker, Oct4, and differentiation markers, PPARγ. However, the FNA cells exhibit positive low expression of osteocalcin, CD34 and Sox9, in which the last two markers were no longer detected over expansion of culture.

The cultured MSCs, both homogenous and heterogeneous cell populations were identified by consistent high expression of an embryonic stem cell marker, Nanog through all selected PDs. Nevertheless, only BCE cells taken from 15PDs were positively confirmed with low expression of Oct4, which was lost over expansion in culture.

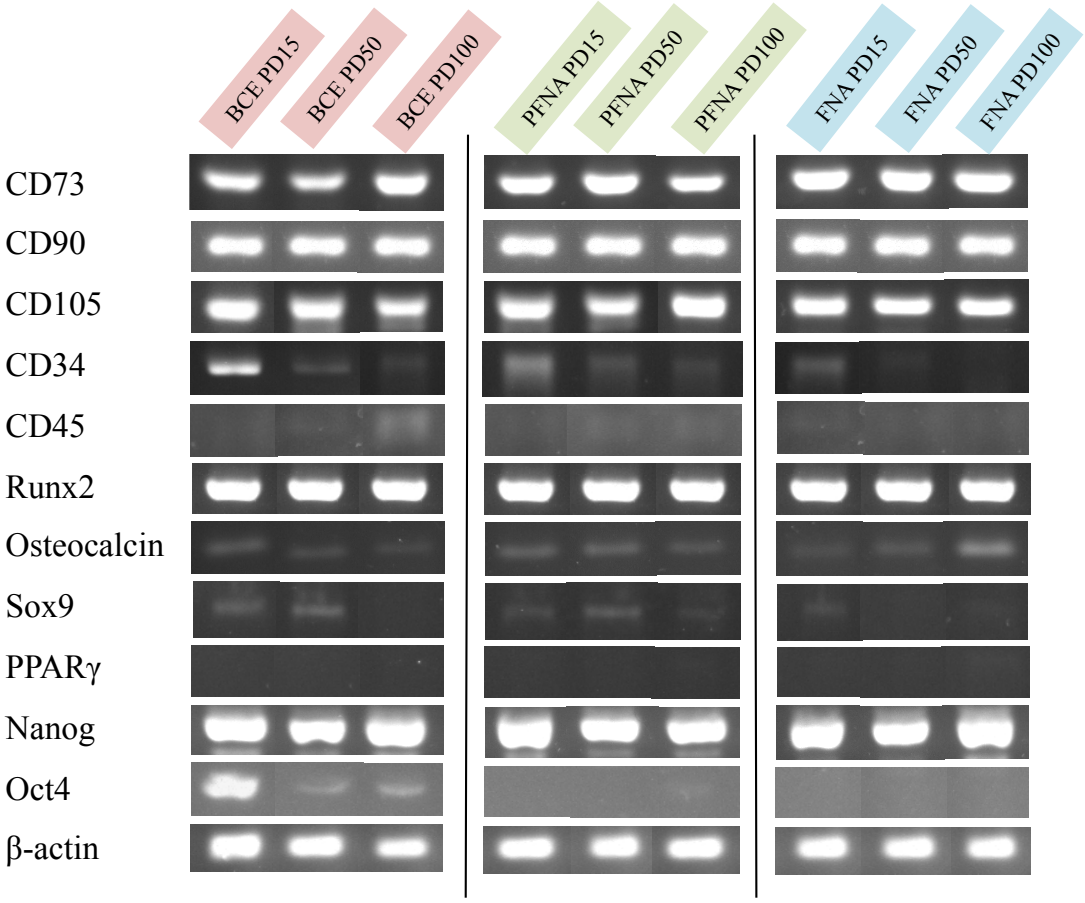

Figure 2.5 Representative expressions of various stem cell surface markers. mRNA isolated from bone marrow and compact bone was subjected to RT-PCR analysis (N, biological replicate=2; n, experimental repeats=2). The expression of mesenchymal cell markers (CD73, CD90 and CD105) was detected. Hematopoietic stem cell marker, CD45, was not detected in all MSC populations, but CD34 was observed in the early PDs and eventually disappeared over time. β-actin was used as the internal control. Negative controls were the PCR runs without mRNA samples. BCE, bone chips explant MSCs; PFNA, plastic and fibronectin adherence BMMSCs; FNA, Histopaque® and fibronectin adherence clonal BMMSCs; PD, population doubling level.

2.2.2 Functional characterisation of MSCs

2.2.2.1 Osteogenic differentiation and mineralised bone formation

The osteogenic potential of rat MSCs isolated using three different methods was tested by culturing PD50 cells from all samples in osteogenic conditioned medium. As early as 10 days in culture, the cultured MSCs exhibited some morphological modifications, with morphological changes from an elongated fibroblastic-like shape to a more cuboidal shape. Following 28 days culture in osteogenic medium, the isolated MSC populations demonstrated the clear formation of stained mineralised bone nodules, with much lower bone formation observed in the clonal MSCs (FNA) compared to the heterogeneous MSC group (BCE and PFNA), as shown in Figure 2.6. To further demonstrate the differentiation potential of the purified cells, the expression of osteoblast-specific markers before and after treatment with the inductive medium was examined. As demonstrated in Figure 2.7, osteogenic differentiation was confirmed by the positive gene expression of osteoprogenitor transcription factor, osterix and later stage of osteoblastic cells marker, osteocalcin that were strongly detected after 28 days induction in osteogenic culture. However, very low expression of osteocalcin and osterix were detected in undifferentiated culture of PFNA cells (day 0), indicating the presence of pro-osteogenic subsets within the heterogeneous bone marrow-derived population. RT-PCR analysis demonstrated the undetectable level of precursor osteoblast marker, osteopontin, in all stages of PDs. In contrast, osteocalcin and osterix mRNA expression were barely noticeable in the non-conditioned medium (day 0). β-actin expression was uniformly detected in samples from all selected PDs.

Western Blotting was performed to validate the osteogenic potential of MSCs at protein level. In Figure 2.8, bands indicating the expression of osteocalcin, osteopontin and housekeeping control, β-actin were seen across all MSC populations after 28 days in osteogenic medium. The osteocalcin fusion proteins were detected at 60kDa, 39kDa and 30kDa molecular weight, while a discrete osteopontin labelling was detected at 62kDa band, with extra bands observed at 55kDa and 75kDa, possibly due to posttranslational modifications.

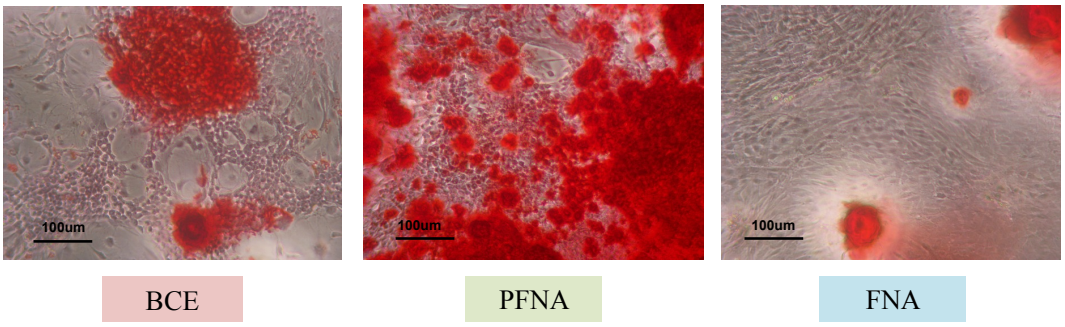

Figure 2.6 Differentiation of MSCs (PD50) isolated from rats bone chips explant and bone marrow, cultured in osteogenic medium for 28 days and stained with Alizarin red. The red colour formation represents calcified deposition of the extracellular matrix. Scale bar= 100µm. BCE, bone chips explant MSCs; PFNA, plastic and fibronectin adherence BMMSCs; FNA, Histopaque® and fibronectin adherence clonal BMMSCs.

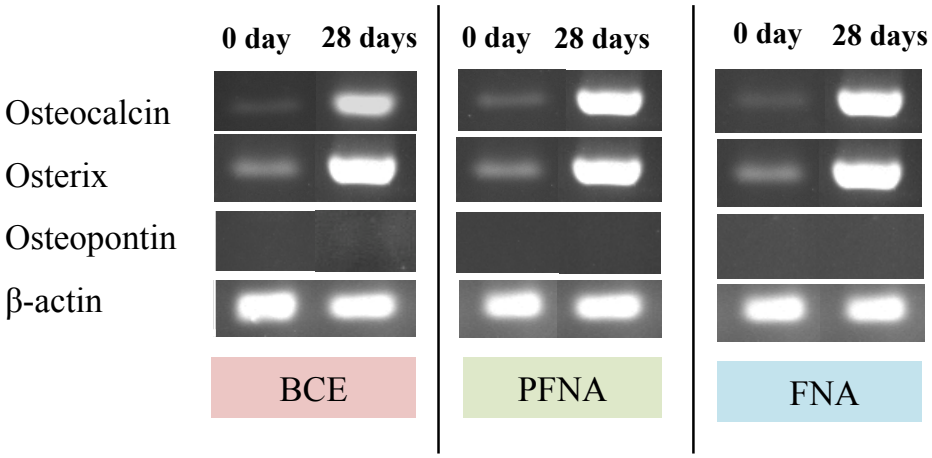

Figure 2.7 Expression of bone specific cell surface markers. mRNA isolated from bone marrow and compact bone, grown in osteogenic medium was subjected to RT-PCR analysis. The expression of osteoblast cell markers (osteocalcin) and transcription factors markers (osterix) were detected following 28 days induction in the osteogenic medium (N=2, n=3). BCE, bone chips explant MSCs; PFNA, plastic and fibronectin adherence BMMSCs; FNA, Histopaque® and fibronectin adherence clonal BMMSCs.

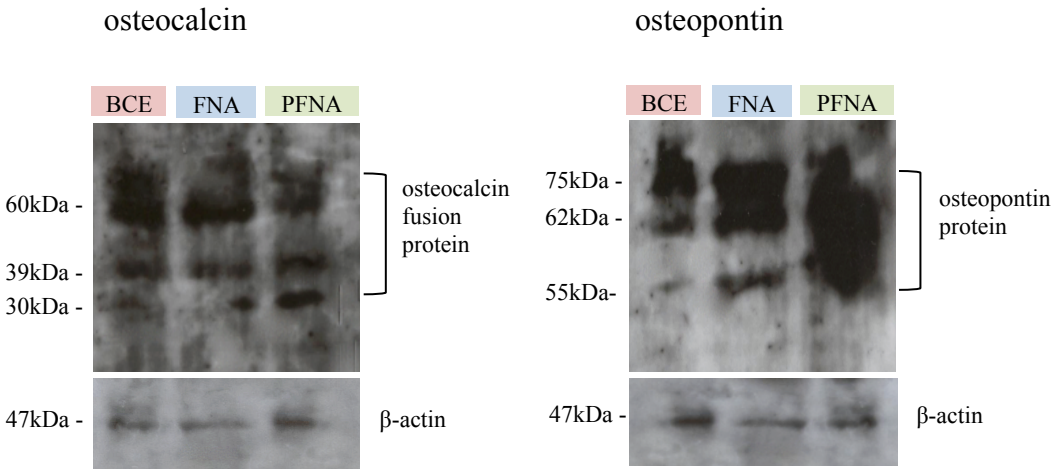

Figure 2.8 Western Blot analysis of osteocalcin and osteopontin in MSC culture grown in osteogenic induction medium for 28 days. BCE, bone chips explant MSCs; PFNA, plastic and fibronectin adherence BMMSCs; FNA, Histopaque® and fibronectin adherence clonal BMMSCs.

2.2.2.2 Quantitative analysis of MSCs osteogenic gene expression

Quantitative real-time RT-PCR was used in this study to examine whether alteration in the differentiation potential of MSCs were accompanied by changes in the expression of osteogenic-related gene markers after 28 days in culture (Figure 2.9). In all cell population, osteocalcin expression was found to be 10-fold higher in osteogenic medium than the control non-conditioned medium on day 2. However, PFNA cells reported a significant increase of osteocalcin expression on day 7 ($p<0.05$), and day 21 ($p<0.01$) in comparison to BCE and FNA cells. Meanwhile, there was a fluctuation in the expression of osteogenic transcription factor, osterix, from day 2 to day 14 in all isolated cultures, with noticeable increased expression in BCE and FNA cells on day 2 ($p<0.05$), followed by evident increase of PFNA ($p<0.05$) on the subsequent week. Moreover, a major significant difference of osterix expression in PFNA cells over BCE and FNA cells was detected on day 21 of bone induction. Interestingly, qRT-PCR also revealed that upregulation of osteopontin expression was only detectable in both heterogeneous cultures (BCE and PFNA) after 21 days culture in osteogenic medium, with significant changes reported on day 21 ($p<0.01$) and day 28 ($p<0.01$), whereas osteopontin was downregulated in clonal bone marrow cultures (FNA) throughout the 28 days of bone induction period.

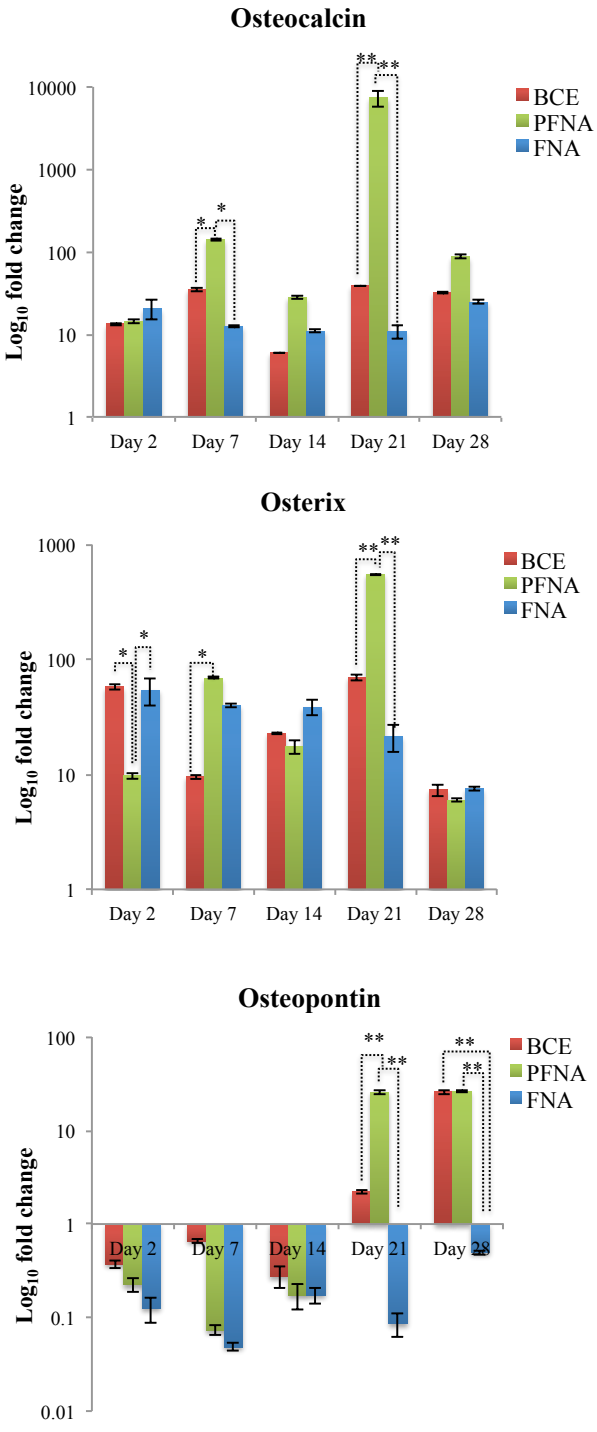

Figure 2.9 Gene expression of osteoblast markers in MSCs at 50PDs. Values were normalised to the expression of β-actin and expression in 28 days osteogenic-induced medium is presented as the fold increase or decrease of that in basal, non-differentiating medium, at day 0. Each bar represent mean fold change±SD. N=2, n=3 and *p<0.05, **p<0.01. All p values were based on two-way ANOVA. BCE, bone chips explant MSCs; PFNA, plastic and fibronectin adherence BMMSCs; FNA, Histopaque® and fibronectin adherence clonal BMMSCs.

2.2.2.3 Adipogenic differentiation and formation of lipid vacuoles

Adipogenic differentiation was successfully induced in the expanded mesenchymal stem cell cultures, by treatment with dexamethasone, insulin, indomethacin and 1-methyl-3-isobutylxanthine. 14 days after induction, the cultured MSCs were successfully stained for the accumulation of lipid-rich vacuoles with LipidTox™ green neutral lipid stain, as demonstrated in Figure 2.10 (a-c). Similar adipocytes staining patterns were obtained with Oil Red O, by detection of red lipid droplets in sample, as shown in Figure 2.10 (d-f). All MSCs induced into differentiation with specific adipogenic medium, demonstrated high potential and capacity to develop into adipocytes lineage cells in culture. The bone marrow MSCs, both PFNA and FNA, showed higher capacity to form adipocytes as the accumulation of lipid vesicles were observed as early as 7 days in culture, in comparison to compact bone-derived MSCs which took a minimum of 11 days to form the lipid droplets. In addition, the observed formation of lipid vacuoles in bone marrow MSCs were found to be much larger in size at day 14, in comparison to the lipid vacuoles formed in compact bone MSCs. Longer treatment in the adipogenic medium resulted in MSC fat-committed lineages, supporting further development of lipid vacuoles formation, which eventually merged and filled up the whole cell. However, the prolongation culture of bone marrow MSCs in the adipogenic medium for more than 16 days, revealed cells rupture due to the progressive droplet formation within these cell populations (data not shown). Therefore, adipogenic induction for 14 days was specifically chosen for this study.

Adipogenic differentiation was further confirmed by RT-PCR analysis, which demonstrated the positive expression of PPARγ, lipoprotein lipase, adiponectin and C/EBPα, as illustrated in Figure 2.11. However, MSCs cultured in basal medium (day 0) also demonstrated positive expression of C/EBPα and lipoprotein lipase, whereas clonal bone marrow cells (FNA) only showed faint expression of adiponectin before the adipogenic treatment.

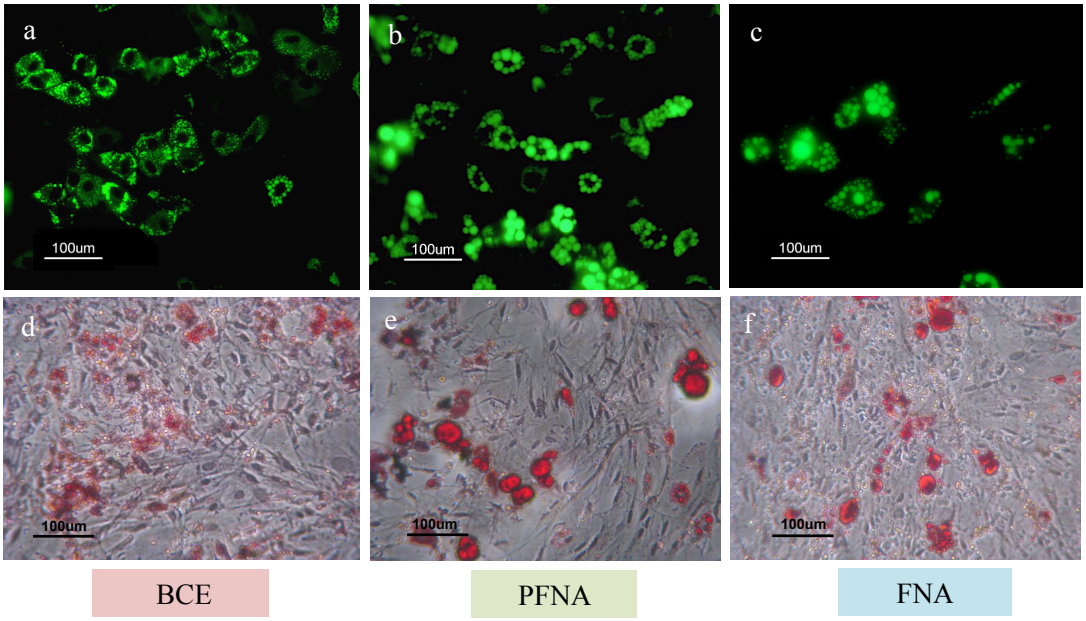

Figure 2.10 Differentiation of MSCs (PD50) isolated from rats bone marrow and compact bone and cultured in adipogenic medium for 14 days before staining with LipidTox™ (a-c) and Oil Red O (d-f). The green and red coloured droplets represent lipid deposition in MSCs, following adipogenic induction. BCE, bone chips explant MSCs; PFNA, plastic and fibronectin adherence BMMSCs; FNA, Histopaque® and fibronectin adherence clonal BMMSCs.

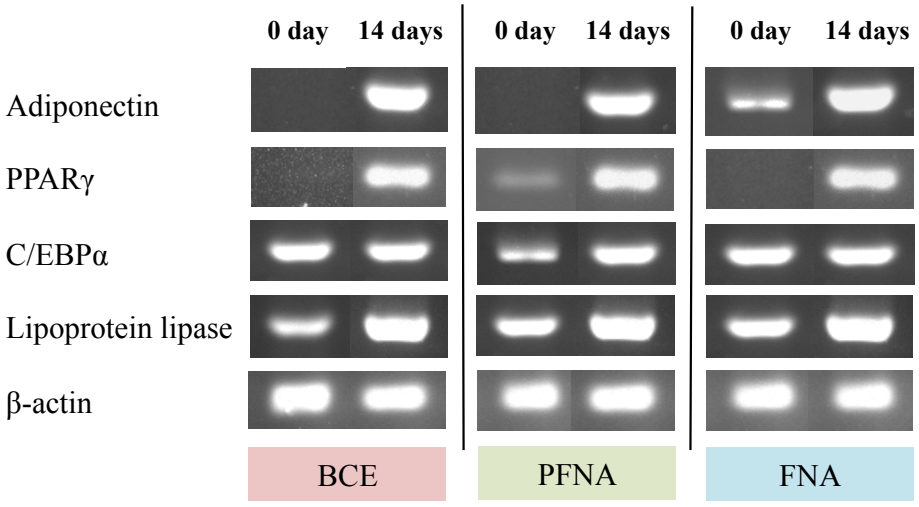

Figure 2.11 Expression of adipocyte cell surface markers. mRNA isolated from bone marrow and compact bone, grown in adipogenic medium, was subjected to RT-PCR analysis. The expression of adipogenic cell markers (adiponectin, PPARγ and lipoprotein lipase) and transcription factor, C/EBPα was detected following 14 days adipogenic induction. (N=2, n=2). BCE, bone chips explant MSCs; PFNA, plastic and fibronectin adherence BMMSCs; FNA, Histopaque® and fibronectin adherence clonal BMMSCs.

2.2.2.4 Quantitative analysis of MSC adipogenic gene expression

Quantitative real-time RT-PCR was performed to examine in further details whether gene expression profiles detected by RT-PCR analysis (Section 2.2.1.3) correlated with changes in the expression of adipogenic related gene markers on a time-based analysis (Figure 2.12). In all tested MSC samples, expression of fatty acid binding protein 4 (FABP4) demonstrated gradual upregulation beginning from day 2, with a marked 1000-fold increase on day 14, with BCE and PFNA significantly demonstrated higher fold change of gene expression compared to clonal bone marrow MSCs ($p<0.01$). The same pattern of elevated gene expression was also identified for transcription factor, C/EBPα, with a 10-fold increase of expression on day 14, with a significant higher expression reported in BCE compared to PFNA and FNA ($p<0.05$). However, adipocytes from the cultured MSCs demonstrated slight variation in the expression of lipoprotein lipase, as the clonal FNA cells showed a consistent high fold expression of lipoprotein lipase ($p<0.01$) from the beginning until the completion of treatment, as opposed to significant lower fold change of lipoprotein lipase seen in PFNA and in particular, CBE cells which indicate a downregulation of lipoprotein lipase on day 2.

Interestingly, qRT-PCR also revealed that 2 days after the induction, adiponectin level in PFNA cells was significantly increased by 44-fold change, whereas in both heterogeneous samples (BCE and PFNA), adiponectin mRNA level was barely detectable. At 14 day, as the MSCs progressed along the adipogenic lineage, endogenous adiponectin level in clonal FNA group has significantly upregulated by 10-fold change compared to BCE and PFNA ($p<0.05$).

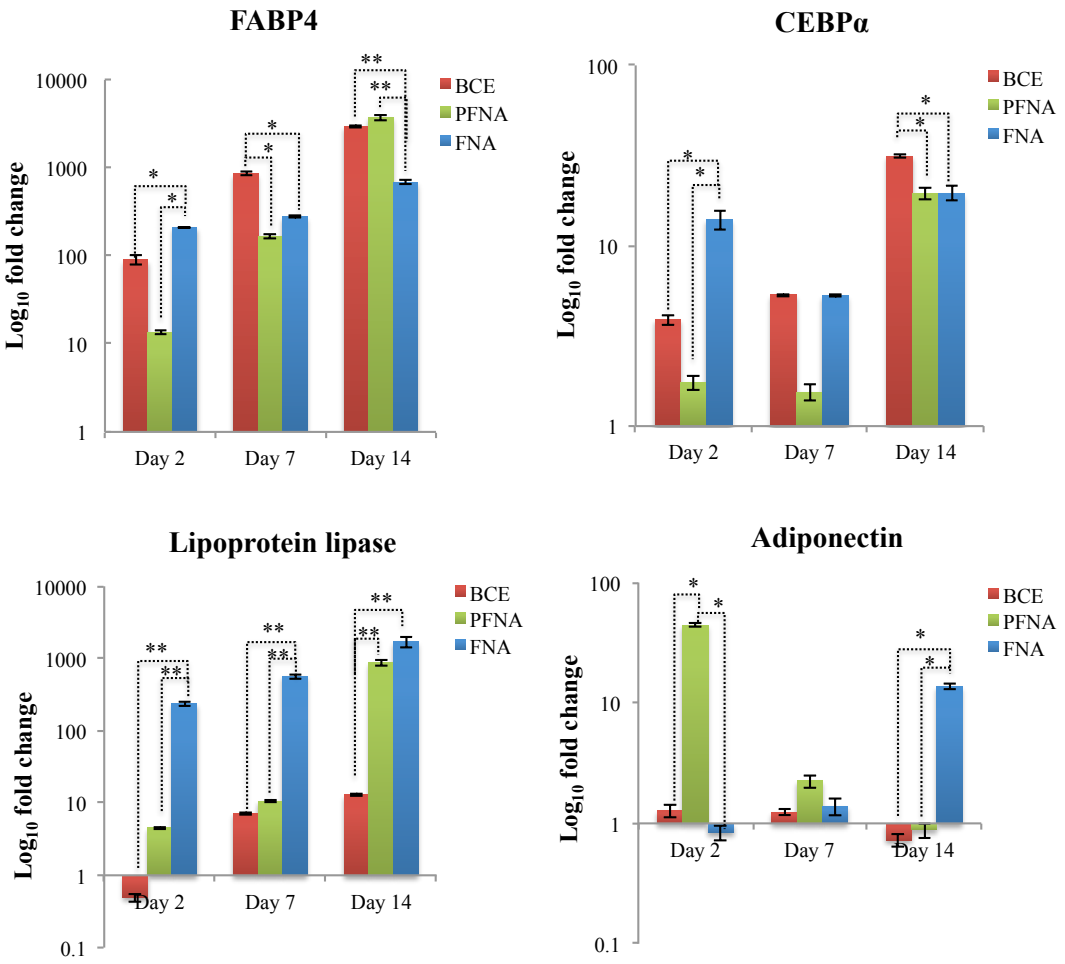

Figure 2.12 Gene expression of adipogenic markers in MSCs at 50PDs. Values were normalised to the expression of β-actin and expression in 14 days adipogenic-induced medium is presented as the fold increase or decrease of that in basal medium. Each bar represent mean fold change±SD. N=1, n=3 and *p<0.05, **p<0.01. All p values were based on two-way ANOVA. FABP4, fatty acid binding protein-4; C/EBPα, CCAAT enhancer binding protein alpha; LPL, lipoprotein lipase. BCE, bone chips explant MSCs; PFNA, plastic and fibronectin adherence BMMSCs; FNA, Histopaque® and fibronectin adherence clonal BMMSCs.

2.3 Discussion

This is a novel comparative study pertaining to isolation, expansion, and characterisation of MSCs from bone marrow and bone chip explants, which does not only combine and compare the application of fibronectin adherence selection with or without gradient density method, but also examines the different niches of bone-derived mesenchymal progenitor cells collected from rats. The data presented in this study portray the purification of adult mesenchymal progenitor cell populations from rats' bone marrow and bone chip explants, providing detailed analysis of the more advantageous protocol for the purification of proliferative MSCs precursors, with the capability of maintaining pluripotency during long-term *in vitro* culture. In addition to cell surface markers expression analysis, the study was extended by fully demonstrating the MSC differentiation properties along two classical mesenchymal pathways; the osteoblastic and the adipocytic lineages. The complete characterisation, along with the multipotency assessment, further allowed for an appropriate definitive hierarchy of these cells, as committed progenitor cells or multipotent MSCs (Bianco and Robey 2000, 2004; Kuznetsov et al. 2004). The most striking finding of the present study had been the discovery of multipotent progenitor cells population derived from bone chips explant culture, which exhibited great proliferative capacity in long-term expansion of *in vitro* culture.

From these observations, all three isolation methods applied in this study led to the successful selection of clonal and non-clonal MSC populations, from both bone marrow and bone chip explant cultures. The combination of gradient density fractionation and fibronectin adherence method permitted the establishment of homogenous MSC populations, with limitation in terms of starting cell numbers due to lower densities of clones observed in culture (data not shown). Interestingly, the clonal MSC expansion demonstrated major differences in terms of cell morphologies, length of the lag-phase, and total cumulative PDs, indicating variations among the isolated clonogenic populations, as suggested by the vast majority of MSCs studies (Caplan 1997; Colter et al. 2001; Harrington et al. 2014). The demonstrated higher proliferation and differentiative capacities of bone marrow clonal cells population in this study might be associated with the proposed hierarchical position of the transit, amplifying cells in relation to the mother stem

cells, as demonstrated in earlier bone marrow clonal cells study (Harrington et al. 2014). Of note, the two morphologically distinct clonal bone marrow MSC observed in separate homogenous culture showed huge discrepancies in their proliferation rates, as the fibroblastoid shaped cells exhibited speedy expansion capacity, whilst the stellate-shaped and wide nucleated cells grew at a slower rate. The presence of stellate cells in culture also suggested the differentiation state of the cells, as shown in cultured pancreatic stellate cells derived from bone marrow and mature osteoblastic culture (Colter et al. 2001; Sparmann et al. 2010). The differences between these two types of cells, with diverse phenotype and growth pattern in *in vitro* cultures has been reported in human and mouse bone marrow MSC cultures (Karaoz et al. 2009; Karaöz et al. 2011; Mareschi et al. 2012). Owing to the increasing trials for application of MSCs in reparative treatments, more cell culture studies have now focus on identifying a rapid and straightforward method for isolating multipotent MSCs. Hence, the disadvantages of using density gradient techniques over plating whole bone marrow stromal cells was shown, as the latter techniques were found to provide higher colony forming efficiency and allowed remarkable expansions of mesenchymal progenitor cells, following the initial plating step (Capelli et al. 2009; Mareschi et al. 2012). Evidence from previous studies also suggests that only a small fraction of clonal bone marrow MSCs has the ability to expand >20 PDs, while maintaining the high proliferative potential, genuine character of MSCs in subsequent passage (Menicanin et al. 2010; Jones and Yang 2011). Taking that into consideration, the application of density gradient techniques possibly acted as a limitation factor in terms of the starting cell numbers for MSCs isolation strategy, with clonal bone marrow MSCs population also exhibited clear evidences of specific MSCs character, showing distinct proliferation rate over the whole cultivation period, thus limiting the potentiality of these cells populations to be used in general cell culture studies due to the presence of variations among clonal bone marrow MSCs.

Therefore, the next experimental approach was initiated based on the modification of previously published protocols, which described isolation of heterogeneous MSCs from either bone marrow or bone explant culture, but without any further long-term cell culture expansion, characterisation or differentiation potentialities (Bruder et al.

1998; Sung et al. 2008; Nakamura et al. 2010b; Huang et al. 2012). The isolation of heterogeneous bone marrow MSCs, which was performed by overnight plating of whole bone marrow stromal onto plastic followed by re-plating the adherence cells onto fibronectin-coated wells, had been proven to positively purify multipotent MSCs. Application of fibronectin in MSCs study was first demonstrated by Jones and Watt (1993), by manipulating the binding capacity of immature progenitor cells towards the RGD domain of fibronectin via cell-surface $\alpha_5\beta_1$ integrin. Recent studies on fibronectin adherence selection performed with $CD14^+$ monocytes demonstrated the presence of multipotential cells within isolated cultures, showing similar morphologic, phenotypic, and functional characteristics of mesenchymal cell types, indicating the potential use of fibronectin in purifying primitive cell populations within multi-differentiation monocytic-derived cells (Seta et al. 2013). However, the detailed processes of intracellular signal transduction via this $\alpha_5\beta_1$ integrin are still unclear due to the use of commercially available fibronectin in many isolation studies, leading to the possible effects of fibronectin degradation products that act by inducing cytokines secretion from progenitor cells rather than intact fibronectin (Feghali and Grenier 2012). Interestingly, the applied technique of digested bone chips explant cultures also exhibited similar success in isolating heterogeneous MSC populations, representing a unique population derived from skeletal tissue, with promising features of multipotent capacity. Hence, based on the total cumulative population doubling levels, the isolated bone chips explant cells (BCE) and bone marrow derived cells (PFNA) demonstrated consistent expandability over prolonged culture periods, respectively. Early culture of heterogeneous MSCs from both tissue sources showed the presence of mixed cell populations in culture, with distinct morphological features that potentially represented the primitive cells, tissue-committed cells, transit amplifying cells or differentiating cells. However, the analysis of mid- and late- PDs MSCs demonstrated the uniform appearance of spindle-shaped cells, which gradually replaced the earlier broad-shaped cells in the culture.

Taken together, the results obtained from this study demonstrated the presence of relevant differences among the different isolated groups, though all the tested MSC populations clearly showed evidence of long-term expansion with highly

proliferative capacity. It was observed that the initial number of heterogeneous MSCs from both bone and bone marrow was likely to be higher, while the proliferation rate was more consistent for each batch of isolated cells compared to homogenous bone marrow MSC populations, as described for human bone marrow MSCs and rat bone marrow MSC studies (Krebsbach et al. 2003; Karaoz et al. 2009). Apart from the different isolation methods, cell heterogeneity, a potential variation, may also be present between the isolated MSCs because they originated from different niche environments, such as the endosteum or periosteum, which consisted of diverse subpopulations, offering various roles in maintenance and supporting the initial growth of cultured MSCs. Rat MSCs isolated by the various techniques in this study also showed similar proliferation ability as human MSCs, if not better in terms of high number of passages and population doubling levels without losing their high clonogenic potential, prime antigenic markers, and differentiation ability throughout the analysed culture period, as opposed to a lower proliferation rate reported in human bone marrow MSCs studies (Muraglia et al. 2000; Tong et al. 2007). However, the major differences seen between human isolated MSCs and rats isolated MSCs in this study may potentially indicate the variation that existed between cells derived from various species.

Regardless of cell origin and isolation techniques, all the purified MSCs populations were found to be positive for selected MSCs markers; CD105 (endoglin), CD90 (Thy-1), and CD73 (ecto-5-nucleotidase), indicating that they were indeed of mesenchyme origin. Nevertheless, no contaminated CD45 hematopoietic cell population was observed throughout the whole culture period, but the presence of CD34+ cells was detected in both early heterogeneous MSCs cultures. In agreement with results obtained from other murine bone marrow MSCs studies, the weak presentation hematopoietic markers in early passage for heterogeneous MSCs, suggested the presence of undefined cells that potentially supported the rapid expansion of isolated cells during *in vitro* culture (Mareschi et al. 2012). Apart from that, CD34+ cells have the ability to transform into CD34- cells in experimental culture, suggesting that CD34 antigen may also serve to define activated stem cells, rather than conclude their hematopoietic origin. Even though it might not be applicable for all adult MSCs, the activation of CD34+ cells hypothetically correlated with the stimulation of hematopoietic components, which directly

controlled the self-renewal activity, as well as proliferative and differentiation capacities of immature cells. Thus, it is important to take this into consideration, as a similar pattern of CD34+ expression was found in both cultured heterogeneous MSCs during earlier culture, which suggested the possible existence of activated CD34+ stem cells that potentially supported the feasibility of primitive MSCs manipulation in the early stages of cell cultivation.

Other than that, the analysis of embryonic stem cells markers in all isolated MSC populations demonstrated the consistent expression of Nanog at all stages of culture, regardless of cell isolation techniques and MSC origin. Furthermore, only BCE MSCs taken from early culture were found to be positive for the expression of Oct4, suggesting a unique characteristics of bone-derived cells originated from the cortical bone niche, comprised of bone-lining cells with heterogeneity in function and degree of differentiation, as demonstrated in other MSCs studies (Kiel and Morrison, 2008; Yin and Li, 2006). In addition, certain Sca-1 populations, derived from compact bone, were found to support the enrichment of osteoblastic markers and differentiation potential, indirectly suggesting the localization of MSCs and skeletal progenitor within the perivascular niche of bone (Nakamura et al. 2010b). The unique heterogeneity observed in early culture of BCE MSCs may also correlate with the presence of contaminating satellite cells in cultured populations. Satellite cells are widely isolated using collagenase digestion, grown in 20% of FBS culture medium with preferential adherence to plastic or ECM component-coated surfaces; and enrichment using $CD45^{-}CD34^{+}$ markers (Danoviz and Yablonka-Reuveni 2012). Therefore, it may be assumed that MSCs derived from bone chips explants contain mixed sub-population of pre-osteoblastic cells, some of which might be immature niche cells that are capable of expressing pluripotent marker–related genes; and other progenitor populations that possess restricted proliferative and differentiation potentials, compared to bone marrow localized, and primitive MSCs.

Meanwhile, Runx2 was reported to promote osteoblast differentiation at an early stage of induction, but inhibited terminal osteoblast differentiation (Komori 2002), whereas endogenous Runx2 expression was detected in non-osteoblastic cells, without activating the differentiation process, suggesting the unknown mechanism in

regulating its expression (Komori et al. 1997). Besides, inhibition of Smad3 in primary cells was reported to induce activation of Runx2 in non-conditioned medium (Hjelmeland et al. 2005). Significantly, Smad3 phosphorylation decreased in cirrhotic rats after bone marrow MSC treatment, suggesting the potential role of bone marrow MSCs in inhibiting Smad3 phosphorylation through modulation of the TGF-β_1/Smad signalling pathway (Jang et al. 2014). Irrespective of population doubling levels, all isolated MSCs in this study showed strong positive expression of Runx2 during expansion culture in basal medium, suggesting the inhibition of Smad3 expression in the isolated MSC populations, which led to the endogenous expression of Runx2 without stimulating osteogenic differentiation.

The mesenchymal cells described in this study had been presented with bi-potential differentiation capacity towards osteogenic and adipogenic lineages, with the presence of variable inductive capabilities. This is in agreement with recent evidence from adult MSCs studies, which proposed the theory of 'trans-differentiation' in stem cells to explain MSCs ability to re-differentiate and de-differentiate into alternate mesenchymal lineages, by solely manipulating and changing the induction medium (Song and Tuan 2004). All isolated MSCs in this study possessed the osteogenic potential, shown by positive expression of osteogenic differentiation and transcription markers, such as osteocalcin, osteopontin, and osterix. The isolated cell populations also exhibited similar patterns of morphological changes during the osteogenic induction process, as previously mentioned in another study conducted by Arrigoni et al. (2009), which indicated alteration from fibroblastic-like shape cells to a rounder cuboidal shape during osteogenic differentiation process. The observed formation of calcified extracellular matrix by alizarin red staining, demonstrated a high capacity of heterogeneous bone marrow MSCs to form bone nodules, with signs of calcified tissue after just 7 days in culture, compared to clonal bone marrow MSCs, which took longer time to produce bone nodules in osteogenic culture. Further analysis via qRT-PCR reported the downregulation of osteopontin in clonal MSCs even after 28 days of osteogenic induction, along with the low expression of osteocalcin and osterix, in comparison to upregulation of all osteoblastic markers in both BCE and PFNA cells populations, with significant differences of fold change expression reported on day 21 (p<0.01). These findings suggested that the clonal

bone marrow MSCs isolated and characterised in this study represented a restricted capacity to differentiate into bone. Moreover, it had been demonstrated in previous studies that only 31-33% of the established clonal bone marrow stem cell populations exhibited *in vivo* bone formed capacity (Kuznetsov et al. 1997; Prins et al. 2014).

From the RT-PCR analysis, the observed high expressions of PPARγ in all MSCs populations following 14 days of culture in adipogenic medium suggested that the isolated cells possessed the capacity to induce key regulator in adipogenesis, PPARγ. In fact, the positive expression of C/EBPα and lipoprotein lipase by confluent MSCs cultured in basal medium, may suggest spontaneous adipogenic differentiation of the cells. In fact, recent findings indicated that the presence of ascorbic acid in pre-adipocytes populations, as applied in this study, might enhance adipogenesis through the upregulation of transcription factor, C/EBPα (Kim et al. 2013). Apart from demonstrating low capacity to form bone nodules during osteogenic differentiation, the low expression of adiponectin observed in basal medium of clonal bone marrow MSCs, might indicate the commitment of these FNA cells towards adipogenesis, as adiponectin is rather well-known in promoting adipocyte differentiation, insulin sensitivity, and lipid accumulation in progenitor cells (Fu et al. 2005; Abbassy et al. 2010; Shin et al. 2012). Within this study, the heterogeneous MSC populations significantly demonstrated 1000-fold change increased expression of FABP4, after 14 days of adipogenic differentiation compared to the clonal MSC ($p<0.01$). The upregulation of FABP4 expression was observed on day 2 and gradually increased as the adipocytes reached the maturity stage. Hence, the presented results further supported findings of similar previous studies, which demonstrated FABP4 expression in mature adipocytes, which play an important role in lipid metabolism and homeostasis (Elmasri et al. 2009). A significant elevation of lipogenic enzyme, lipoprotein lipase, was observed in bone marrow-derived MSCs, compared to bone chip explants cells, indicating the differences in lipid metabolism and transport between adipocytes differentiated from bone marrow and periosteum-derived progenitor cells. Similarly, enhanced capacity of bone marrow MSCs to express lipoprotein lipase compared to bone explants MSCs, following adipogenic induction was demonstrated in human cell study (Eyckmans et al. 2012). In light of the significant findings derived from this study, it is reasonably appropriate to include

adiponectin and osterix for osteogenic and adipogenic differentiation analysis of stem cells, to conclusively define the pro-lineage commitment of the cells, due to the complexity of progenitor cells behaviour in various *in vitro* culture conditions.

Together, the results gathered from this chapter have provided important insights in understanding the cellular characteristics of clonal and non-clonal derived MSCs, from either bone marrow or bone explant cultures, with respect to their proliferative and differentiation capacities. These MSC populations were assessed after cryopreservation and no difference was observed at any passage time-point, following the initial isolation period, suggesting their potential use for bone repair and regeneration. In addition, the simplicity of the protocols for the isolation of MSCs from digested bone chip explants acted as another promising platform for obtaining characterised skeletal stem cells for bone repair studies. In fact, bone chip explant MSCs possessed an outstanding proliferative capacity and differentiation potential into osteogenic and adipogenic lineages, which indicated the prospective application of these cells for the development of an *in vitro* disease model, such as Type 2 Diabetes Mellitus. Therefore, investigation depicted in the next Chapter investigated the effects of high glucose medium on proliferation and differentiation potentials of bone chip explant MSCs to characterise the behaviour of the cells within diabetic environment and further elucidate their role in diabetic bone repair.

Chapter 3

Effect of High Glucose Level on Expansion Cultures of Bone Chip Explant-Derived, Mesenchymal Stem Cells

3.0 Introduction

MSCs have been isolated from various adult tissues and organs, demonstrating the ability to differentiate into multiple mesodermal cell types, such as osteoblasts, adipocytes, chondrocytes, hepatocytes, and neuronal cells (Mareschi et al. 2012; Sharma et al. 2014). The immunosuppressive properties of these cells also offer great potential in improving transplantation tolerance (Ding et al. 2010). The extended knowledge on stem cells metabolism has facilitate in treating a wide variety of diseases, such as myocardial infarction, diabetes, and Parkinson's disease (Lovell-Badge 2001; Kuo et al. 2011; Choudhery et al. 2012). Moreover, the promising hope of stem cell replacement therapy has extended to tissue regeneration and repair during bone, spinal cord, periodontal, and craniofacial reconstructive procedures.

High glucose levels act as an independent risk factor for short- and long-term deterioration in the progression of micro-vascular damage in the affected organs (as reviewed by Rolo and Palmeira in 2006). *In vivo*, chronic hyperglycaemia had been proven to have detrimental effects on insulin secretion by limiting the response of cellular glucose uptake level (Rossetti et al. 1987). In fact, most studies that investigated the influence of hyperglycaemia on cellular behaviour were performed *in vitro*, with the assumption that glucotoxicity-induced in culture might reflect the actual mechanisms with *in vivo* systems. High glucose is associated with induction of early senescence and potentially leads to numerous perturbations in cellular behaviour and metabolic activity in the skeletal system (Stolzing et al. 2006). Experimental data suggested reductions in cells proliferative capacity in high glucose concentrations, followed by preferential differentiative capacity of cells towards adipogenic lineages, while both osteogenic and chondrogenic potentials were suppressed (Dominici et al. 2006; Cramer et al. 2010). Osteoblastic culture in high glucose medium also displayed a marked reduction in the number of nodules formed and calcium deposition (Zhen et al. 2010). In fact, both murine and primate stem cell studies demonstrated impaired interplay between osteoblast and osteoclast lineages in hyperglycaemic condition (Steiler et al. 2003).

The actual mechanism by which high glucose-levels might have altered MSC behaviour in both *in vivo* and *in vitro* systems is still unclear. High glucose increased

osteoprotegerin (OPG) expression over RANKL, while suppressed ALP production, induced defects in matrix mineralisation and led to impaired bone remodelling (Cunha et al. 2014). Furthermore, it had been found that hyperglycaemia stimulated the production of reactive oxygen species (ROS) and the secretion of growth factors; TGF-β_1 through PKC and hexosamine pathways (Kolm-Litty et al. 1998; Inoguchi et al. 2000). In other studies, high glucose levels were shown to reduce Runx2 expression in stem cells, which resulted in altered wound healing through AR polyol pathway (D'Souza et al. 2009). In T2DM models, alterations in mitochondrial DNA and oxidative stress had been associated with glucose-stimulated and insulin resistance of β-cell (Rolo and Palmeira 2006). Persistent exposure to high glucose levels increased ROS and the production of advance glycated end products (AGEs) (Kume et al. 2005). Moreover, prolonged high glucose levels also inhibited stem cell function and proliferative capacity; besides inducing apoptosis through production of ROS (Li et al. 2007; Petrelli et al. 2012). High glucose levels and hyperosmotic conditions were also involved in provoking increased susceptibility of osteoblastic cells towards osmotic stress, leading to somatic reprogramming of stem cells (Madonna et al. 2013).

Although hyperglycaemia is known to represent a major feature in diabetic progress, the on-going debate about hypothetical effect of high glucose on MSCs functions has remained controversial. High glucose had been reported to enhance the ESCs proliferations growth (Kim et al. 2006), but decreased that in rat MSCs (Stolzing et al. 2012). Meanwhile, glucose has no effect on proliferation of human bone marrow-derived MSCs (Weil et al. 2009). These contradictory findings serve as important evidence to further investigate the critical use of stem cells as treatment in disease conditions associated with high glucose environments, elucidating the actual mechanisms involved in alterations to progenitor cells growth and function.

Moreover, bone-derived MSCs have only been studied in recent years, owing to the successful isolation and characterisation of these progenitor cells from trabecular bone chip explant culture of murine and human origin (Nöth et al. 2002; Sottile et al. 2002; Guo et al. 2006; Zhu et al. 2010). Bone-derived MSCs have demonstrated the capacity for *in vitro* multilineage differentiation and offer remarkable potential for application in tissue engineered therapy, as well as the development of

musculoskeletal disease model, due to their straightforward isolation protocols, highly proliferative features, and great differentiation capacity into mesenchymal lineages. However, little is known about the main elements in typical cell culture medium, such as glucose, which provides the main fuel source for bone chip explant MSCs and a great potential in affecting cells proliferation rate, as well as differentiation capacity.

In spite of recent advance in using MSCs as key components in cell-based therapy for treating degenerative disorders and accelerating repair of tissue injury, studies providing an exhaustive model of glucose-induced toxicity in 2D culture are still lacking. Precisely, the most strategic way to improve MSC-based therapies for skeletal repair with diabetes complications must first embrace a deeper insight on the influence of glucose on MSCs, even prior to their clinical administration. To date, this issue is only partially discovered. Therefore, further understanding on the effects of glucose on MSCs does not only assist in identifying and clarifying the pathophysiology of hyperglycaemia, but more importantly, it provides an alternative approach in minimising the impact that glucose has on the metabolism and the therapeutic potential of MSC populations.

With that, this chapter offers understanding of bone progenitor cells proliferation and survival, in response to hyperglycaemic conditions, and further elucidates if the diabetic environment significantly promoted alterations in cellular behaviour. The information gained from this study would further assist in our better understanding of cellular and biological functions of MSCs, for application in disease models, and regenerative therapies.

3.1 Materials and Methods

3.1.1 Animals

Briefly, bone explants were obtained from the femurs and humerus bone of 28 days Wistar rats, as described in Section 2.1.1.

3.1.2 Cell culture

The previous chapter provided details about the isolation, expansion and characterisation of MSCs derived from rat bone chips explants, as described in Section 2.1.1.3. Bone chip explant MSCs showed great potential in maintaining high proliferative rate in long-term culture, without losing the prime features of differentiation along the osteogenic lineage. Within this chapter, bone chip explant MSCs (BCE-MSCs) taken from population doubling levels (PD) 10 of earlier cultures, were thawed from nitrogen storage and maintained for ~200days in different glucose level medium, to monitor the effect of high glucose level on MSCs proliferation potential and differentiation capacity. The experimental culture was incubated in high-glucose culture medium (HGCM), which consisting of complete culture medium (CCM, as described in Section 2.1.1.1) supplemented with sterile D-glucose 100g/L (Sigma Aldrich, Dorset, UK) to reach a final concentration of 25.0mM glucose. Meanwhile, experimental control of BCE-MSCs was maintained in CCM (5.5mM glucose). Both cultured BCE-MSCs was incubated at 37^{o}C in a humidified atmosphere containing 5% CO_2. Images of cultured cells were captured using light microscopy at each PD.

3.1.3 Assessment of cell proliferative capacity

PDs of BCE-MSCs cultures were assessed, as described in Section 2.1.1.4, up to 200 days.

3.1.4 Differentiation along the osteogenic lineage and assessment of bone formation

Prior to osteogenic differentiation, BCE-MSCs taken at PD50 and PD150 for each cell population were plated at 4000 cells/cm^2 in 6-well plates (for RNA extraction and immunohistochemical analysis) and also in T25 flask (for protein extraction).

The cells were cultured in either CCM or HGCM for 24hr, prior to supplementation of osteogenic induction medium. BCE-MSCs were differentiated for 28 days in either 5.5mM control osteogenic medium (COM), as described in Section 2.1.3.2; or D-glucose (Sigma Aldrich) supplemented 25.0mM high-glucose osteogenic medium (HGOM), with 2 to 3 days change of culture medium. At day 28, adhered cells in the 6-well plate were prepared for cellular staining with Alizarin Red (as performed in Section 2.1.5.1). RNA was extracted (as described in Section 2.1.4.4) from cultured BCE-MSCs on day 2, 7, 14, 21 and 28, to assess the temporal expression of osteogenic-related differentiation gene markers, osteocalcin (OCN), osteopontin (OPN) and osterix (OSX) using qRT-PCR analysis (as described in Section 2.1.4.4). Details of the selected osteogenic differentiation markers are summarised in Table 3.1. RNA extraction and reverse transcription reactions were performed on the osteogenic and control-treated cultures, as described in Sections 2.1.3.3 and 2.1.3.4. PCR reactions were carried out using the same cycling condition as stated in Section 2.1.3.5, with exception to OCN, as the annealing temperature was set at 62°C. Control-treated culture, supplemented with CCM (as described in Section 2.1.1.1) was used as pre-differentiation negative control; and the RNA was collected once the culture reaches confluent. Meanwhile, another control culture was carried out alongside the differentiation culture to act as a negative control, supplemented with CCM for 28 days.

Table 3.1 Primer sequences and product sizes of selected osteogenic and adipogenic differential markers for qRT-PCR analysis.

Gene	cDNA sequence (5'-3') F, Forward; R, Reverse	Length (bp)	References
β-actin	F: GGGTCGAGTCCGCGTCCAC R: CGACGAGCGCAGCGATATC	108	Park et al. 1997
OCN	F: ACAGACAAGTCCCACACAGCAACT R: CCTGCTTGGACATGAAGGCTTTGT	161	Owen et al. 2012
OPN	F: TCCAAGGAGTATAAGCAGAGGGCCA R: CTCTTAGGGTCTAGGACTAGCTTGT	200	Singh et al. 1992
Osterix	F: GCTTTTCTGTGGCAAGAGGTTC R: CTGATGTTTGCTCAAGTGGTCG	136	Georgiou et al. 2012
LPL	F: AGGTCAGAGCCAAGAGAAGCA R: GGAGTAGGTTTTATTTGTGGCG	215	Levak-Frank et al. 1995
FABP4	F: GGAATTCGATGAAATCACCCC R: TGGTCGACTTTCCATCCCACT	104	Minoura et al. 2007
C/EBPα	F: GGGAGAACTCTAACTCCCCCAT R: CTCTGGAGGTGGCTGCTCATC	82	Calkhoven et al. 2000
Adiponectin	F: GAATCATTATGACGGCAGCAC R: CTTGGAGCCAGACTTGGTCTC	224	Puerta et al. 2002

3.1.5 Differentiation along the adipogenic lineage and assessment of lipid vacuoles formation

The CCM-treated and HGCM-treated BCE-MSCs were taken at PD50 and PD150 for adipogenic induction process. For adipogenesis, protocol was performed as previously described in Section 2.1.3.3. In addition, cells were also maintained in different glucose levels in adipogenic induction medium, with the addition of D-glucose at 5.5mM and 25.0mM, respectively. Along the adipogenic induction process, RNA extraction and qRT-PCR analysis was conducted on day 2, 7 and 14, to assess transcription of adipogenic genes, lipoprotein lipase (LPL), FABP4, C/EBPα and adiponectin during the induction procedure (as described in Sections 2.1.3.3 to 2.1.3.5). Details of the selected adipogenic differentiation markers are summarised in Table 3.1. On day 14, the cultured cells were processed for LipidTOX™ staining (Life Technologies, Paisley, UK) and images were viewed under UV microscopy, as previously described in Section 2.1.2.2. RNA extraction and reverse transcription reactions were performed on the adipogenic and control-treated cultures, as described in Sections 2.1.2.3 and 2.1.2.4. PCR reactions were carried out using the same cycling condition as stated in Section 2.1.3.5. Control-treated culture, supplemented with CCM (as described in Section 2.1.1.1) was used as a pre-differentiation negative control, and the RNA was collected once the culture reaches confluent. Meanwhile, another control culture was carried out alongside the differentiation culture to act as a negative control, supplemented with CCM for 28 days.

3.1.6 Statistical analysis

Values are expressed as means ± standard deviation (SD). Analyses were performed by the software package, SPSS 20.0 (IBM, NY, USA). The statistical significance of differences among experimental group was evaluated by two-way and three-way ANOVA followed by multiple comparison using Tukey's test with*$p<0.05$, **$p<0.01$ being considered statistically significant. The number of replicates used is stated in the figure legends.

3.2 Results

3.2.1 Morphology of bone chip explant MSCs in high glucose medium

Within this chapter, the study explored potential morphological changes of BCE-MSCs during long-term culture in control/normoglycaemic level (5.5mM) and hyperglycaemic level (25.0mM) culture medium. Over 200 days during the total expansion period, the cultured BCE-MSCs exhibited considerable alterations in cellular features as time increased. As displayed in Figure 3.1a and 3.1b, MSCs derived from early PD (PD15) demonstrated no difference in cell morphology between the different glucose cultures, with the presence of uniform spindle-like shaped cells when viewed under light microscopy. At PD50, cells of normoglycaemic-cultured medium (Figure 3.1c) exhibit the presence of heterogenous cells with two morphological phenotypes; with one group consist of thin, spindle-like features and another type with broadened cell body and shorter projectors. In contrast, PD50 HGCM-treated c consisted of cells with bigger nucleated bodies (Figure 3.1d). No difference was observed between PD150 BCE-MSCs cultured in normoglycaemic or hyperglycaemic treatments, as the cells demonstrated homogenous features with broadened, flat-shaped cells with dispersed cytoplasm (Figure 3.1e and 3.1f).

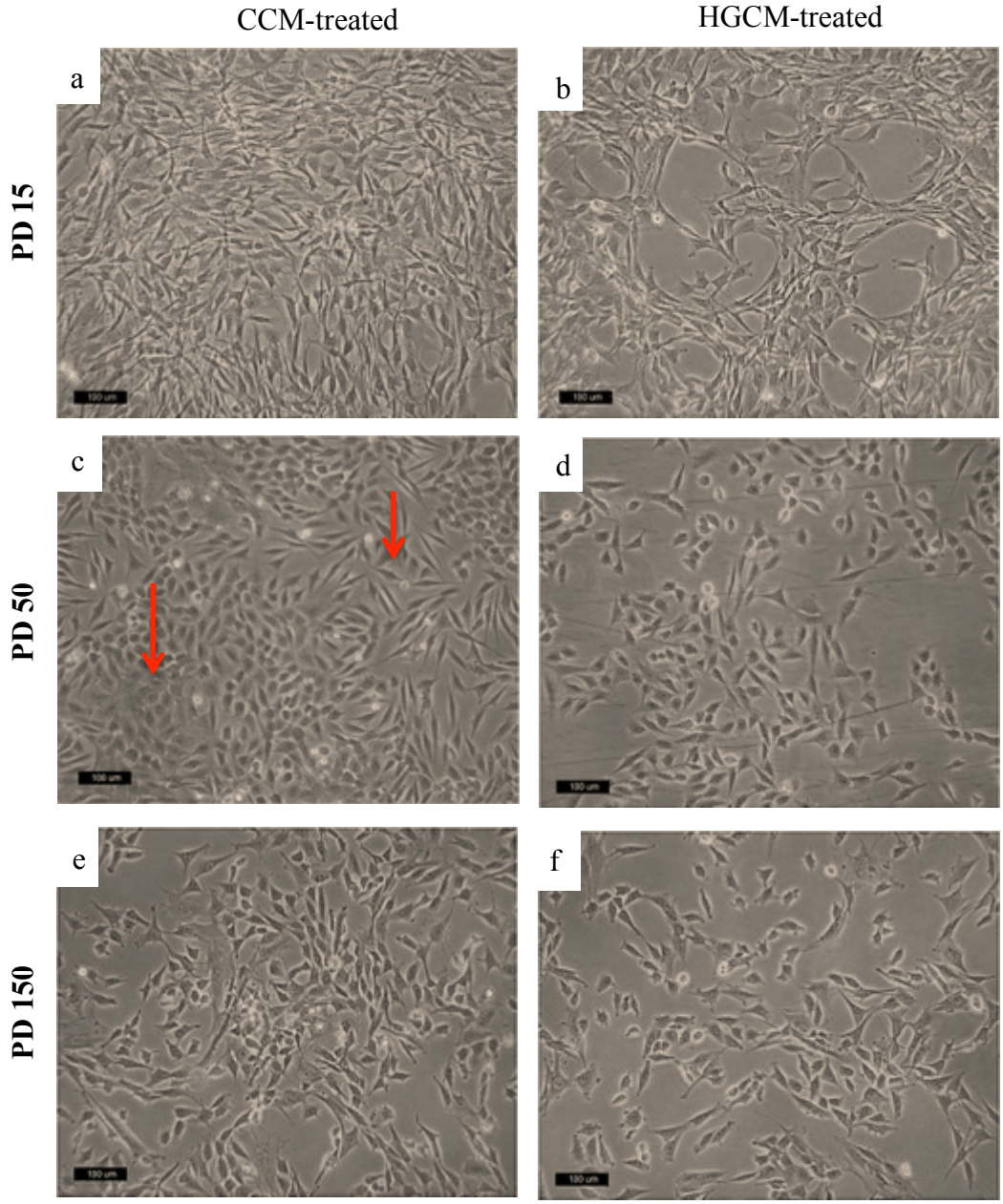

Figure 3.1 Morphology of long-term BCE-MSCs cultured in CCM (Figure 3.1 a,c and e) and in HGCM (Figure 3.1 b, d and f). Arrows indicate the presence of two distinct morphological phenotypes within the culture. PD, population doubling level; CCM, complete culture medium; HGCM, high-glucose culture medium.

3.2.2 Proliferative capacity of bone chip explant MCSs in different glucose level

The assessment of BCE-MSC PDs was performed to investigate the influence of high glucose concentration on cell expansion rates (Figure 3.2). Initially, high glucose concentrations were found to promote BCE-MSCs proliferation because within 58 days following initial incubation, cells cultured in high glucose level exhibit slight elevations in doubling time, in comparison to normoglycaemic medium. However, subsequent culture of BCE-MSCs in high glucose concentration demonstrated major discrepancies in proliferation rate, as the 5.5mM glucose-treated cells showed consistent highly proliferative capacity reaching up to 226 PDs in over 200 days, in contrast to high glucose-treated cells, which exhibited much lower doubling time (only 182 PDs) over the same experimental period. The data suggested that 25mM glucose medium has a notable effect on BCE-MSCs proliferation rate. Further analysis on cell doubling times revealed strong evidence of changes in the proliferative growth between different conditioned media. An average of 10.51 PD/week was recorded for CCM-treated cells, whereas much lower 8.89 PD/week reported in HGCM-treated cells. Although reduction of cells doubling time was seen during later stage of culture, BCE-MSCs cultured in both conditioned medium maintained a good proliferative capacity without showing signs of senescence. Collectively, the results suggested that increased glucose concentration in culture potentially decreased MSCs proliferation rate in long-term expansion culture.

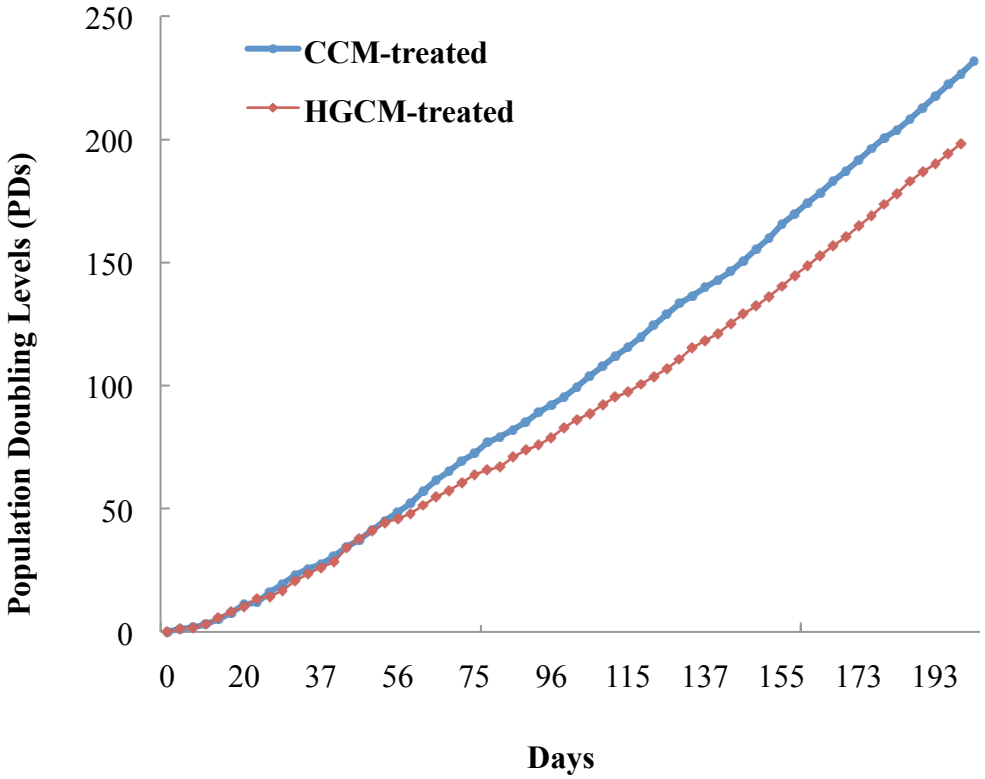

Figure 3.2 Cell proliferation of BCE-MSCs subjected to 5.5mM and 25.0mM glucose variations in culture. Cell doublings time for populations of CCM-treated and HGCM-treated BCE-MSCs during exponential growth for 200 days period of culture showed distinct proliferative capacity. Data is presented as calculated PDs at each time point, plotted on a linear scale. CCM, Complete culture medium; HGCM, High glucose culture medium.

3.2.3 Osteogenic staining of high glucose-cultured bone chip explant MSCs

As glucose level were known to effect differentiation capacity of adherent MSC cultures, the CCM-treated and HGCM-treated BCE-MSCs were further incubated for 28 days under two different osteogenic medium (OM) configurations; 5.5mM OM and 25.0mM OM. The early PD cell populations exhibited distinctive capacity to form bone nodules in both glucose level of osteoblastic medium (Figure 3.3a-d). In contrast, marked decreases in Alizarin red staining patterns were observed in BCE-MSCs at PD150, regardless of glucose supplementation in culture medium or induction medium (Figure 3.3 e-h), indicating an overall perturbations in BCE-MSC capacity to form new bone at higher PDs.

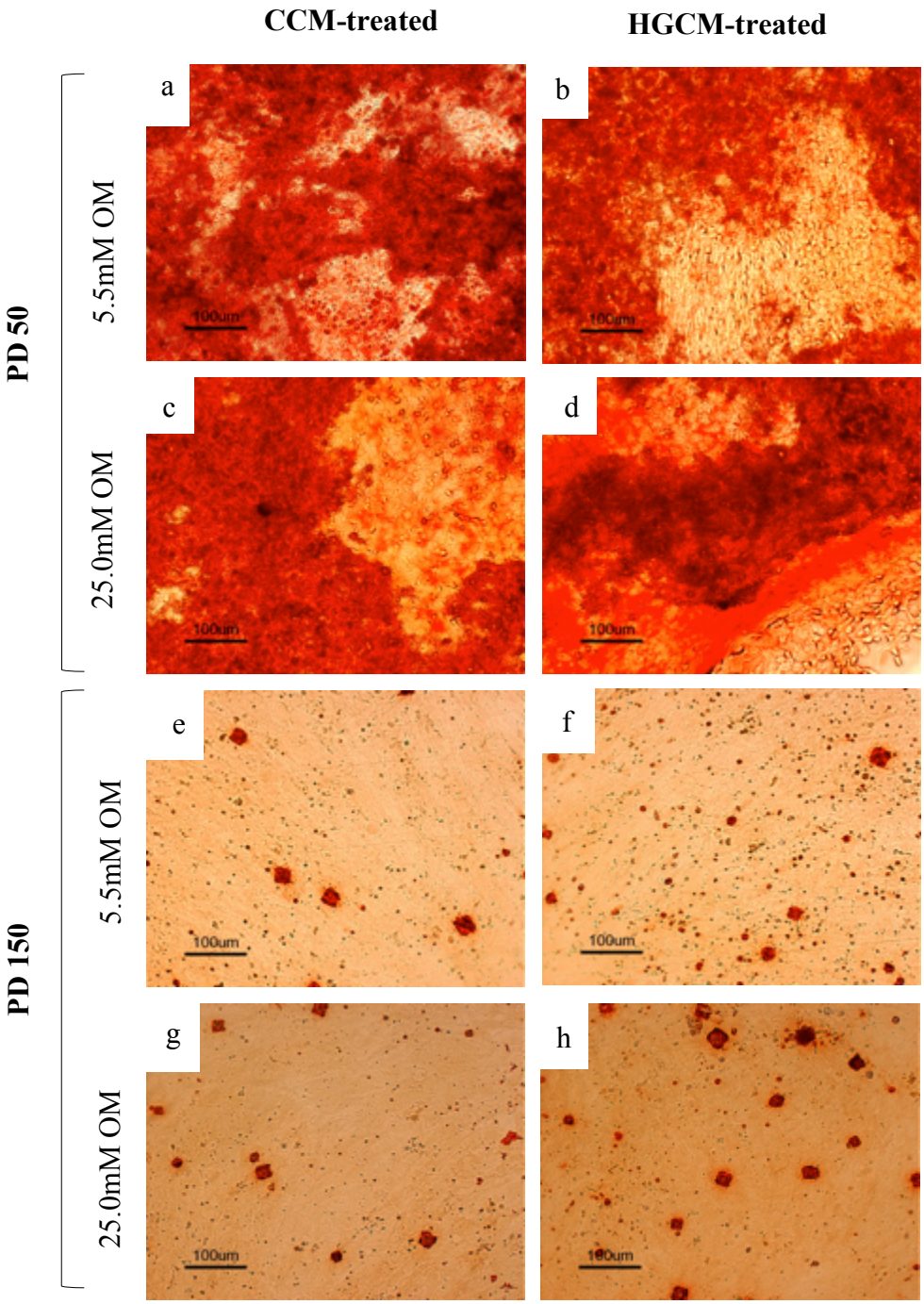

Figure 3.3 Histological analysis by light microscopy of CCM-treated and HGCM-treated BCE-MSCs. Monolayer cultures of early-PD (a-d) and late-PD (e-h) cells in six–well plates were induced for osteogenesis in 5.5mM and 25.0mM osteogenic medium (OM) for 28 days. Osteogenesis was indicated by bone nodules deposition that stained with Alizarin Red. PD, population doubling level; CCM, Complete culture medium; HGCM, high glucose culture medium.

3.2.4 Osteogenic gene expression of bone chip explant MCSs in high glucose medium

Multivariate analysis was performed to investigate BCE-MSCs gene expression data, to provide in depth analysis of glucose-induced alteration in osteblastic gene expression during differentiation. As shown in Figure 3.4, high glucose significantly increased calcification in PD50 BCE-MSCs derived from CCM-treated cultures, in comparison to HGCM-treated cells. 28 days induction process in 25.0mM osteogenic medium seems to suggest that short-term high glucose-supplemented induction medium has a profound effect in increasing the expression of osteogenic markers. Significant differences were seen in OSX (osterix) expression on day 2 ($p<0.05$) and 7 ($p<0.01$), accompanied by elevated OCN (osteocalcin) expression on day 2 ($p<0.01$) and 14 ($p<0.05$). Conversely, a significant reduction in OPN (osteopontin) expression was reported in high glucose-treated cells on day 28 ($p<0.01$).

The most striking observation to emerge from the qRT-PCR gene expression data was derived from the PD150 cell populations (Figure 3.5). Discrepancies in osteogenic differentiation potential were observed between CCM-treated cells and HGCM-treated cells, reflected by the statistically significant increase in expression of OSX ($p<0.01$) and OCN ($p<0.01$) on day 28 of osteogenic induction. Analysis made on the same data, however, showed no significant differences in expression of OSX and OCN between 5.5mM and 25.mM osteogenic differentiation medium. The results on day 21, demonstrated statistically significant increase of OSX ($p<0.05$), and OCN ($p<0.01$) expression in CCM treated cells, differentiated in high glucose osteogenic medium, compared to the normoglycaemic osteogenic medium. Hence, these findings may suggested that a combination of long-term high glucose culture and high glucose in osteogenic induction medium significantly induced the expression of osteogenic markers, OSX and OCN by BCE-MSCs. Furthermore, the upregulation of OPN expression in HGCM-treated late PD MSCs was detected as early as 7 days, in comparison to 21 days reported in early-PD MSCs. The CCM-treated late PD cells, which were differentiated in high glucose osteogenic medium, exhibited a statistically significant increased of OPN ($p<0.01$) along the differentiation process, beginning from day 2 until day 28, with the highest peak reached on day 21 which demonstrated 1000-fold elevation in expression on OPN.

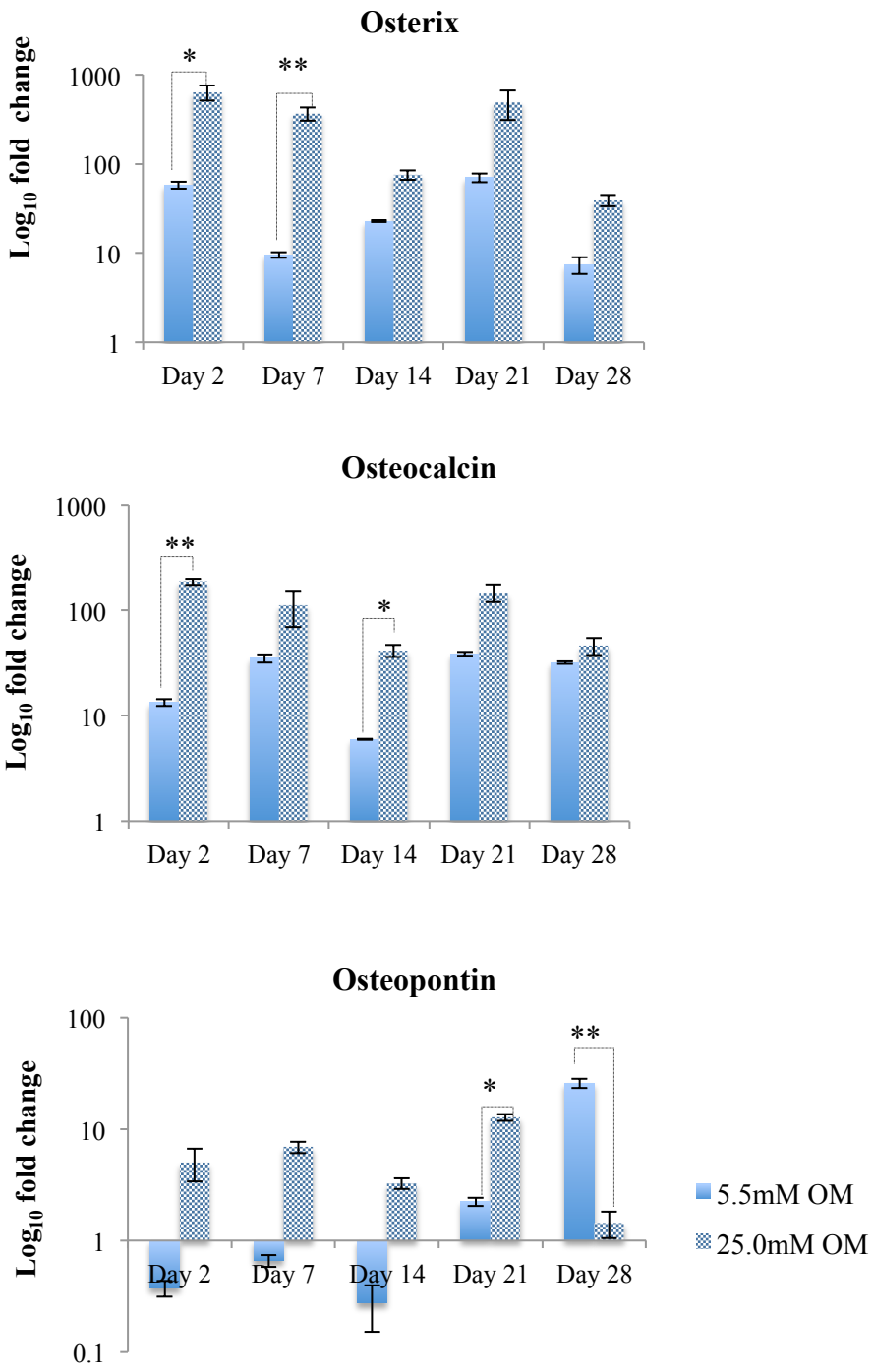

Figure 3.4 qRT-PCR gene expression data of PD50 BCE-MSCs, induced for osteogenesis in normoglycaemic and hyperglycaemic osteogenic medium (OM). Values were normalised to the expression of β-actin and expression in 28 days osteogenic-induced medium is presented as the fold increase or decrease of that in basal, non-differentiating medium at day 0. Each bar represent mean fold change±SD. N=2, n=3 and *p<0.05, **p<0.01. All p values were based on two-way ANOVA.

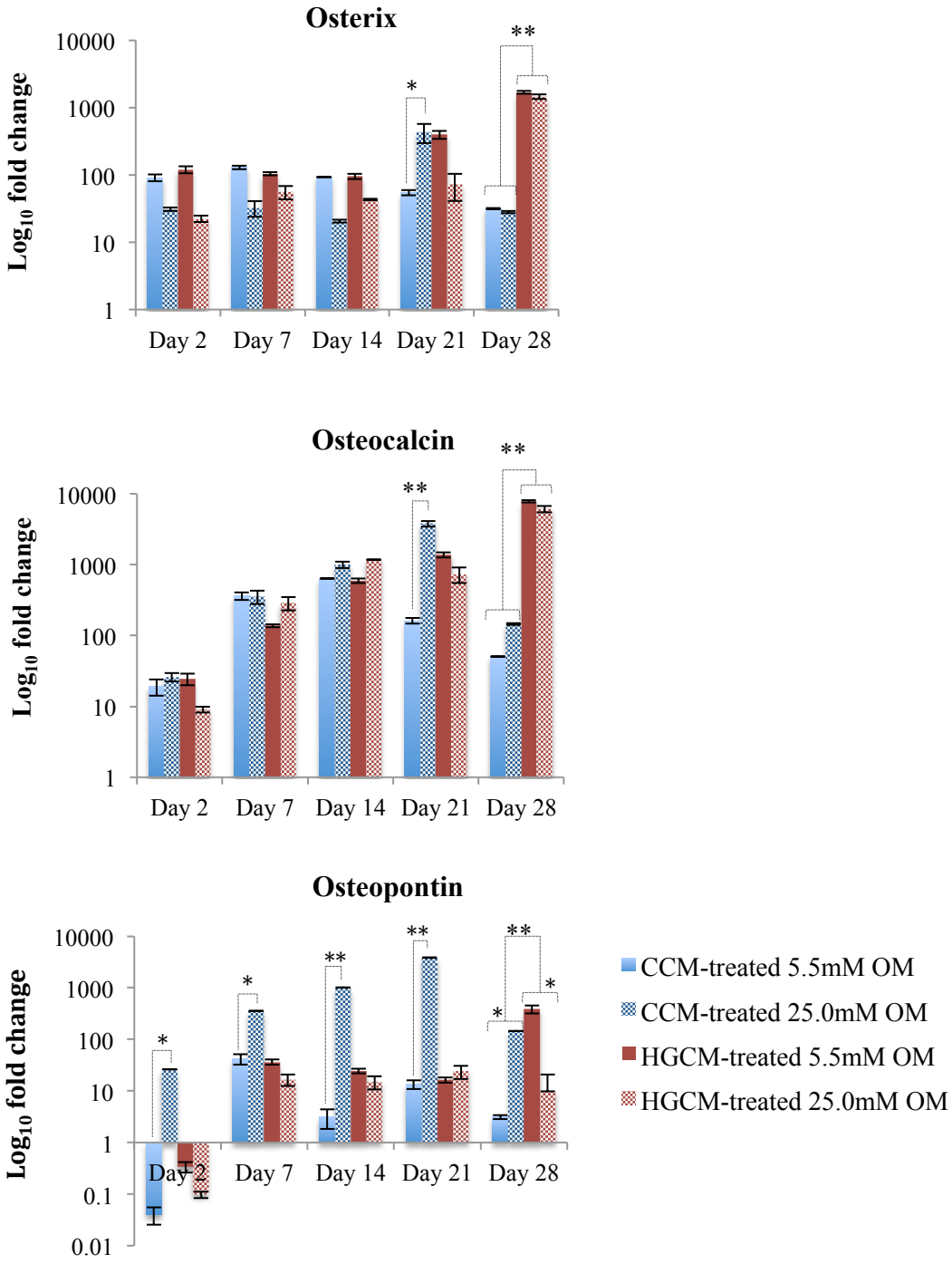

Figure 3.5 qRT-PCR gene expression data of CCM-treated and HGCM-treated PD150 BCE-MSCs, induced for ostenegenesis in normoglycaemic and hyperglycaemic osteogenic medium (OM). Values were normalised to the expression of β-actin and expression in 28 days osteogenic-induced medium is presented as the fold increase or decrease of that in basal, non-differentiating medium. Each bar represent mean fold change±SD. N=2, n=3 and *p<0.05, **p<0.01. All p values were based on three-way ANOVA.

3.2.5 Adipogenic staining of high glucose-cultured bone chip explant MSCs

To examine the effects of high glucose on the expression of adipogenesis-related markers, pre-adipocytes derived from CCM-treated and HGCM-treated groups were cultured in 5.5mM or 25.0mM glucose adipogenic medium (AM), for 2, 7 and 14 day. The Oil Red O staining pattern of lipid vacuoles from both cell group indicated comparable ability of each BCE-MSCs to differentiate into adipogenic lineage (Figure 3.6), with each group showing consistent formation of lipid vesicles in the cellular compartment. The data seemed to suggest that early-PD BCE-MSCs populations demonstrated similar capacity to form adipocytes, following the induction protocol. Both PD50 CCM-treated and HGCM-treated cells demonstrated capacity to form lipid deposition within the cellular compartment of thin, elongated-shaped of early PD cells (Figure 3.6a-d). The cellular morphology of HGCM-treated PD150 cells (Figure 3.6f and h) exposed to either normoglycaemic or hyperglycaemic adipogenic medium exhibit broadened shape, with slightly larger size of lipid vacuoles formed in clusters within the cytoplasm areas, in comparison to early-PD cells. Similarly, the CCM-treated cells cultured in 25.0mM adipogenic medium demonstrated parallel findings to the PD150 HGCM-treated cells. Collectively, the results suggested that lipid formation in the cellular compartments of pre-adipocytes correlated with glucose level supplementation in both normal culture and differentiation medium.

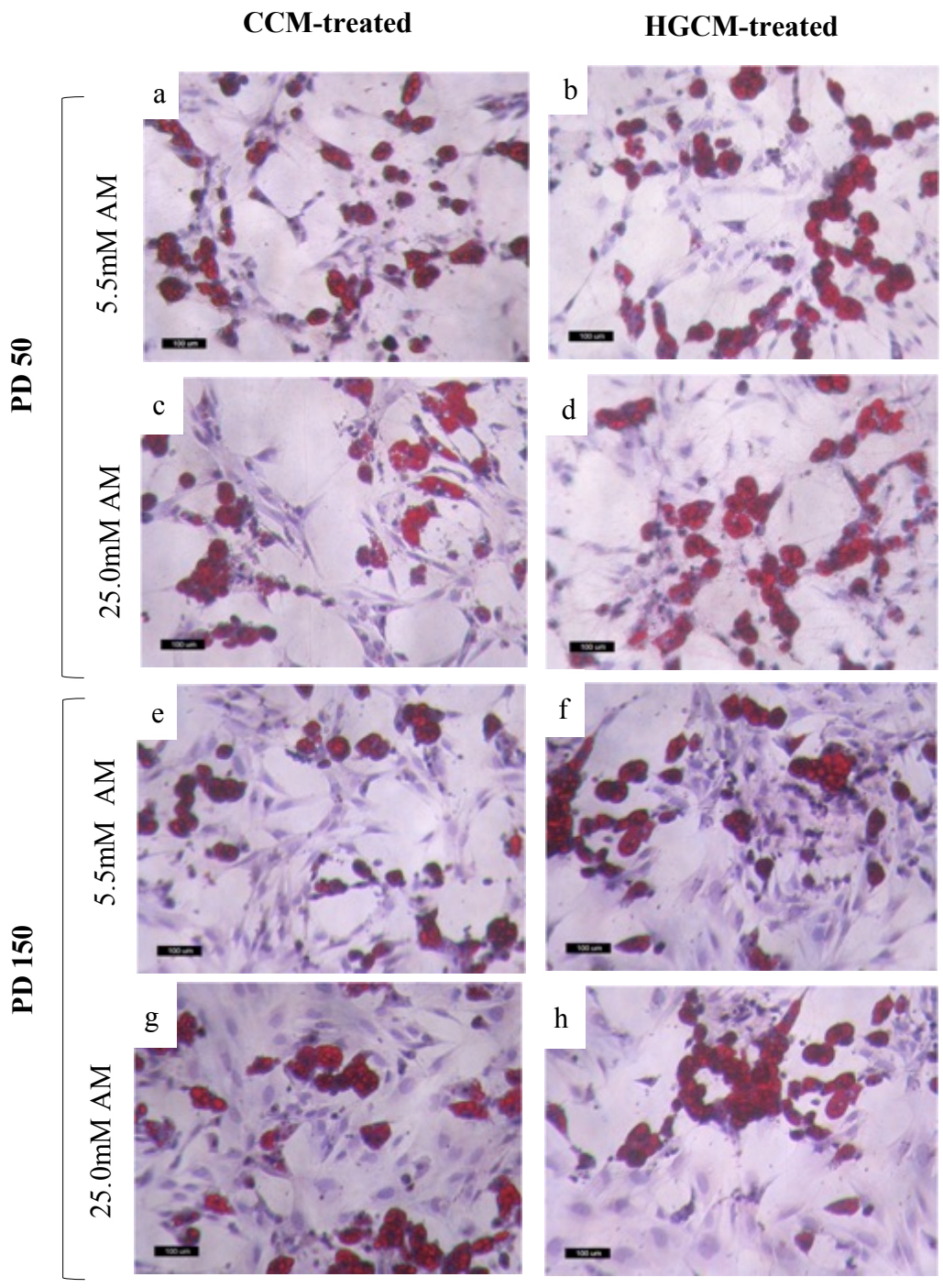

Figure 3.6 Histological analysis by light microscopy of CCM-treated and HGCM-treated BCE-MSCs induced to undergo adipogenesis. Monolayer cultures of mid-PD (a-d) and aged-PD (e-h) cells in six–well plates were induced in 5.5mM and 25.0 mM adipogenic medium (AM) for 14 days. Adipogenesis was indicated by vesicles formation, stained with Oil Red O. PD, population doubling level; CCM, Complete culture medium; HGCM, high glucose culture medium.

3.2.6 Adipogenic gene expression of bone chip explant MCSs in high glucose medium

Quantitative PCR analysis of CCM-cultured PD50 BCE-MSCs demonstrated that high glucose adipogenic medium significantly induced an overall increase in expression of adipogenic markers, FABP4, C/EBPα and LPL, with adiponectin exhibit the most prominent increase in gene expression in glucose-induced environment, as demonstrated on day 2, 7 and 14 (Figure 3.7). As we analyses further, qRT-PCR analysis conducted on PD150 BCE-MSCs (Figure 3.8) revealed 10-fold lower overall expression of FABP4, in comparison to PD50 BCE-MSC, whereas C/EBPα, LPL and adiponectin gene expression remained comparable with PD50 cells.

The adipogenic gene expression in PD150 HGCM-treated cells revealed a distinctive alteration in glucose-induced cultures, showing significant elevation of FABP4 and LPL ($p<0.01$) on day 7 and 14 following the induction protocol. Likewise, significant increases in C/EBPα level were observed in PD150 HGCM-treated cells on day 7. The data also indicated a significant upregulation of adiponectin expression in PD150 HGCM-treated BCE-MSCs, as oppose to the downregulation seen in CCM-treated cells. The results suggested that short-term, high glucose adipogenic medium has significantly induced upregulation of adipogenic lineage within the younger MSCs. However, introduction of high glucose adipogenic medium to long-term expanded MSCs does not revealed a similar stimulatory effect on adipogenesis marker expression. In fact, the long-term hyperglycaemic-induced cell culture protocol has significantly increased adipogenesis gene expression when exposed to either 5.5mM or 25.0mM adipogenic medium.

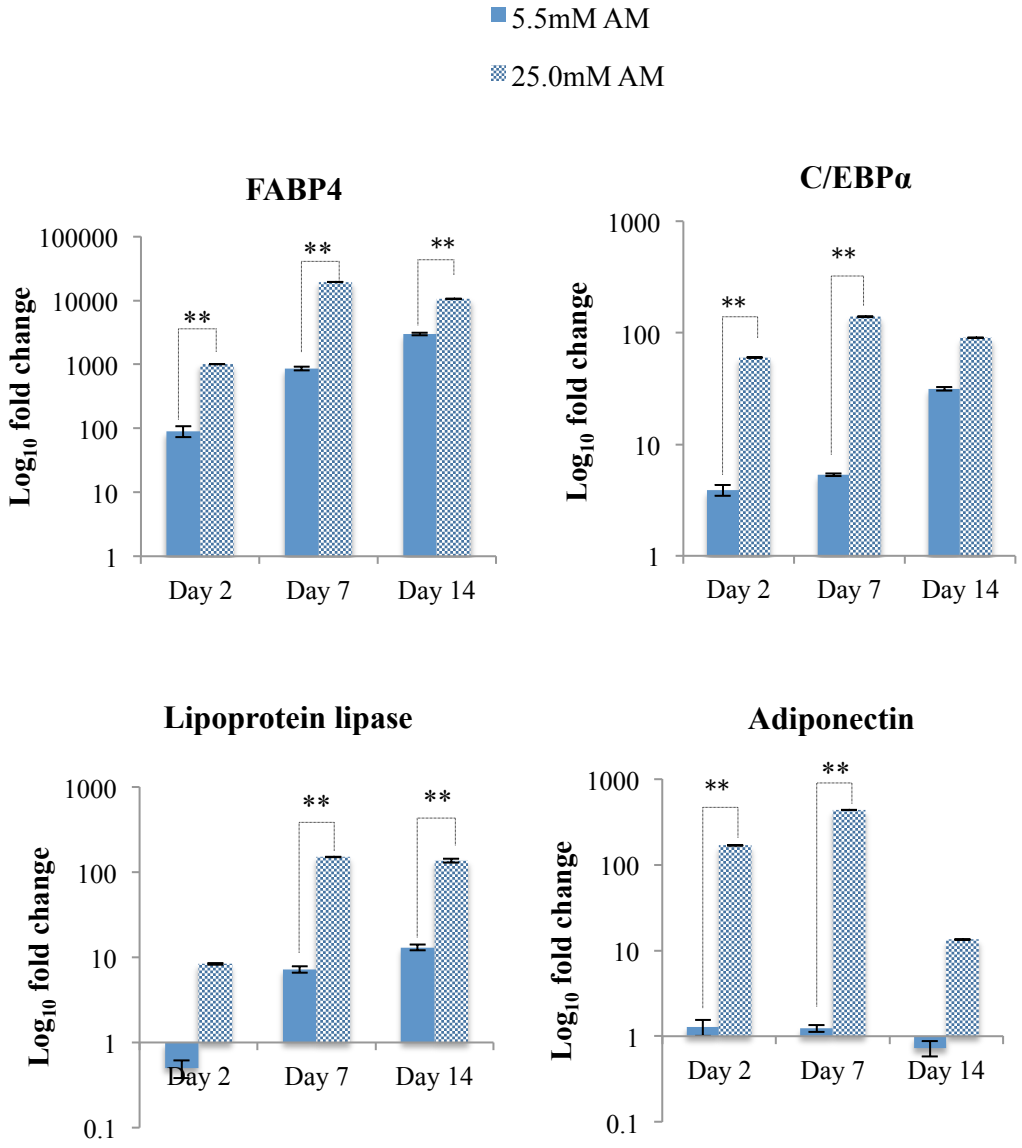

Figure 3.7 qRT-PCR gene expression data of PD50 BCE-MSCs, induced for adipogenesis in normoglycaemic and hyperglycaemic adipogenic medium (AM). Values were normalised to the expression of β-actin and expression in 14 days adipogenic-induced medium is presented as the fold increase or decrease of that in basal, non-differentiating medium. Each bar represent mean fold change±SD. N=2, n=3 and *p<0.05, **p<0.01. All p values were based on two-way ANOVA. FABP4, fatty acid binding protein-4, C/EBPα, CCAAT/enhancer binding protein.

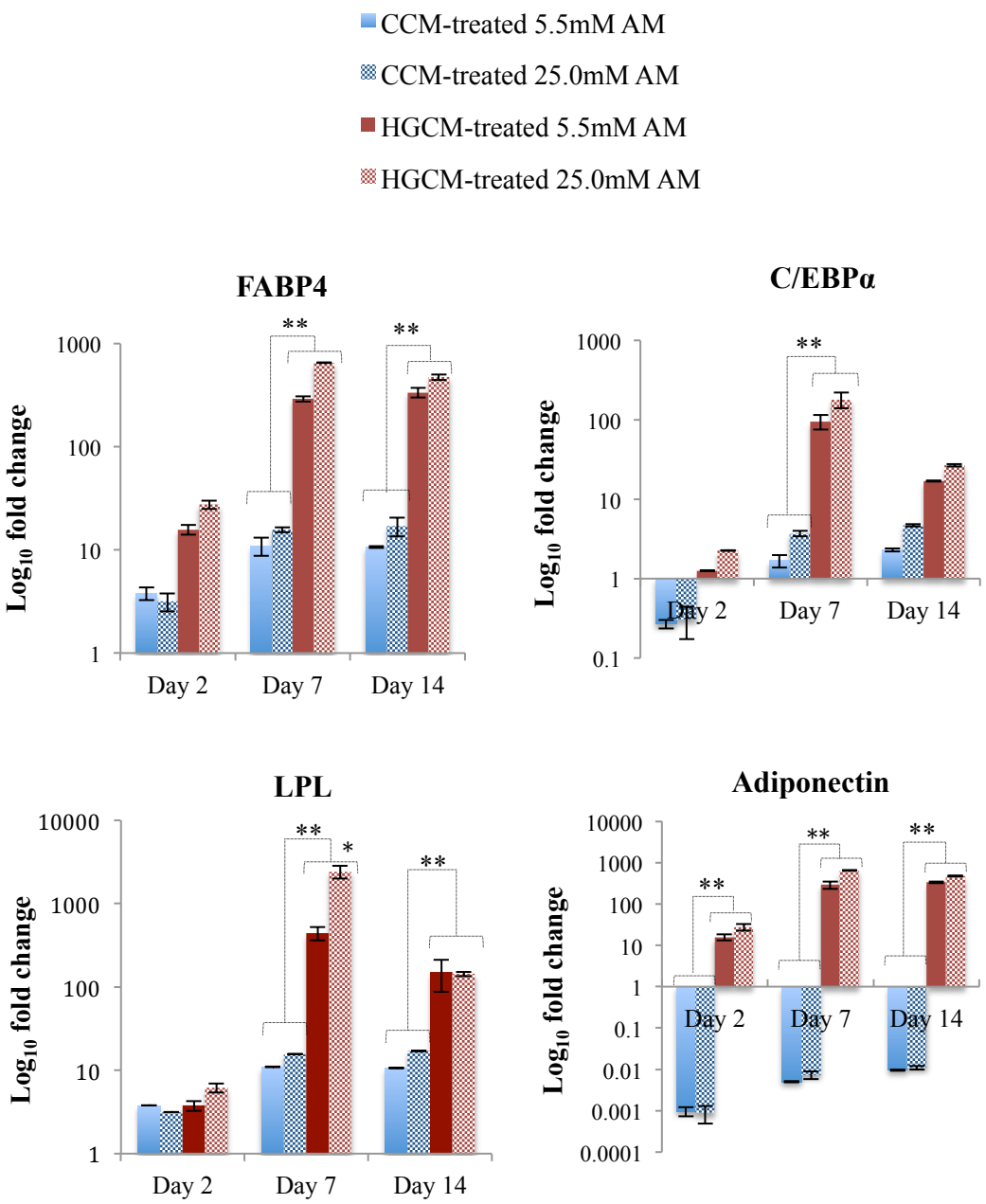

Figure 3.8 qRT-PCR gene expression data of CCM-treated and HGCM-treated PD150 BCE-MSCs, induced for adipogenesis in normoglycaemic and hyperglycaemic adipogenic medium (AM). Values were normalised to the expression of β-actin and expression in 14 days adipogenic-induced medium is presented as the fold increase or decrease of that in basal, non-differentiating medium. Each bar represent mean fold change±SD. N=2, n=3 and *p<0.05, **p<0.01. All p values were based on three-way ANOVA. FABP4, fatty acid binding protein-4, C/EBPα, CCAAT/enhancer binding protein.

3.3 Discussion

The current Chapter represents a novel *in vitro* study of bone explant-derived MSCs, to assess the long-term effects of hyperglycaemic culture condition on bone progenitor cells behaviour and activities. Briefly, evidence gathered from the present 2D cell culture study revealed that prolonged high glucose concentrations had a detrimental impact on BCE-MSC proliferative rates. However, prolonged and short-term hyperglycaemia were found to induce the differentiation capacity into osteogenic and adipogenic lineages. For the first time, this study had provided great evidence to support the claim that persistent hyperglycaemia plays an important role in generating overall cellular perturbations that may indirectly impair MSCs reparative role in bone repair processes. Comparisons were made between the two different stages of progenitor cells, taken at early and late PDs in the hyperglycaemic-induced state also revealed the various impacts of intermittent high-glucose induction on cellular differentiative capacity towards different mesenchymal lineages. Hence, the data also suggested the importance of glycaemic control in controlling bone repair progress.

The exact mechanism by which glucose levels might exert the impact on the behaviour of stem cells and the rate of expansion is a highly fascinating subject. Of note, the *in vitro* experiments conducted in this Chapter revealed very interesting evidences, indicating partial agreement with the stereotypical negative influence of glucose-inducing condition on MSCs behaviour. Contrary to the initial hypothesis, the short-term exposure to high glucose was found to increase the proliferative capacity of MSCs and their differentiation potential, showing stimulation of growth and differentiation ability. Within 50 days of culture in high glucose medium, the BCE-MSCs showed higher doubling time per week, in comparison to normoglycaemic conditions. Similarly, the short-term culture of MSCs displayed higher cell population doubling when cultured in higher glucose concentrations (Deorosan and Nauman 2011). In comparison, experiments conducted using human MSCs demonstrated insignificant effect on the proliferation rates and growth factor production in cells, following short-term high glucose condition (Weil et al. 2009). Therefore, the present data postulated that short-term effects of high glucose had been heavily dependent on the cell-type and the cell source in question.

On top of that, the stemness of MSCs might play a role in exerting the resistance effect of stem cells towards high glucose toxicity (Weil et al. 2009). However, this study confirmed that a long-term culture in high glucose medium eventually suppressed rat BCE-MSCs proliferative capacity. These perturbations led to lower PDs in high-glucose cultures, in comparison to parallel normoglycaemic cultures. Similarly, adipose–derived MSCs obtained from T2DM patients showed significantly decreased proliferative capacity, as well as induced cellular senescence and apoptosis, compared to normal patient MSCs (Cramer et al. 2010). The observed morphology of BCE-MSCs taken from mid-PDs also indicated relative differences in phenotype upon culture under these differing conditions. Comparatively, glucose-induced endothelial cells demonstrated a significant alteration in actin pattern and total cellular cytoplasmic area (Salameh et al. 1997). The observation that there was a parallel change in cell morphology is consistent with the idea that intracellular defects are responsible for the abnormalities of MSCs glucose metabolism, seen in patients with a T2DM condition. Collectively, these data evidenced that high glucose concentrations caused prominent disparities in cell behaviour and activity. However, in light of the insufficient available data, it is practically inappropriate to assume that the alteration in cellular behaviour discovered within this study is solely dependent on high glucose-induced stress, without consideration of the aging factor effect on MSCs.

Significantly, the present data revealed that short- and long-term exposure to hyperglycaemic medium induced higher mRNA expression of both osteogenic and adipogenic markers. This study demonstrated high tendencies of the hyperglycaemic condition to induce early expression of OPN and OCN in BCE-MSCs, confirming the alterations to matrix formation and the mineralisation process within high glucose environments. Similarly, high glucose was found to stimulate biomineralisation in osteoblastic cells and increased mRNA expression of OCN, Runx2, together with bone matrix protein synthesis, in mouse embryonic stem cells (ESC) studies (Chen et al. 2006; Kim et al. 2006; García-Hernández et al. 2012). However, analysis on bone structural properties demonstrated marked deterioration in the quality of the mineral produced, despite increased mRNA expression of osteoblastic genes (García-Hernández et al. 2012). The present analysis on

osteogenic induction of BCE-MSCs from late-PDs also demonstrated 10-fold increase of OCN, OSX, and LPL, in comparison to mid-PD cells, particularly in the high glucose-treated group. MSCs exhibited decreased proliferative properties as the cells progressed towards differentiation lineage (Chan et al. 2004). However, the effect of high glucose on the transient amplifying compartment was different to mature and developed functional cells (Li et al. 2007). Within this study, further proliferation of BCE-MSCs in the 2D system was found to subsequently reduce the presence of quiescent stem cells in the culture, nurturing a pool of more differentiated transit amplifying (TA) cells, with the capacity to rapidly proliferative and further develop into fully functional cells. Knowing that stem cells will preferentially undergo either a proliferation or differentiation route at one time-point, the data potentially suggested that high glucose might alter the biological activity of MSCs, particularly in generating pools of TA cells, which have a primary role in responding to cues generated for bone repair. Hence, the overall perturbations discovered from the hyperglycaemic level might be potentially caused by the shift of cells' proliferative capacity towards the differentiation route, thus limiting the regenerative potential, which led to impairment or delay in tissue healing.

The data also reported an increase in all adipogenesis markers, particularly adiponectin, which demonstrated a significant upregulation in hyperglycaemic cultures, in comparison to normoglycaemic control. Besides, it had been postulated that hyperglycaemia seemed to alter gene expression and skewed the differentiation of MSCs towards the adipogenic lineage (Bastianelli et al. 2014). Recent studies suggest the important role of adiponectin in T2DM as an insulin-sensitizing adipokine, due to the anti-inflammatory properties. Therefore, the present study proposed that a long-term culture in high glucose could cause major alteration in MSCs behaviour, resulting in preferential osteogenesis and adipogenesis. Unfortunately, the actual mechanism of how adiponectin might exert their effect on MSCs phenotypic alteration, to drive differentiation in the MSC populations, has remained unknown.

The cellular functions of MSCs is paramount in maintaining the ability of these cells to release beneficial growth factors to protect the cells and the surrounding matrix

components against injury during tissue repair. *In vitro* evidence demonstrated that various technical manipulations were applied to optimise the MSCs biological properties in *ex vivo* culture, including alterations of culture conditions with growth factor pre-conditioning, hypoxia treatment, genetic modifications, and pre-transplantation adjustment (Bouletreau et al. 2002; Song et al. 2005; Yu et al. 2011). However, much of the performance of the stem cells observed to this point had been limited to early passage MSCs that were grown in normoglycaemic culture, without considering the fact that a large number of transplanted cells failed to survive and proliferate. It might be partly due to major dissimilarities that existed between the 2D cell culture element and complex physiological environment within the 3D transplanted organ (Brinster 2002). The cited problem is particularly relevant, given that the presence of hyperglycaemia is a commonly encountered condition in many of the potentially treated diseases, which MSC transplant might bring substantial positive impact, such as T2DM.

Significantly, this Chapter has demonstrated that proliferation potential, metabolic activity, and differentiation capacity of *in vitro* cultured progenitor stem cells were influenced by high glucose concentrations. Hyperglycaemic culture seemed to suppress the proliferative capacity of the cells for a long-term, but induced their functional role towards a differentiation route, particularly the adipogenic lineage. Moreover, further damage and alterations caused by the high glucose level exerted a negative impact on stem cell properties in the long-term and irreversible fashion, leading to impaired regenerative capacity, as well as promoting the progression of diabetic perturbations in the affected tissues. Therefore, more investigations would be valuable to gain better insight into the exact molecular mechanisms of high glucose-induced alterations in MSCs using different cell types and origins, in order to develop a suitable *in vitro* bone repair model of T2DM. Therefore, the next Chapter portrays the investigation on growth factors responsiveness in BCE-MSCs during diabetic bone repair, by using both *in vivo* and *in vitro* animal models. Attention was also given to look into the potential alterations in proteoglycans expression within the ECM compartment, which potentially influenced growth factor signalling and MSCs reparative role in T2DM.

Chapter 4

Growth Factor Responsiveness of MSCs During Bone Repair in Type 2 Diabetes Mellitus (T2DM)

4.0 Introduction

Diabetes has long been associated with physiological and pathological disturbances that have led to the impairment of biological activities within the skeletal environment. A number of experimental studies, from immunohistological and ultrastructural observation, to *in vitro* analysis; have indicated the correlation of diabetes with progressive alteration in cellular functions and delayed bone metabolism, resulting in lower bone quality and mechanical properties (Prisby et al. 2008; Yaturu et al. 2009; Retzepi et al. 2010). Various hypotheses have been proposed to elucidate the underlying mechanisms of diabetic alterations in a hyperglycaemic environment. However, these experimental analyses often neglected the fact that there is a distinct pathological progress between the different types of diabetes. Moreover, from the vast majority of osseointegration studies in diabetic animals, only a few studies specifically focused on Type 2 Diabetes Mellitus (T2DM) repair models, either using genetically modified or selective inbreeding animals, which developed late onset hyperglycaemia and obesity that mimicked human T2DM (Casap et al. 2008; Sakai et al. 2008; Wang et al. 2010b; Colombo et al. 2011). In view of the lack of evidence of osseointegration studies in the T2DM microenvironment, it further justifies the necessity to perform more studies to obtain better insight of bone healing mechanisms in T2DM model.

Mesenchymal stem cells (MSCs) are multipotent progenitor cell populations derived from adult tissues, which exhibit great capacity to differentiate into a multiple type of functional cells. Successful isolation of bone progenitor cell populations from trabecular bone has emerged as an attractive cell source for bone repair studies, particularly in the development of diabetic-induced *in vitro* models (Guo et al. 2006; Sung et al. 2008; Zhu et al. 2010). Besides, MSCs play an important role during reparative phases to co-ordinate the expression of growth factors and stimulate the production of matrix proteoglycans, which resulted in overall tissue remodelling within the healing site (Lieberman et al. 2002). Meanwhile, growth factors, such as TGF-$\beta_{1,}$ have been demonstrated to influence bone resorption and bone formation (Tang et al. 2009). TGF-β_1 also acts as a mediator in the formation of collagen matrix during bone healing process (Ignotz and Massagué 1986). However, to the best of the researcher's knowledge, nothing has been reported so far concerning the

role of growth factor activity, particularly TGF-β_1, in response to glucose stress within bone progenitor cell populations. Thus, the question of whether TGF-β_1 has any role in the biological response to glucose in bone chip explant MSCs has remained unexplored. The present Chapter depicts the investigation of the *in vitro* short- and long-term effects of TGF-β_1 bioavailability in bone-derived MSCs, in response to high glucose concentrations, as their significance in the pathogenesis of T2DM remains to be clarified.

Proteoglycans are integral biomolecules of the extracellular matrix (ECM) in all tissues that play various important roles in regulating innate immunity, inflammation, and regulating matrix assembly (Bianco et al. 1990; Frey et al. 2013). Biglycan and decorin are among two of the most commonly studied small leucine rich proteoglycans (SLRPs) family found to be highly expressed in skin and bone, respectively (Corsi et al. 2002; Waddington et al. 2003). Evidence indicates a critical role for biglycan in modulating the osteogenic differentiation of MSCs by regulating the early stages of cell proliferation and differentiation (Chen et al. 2004; Roberts et al. 2008). Biglycan and decorin also act as important modulators in the inhibition and sequestration of growth factors within ECM, such as TGF-β, FGF, and BMP-4, by modulating the cell-matrix cross-talks (Fernig and Gallagher 1994; Corsi et al. 2002; Bi et al. 2005; Merline et al. 2009). Apart from their primary roles in assembling matrix ultrastructures, both biglycan and decorin also interact with various cell surface receptors and indirectly control cellular proliferation, differentiation, and apoptosis, depending on the cell type and signalling milieu (Frey et al. 2013). Moreover, *in vitro* analysis of primary bone cells revealed temporal expression of both biglycan and decorin, which were linked to their co-operative role in regulating cell proliferation, matrix deposition, and mineralisation (Waddington et al. 2003).

Furthermore, hyperglycaemia has been reported to produce significant alterations in biglycan and decorin expression of matrix tissues, leading to further perturbations in wound repair and progressive development of diabetic pathogenesis (Roberts et al. 2008; Yang et al. 2009; Nikolovska et al. 2014). Hyperglycaemia-induced expression of TGF-β_1 through Smad2/3 and p38 MAP kinase led to GAG elongation during proteoglycan synthesis and increased affinity of progenitor cells to bind to low density lipoprotein (Dadlani et al. 2008). To date, hyperglycaemia has been

associated with induced proteoglycan synthesis, increased expression of TGF-β_1, and stimulation of collagen expression, as demonstrated in the vast majority of mesangial cells and endothelial cells culture studies (Kolm-Litty et al. 1998; Iglesias-de la Cruz et al. 2002; Vogl-Willis and Edwards 2004). However, no studies has addressed the actual mechanism of TGF-β_1 mediated, biglycan and decorin activity, in regulating the proliferative and osteogenic potential of MSCs, in view of their bone restorative capacity.

Hence, this Chapter provides substantial evidence on bone progenitor cell proliferation and survival in response to hyperglycaemic conditions. By using non-obese type 2 diabetic models, the study further elucidated if hyperglycaemia alone could significantly promote alterations in cellular behaviour and responsiveness towards growth factors administration and matrix proteoglycans in both *in vitro* and *in vivo* conditions**.**

4.1 Materials and methods

4.1.1 *In vivo* analysis of diabetic bone repair

4.1.1.1 Animal

Twelve male diabetic GK rats and twelve male Wistar rats were used in the experiment (Shimizu Laboratory Supplies Co. Ltd., Kyoto, Japan). Each of the diabetic and control group consisted 6 of 10 weeks-old rats and 6 of 18 months-old rats. Implantology method was carried out by Professor Diago Sakai and Professor Joji Okazaki, at the Dental University of Osaka, Japan, for 3 weeks and 9 weeks, on both groups of male Wistar and Goto Kakizaki rats, as described in previous studies (Sakai et al, 2008). All experiments performed were reviewed and approved by the Animal Committee of Osaka Dental University (with approval number of 08-03009) and conformed to the procedures described in the "Guiding principles for the Use of Laboratory Animals Handbook" at the Laboratory Animal Facilities in the Institute of Osaka Dental Research, Osaka Dental University.

4.1.1.2 Implant procedure

Implant procedures were conducted by our collaborators from Institute of Osaka Dental Research, Osaka Dental University, Osaka, Japan. The erupting incisors of the rats were trimmed at 14, 11, 7 and 4 days prior to extraction in order to stimulate eruption. The trimming step helps to loosen the incisors and facilitate the later extraction process. Pre-treatment trimming procedures were carried out under infiltration anaesthesia with isoflurane (Isoflurane Rhodia TM, Nissan Chemical Industries Ltd, Tokyo, Japan). Weights of all rats were measured prior to tooth extraction, which were carried out under the general anaesthesia sodium pentobarbital (Nembutal R, Dainippon Pharmaceutical Co. Ltd, Osaka, Japan), delivered by intraperitoneal injection. The blood glucose level was measured as an indicator of diabetes at the time of extraction using the enzymatic method (Medisafe Mini Terumo, Tokyo, Japan). The implant socket was curetted to remove any remaining debris and the majority of periodontal ligament. Sterilised titanium alloy (Ti-6A1-4V) implants, with a length of 17.0mm and 1.2mm diameter (SNK

screwpost Ti-tan R, Dentsply-Sankin K.K., Tokyo, Japan), were immediately placed in the socket of left mandibular incisor and stabilized via the alveolar plate, while the right mandibular incisor was left alone for food ingestion.

4.1.1.3 Preparation of mandibles and fixation

At 3 and 9 weeks after the implant placement**,** both groups of rats were euthanised by intraperitoneal injection of sodium pentobarbital, 30min after an intraperitoneal injection of the anticoagulant sodium heparin (Novo-Heparin Injection 1000®; Mochida Pharmaceutical, Tokyo, Japan). After perfusion fixation with 10% neutral-buffered formalin according to standard methods for 7 days, the entire mandible was removed and dissected centrally into left and right halves, with a surgical scalpel. The left side was retained as a control sample. Finally, the mandibles were put into 10% neutral-buffered formalin solution and transported to Cardiff University, UK.

4.1.1.4 Microtomy and embedding process

Implants were carefully removed from each mandible by gently unscrewing them out from the socket. After removal of the ramus and condyle, the mandibles were then cut into approximately 2mm thick sections running perpendicular to the implant socket, using a bone saw; and placed in 10% formic acid with agitation for 72h to demineralise the tissue sections. The tissue sections were then placed in embedding cassettes for automatic processing machine, Leica ASP300S (Leica Microsystems UK Ltd., Milton Keynes, UK, through a series of 70%, 90% and 100% graded alcohol solutions, which served to dehydrate them; and cleared with a xylene rinse. Tissue sections were then removed from the processing machine and embedded in molten paraffin wax (Thermo Scientific Raymond Lamb, Loughborough, UK). 5µm sections were cut using Leica SM2400 sliding microtome (Leica) and mounted on poly-L-Lysine coated glass slide (Sigma Aldrich, Poole, UK), before being placed in an oven at 65°C overnight.

4.1.1.5 Haematoxylin and eosin staining

Sections were stained with haematoxylin and eosin (H&E) using an automated staining machine, in order to visualize the tissue and cell architecture around the

implant site. First, the automated staining system passed the slide mounted sections through a series of xylene, graded alcohol and water rinses, in order to remove all paraffin and to rehydrate them. The sections were then immersed in haematoxylin to colour the nucleus of cells, washed and blued in Scott's tap water; and differentiated in 1% alcohol. After further rinse in tap water, sections were stained with eosin which stains cytoplasmic components red. Finally, the sections were rinsed in tap water, dehydrated in alcohol and immersed in xylene. Cover slips were mounted onto the sections using DPX mounting medium (Thermo Scientific). Images were captured using Olympus AX-70 microscope (Olympus Co. Ltd., Tokyo, Japan) incorporating a Nikon DXM1200 digital camera and ACT-1 software (Nikon Instruments UK, Surrey, UK). Sections were examined by analysing the healing sockets along the entire length of the implant, starting from the insertion site to the tip of the implant, where the growing root tip had once been.

4.1.2 Transmission electron microscopy (TEM) analysis

4.1.2.1 Tissue preparation

Specimens for histological and immunohistochemical staining were prepared and fixed, as described in Sections 4.1.1.2 and 4.1.1.3. Then, 2mm thick blocks obtained from Section 4.1.1.3 were cut into four pieces with each piece encompassing the hole and being placed in phosphate-buffered saline (PBS). The sections were demineralised using 6% ethylenediaminetetraacetic acid (EDTA) solution (pH 7.4) for 4 weeks, followed by calcium oxalate test to ensure complete decalcification. Briefly, 5ml of decalcifying solution was transferred into bijoux bottle and followed by drops of ammonia hydroxide until litmus indicated pH 7.0. 5ml of saturated ammonium oxalate was added and solution is allowed to stand for 30min. Clear solution indicated completion of decalcification. Specimens were thoroughly washed in PBS, dehydrated in graded concentrations of ethanol and embedded in Lowicryl HM20 (Agar Scientific Elektron UK Ltd., Stansted, UK) by using Progressive Lowering of Temperature (PLT) Protocol, as previously described in Hobot and Newman (1996). Sample pieces were then placed into gelatine capsules (size '0'/vol 0.68ml), followed by indirect UV-light polymerisation at 35°C for 24h and direct UV-light for another 72h at room temperature.

4.1.2.2 Primary antibodies and secondary probes

Affinity-purified polyclonal rabbit IgGs, raised against rat transforming growth factor-β_1 (TGF-β_1) were obtained from Santa Cruz Biotechnology (Insight Biotechnology, Wembley, UK). Goat anti-rabbit IgGs (Sigma) tagged to 10nm colloidal gold (GAR-10) was conjugated in house (Bioclinical Services, Cardiff, UK). GAR-10 stock was diluted 1/5 in filtered 20mM Tris-HCl (pH 8.2) and centrifuged, prior to use for 4min at 10,000g to remove larger gold clusters. A modified 0.01M PBS containing 0.6% w/v BSA (pH 7.4) was used throughout all the following procedures for all dilutions of antibodies or serum.

4.1.2.3 Immunogold labelling of selected growth factors

Established methods were used to perform immunogold TEM (Newman and Hobot 1999). Four μm sections from each diabetic and control groups, embedded in Lowicryl HM20 were cut using a LKB III ultramicrotome (Cambridge Instruments, Cambridge, UK) and collected on 400 mesh nickel grids. For negative controls, antibody was omitted and only PBS and BSA were used. Immunolabelling of sections was by immersing the grids in 50μl of solution, initially in PBS and BSA solution for 10min, then in the appropriate antibody (diluted 1:10) for 60min (or PBS and BSA for controls). Sections were then washed with (1 x 1min) PBS and BSA and (2 x 1min) 20mM Tris-HCl (pH8.2), followed by 60min in GAR-10; washed once for 1min with Tris-HCl and twice for 1min with water from Elga Option 7 water purifier (Elga Labwater, High Wycombe, UK) and post-stained in 4% w/v aqueous uranyl acetate for 20min, water washed (500μl) and air dried. The sections were viewed in a Philips CM12 (Phillips Ltd., Cambridge, UK) operating at 80kV. Images were recorded using a SIS MegaView III (SIS Company, Münster, Germany) digital camera. The immunogold labelling was counted from at least 25 random field of 30μm area.

4.1.3 *In vitro* cell culture study

4.1.3.1 Time-based analysis of rat progenitor cells osteogenic culture

Rats MSCs were isolated by the explant method and expanded in culture as previously described in Chapter 2, (Section 2.1.1 and 2.1.1.3). The BCE-MSCs used in this study were assessed at early population doubling levels (PD) of PD15 and late PDs (PD150). These cells were grown in either complete culture medium (CCM) or high glucose culture medium (HGCM), to represent cells of different proliferation rate and glucose-induced treatment, as previously described in Chapter 3, (Section 3.1.2). Cultures were maintained at 37°C in 5% CO_2/95% air, with the medium changed every 2 or 3 days.

4.1.3.2 RNA extraction and qRT-PCR reactions

At selected PDs, following a StemPro® Accutase® digestion step, BCE-MSCs were seeded at density of 4000 cell/cm^2 into 3 of 6-well plates and maintained in either CCM or HGCM at 37°C in 5% CO_2/95% air. At 24h, CCM and HGCM were replaced with osteogenic induction medium, 5.5mM OM or 25.0mM OM (as described in Section 2.1.3.2. The cells were further incubated at 37°C in 5% CO_2/95% air, with samples taken at 2, 7, 14 and 21 days, to assess the expression of TGF-β_1, biglycan and decorin by the MSCs. At the specific time intervals, the culture medium was removed and total mRNA was extracted from approximately 600,000 cells using the RNeasy® Mini Kit and QIAShredder (Qiagen Ltd., Crawley, UK); and transcribed into cDNA as described in Section 2.1.2.3 and 2.1.2.4. For qRT-PCR reactions, cDNA was pre-diluted 1:10 with RNA free water immediately, prior to analysis. Each qRT-PCR reaction was performed using 2.5µl 3µm primers (forward and reverse), 5µl diluted cDNA sample and 10µl SYBR Green Precision qRT-PCR Master Mix (Primer Design Ltd, Southampton, UK) and RNA-free water added for a final volume of 20µl. All samples were triplicates in Bright White 96-well plates (Primer Design) using ABI Prism 7000 Sequence Detection System and ABI Prism 7000 SDS Software V1.0 (Applied Biosystems, Warrington, UK). Reactions conditions were: 1 cycle of 95°C for 10 min, 40 cycles of 95°C for 15s, 55°C for 30s and 72°C for 30s. Specific primers for the detection of selected growth factor and

proteoglycans gene markers are described in Table 4.1 and the primer sequences were ordered from Eurofins MWG Operon, Ebersberg, Germany.

Table 4.1 Specific primers for the detection of selected growth factor and proteoglycans gene markers.

Gene	cDNA sequence (5'-3') F, Forward; R, Reverse	Length (bp)	References
β-actin	F: TGAAGATCAAGATCATTGCTCCTCC R: CTAGAAGCATTTGCGGTGGACGATG	155	Gao et al. 2009
Decorin	F: ACCCGGATTAAAAGGTGGTGA R: TCTCTGCTCAAATGGTCCAGC	104	Roberts et al. 2008
Biglycan	F: CCTCCAGCACCTCTATGCTC R: ACTTTGAGGATACGGTTGTC	186	Roberts et al. 2008
TGF-β_1	F: AAGAAGTCACCCGCGTGCTA R: GGCACTGCTTCCCGAATG	82	Gao et al. 2009

4.1.3.3 Protein extraction and dialysis

Protein synthesis and localisation was investigated in three ways within this study. First, by detecting the protein that was released into the culture medium (CM); second, by examining the intracellularly produced TGF-β_1 by analysing the cells lysate extracts (CE) and third, by analysing the expression of TGF-β_1 localised and sequestrated within the extracellular matrix (ECM) component. Collectively, the results of Western blot analysis may provide conclusive evidence on TGF-β_1 expression by MSCs derived from different expansion period, in response to normoglycaemic and hyperglycaemic exposure. Prior to protein analysis, immediately after the Accutase digestion step, each different group of BCE-MSC were seeded in two T25 tissue culture flasks (BD Biosciences, Oxford, UK), incubated either with 5ml of CCM or HGCM at a plating density of 4000cells/cm^2; and maintained at 37°C in 5% CO_2/95% air. At 24h, culture medium was replaced with 5ml of osteogenic induction medium, each containing 5.5mM glucose or 25.0mM glucose, respectively. MSCs were maintained at 37°C in 5% CO_2/95% air. At day 2, 7, 14 and 21, the osteogenic induction medium was collected and centrifuged (8,000 rpm, 5min) to pellet cell debris. MSCs were washed twice in ice-cold PBS (2x), and cell extracts was obtained by addition of 2ml of extraction buffer I (0.1% TritonX-100, 0.05M sodium acetate buffer, pH 6.8, supplemented with Complete™ protease inhibitor cocktail (Roche, Diagnostics Ltd, Burgess Hill, UK) as per manufacturer's instruction) and cell were further incubated at 37°C for 15 mins before the cell extracts suspension was collected. The remaining matrix in the flask were washed twice in ice-cold PBS, prior to addition of 2ml of extraction buffer II (2% TritonX-100/4M guanidinium hydrochloride, 0.05M sodium acetate buffer, pH 6.8, supplemented with Complete™ protease inhibitor cocktail (Roche); and further incubated and collected, as previously mentioned above. The collected cell supernatants, cell extracts and extracellular matrix extracts were put into 33mm width cellulose membrane dialysis tubing. Tubing contents was dialysed for 3 days in protease inhibitor solution (0.5mM iodoacetic acid, 0.5mM benzamidine, and 0.1mM N-ethylmaleimide) at 4°C on magnetic stirrer for continuous agitation. Dialysed contents were subsequently lyophilised (Edwards Freeze-dryer Modulyo, Crawley, UK). The protein concentration of the cell supernatants, cell lysates and

ECM extracts were quantified using Pierce® BCA Protein Assay Kit (Thermo Fisher Scientific, Loughborough, UK) according to manufacturer's instructions.

4.1.3.4 Protein separation and Western blot

20µg of proteins samples were diluted 1:1 with 1X Laemmi buffer (62.5mM Tris-HCL pH 6.8, 2% (v/v) SDS in distilled water, 10% (v/v) glycerol, 0.5% (w/v) bromophenol blue in distilled water and 2.5% (v/v) β-mercaptoethanol) and boiled for 5min. Samples were loaded onto 4-15% Mini-PROTEAN® TGX™ Precast Gels (BioRad, Hemel Hempstead, UK) along with 10µl Kaleidoscope™ Prestained Standard (Bio-Rad). Separation of protein was performed under reducing conditions by sodium dodecyl sulphate-polyacrylamide gel electrophoresis (SDS-PAGE) at 200V for 40min, using the Mini-Protean® Tetra Cell System (Bio-Rad). The proteins were electrotransferred onto polyvinylidene difluoride membranes (Hybond™-P, Thermo Fisher Scientific) at 15V for 30min, using the Semi-Dry Trans-Blot System (BioRad). Membranes were then blocked with 5% semi-skimmed milk/1% Tween 20 (Thermo Fisher Scientific) in Tris-buffered saline (TBS), at 4^{o}C overnight.

4.1.3.5 Protein detection

Following the blocking procedure, membranes were probed with polyclonal anti-goat TGFβ_1 (1:100) (Santa Cruz, Middlesex, UK), monoclonal antibodies against the core protein of decorin and biglycan (generous gifts from Professor Bruce Caterson, School of Biosciences, Cardiff University) and monoclonal anti-rabbit Smad 2/3 (1:1000, New England Biolabs, Hitchin, UK) in 5% semi-skimmed milk /1% Tween 20, at room temperature for 1h. Addition of 10X amount of TGF-β_1 blocking peptide (1:10, Santa Cruz) to primary antibody, prior to incubation served as a negative control. Normalised protein loading was confirmed by β-actin loading control probing (1:1000, Abcam, Cambridge, UK). Membranes were washed 3 times in 5% semi-skimmed milk/1% Tween 20/TBS and incubated for 1h in secondary antibody for TGF-β_1 (1:3000, HRP-conjugated rabbit anti-goat IgG, Santa Cruz), decorin and biglycan (1:50,000, HRP-conjugated rabbit anti mouse IgG, Abcam); diluted in 5% semi-skimmed milk/1% Tween 20/PBS; at room temperature for 1h. In parallel, the β-actin loading control samples were incubated in secondary antibody (1:3000, HRP-

conjugated polyclonal swine anti-rabbit Ig's, Dako UK Ltd, Cambridge, UK) in 5% semi-skimmed milk/1% Tween 20/PBS; at room temperature for 1hr. Membranes were washed (x3) as above and chemiluminescent detection was performed using the ECL™ Prime Detection Reagent (GE Healthcare, Chalfont St., Giles, UK). The enhanced chemiluminescents substrate were captured and developed on autoradiographic films (Hyperfilm™-ECL, GE Healthcare) according to manufacturer's instructions. Immunoblots were later scanned to digital images, using a transparency scanner Epson Perfection V600 (Epson UK Ltd. Hemel Hempstead, UK) and further analysed.

4.1.4 Statistical analysis

Unless otherwise stated, values are expressed as means ± standard deviation (SD). Analyses were performed by the software package, SPSS 20.0 (IBM, NY, USA). The statistical significance of differences among experimental group was evaluated by three-way ANOVA or mixed ANOVA, followed by multiple comparison using Tukey's test with $*p<0.05$ and $**p<0.01$ being considered statistically significant. The number of replicates used is stated in the figure legends.

4.2 Results

4.2.1 Histological observation of bone repair site

Histological sections of bone-implant area following haematoxylin and eosin staining in young group and aged group, are shown in Figure 4.1 and 4.2. In the young-control group (Figure 4.1a), observations made within the repair site at 3 weeks post-surgery demonstrated that large areas of the healing site were filled with pink coloured immature soft tissues, consisting of an irregular deposition of collagen fibres. However, at 9 weeks after implant placement (Figure 4.1b), the healing socket revealed a clear formation of new bone, represented by dense red-coloured staining of the tissue. Magnified images showed osteoid deposition rimmed by osteoblasts in the newly formed bone. In contrast, histological examination in young-diabetic group after 3 weeks of surgery procedure showed that the bone-implant contact is mainly occupied with non-collagenous matrix (Figure 4.1c). Later on, at 9 weeks post-surgery (Figure. 4.1d), the young-GK group showed slight increases in new bone formation, as oppose to the 3 week time-point. The newly formed mandibular bone tissue was represented by a red-staining pattern within the healing site, accompanied by a small proportion of soft pink matrix formation. Briefly, histological observations of bone-implant contact from the young group within the present study showed that new bone formation is higher in 9 week groups, compared to 3 week groups, which suggested that the healing processes within the insertion site is considerably increasing with time.

Next, analysis was made within the aged animal groups. In general, the findings demonstrated that new bone formation in the aged-control group was much less, in comparison to young-control group, at both time-point post-surgery. However, aged-control tissue exhibits considerable progress in healing capacity as time progressed (Figure 4.2a and 4.2b). Interestingly, comparison made within the aged group alone, exhibited a clear delay of osseointegration in diabetic rats in comparison to control animal, regardless of the chosen time-point of analysis (Figure 4.2c and 4.2d). The aged-diabetic tissue displayed less organised collagen fibres architecture around the implant. The healing site was also occupied with immature non-collagenous matrix components and a high presence of inflammatory cells. Clearly, the longer period given for the repair process does not considerably improve the progress of bone

formation in aged-diabetic groups, as oppose to better healing capacity observed in control animals.

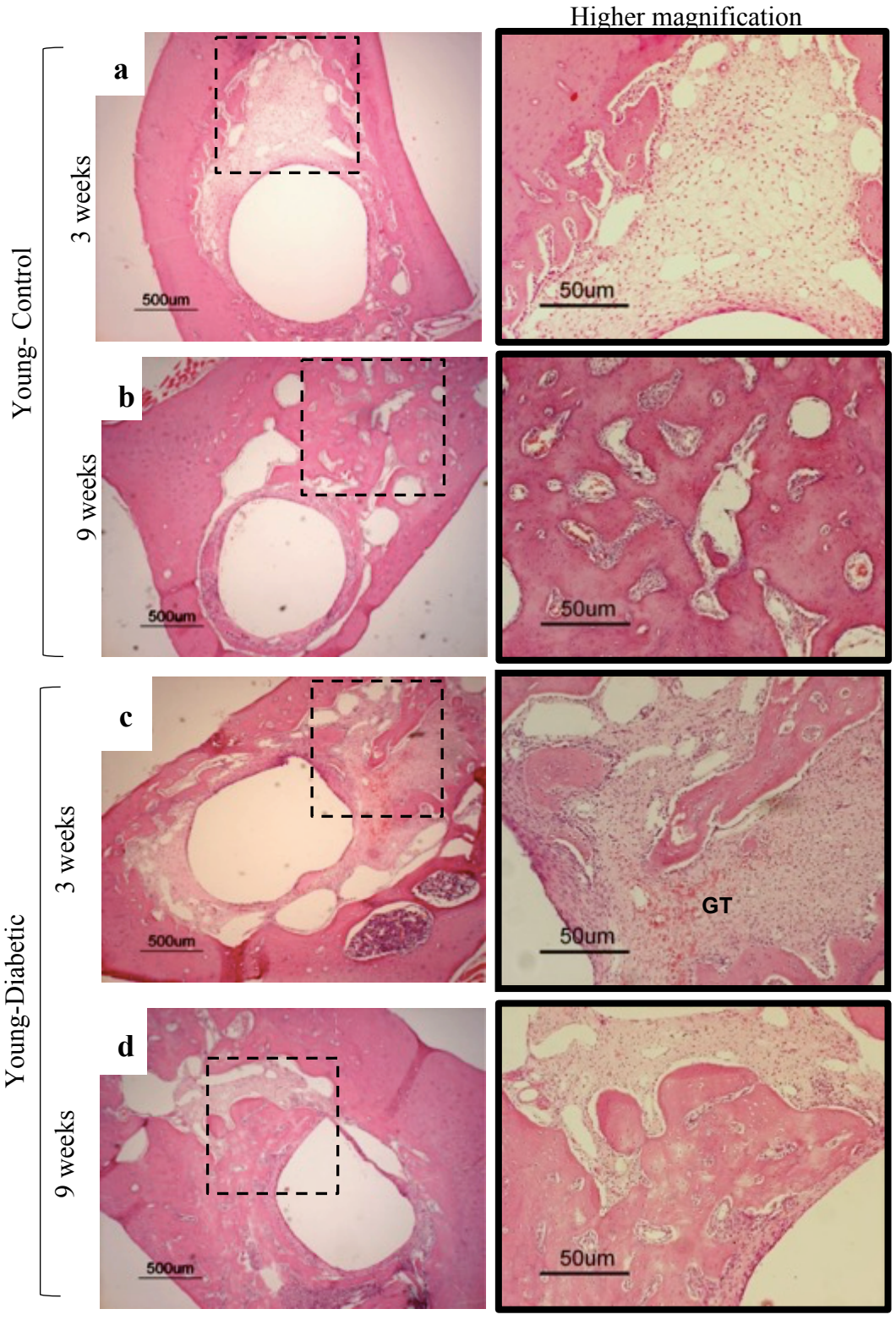

Figure 4.1 Haematoxylin-eosin section from the young Wistar and GK rats, at 3 weeks and 9 weeks post-surgery. a) young-Wistar 3 weeks, b) young-Wistar 9 weeks, c) young-GK 3 weeks, d) young-GK 9 weeks. GT: Granulation tissue.

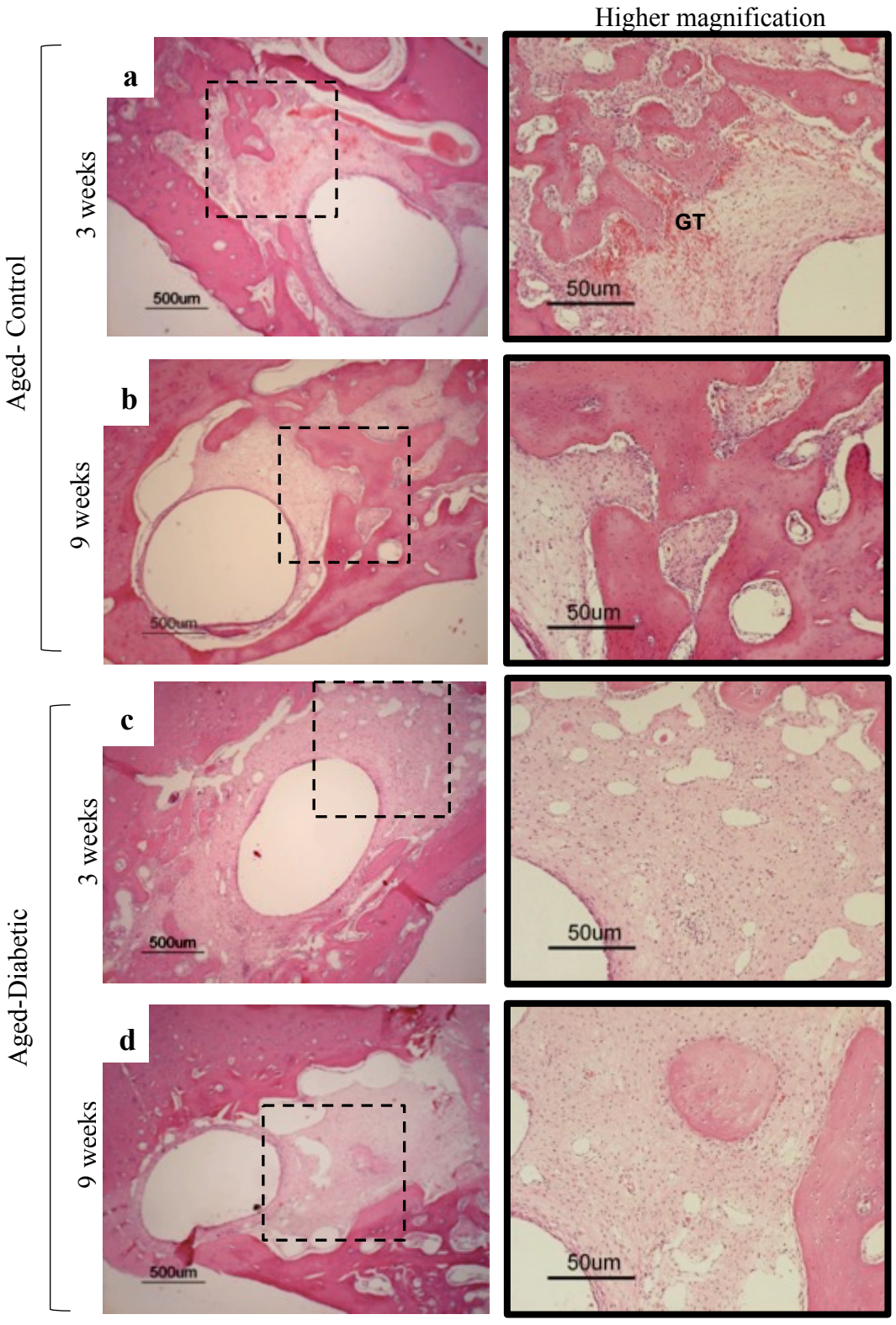

Figure 4.2 Haematoxylin-eosin section from the aged Wistar and GK rats, 3 weeks and 9 weeks post-surgery. a) aged-Wistar 3 weeks, b) aged-Wistar 9 weeks, c) aged-GK 3 weeks, d) aged-GK 9 weeks. GT: Granulation tissue.

4.2.2 Immunolocalisation of TGF-β_1

Localisation of TGF-β_1 within the bone-implant contact region showed moderate sequestration of TGF-β_1 throughout the ECM of healing tissue sites in young–control and young-diabetic tissue (Figure 4.3c and 4.3d). TGF-β_1 labelling was predominantly deposited along the formation of collagen fibres and woven bone structure within the ECM region, but only at intermittent points. Observation of TEM images also demonstrated that TGF-β_1 was intracellularly synthesised, before being transported and incorporated into the ECM (Figure 4.3c). The image also revealed specific gold labelling in cellular regions for TGF-β_1, but none over the bare resin showing that the specificity of labelling is fairly good even though the tissue was initially perfused fixed in formalin. Negative-control image over areas of collagen fibres show no gold labelling (Figure 4.3d), indicating that the labelling was specific. This evidence demonstrated that prolonged formalin fixation did not significantly reduce immunoreactivity for TGF-β_1 antigen, even if fixation was prolonged to 120 days. Hence, it further justified the semi-quantitative analysis performed on TGF-β_1 immunogold-labeled particles in the next section.

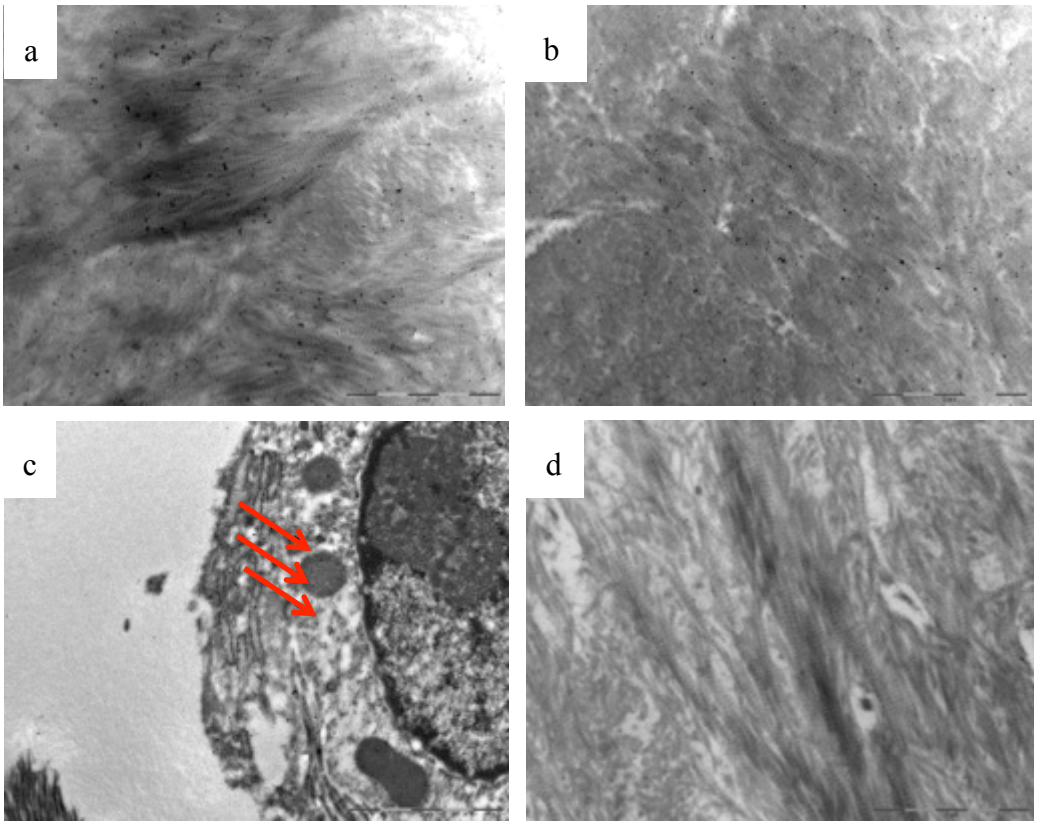

Figure 4.3 a) Immunolocalisation of TGF-β_1 in young-Wistar rats sample at 3 weeks post-implant surgery. Regular labelling is seen around the collagen fibres. b) Immunolabelling of young-GK samples with TGF-β_1 at 3 weeks. c) Specific gold label is seen only within the cellular regions (arrowed). The resin background is free of any gold particles indicating high spesificity of TGF-β_1 labelling within the tissue sample. d) Immunolabelling of young-Wistar rat with antibody omitted. The negative control showed no gold labelling throughout the tissue. Scale bar =2μm.

4.2.3 Quantification of TGF-β_1 immunolabelling

Following the successful TGF-β_1 immunolabelling techniques, further analysis was conducted by quantifying the number of gold-labelled particles in a random field of 30μm^2-sized ECM of the bone-implant contact area. Minimums of 23 images were counted per experimental group. Based on three-way ANOVA analysis results, a significant increase of TGF-β_1 localisation in the matrix area ($p<0.01$) was reported in the young-diabetic group, in comparison to young-control group at 9 weeks, following surgical implant insertion (Figure 4.4). Similarly, comparisons made within the diabetic group at 9 weeks post-surgery, between young and aged animals, also showed significant differences in TGF-β_1 sequestration within the ECM. However, further analysis made between aged-control and aged-diabetic groups, either at 3 week or 9 weeks post-surgery, did not reveal any significant differences in TGF-β_1 localisation within the bone repair sites.

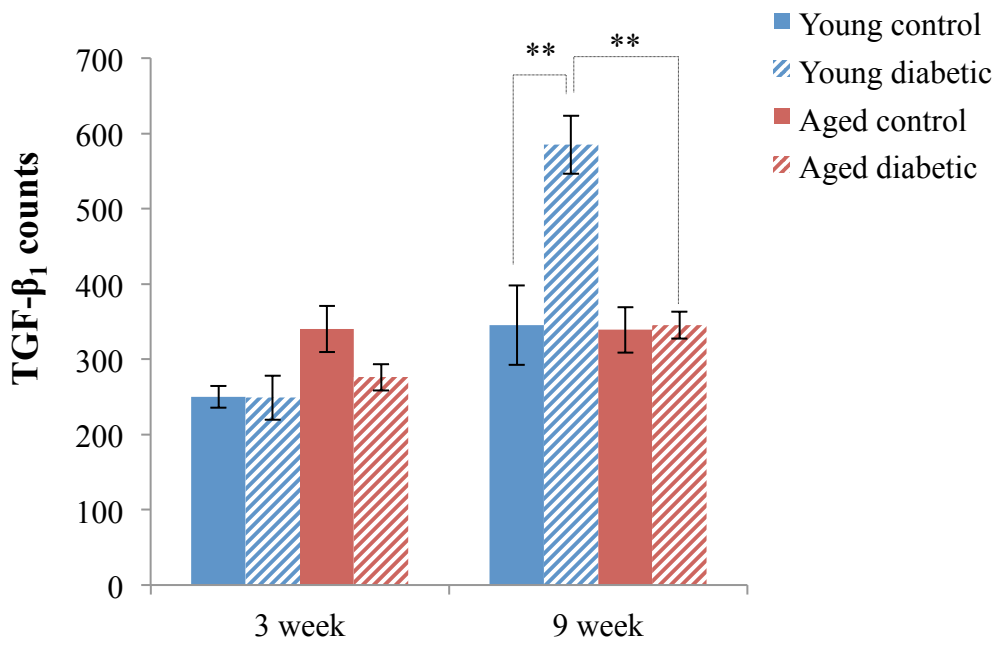

Figure 4.4 Quantification of TGF-β_1 immunolabellling from diabetic and control group. Each bar represent mean ± SEM. N=3, n=23 and $^{**}p<0.01$ accepted as statistically significant between experimental groups. All *p* values were based on three-way ANOVA.

4.2.4 Validation of high glucose effect on TGF-β_1 gene expression and protein synthesis

MSC gene expression patterns for TGF-β_1 were examined at different time point, leading to matrix deposition and bone formation within bone repair sites (Figure 4.5). Relative to housekeeping gene as controls, the results suggested downregulation of TGF-β_1 expression in early PD cells. No significant differences of TGF-β_1 expression were observed between PD15 cells that were cultured in either 5.5mM or 25.0mM osteogenic medium. On the other hand, a significant variation in gene expression was seen among PD150 cells induced in different glucose levels within osteogenic medium. At day 21, PD150 cells which were long-term expanded in normoglycaemic culture medium exhibit significant increases in TGF-β_1 expression ($p<0.01$), when differentatiated in high glucose osteogenic medium. In contrast, hyperglycaemic-cultured PD150 cells demonstrated downregulation of TGF-β_1 expression ($p<0.01$) following osteogenesis in high glucose medium, in comparison to 5.5mM osteogenic medium. These results are likely to suggest that hyperglycaemic osteogenic medium exerts different effects on late PD cells, which are closely linked to the glucose-stimulation applied during the expansion period. Moreover, comparison made between PD150 cells which were differentiated in 25.0mM osteogenic medium, demonstrated that CCM-expanded cells posses significantly higher capacity to upregulate TGF-β_1 on day 21, as opposed to HGCM-expanded cells. The data indicated that high glucose exposure throughout the expansion period might alter MSCs responsiveness on TGF-β_1 expression, in subsequent exposure to osteogenic medium.

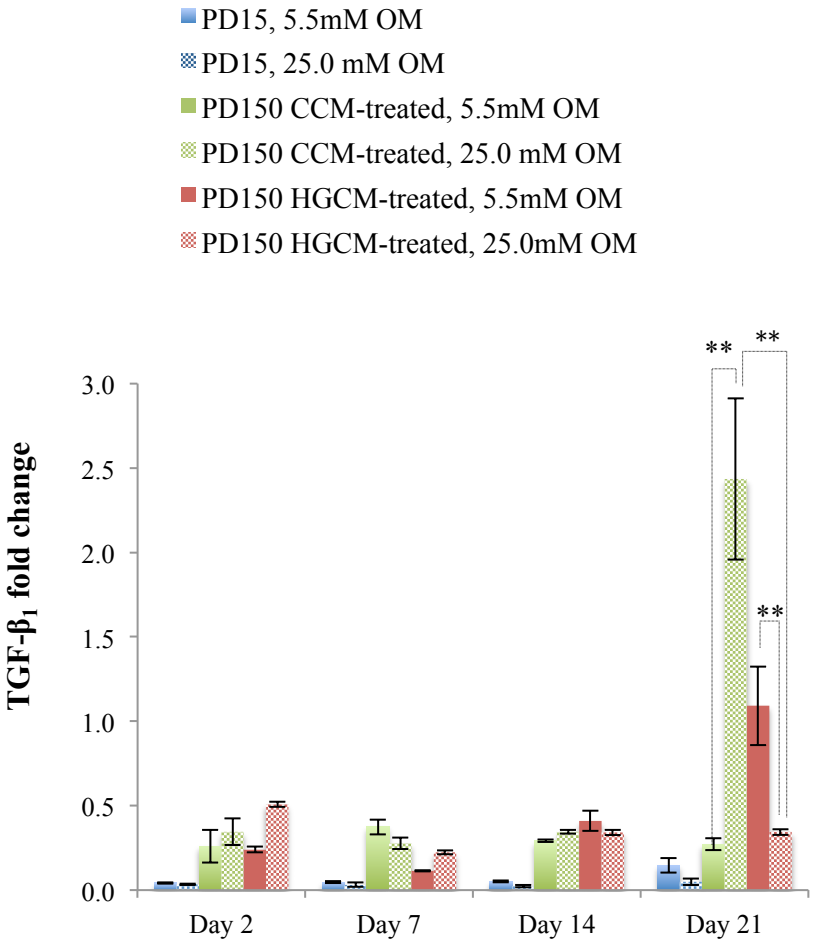

Figure 4.5 BCE-MSCs were induced to undergo osteogenesis in normoglycaemic and hyperglycaemic osteogenic medium (OM). TGF-β_1 expression levels of BCE-MSCs assessed by qRT-PCR are reported as fold changes from day 0. Solid boxes represented 5.5mM OM-cultured and hatched box represented 25.0mM OM-cultured cells. Each bar represent mean±SD. N=2, n=3. *p<0.05, **p<0.01, when statistically compared between group. All p values were based on mixed ANOVA. PD, population doubling; CCM, complete culture medium; HGCM, high-glucose culture medium.

The expression of TGF-β_1 by MSCs at protein level was determined by Western blot over the full duration of the culture. As shown in Figure 4.6, PD15 BCE-MSCs cell culture extracts revealed a few TGF-β_1 band at different molecular weights, corresponding to one high molecular weight protein with approximate size of 110kDa and fewer proteins at 45kDa and 25kDa. However, the 110kDa band was not observed in the ECM extracts.

The control sample, which only contain 10% FBS+OM without any cells showed detection of TGF-β_1 precursor protein bands at 45kDa and 110kDa. Similarly, abundance of TGF-β_1 expression was present in the culture medium extracts, with strong blotting patterns observed in the high glucose osteogenic medium. The same trend of staining was seen in cell extracts, with distinct TGF-β_1 expression of 110kDa protein, stimulated on day 7 and 21, in high glucose OM. In contrast, examination on ECM extracts showed the presence of one strong band detected at approximately 45kDa on day 21 following culture in 25.0mM osteogenic medium and less amount of TGF-β_1 expression observed on day 14 and 21 in the 5.5mM osteogenic medium. Similar analysis on culture medium extracts of PD150 BCE-MSCs (Figure 4.7) demontrated a greater amount of TGF-β_1 band expression in CCM-treated pools, compared to HGCM-treated cells. However, comparison made between induction medium of different glucose levels revealed almost similar patterns in the normoglycaemic-culture expended cells, as oppose to contrasting patterns of expression observed in the HGCM-treated cells.

The specificity of these TGF-β_1 bands was determined by preincubating the antibody with the blocking peptide against which the antiserum was raised. The antibody was preincubated in a 10-fold excess of peptide overnight at 4°C and then used for immunoblotting. Preincubation with TGF-β_1 blocking peptide led to disappearance of all associated bands (data not shown). Therefore, this data suggests that the antibody used in this study specifically recognised the TGF-β_1 protein.

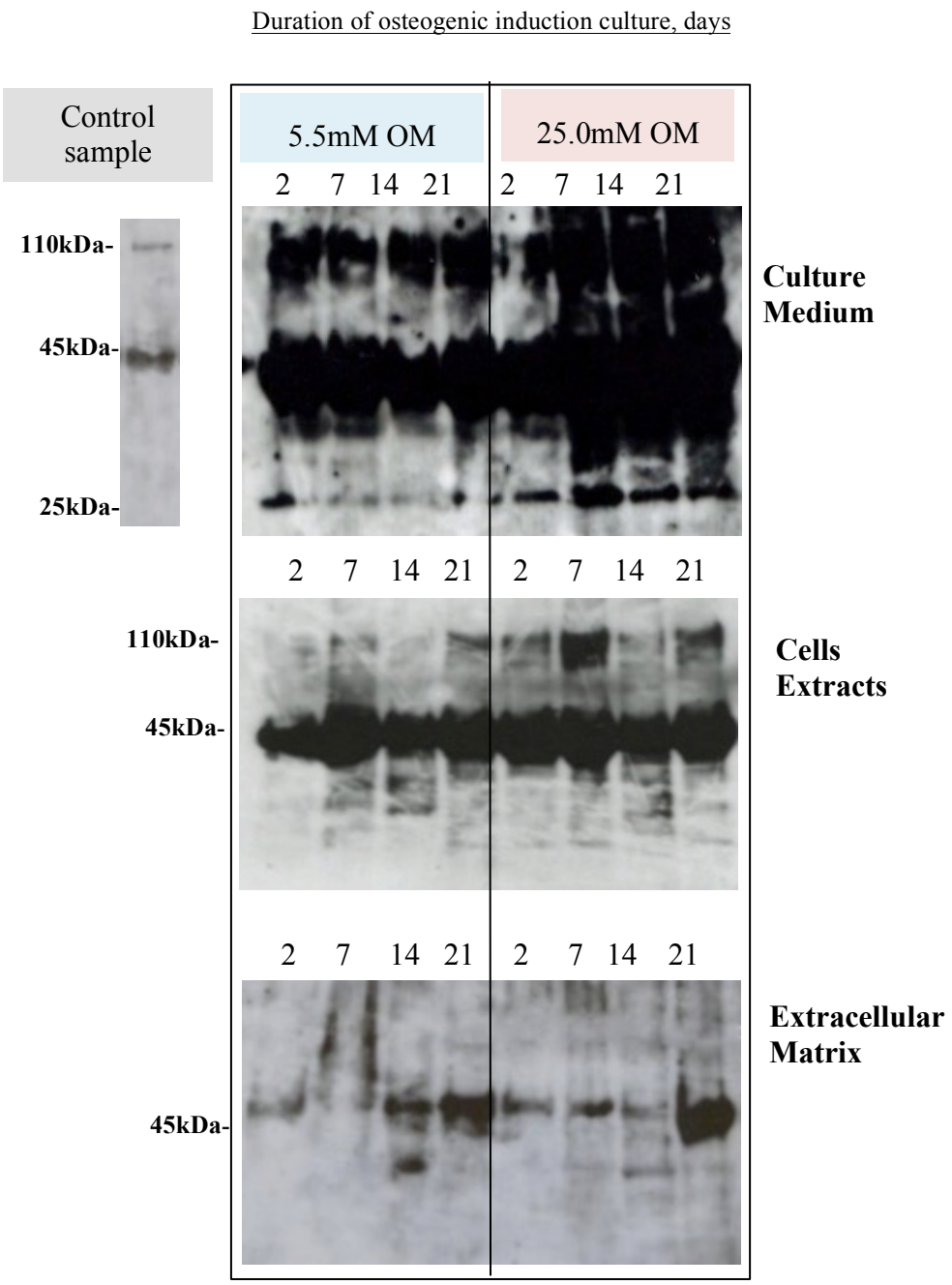

Figure 4.6 Representative blot of a time-course high glucose level effect on TGF-β_1 synthesis of PD15, CCM-cultured BCE-MSCs. The BCE-MSCs were differentiated in 5.0mM OM and 25.0mM OM for the indicated time period. 20µg of protein derived from culture medium, cell lysates and extracellular matrix extracts were loaded onto SDS-PAGE gels and electrotransferred onto PVDF membranes. The blots were then developed with TGF-β_1 antibody. Control sample, which contain 10% FBS+OM without any cells showed detection of TGF-β_1 precursor protein bands. OM, osteogenic medium; PD, population doubling level; CCM, complete culture medium.

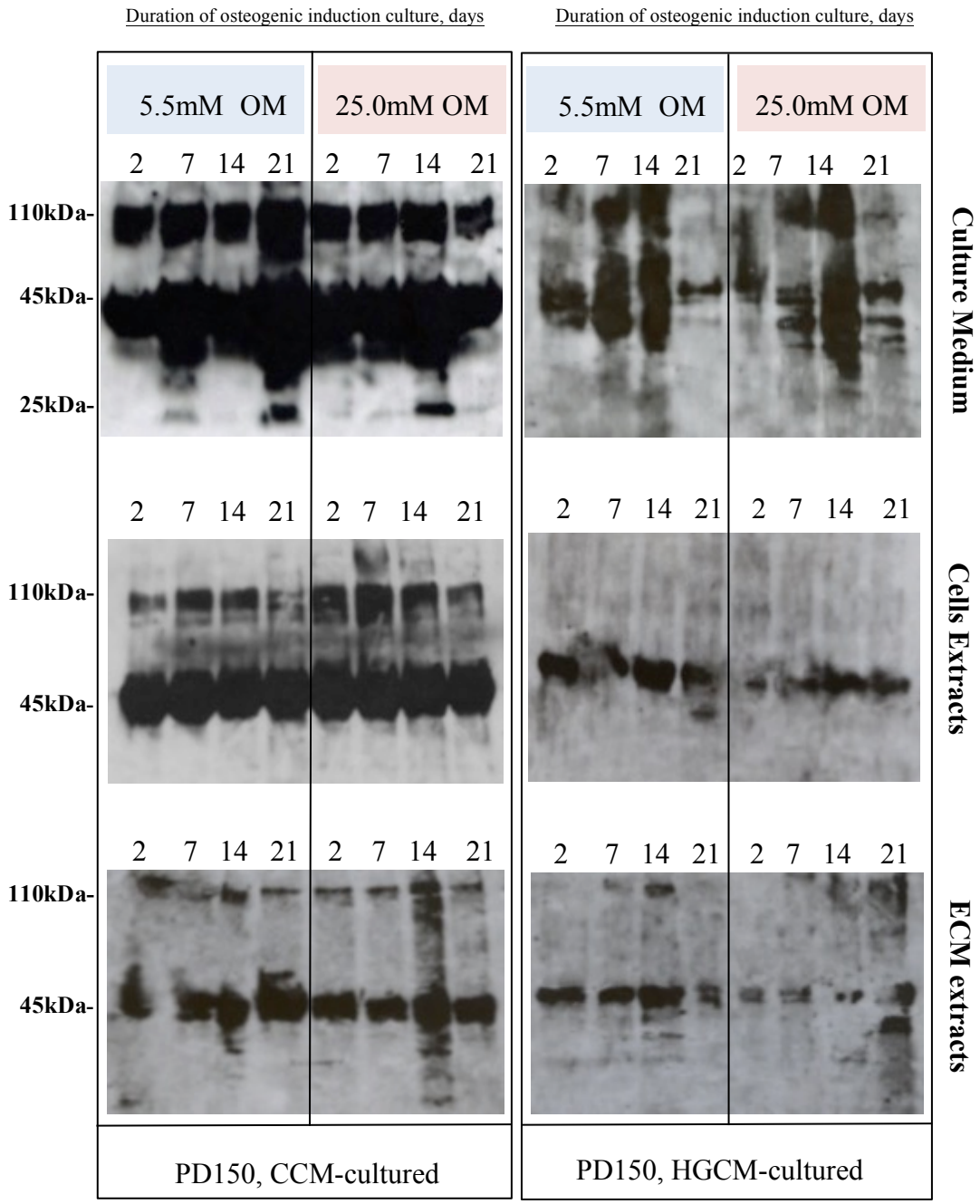

Figure 4.7 Representative blot of a time-course high glucose level effect on TGF-β_1 synthesis by PD150 MSCs from CCM-treated and HGCM-treated group. The BCE-MSCs were differentiated in 5.0mM OM and 25.0mM OM for the indicated time period. 20μg of protein derived from culture medium, cell lysates and extracellular matrix (ECM) extracts were loaded onto SDS-PAGE gels and electrotransferred onto PVDF membranes. The blots were then developed with TGF-β_1 antibody. PD, population doubling level; OM, osteogenic medium; CCM, complete culture medium; HGCM, high-glucose culture medium.

4.2.5 Validation of high glucose level on biglycan gene expression and protein synthesis

TGF-β_1 is mainly associated with stimulation of biglycan core protein synthesis. To determine whether TGF-β_1 regulation and localisation within the ECM was directly affected by the relative amount of proteoglycans existed within the cellular environment, both qRT-PCR and Western blot analysis were conducted to detect the expression of biglycan by the osteo-induced MSCs. Biglycan gene expression profiling was performed on PD15, PD150 CCM-treated and PD150 HGCM-treated MSCs, which were differentiated in either 5.5mM osteogenic medium or 25.0mM osteogenic medium (Figure 4.8). Under osteogenic conditions, biglycan expression observed in the early proliferative stage of BCE-MSCs osteogenic culture (PD15) exhibit an average fold change below 1.0, indicating the downregulation of the gene. While hyperglycaemic osteogenic medium did not reveal considerable changes in biglycan expression in the early PD cells, statistically significant biglycan upregulation in cells of late PD were observed, particularly between the CCM-cultured and HGCM-cultured cells.

Bone explant cells which were long-term expanded in normal glucose medium showed significant increases in biglycan expression at day 21 ($p<0.01$), when induced for osteogenesis in high glucose medium, indicating the stimulation effect of short-term high glucose on diabetic-induced MSCs to produce higher biglycan levels. Likewise, analysis made on cells from late PD HGCM-cultured MSCs, that was induced in 25.0mM of osteogenic medium showed a significant increased in mRNA expression for biglycan on day 2 of osteogenesis ($p<0.01$). However, subsequent observation at day 14 and 21, reported significantly marked reduction of biglycan expression in late PD HGCM-treated cells in the hyperglycaemia induced medium. Overall, these results suggested different alterations in biglycan gene expression of MSCs induced in different level of glucose, in respect to prior short- or long-term exposure in diabetic-induced medium.

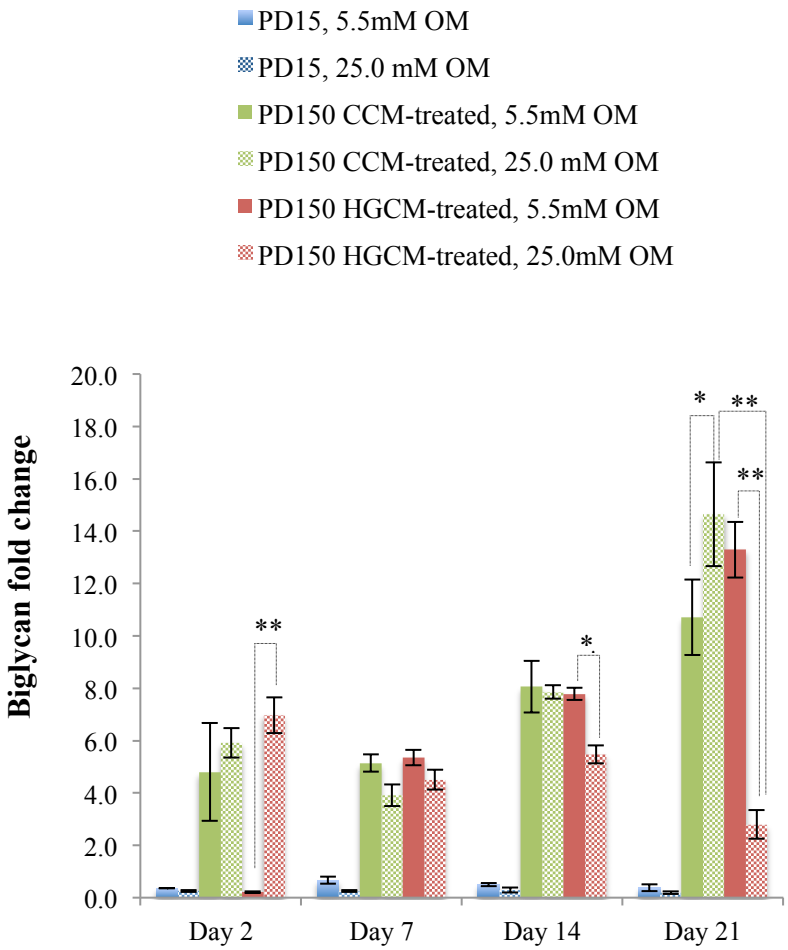

Figure 4.8 Biglycan expression levels in BCE-MSCs assessed by qRT-PCR are reported as fold changes. Solid boxes represented 5.5mM OM-cultured and hatched boxes represented 25.0mM OM-cultured cells. Data is presented as means ± SD. N=2, n=3. *p<0.05, **p<0.01, when statistically compared between group. All p values were based on mixed ANOVA. PD, population doubling level; OM, osteogenic medium; CCM, complete culture medium; HGCM, high-glucose culture medium.

Biglycan core protein synthesis by MSCs was examined using Western blot. Observation made on secreted proteoglycans from early (Figure 4.9) and late PD BCE-MSCs (Figure 4.10), revealed the presence of one particular biglycan band at 45kDa in all extracts. There are considerable changes in biglycan band formation in early PD cells, particularly observed on cells extracts and ECM extracts samples. The results demonstrated that stronger biglycan bands were formed in high glucose osteo-induction medium, compared to normolycemic medium, throughout culture from day 2 until day 21 of induction in PD15 cells.

Further analysis of biglycan core protein was conducted on PD150 cells group, which was either previously prolonged cultured in normoglycaemic level or diabetic-induced condition. Less staining pattern of biglycan core protein band was observed in the cell extracts sample of BCE-MSCs grown in prolonged high glucose culture medium. Moreover, short-term high glucose osteo-induction medium seems to reveal no changes for the staining pattern in biglycan band between the CCM-treated and HGCM-treated, PD150 cells. Analysis on ECM extracts displayed a presence of strong biglycan protein band in the 5.5mM OM on day 2, whereas the band only appear in the 25.0mM treated group on day 7 after ostegenic induction. Similarly, a pattern of delayed biglycan localisation in the extracellular matrix compartment was seen in ECM extracts of HGCM-treated cell, as biglycan protein band was observed on day 7 in normal OM and was later observed on day 14 in the 25.0mM induction medium. Indirectly, these findings are likely suggesting a relative alteration and delay of biglycan expression by the bone progenitor cell populations within the uncontrolled high glucose-induced environment, which possibly occurs in the inflammatory stage of diabetic bone repair.

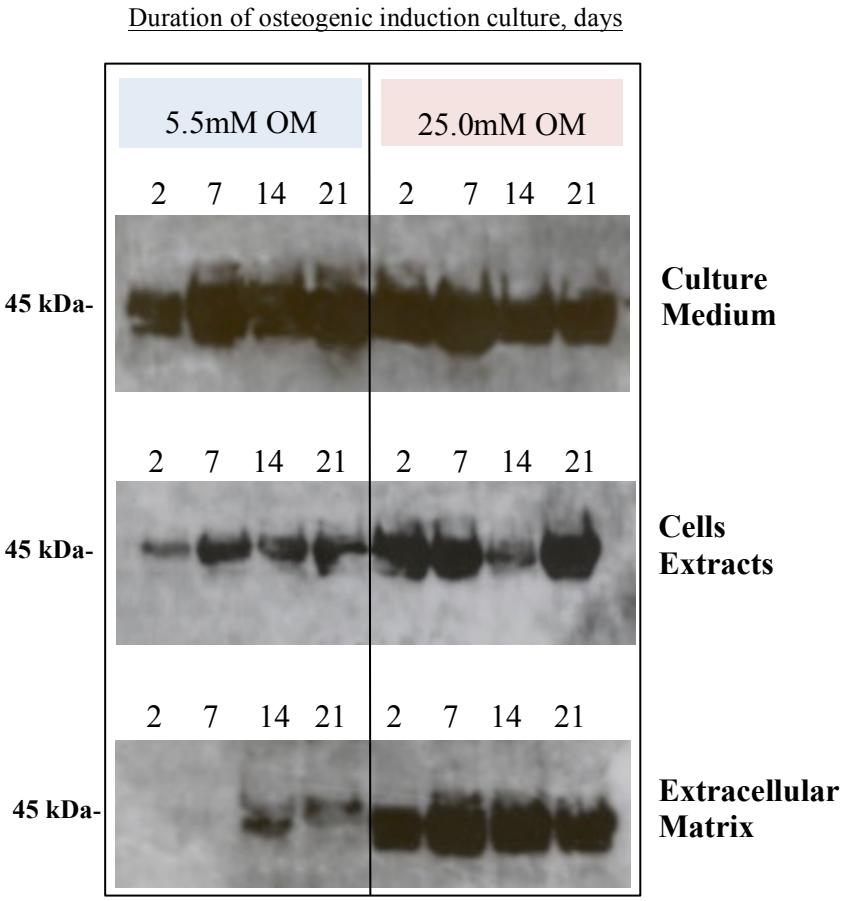

Figure 4.9 Representative blot of a time-course high glucose level effect on biglycan core protein synthesis by MSCs from PD15 CCM-treated cells. Rat BCE-MSCs were cultured in 5.5mM OM and 25.0mM OM for the indicated time period. 20μg of protein derived from culture medium, cell lysates and extracellular matrix extracts were loaded onto SDS-PAGE gels and electrotransferred onto PVDF membranes. The blots were developed with biglycan antibody. PD, population doubling level; OM, osteogenic medium; CCM, complete culture medium.

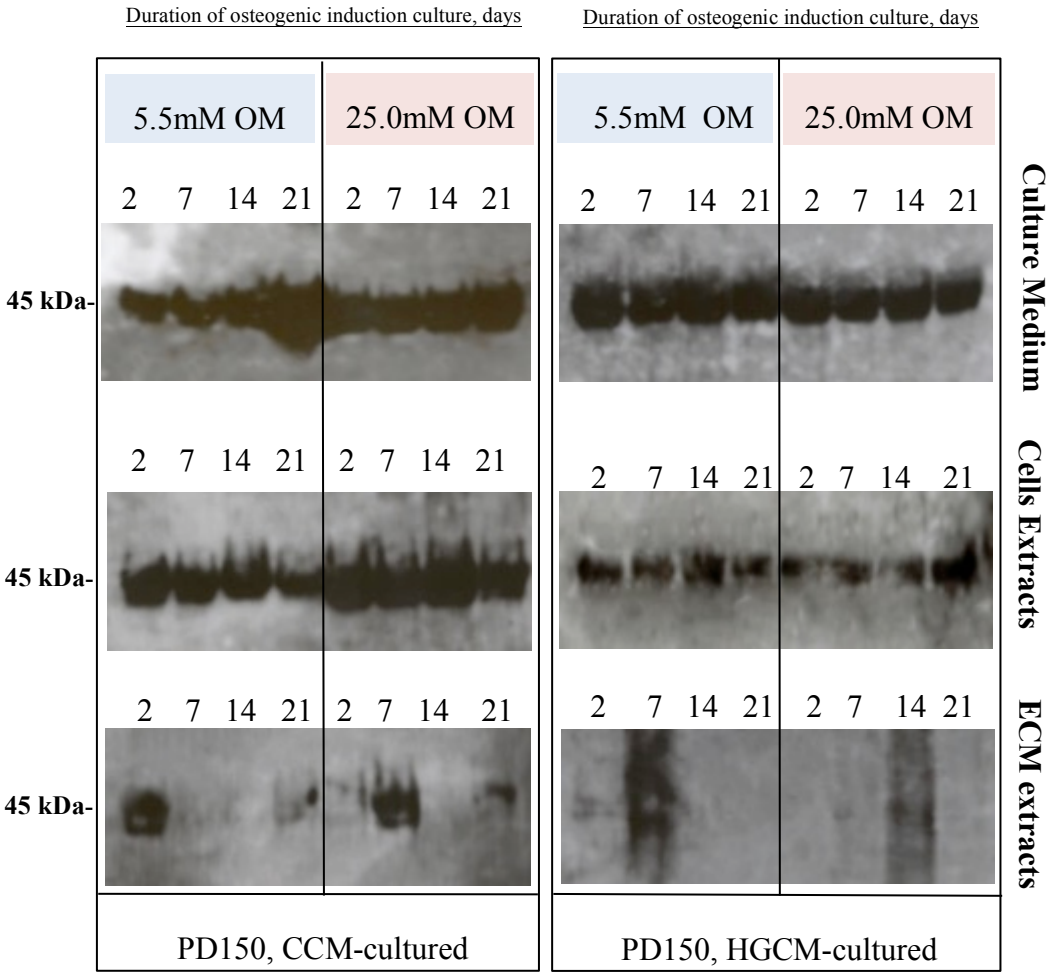

Figure 4.10 Representative blot of a time-course high glucose level effect on biglycan core protein synthesis by MSCs from PD150, CCM-treated and HGCM-treated group. Rat BCE-MSCs were cultured in 5.5mM OM and 25.0mM OM for the indicated time period. 20μg of protein derived from culture medium, cell lysates and extracellular matrix (ECM) extracts were loaded onto SDS-PAGE gels and electrotransferred onto PVDF membranes. The blots were developed with biglycan antibody. PD, population doubling level; OM, osteogenic medium; CCM, complete culture medium; HGCM, high-glucose culture medium.

4.2.6 Validation of high glucose effect on decorin gene expression and protein synthesis

Decorin is another type of relevant proteoglycan that are commonly linked with TGF-β_1 regulation and sequestration within the ECM. MSC gene expression of decorin was analysed over a period of 21 days, in normal and high-glucose osteogenic medium. From Figure 4.11, the gene expression levels of decorin in early PD cells were not significantly changed throughout the differentation period, with the level of expression maintained at relatively low levels. Conversely, the expression of decorin in late PD CCM-cultured cells indicated a significant decrease with strong fold changes ($p<0.01$), reported on days 2 following the osteo-induction in high glucose level. However, observation on day 21, demonstrated that decorin expression was significantly elevated in CCM-cultured cells, which undergo osteo-induction in hyperglycaemic environments ($p<0.01$). A similar pattern of alteration in decorin gene expression was seen in the diabetic-induced MSCs, particularly in the hyperglycaemic osteoblast cultures, although the data did not reveal statistically significant differences between the treated group. Although decorin gene expression in PD150 HGCM-treated cells was only reported to be significantly increased on day 21 in 5.5mM osteogenic medium, the results suggested that subsequent hyperglycaemic osteo-inductions, however, may play a role in suppression of decorin gene expression and influence the regulatory mechanism of TGF-β_1 activity, at a cellular level.

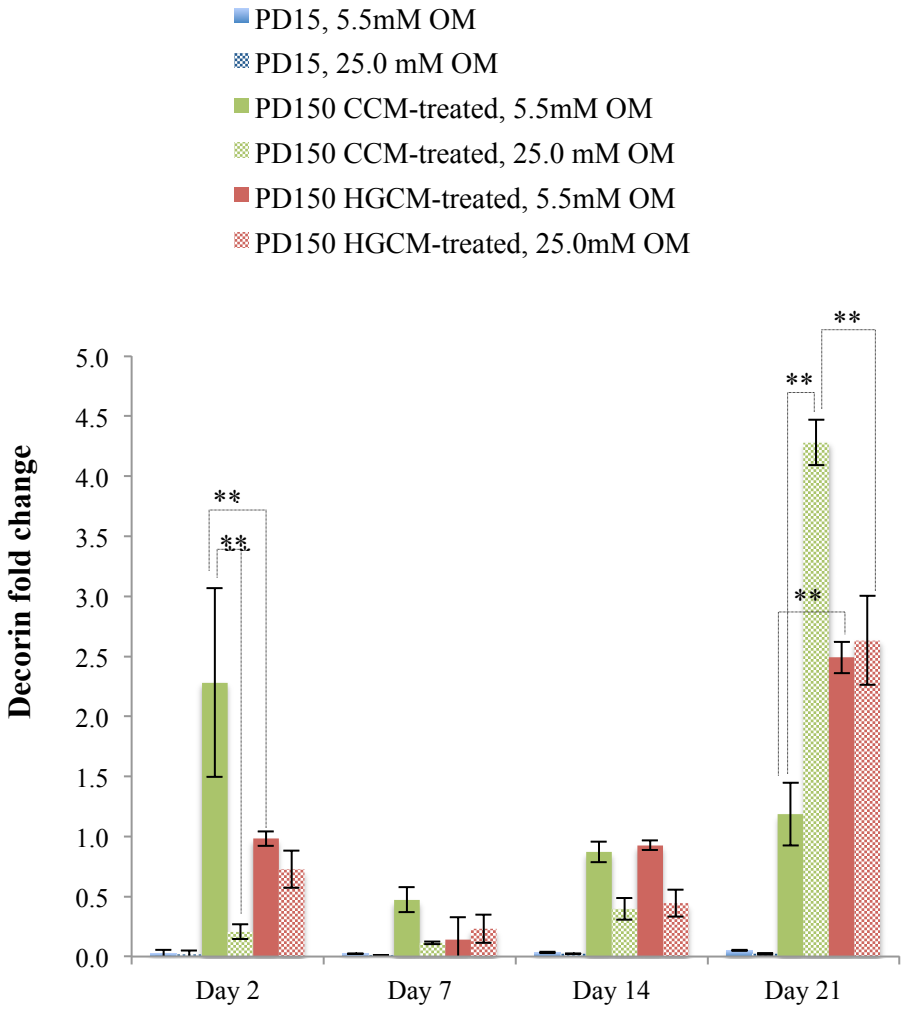

Figure 4.11 Comparison of decorin expression levels in BCE-MSCs measured with qRT-PCR is reported in fold changes. Solid box represented 5.5mM OM-cultured and hatched box represented 25.0mM OM-cultured cells. Data is presented as means ± SD. N=2, n=3. *p<0.05, **p<0.01, when statistically compared between group. All p values were based on mixed ANOVA. PD, population doubling level; OM, osteogenic medium; CCM, complete culture medium; HGCM, high-glucose culture medium.

MSCs decorin synthesis over a 21 day period in either normoglycaemic or hyperglycaemic osteo-induction medium was determined by Western blot. From the SDS-PAGE of culture medium extracts (Figure 4.12), 3 distinct protein bands with the size of approximately 120kDa, 90kDa and 40kDa were detected in high glucose osteo-induction PD15 BCE-MSCs culture, while the normoglycaemic level only revealed the formation of 40kDa protein bands. Further analysis on cell extracts cultured in 25.0mM osteogenic medium revealed the presence of single decorin protein at 40kDa, compared to none or very low level of bands formation observed in the 5.5mM osteo-induction medium. On the other hand, analysis of ECM extracts of PD15 samples exhibited the presence of few decorin bands at different molecular weights corresponding to approximate size of 110kDa, 40kDa and 25kDa. However, comparisons made between different osteogenic treatments likely suggest that decorin band formation on days 14 and 21 in high glucose level is more concentrated compared to similar days synthesis in the normolycemic condition.

Western blots of culture medium extracts from PD150 MSCs (Figure 4.13) revealed the presence of 4 decorin protein bands, with approximate size of 120kDa, 90kDa and 40kDa, as previously decscribed in early PD BCE-MSCs. Analysis on cell extracts and ECM extracts revealed considerable reductions in decorin band staining pattern of BCE-MSCs which had undergo long-term diabetic-induced culture, in comparison to the normoglycaemic-expanded cultures. An additional band was detected in PD150 HGCM-cultured cells, at an approximate size of 25kDa. Decorin protein band of PD150, ECM extracts from 5.5mM osteogenic medium were detected at day 7, while a band with similar staining pattern were only present in hypeglycaemic-OM cells at days 14 and 21, which likely suggests a delay in decorin localisation into the ECM compartment.

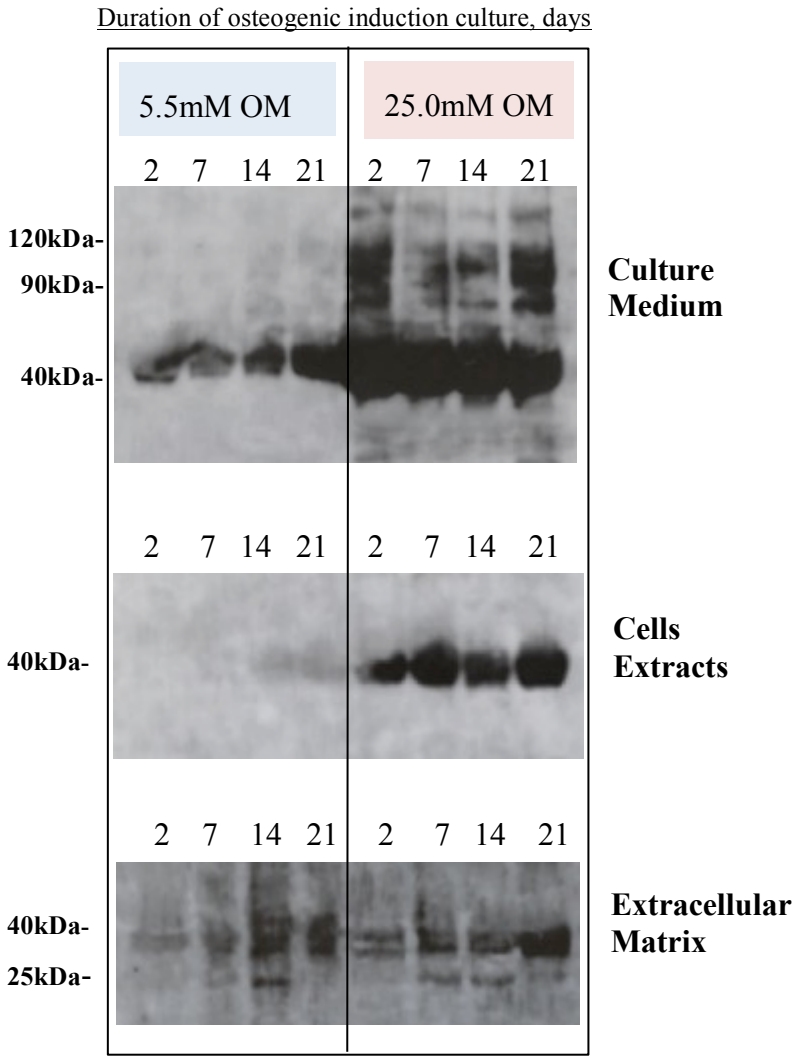

Figure 4.12 Representative blot of a time-course high glucose level effect on decorin synthesis by MSCs from PD15, CCM-treated cells. Rat BCE-MSCs were cultured in 5.5mM OM and 25.0mM OM for the indicated time period. 20μg of protein derived from culture medium, cell lysates and extracellular matrix (ECM) extracts were loaded onto SDS-PAGE gels and electrotransferred onto PVDF membranes. The blots were developed with decorin antibody. PD, population doubling level; OM, osteogenic medium; CCM, complete culture medium.

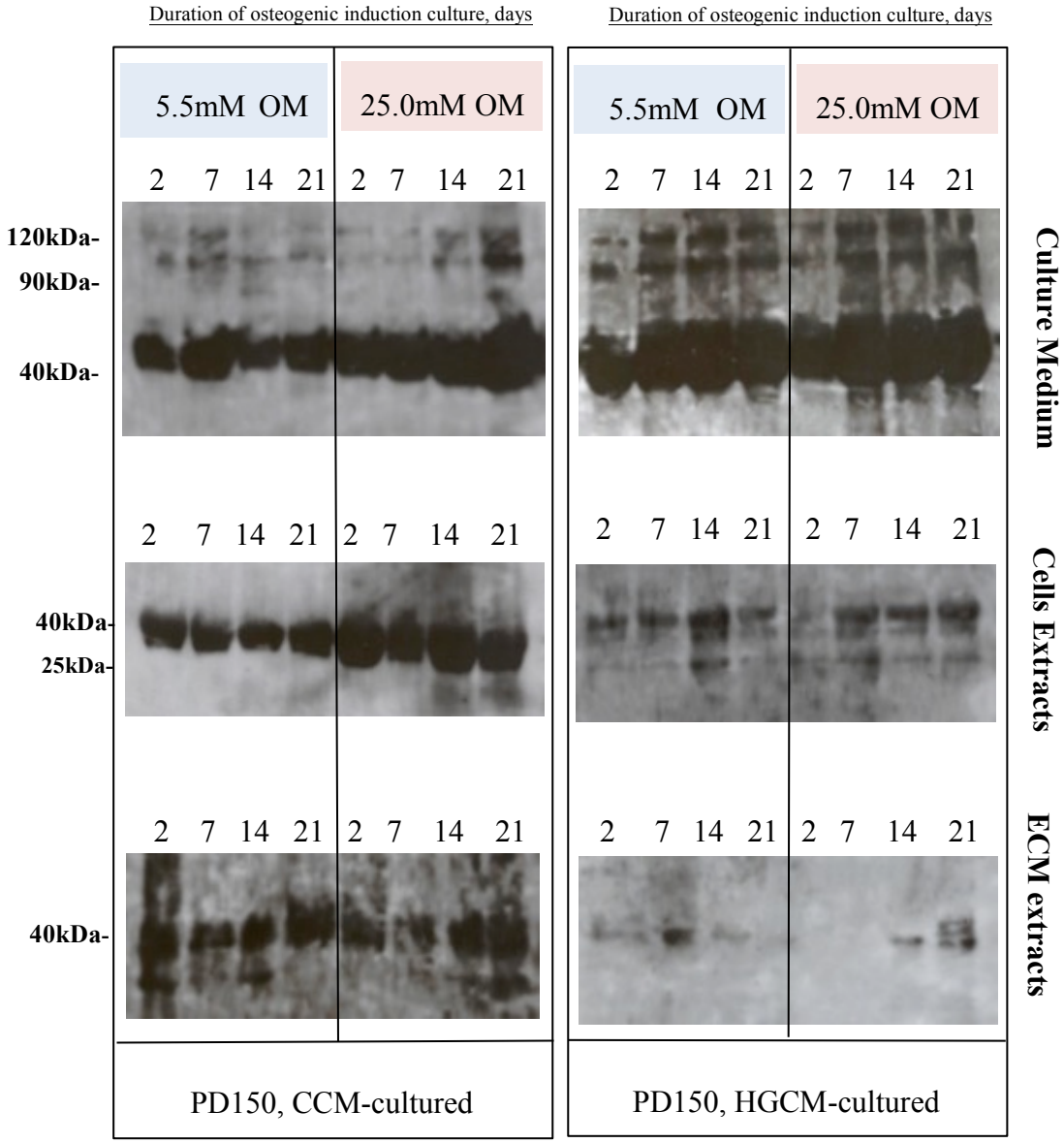

Figure 4.13 Representative blot of a time-course high glucose level effect on decorin synthesis by MSCs from PD150, CCM-treated and HGCM-treated cells. Rat BCE-MSCs were cultured in either 5.5mM OM or 25.0mM OM for the indicated time period. 20μg of protein derived from culture medium, cell lysates and ECM extracts were loaded onto SDS-PAGE gels and electrotransferred onto PVDF membranes. The blots were developed with decorin antibody. PD, population doubling level; OM, osteogenic medium; CCM, complete culture medium; HGCM, high-glucose culture medium.

4.2.7 SMAD expression in osteo-induced rat BCE- MSCs

Immunoblotting was performed with anti-Smad2 antibodies that cross reacts with Smad3. As shown in Figure 4.14, particularly from PD150 CCM-treated samples, the antibody revealed two bands: one at 60kDa, the expected size of Smad2, and one at 52kDa, the expected size of Smad3. Although Smad3 protein was consistently expressed during the differentation period in PD150 CCM-treated MSCs, the result reported an absence of Smad2 protein band on day 7 of induction in normoglycaemic osteogenic medium. In contrast, Smad2/3 protein bands from PD15 and PD150 HGCM-treated cells only show one strong band located between the sizes of 52kDa to 60kDa, which potentially resulted from the fusion of two separate bands. Smad 2/3 protein expression seen in PD15 and PD150 HGCM-treated cells is also relatively unchanged during the osteogenic induction, regardless of the different glucose levels.

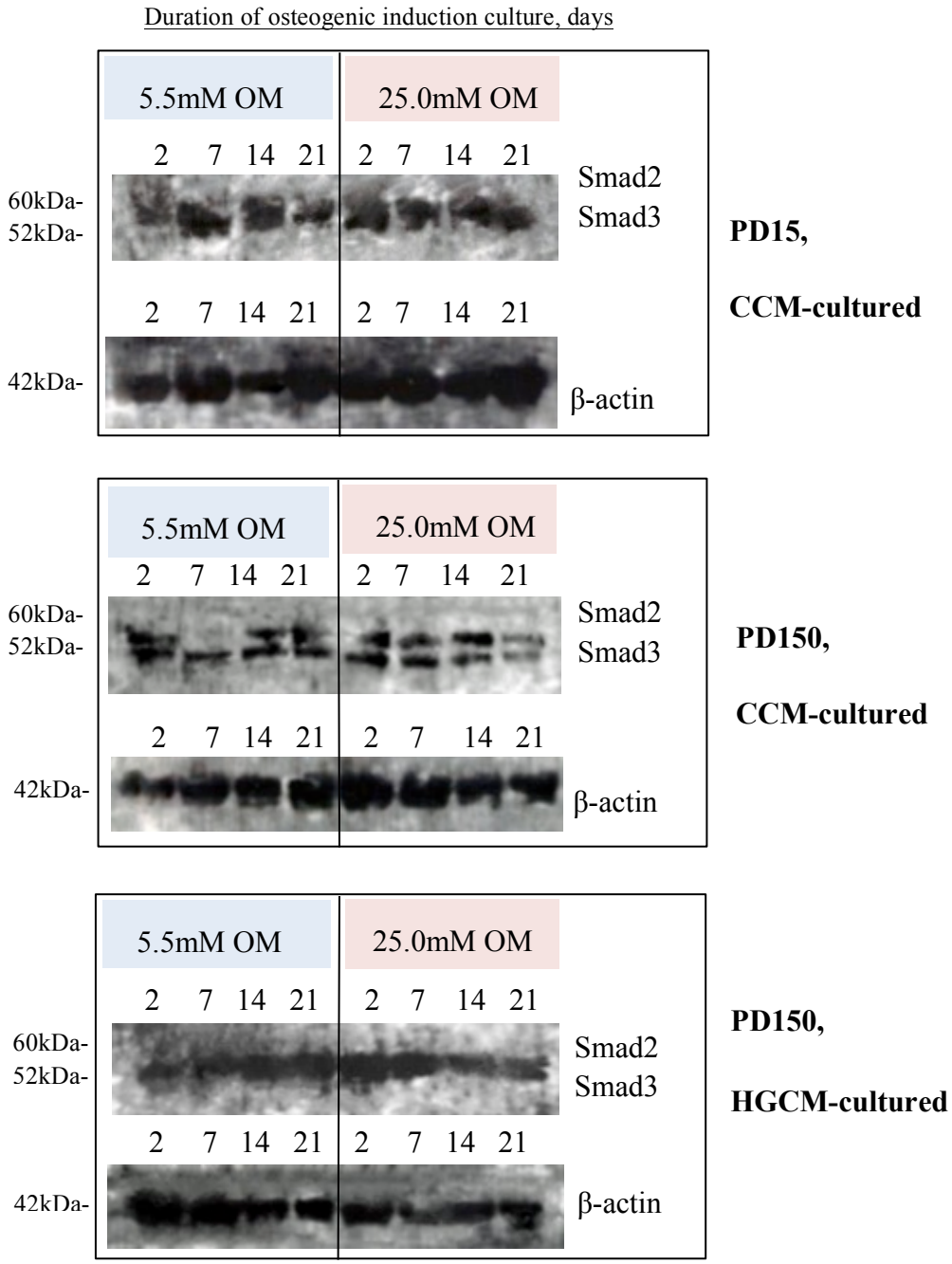

Figure 4.14 Representative blot of a time-course high glucose level effect on Smad 2/3 expression by MSCs from PD15 and PD150, CCM-treated and HGCM-treated cultures. BCE-MSCs were cultured in normal OM and high glucose OM for the indicated time period. 20μg of protein derived from cell lysates, were loaded onto SDS-PAGE gels, electrotransferred onto PVDF membranes and the blot were developed with anti-Smad 2/3 antibody. β-actin was used as a loading control.

4.3 Discussion

The present Chapter provides detailed investigation of T2DM environment effects on implant osseointegration, with attention given for investigating the responsiveness of bone-derived MSC populations to stimulate the expression and to modulate the bioavailability of matrix bound-growth factors. Immunohistochemical and histological staining enabled characterization of new bone tissue formation at the bone-implant interface in the *in vivo* study, which allowed further representation of cellular changes within the healing area. Profound impairments were observed in the aged and diabetic groups, even after longer duration was given for the reparative process to take in place, suggesting a delay in bone repair capacity. These results had further extended previous studies on bone repair impairment, which had been reported in much younger animal models (Hasegawa et al. 2008; Sakai et al. 2008; Wang et al. 2010a; Colombo et al. 2011). Therefore, this study has extended the current knowledge on bone repair capacity in aged animal populations that confirmed the role of aging in the deterioration of regenerative capacity, which was progressively worsened by diabetic condition.

A significant increase of TGF-β_1 expression was observed in young diabetic rats, in comparison to healthy controls, at nine weeks post-implant surgery, as previously demonstrated in similar *in vivo* studies of T2DM models in young animal models (Colombo et al. 2011). However, the present data showed insignificant difference in TGF-β_1 localisation within the ECM of the healing area in the aged group, regardless of implant duration and diabetic status. TGF-β_1 localisation in the bone area had been highly associated with the functional role of bone progenitor cell populations to produce and to control the availability of growth factor within cellular microenvironment (Janssens et al. 2005). Again, the data suggested that both diabetic and aging potentially altered growth factor expression by MSCs, particularly TGF-β_1 during the healing progress, which affected their essential roles in bone metabolism, and led to subsequent delays in bone repair and remodelling. This interpretation has never been mentioned in any previous osseointegration studies in T2DM animal models (Hasegawa et al. 2008; Sakai et al. 2008; Wang et al. 2010a; Colombo et al. 2011), due to the lack of evidence provided in aged populations.

TGF-β_1 serves a major role in inducing the migration of MSCs to the repair site in order to co-ordinate new bone formation (Tang et al. 2009). Therefore, TGF-β_1 alterations within the healing site of diabetic animals from the *in vivo* study might potentially be associated with the response properties of MSCs within diabetic-induced condition. To further explain the *in vivo* results, the present study continued to analyse *in vitro* evidence of the cellular and molecular responses of bone progenitor cell populations within hyperglycaemic-induced environments. In order to investigate the cellular mechanisms in diabetic alterations, cells that were isolated and expanded in long-term culture had been induced in osteogenic medium and investigated for their capacity to express and synthesis TGF-β_1, in response to different glucose stimulation. The result might not be interpreted as a direct comparison to the *in vivo* model, which was represented by young and aged animal groups, but it fit the main purpose of studying ageing influence on cells' regenerative capacity, in which both aged cells from *in vivo* or *in vitro* experiments involving cells that had undergone a large number of population doubling levels.

Within this study, reduced regenerative capacity of MSCs was found to mask the delayed diabetic influences on healing cascades. TGF-β_1 expression in cultured mature osteoblasts was significantly altered, depending on the duration of exposure to high glucose medium. Bone marrow-derived MSCs isolated from aged animals were reported to have lower proliferative capacity and less regenerative potential (Scutt et al. 1996). Therefore, the present data suggested a possible association between MSCs proliferative capacity and TGF-β_1 production, which is related to the capacity of MSCs to differentiate bone-forming cells and to further synthesise the reparative endogenous molecules. Besides, prolonged hyperglycaemic-cultured MSCs demonstrated a delay in TGF-β_1 protein synthesis and sequestration within the ECM. Although the mechanisms of how hyperglycaemic might induce differentials expression and synthesis level of TGF-β_1 are partially understood, as the present findings suggested that MSCs demonstrated similar responsiveness towards growth factor expression, either *in vivo* or *in vitro*. Growth factors had been proposed to have a role in regulating glucose uptake and co-ordinating the metabolic pathway for cell growth (Vander Heiden et al. 2001). Thus, it might be possible that the delayed expression of TGF-β_1 in MSCs may potentially compromise their metabolic capacity

and proliferative rate, leading to a weakened repair process in aged and diabetic animals.

Knowing that biglycan and decorin are bound to growth factors, the present study also investigated potential alterations in these SLRPs, in response to hyperglycaemic-induced condition. For the first time, this study demonstrated a positive correlation between biglycan and decorin production with increased *in vitro* cell maturity. The *in vitro* study demonstrated that high biglycan production is relatively important to support the osteogenic pathway of MSCs by activation of TGF-β_1 signalling, stimulating the expression of osteoblastic gene markers, and matrix mineralisation (Wu et al. 2013). Biglycan also plays an important role in controlling osteoblast differentiation and supporting the skeletal maturation by modulating BMP-4-induced signalling (Young et al. 2002; Chen et al. 2004). Hence, biglycan deficient-mice and decorin null-mice showed lower capacity to produce bone precursor cells, poor responsiveness to TGF-β_1, reductions in collagen type I synthesis, and diminished osteogenic capacity, leading to increased skin and bone fragility (Danielson et al. 1997; Young et al. 2002). Within the present study, the results suggested that Smad2 and Smad3 were activated in response to both TGF-β_1-induced glucose exposure in osteoblastic cultures of rat bone derived-MSCs. Parallel to mRNA analysis, protein extracts from prolonged diabetic-induced cells revealed less biglycan and decorin band staining. Protein extracts from the ECM showed delays in biglycan and decorin protein sequestration under hyperglycaemic condition. Owing to the fact that SLRPs expression are expressed in a temporal pattern during mineral deposition (Waddington et al. 2003), the limitation of time-based analysis performed within this study might have missed an important timeframe whereby these SLPRs reached their highest peaks in expression. In view of the existing limitation in interpreting the data, the results could only suggest that prolonged high glucose exposure has a potential role in causing the delay of biglycan and decorin expressions and syntheses. The delayed expressions of biglycan and decorin may involve a causative role in diminishing the protective capacities of these SLRPs to inhibit the digestion of bone matrix during bone remodelling, resulted in alteration of TGF-β_1 bioavailability, which led to impaired osseointegration.

Collectively, evidences obtained from the present Chapter has provided a deeper understanding of the relative functions of MSCs in the regulation, growth factor availability, and proteoglycan localisation in the ECM compartment during reparative phase of diabetic bone healing. This may further explain important factors that determine MSC survival, migration, and activities, which are inter-dependant on various signalling molecules and matrix component within the repair site. Although the data seem to best fit with the overlapping of *in vivo* and *in vitro* models, the interpretation of results only represented a specific type of diabetic animal model and cell culture types. Further experimental procedure, including other types of relevant growth factors and the direct mapping of alternative activated signalling pathways that are involved in the diabetic alterations, would be required to further validate the underlying perturbation of healing progress in these model. Apart from MSCs, inflammatory components, such as macrophages, are well associated with alterations in growth factor signalling during diabetic tissue repair. Therefore, the next Chapter portrays the investigation on the potential involvement of macrophages population in regulating TGF-β_1 expression, within hyperglycaemic conditions. The potential causal relationships identified among these identified inflammatory biomolecules may provide relative evidence for finding the therapeutic target for bone reparative treatment in T2DM.

Chapter 5

Investigating the Role of Macrophages TGF-β_1 Expression in High Glucose Environment

5.0 Introduction

Macrophages are well-known to play an important role in innate and adaptive immune responses, by controlling tissue homeostasis and various biological functions, including the complex stages of wound and bone healing. These cells produce a vast majority of important cytokines throughout the inflammatory phase of tissue repair (Murray and Wynn 2011). Evidence obtained from *in vitro* studies of activated-macrophages population showed that the combination of cytokines stimulation and choice of basal medium were found to have a significant influence on macrophages polarisation (Rey-Giraud et al. 2012). Depending on the variation of stimulus, different types of macrophages activation might be triggered and further maintained by simultaneous activity of the inflammatory cascade. These different types of activated-macrophages also play an important role in coordinating the expression of growth factors and other inflammatory molecules that regulate tissue regenerative properties.

Macrophage studies in animal models suggest a causal role of macrophages in the development of diabetic complications. Impaired macrophage functions have been associated with the deterioration in immunity, which has led to the elevated rate of infection (Espinoza-Jimenez et al. 2012). Furthermore, a study on insulin–resistant adipose tissue in humans demonstrated increased localisation and activity of transforming growth factor-β (TGF-$\beta_)$, associated with M2 macrophages, which led to overall increase in fibrosis (Spencer et al. 2010). Significantly, macrophages of T2DM patients also demonstrated alterations in fatty acid content, which resulted in permanent alterations of cytokine signalling and impaired IL-4 anti-inflammatory responses (O'Connor et al. 2007; Senanayake et al. 2007).

Macrophage polarisation is a recent mechanism proposed to explain two distinct types of activated-macrophage populations, involved in immunological response. From gene expression and phenotype analysis, M1-like macrophages represent the classical activated macrophage pathway, primarily induced in early stages of tissue repair to stimulate the expression of various pro-inflammatory molecules (Liu et al. 2012). Meanwhile, the M2 macrophages phenotype is associated with the alternatively activated pathway and is predominantly represented by anti-

inflammatory features. M2 macrophages are mainly involved in later stages of healing due to their vital role in sustaining proper tissue repair capacity by secreting growth factors and cytokines. This activation may further regulate progenitor stem cells activity, supporting angiogenesis and extracellular matrix (ECM) deposition (Kharraz et al. 2013). The phagocytic role of macrophages also plays an important role during osseointegration stages, to remove unwanted foreign molecules, such as implant debris and dead cells, within the healing site. However, alterations in bone metabolism and local glycaemic levels were identified to impair osseointegration and might lead to early implant failure (Olmedo et al. 2003).

Moreover, elevated expression of circulating inflammatory markers, such as C-reactive protein and interleukin-6 (IL-6), has long been associated with the pathological progress of T2DM (Pickup 2004). Widespread activation of pro-inflammatory responses, and the prolongation of the innate immune system, have a significant impact on the associated complications observed during the reparative phase of wound healing. Osseointegration studies on healing T2DM bone tissue demonstrated alterations in growth factor production, prolongation, and increased expression of pro-inflammatory cytokines, such as interleukin 1β (IL-1β), tumour necrosis factor-α (TNF-α), and macrophages (Colombo et al. 2011). The associated hyperglycaemic condition in diabetes was also established to promote pro-inflammatory, pro-fibrotic, and diminished capacity of the alternatively activated macrophages phenotype (Reddy et al. 2014). The alterations to the pro-inflammatory stage might potentially influence the activities of MSCs and their differentiation towards bone synthesising osteoblasts, mediated by growth factors bioavailability within the healing site. Furthermore, high glucose levels were postulated to promote alterations in the fatty acid component of macrophages, resulting in the progression of diabetic pathology and insulin resistance (Senanayake et al. 2007). In addition, TGF-β_1 plays a critical role in T-cell immunity and has been identified to promote alternative activation in macrophages. TGF-β_1 signalling is impaired in hyperglycaemic states, as shown in a study of alveolar-derived macrophages (Sunahara and Martins 2012). The combination of various components in T2DM pathology, which includes hyperglycaemia, accumulation of AGE products; and increased production and binding affinity of macrophages to lipoprotein lipase

(LPL), may cumulatively set an overall transformation on the availability and the functional activity of macrophages that exist within the diabetic tissue (Tesch 2007).

Moreover, lack of *in vitro* studies on macrophages polarisation, added to the plasticity of macrophages switching between the two distinct phenotype, might have hindered further characterisation on the different macrophage activated phenotypes. Therefore, an *in vitro* analysis of bone marrow macrophage phenotypic characterisation seems promising to assist better understanding of their role in regulating tissue repair, particularly in looking the cellular inflammatory response towards high glucose levels. This study hypothesised that the hyperglycaemic-induced condition might affect the monocyte differentiation process, resulting in altered macrophage phenotypes and cytokine/growth factor production at the healing site, which would subsequently impair overall tissue restorative capacity. On completion of this Chapter, better understanding of monocyte maturation and cytokine/growth factor production in both activated macrophage phenotypes is offered. In fact, more focus had been given to the influence of high glucose level on *in vitro* culture of bone marrow-derived monocytes.

5.1 Material and methods

5.1.1 Isolation of bone marrow-derived macrophages

Bone marrow cells were flushed from femurs and tibia of combined 2 Wistar rats, at 4 weeks old (Charles River UK Ltd., Margate, UK), using 21-gauge syringe filled with ice-cold PBS, passing through a 70μm cell strainer. After centrifugation at 1800rpm for 5min, the cell pellets were resuspended with 2ml of Lysing Buffer (BD Biosciences, Oxford, UK) and gently agitated for 2min. The samples were centrifuged and the pellets were washed twice, resuspended and counted before seeded at density of 1x 10^6 cells/cm^2 in T25 flasks (Sarstedt Ltd., Beaumont Leys, UK). The cells were cultured in RPMI 1640 (Invitrogen, Renshaw, UK) contained 10% FBS, supplemented with either granulocyte-macrophage colony-stimulating factor (GM-CSF, 10ng/ml)(Peprotech, London, UK), or a combination of macrophage colony-stimulating factor (M-CSF, 10ng/ml) and interleukin-4 (IL-4, 10ng/ml), to allow differentiation of monocytes into M1 or M2 macrophages, respectively. The monocytes were incubated in 37°C, 5% CO_2 for 7 days. The supernatant was collected and the medium was changed on days 1, 3, 5 and 7.

5.1.2 Cell morphological analysis by light microscopy

Comparison of cellular morphology was made between different types of isolated M-CSF-induced and GM-CSF and IL-4-induced macrophages populations by light microscopy with serial images captured on digital cameras Canon PC1234 (Canon UK Ltd., Surrey, UK).

5.1.3 RNA extraction, PCR and qRT-PCR

At day 7, adherent cells were harvested and the RNA collected for both RT-PCR and qRT-PCR analysis. The culture medium was removed and total mRNA was extracted from approximately 600,000 cells, using the RNeasy® Mini kit and QIAShredder (Qiagen Ltd., Crawley, UK) and transcribed into cDNA, as described in Sections 2.1.2.3 and 2.1.2.4. PCR was then carried out, as previously described in Section 2.1.2.4. For qRT-PCR reactions, cDNA was pre-diluted 1:10 with RNA-free water immediately prior to analysis and qRT-PCR reaction was performed, as described in Section 2.2.4.4. All the PCR and qRT-PCR analysis was performed using forward

and reverse primer (as shown in Table 5.1). Reactions conditions were: 1 cycle of 95°C for 10min, 40 cycles of 95°C for 15s, 55°C for 30s and 72°C for 30s.

Table 5.1 Primer sequences and product sizes of selected macrophages markers

Gene	cDNA sequence (5'-3') F, Forward; R, Reverse	Length (bp)	References
β-actin	F: TGAAGATCAAGATCATTGCTCCTCC R: CTAGAAGCATTTGCGGTGGACGATG	155	Gatto et. al, 2008
ArgI	F: GCAGAGACCCAGAAGAATGGAAC R: CGGAGTGTTGATGTCAGTGTGAGC	144	Kanyo et al. 1992
IL-12p40	F: CAAGGCCCAGCAGCAGAATAAATA R: GTGCTCCAGGAGTCAGGGTACT	153	Winnall et al. 2011
IL-6	F: GAGTCACAGAAGGAGTGGCTAA R: ACAGTGAGGAATGTCCACAAAC	146	Simonic-Kocijan et al. 2012
TNFα	F: TGTCTGTGCCTCAGCCTCTTC R: TTTGGGAACTTCTCCTCCTTGT	114	Zhang et al. 2011
iNOS	F: CTTGGAAGAGGAACAACTACTGCT R: GCCAAATACCGCATACCTGAA	139	Li et al. 2013
MRC1	F: AAGGTTCCGGTTTGTGGAG R: TGCATTGCCCAGTAAGGAG	98	Ohnishi et al. 2012
TGF-β_1	F: AAGAAGTCACCCGCGTGCTA R: GGCACTGCTTCCCGAATG	118	Gao et al. 2009
VEGF	F: ATCATGCGGATCAAACC R: ATTCACATCTGCTATGCT	73	Bastide et al. 2008
CD163	F: TGTAGTTCATCATCTTCGGTCC R: CACCTACCAAGCGGAGTTGAC	97	Zhang et al. 2012

5.1.4 Enzyme Linked-Immunosorbent Assay (ELISA) of rat TGF-β_1 in media from macrophages culture

Macrophages cell culture medium samples were collected at days 1, 3, 5 and 7. The secreted TGF-β_1 in the supernatants were evaluated using TGF-β_1 Platinum ELISA Kit (eBioscience, Hatfield, UK). The assay was performed according to the manufacturer's protocol. Briefly, the wells of a microtiter plate coated with a pre-tittered amount of anti-rat TGF-β_1 monoclonal antibodies were loaded and incubated with 20µL volumes of duplicate pre-diluted medium samples and TGF-β_1 standards in order of ascending concentration. The wells were washed five times with assay buffer (phosphate-buffered saline, with 0.1% Tween 20 and 1% bovine serum albumin (BSA). Biotinylated anti-rat polyclonal antibody was added to each well and washed, as the above. 100µL of enzyme solution (streptavidin-horseradish peroxidase) and 100µL of substrate solution (3,3,5,5-tetramethylbenzidine) were added to each well with five washing steps in between. The enzyme activity was terminated by addition of stop solution (1M phosphoric acid), and the microtiter plate measured spectrophotometrically at 450nm, with 620nm as the reference wavelength. The amount of captured TGF-β_1 in the samples was calculated from a reference curve generated in the same assay with reference standards of known concentrations of TGF-β_1. Experiments were performed in triplicates of two independent experiments (n=6) and results were expressed as pg/ml.

5.1.5 Statistical analysis

Unless otherwise stated, data was expressed as mean ± standard deviation (SD). All statistical analyses were performed using SPSS version 20.0 (IBM, NY, USA). Data were analysed by two-way and mixed analysis of variance (ANOVA), with a significance level accepted at $*p<0.05$ and $**p<0.01$.

5.2 Results

5.2.1 Morphological observation of macrophages culture

Monocytes from either GM-CSF or M-CSF and IL-4 supplemented culture medium exhibited a homogenous round shape with short processes, 24hr after initial plating (Figure 5.1a-b). During 7 days in culture, the monocytes showed considerable changes in cell morphology and increased in cell size. Stimulation with GM-CSF in RPMI 10% fetal bovine serum (FBS) revealed a comparable morphology with M-CSF and IL-4 in RPMI 10% FBS media, which demonstrated the formation of mostly stretched, spindle-like shaped cells on day 3, possessing long cytoplasmic processes (Figure 5.1 c-d). These elongated-shaped macrophages exhibit rapid expansion capacity, compared to the round-shaped cells observed at earlier time-points. At day 7, the cultured monocytes have fully differentiated into morphologically heterogeneous populations, depending on the cytokine stimulation used. Both GM-CSF in RPMI 10% FBS and M-CSF and IL-4, in RPMI 10%, led to formation of mostly round or oval macrophages, with the fried egg morphology (Figure 5.1e and 5.1f). Similar tendencies were observed among monocytes culture of RPMI 10% FBS when supplemented with 25.0mM glucose, for each cytokines stimulation.

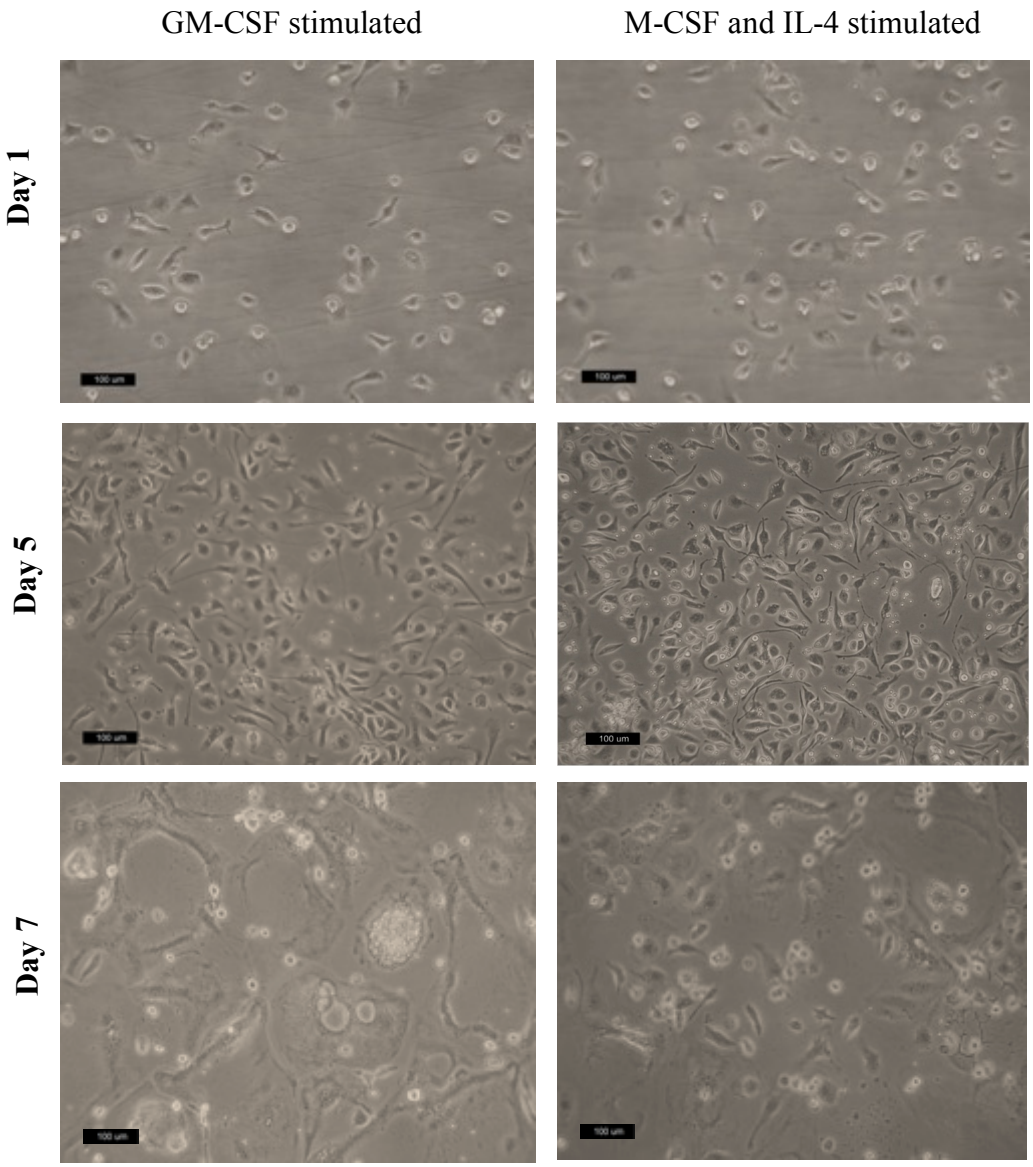

Figure 5.1 The identified macrophage populations of GM-SCF and M-CSF and IL-4 stimulated monocytes activation. Images were taken at day 1 (a,b), day 3 (c,d) and day 7 (e,f) in culture.

5.2.2 Gene expression of M1 and M2 activated macrophages

Preliminary RT-PCR confirmed the expression of TGF-β_1 in the differentiated macrophages population. Regardless of glucose concentration in the culture medium, GM-SCF in RPMI 10% FBS (M1-activation) and combination of M-CSF and IL-4 in RPMI 10% FBS (M2-activation) showed monocyte activation and induced the expression of TGF-β_1, IL-6 and TNF-α. However, high concentration of glucose in each macrophage induction media seems to differentially stimulate the expression of IL-6, in comparison to the normoglycaemic medium.

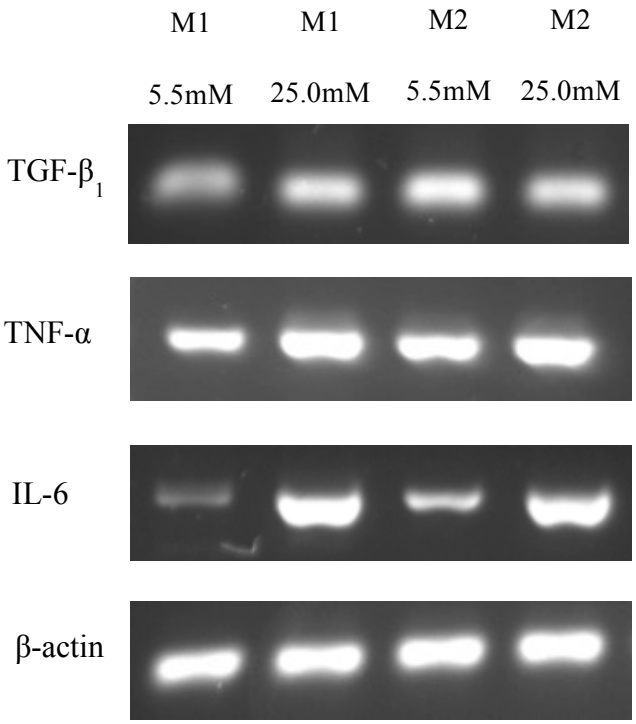

Figure 5.2 PCR analysis of macrophages induction in different cytokines stimulation and glucose level. β-actin was used as an internal control.

5.2.3 Quantitative RT-PCR analysis of M1 and M2 activated macrophages

The phenotype of the differently activated macrophages was further assessed by investigating macrophage marker expression, using quantitative RT-PCR analysis. Activated M1 macrophages in GM-CSF-stimulated cultures displayed increased TNFα, IL-6 and iNOS expression (Fig. 5.3). The data displayed marked differences in M1 populations, dependent on the concentration of glucose used in the culture medium. High glucose seems to inhibit the expression of IL-6 and iNOS in the M1 culture, but no significant differences were seen in TNF-α expression.

In contrast, the M2 differentiated macrophages demonstrated a statistically significant increase in expression of CD163, arginase 1 (Arg1) and mannose receptor C; type 1 (MRC1), in comparison to M1 macrophages. The upregulation was also observed in the expression of growth factors, such as TGF-β_1 and VEGF (Figure 5.3). However, the M2-stimulated population cultured in high glucose exhibited a significant reduction in the expression of M2-related markers, indicating changes in the regulation of gene expression under high glucose, M-SCF and IL-4 medium.

Another important finding observed was with IL-12p40 expression, which was the most common M1-associated marker. The data showed a significant increased in IL-12p40 in M2 activated populations, as opposed to M1 activated cells. Moreover, high glucose levels in M-SCF and IL-4 medium were found to inhibit expression of IL-12p40 in the M2 activated cells.

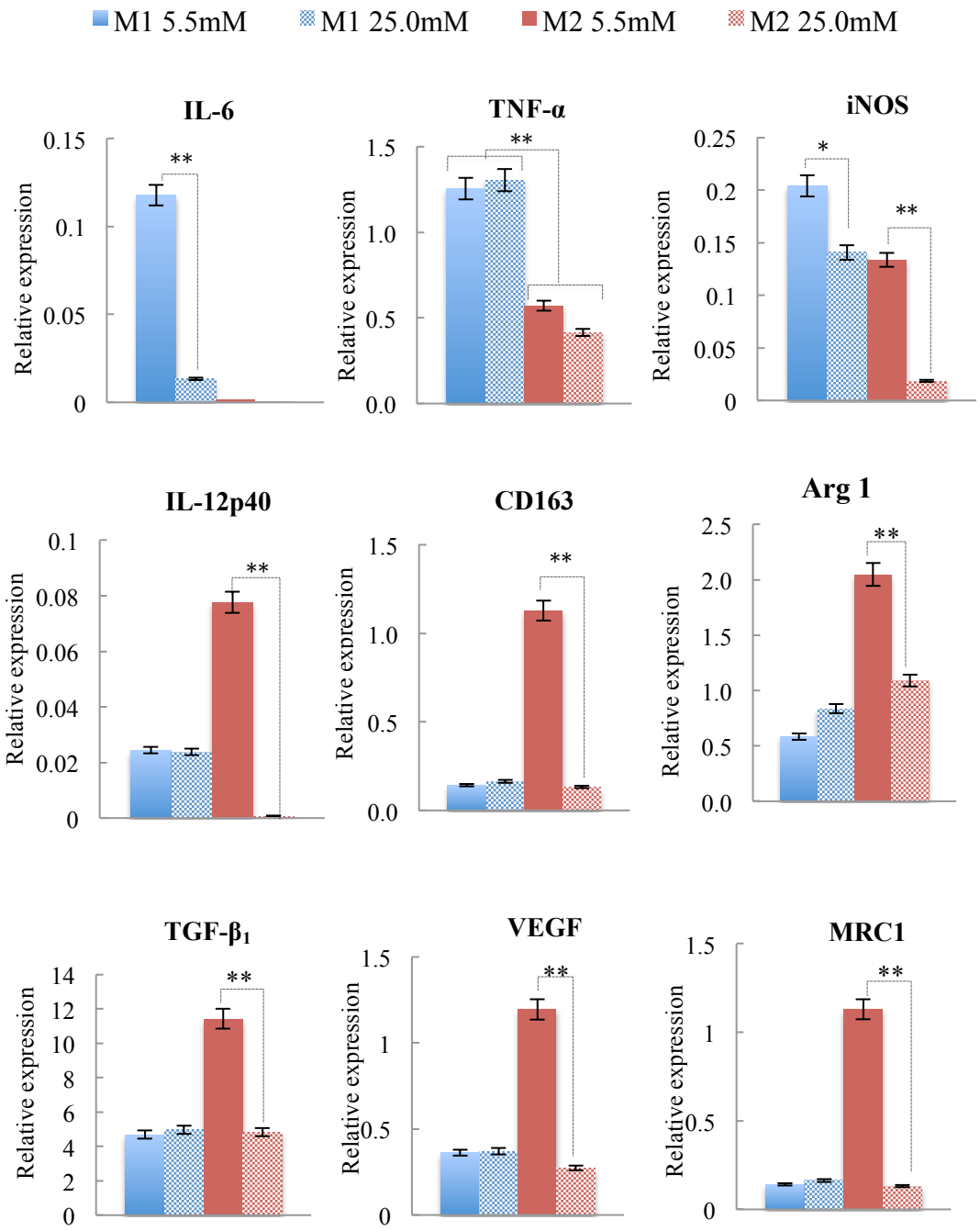

Figure 5.3 Quantitative PCR analysis of M1 and M2 macrophage gene expression, following different cytokines stimulation and glucose levels. M1-activated macrophages showed increase TNFα, IL-6 and iNOS expression, while M2-activated macrophages demonstrated increases CD163, Arg1, MRC1, TGF-β_1 and VEGF. Results are presented in relative expression to β-actin as the internal control. Each bar represent mean±SD. N=2, n=6, *p<0.05 and **p<0.01. All p values were based on two-way ANOVA.

5.2.4 Determination of released TGF-β_1 in the cell culture medium

ELISA was performed to measure the released TGF-β_1 in cell culture, at day 1,3,5 and 7 (Figure 5.4). Statistically significant increase in early expression of TGF-β_1 (p<0.01), from hyperglycaemic culture of M1- and M2-activated macrophages was observed on days 1. At day 3, TGF-β_1 was significantly decreased in high glucose M1- and M2- stimulated medium (p<0.01). However, at day 5 the M2-activated macrophages cultured in high-glucose levels demonstrated marked reduction in TGF-β_1 levels, as opposed to the marked elevation of TGF-β_1 observed in the M1-activated cells. The subsequent culture of monocytes in high-glucose levels, at day 7 also inhibited the release of TGF-β_1 from M2-activated macrophages, although the M1-activated cells demonstrated slight increased in TGF-β_1 level. Together, the present data indicated that TGF-β_1 production within the macrophage population was highly associated with the type of macrophages formed and the relative levels of glucose exposure presented in culture condition.

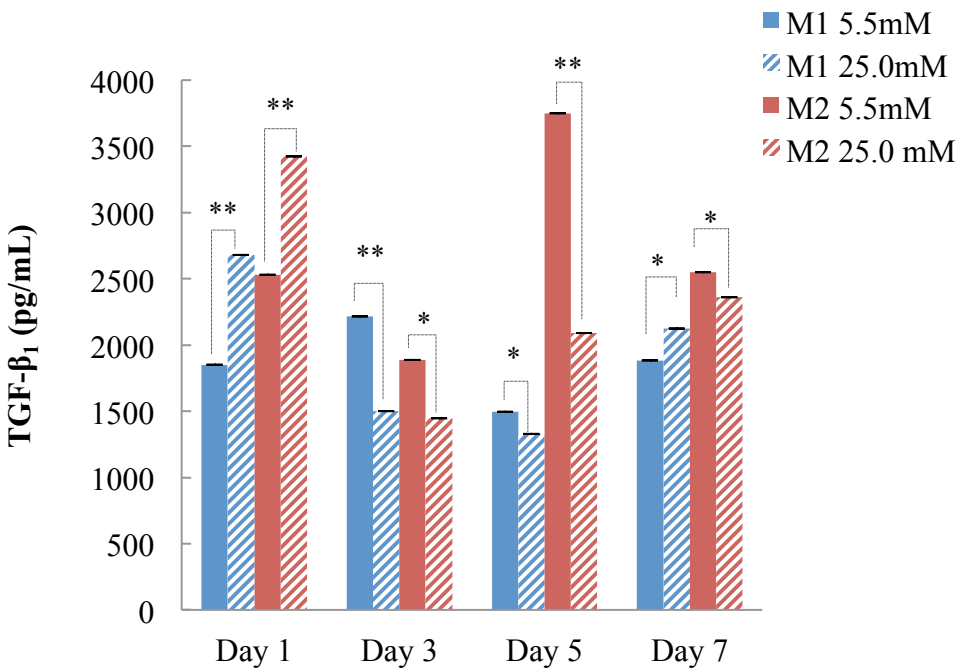

Figure 5.4 Phenotype of bone marrow-derived macrophages at a translational level, in culture. The released cytokines was measured and the data presented as mean±SD. N=2, n=6, *p<0.05, **p<0.01, accepted as statistically significant. All p values were based on mixed ANOVA. Comparison made between macrophages activated group and between days in culture, within different glucose levels. Released TGF-β_1 was measured by an enzyme-linked immunosorbent assay (ELISA) at days 1,3,5 and 7. From day 3 onwards, TGF-β_1 release from high-glucose macrophages cultures was suppressed.

5.3 Discussion

The previous *in vitro* study confirmed that the activation of bone marrow macrophages phenotype is associated with cytokine stimulation present in the culture medium (Rao et al. 2014). Although this study did not seem to demonstrate clear distinction of phenotype switch between M1 and M2 populations, which potentially associated with prolonged inflammatory responses, the present results established that high glucose concentrations might suppress TGF-β_1 and VEGF expressions from alternatively activated macrophages, within high glucose environments. Significantly, this is the first study to investigate the potential involvement of macrophages polarisation, in response to hyperglycaemic conditions to further investigate their role in growth factors expression during the inflammatory stage of bone repair.

Within this study, GM-CSF and M-CSF with IL-4 in RPMI 10% FBS activated macrophages revealed no distinct morphological appearances when the monocytes differentiated from homogenous round-shaped cells to heterogeneous populations consisting of oval and flattened-shaped macrophages. These findings are partly in agreement to those described recently, when human monocytes were differentiated by GM-CSF in RPMI 10% FBS, whereas the M2 activated macrophages of human monocytes tended to exhibit stretched, elongated fibroblast-like shaped cells with prominent processes; as opposed to round and oval shapes morphology, as seen in rat bone marrow macrophages (Rey-Giraud et al. 2012). Phenotypic and functional heterogeneity is known to be highly dependent on a wide range of factors, including the type of precursor cells, differentiation stages, cellular microenvironments, and variations in key stimulatory cytokines (Chakraborty et al. 2005). Moreover, the basal medium used for macrophage culture showed profound effect on macrophages morphology, as comparison made between RPMI with 10% FBS and X-Vivo medium revealed the production of different macrophages phenotypes, whereas the latter is found to produce macrophages with elongated morphology and increased adherence properties (Rey-Giraud et al. 2012).

Within this study, the data revealed that *in vitro* macrophages polarisation might possibly be activated without lipopolysaccharides (LPS) stimulation, to produce a similar characteristic of LPS stimulated bone marrow M1 macrophages (high iNOS

and TNF-α) and M2 type that correlated with elevated level of Arg1 (Zheng et al. 2013). Moreover, gene expression analysis indicated that two distinct populations of rat macrophages were successfully isolated and activated following the adapted induction protocol, as described in earlier murine macrophages isolation and characterisation studies (Davies and Gordon 2005; Ho and Sly 2009). GM-CSF clearly stimulated expression of IL-6, TNF-α, and iNOS, which fit the characteristics of M1-like macrophage phenotype, as proposed by earlier studies of adipose-derived M1 macrophages in a mouse model (Fujisaka et al. 2009). Meanwhile, M-CSF and IL-4 displayed the capacity to stimulate the production of M2 activated macrophages, showing relative increment in the expression of cytokine and related growth factors, including CD163, Arg1, MRC1, TGF-β_1, and VEGF. The correlation of these gene expression markers and M2 activated phenotype was previously established in macrophages polarisation studies, which proposed that alternatively activated macrophages can be defined by expression of the above markers, as identified within the present study, along with expression of IL-10, CD206, CXCL2, SOCS1, Ym1, and Fizz1 expression (Stout 2010).

Moreover, the data showed thrice higher expression of IL-12p40 in M2 activated macrophages than the level observed in M1 activated populations, suggesting an association between IL-12p40 and elevated TGF-β_1 expression in non-LPS activated macrophages. Although LPS activation was found to be unrelated to TGF-β mRNA expression, it might likely induce the secretion of TGF-β in alveolar macrophages (Assoian et al. 1987). Therefore, recent evidence postulated that IL-12p40 might upregulate TGF-β_1 expression and exhibited a potential role in driving macrophage polarisation (Bastos et al. 2002; Sindrilaru et al. 2011; Zhang et al. 2013). However, ELISA analysis of M2 activated macrophages in the present study revealed that hyperglycaemic culture inhibited the secretion of TGF-β_1 in culture medium. In view of this relevant evidence, the present study demonstrated a further influence of high glucose concentration on macrophage function and phenotype switching capacity, without the presence of LPS stimulation. Thus, it further suggests a high degree of complexity for macrophages polarisation, which is strictly controlled by various microenvironments, particularly the sensitive M2 phenotype.

In addition, experimental evidence suggested that diabetes promotes pro-inflammatory and pro-fibrotic stages in tissue repair, which exacerbate the dysfunction of the M2 macrophage phenotype (Brown et al. 2012). In fact, recent analyses showed that diabetes altered levels of several long non-coding RNAs, which play a functional role in activation of pro-inflammatory genes in T2DM macrophages (Reddy et al. 2014). Furthermore, *in vivo* implant osseointegration in T2DM animal models revealed prolonged expression of pro-inflammatory cytokines, IL-1β, and TNF-α during bone repair, along with increased levels of TGF-β_1, suggestively in part of increased macrophage activation (Colombo et al. 2011). Significantly, the data derived from the present study suggested the involvement of the M1-activated phenotype to increase the level of TNF-α in hyperglycaemic cultures, which further explained the prolonged and delayed pro-inflammatory stage seen in healing diabetic tissues. Likewise, qRT-PCR analysis reported the late expression of macrophage activity following the onset of hyperglycaemia in diabetic animals (Doxey et al. 1998; Barbu-Tudoran et al. 2013). Macrophages from insulin-resistant subjects also indicated the dominant feature of anti-inflammatory M2-like character, with high susceptibility to produce extensive amounts of pro-inflammatory cytokines that are closely linked to increase the rate of fibrosis and the development of further insulin resistance (Zeyda et al. 2007; Spencer et al. 2010). Experiment of bone marrow stem cells exposed to diabetic conditions exhibited alteration in TLR4 response, which resulted in elevated expression of IL-12p40, TNFα, IL-6, and iNOS, which further explain the alterations of inflammatory responses discovered in diabetic-mediated complications (Mohammad et al. 2006). In addition, the present study revealed that essential growth factors (VEGF and TGF-β_1) and pro-inflammatory cytokines (IL-6 and TNFα) of M1 and M2 activated macrophages population were both inhibited in high glucose.

Collectively, the present study demonstrated for the first time that high glucose levels might restrict M2 activated polarisation in bone marrow-derived macrophages; and might further enhance the pro-inflammatory stages during the healing process. The proposed mechanisms of hyperglycaemic-induced response might either be initiated by inducing M2 to M1 phenotype transformation, to prolong the pro-inflammatory stage, or by limiting the production of TGF-β_1, which led to defective

signalling and regulatory interactions; resulting in overall delayed tissue repair process. Collectively, the findings extend our current understanding of rat macrophage phenotype upon stimulation in various cytokines and offer huge potential for *in vitro* application of a disease model in studying immunological responses. Further studies on high glucose-mediated macrophage polarisation, particularly in regard to growth factors production, may clarify the exact mechanisms and enhance understanding of immune responses in T2DM environments.

Chapter 6

General Discussion

6.0 General discussion

The role of growth factor in bone repair is widely recognized, particularly the TGF-β_1. *In vivo* findings, as well as *in vitro* studies of osteoprogenitor cell populations in this study, strongly suggested that diabetes induced the alterations of TGF-β_1 bioavailability within hyperglycaemic environments. *In vivo* implant osseointegration studies demonstrated increased expression of TGF-β_1 in the diabetic healing bone of the young group, at 9 weeks of post-implantation, which was not apparent in the aged group. Likewise, in a previous study on TGF-β_1 expression in the bone repair area, TGF-β_1 was reported to be significantly increased in a comparable young diabetic group at similar post-implant time intervals (Colombo et al. 2011). However, insignificant differences in TGF-β_1 immunolabelling had been observed in the bone-implant area of aged-diabetic animal, suggestive of masked TGF-β_1 alterations in ageing cells, which is represented by the higher proliferative cells populations, from *in vitro* culture. However, *in vitro* analysis on mature osteoprogenitor cells populations exhibited marked increase of responsiveness to express and synthesise TGF-β_1, along with biglycan and decorin, but the capacity was markedly reduced in hyperglycaemic differentiation medium. In normal healing bone, TGF-β_1 acts through paracrine signalling, as these cells are secreted by osteoblast, but at the same time, involved in recruitment and inducing proliferative capacity of mesenchymal progenitor cells towards osteoblastic lineage (Ehnert et al. 2010). Besides, the temporal expression of TGF-β_1 is highly correlated with the specific stage of bone healing progress (Würgler-Hauri et al. 2007). TGF-β_1 plays an important role during the early phase of osteoblast differentiation pathway, particularly within the injury site, to induce migration and proliferation of progenitor cells that are capable of forming bone cells and further synthesising new bone. Within this study, Western blot on the extracellular matrix (ECM) protein of cultured osteoblastic cells indicated a delay in TGF-β_1 expression in the hyperglycaemic-induced cells. The late expression of TGF-β_1 had been related to their functional role to inhibit terminal differentiation of osteoblast, during the late stage of mineral deposition and lamellar bone formation. Together, the significant alterations of temporal expression seen within the diabetic tissue and hyperglycaemic-induced MSCs may, therefore, be an indicator of significant changes in the signalling cascade and extracellular matrix (ECM) protein modifications, which modulate the

bioavailability of TGF-β_1 expression, synthesis, and sequestration within the repair site.

Biglycan and decorin are mainly expressed and localised in a range of specialised developing tissues, with the main role to regulate the sequestration of matrix-bound growth factors, such as TGF-β_1 (Bianco et al. 1990). Biglycan and decorin may protect TGF-β_1 from degradation and modulating their survival and release to the progenitor cells (Baker et al. 2009). *In vitro* studies on vascular smooth muscles and mesangial cells have suggested an association between hyperglycaemia and elevated TGF-β_1, which acts as a potent regulator of ECM synthesis leading to accelerated progression of atherosclerosis and glomerulosclerosis (Kolm-Litty et al. 1998; Yang et al. 2010). However, less evidence and relevance information was found to explain on how high glucose exposure may alter TGF-β_1 expression and availability, particularly with the known mediating role of biglycan and decorin in supporting the ECM synthesis. Furthermore, *in vitro* studies investigating the effects of hyperglycaemia on proliferation and functional activities of bone mesenchymal progenitor cells is still lacking, particularly concerning their biological functions in pathological progress of diabetic bone healing. Hence, to the researcher's knowledge, this thesis is the first to document that long-term and short-term high glucose exposure could upregulate the mRNA expression and protein synthesis of biglycan and decorin in long-term *in vitro* expanded cells, as well as exerting a delay on their sequestration within the ECM. However, owing to the temporal expression of TGF-β_1 and SLRPs during bone formation (Waddington et al. 2003), caution should be taken in interpreting the present data because the peak of gene expression for these biomolecules might have been missed between the chosen sampling points. Significant elevations in biglycan and decorin expression and synthesis were also observed in the cells with higher proliferative stage. These novel results might explain, in part, the molecular mechanism underlying the impaired bone healing potential in diabetic and aged population. Collectively, findings from this study suggest a strong correlation between the stemness of progenitor cells and expression of SLRPs (biglycan and decorin), to regulate the bioavailability and the bioactivity of sequestrated TGF-β_1 in the bone-implant contact area, in order to maintain the cues for bone remodelling and repair.

Prior to the 21st century, the discussion on proposed bone repair mechanisms in Type 2 Diabetes Mellitus (T2DM) mainly consists of speculations, owing to the lack of reasonably supported data derived from both *in vitro* and *in vivo* experiments. Growing evidence on osseointegration has now confirmed the delay and impaired bone repair capacity in T2DM subjects (Jung et al. 2013; Tatarakis et al. 2014). Histological observations on bone-implant contact area of T2DM animal demonstrated extended formation of soft, fibrous tissue, and less mature bone, compared to control subjects (Casap et al. 2008; Hasegawa et al. 2008; Sakai et al. 2008; Wang et al. 2010a). Likewise, delayed osseointegration has been reported in adult populations, which indicated a significant increase of tooth loss in mature groups, when compared to young groups (Jung et al. 2013). Within this study, the diabetic group demonstrated impaired bone healing progress, with the worst effect seen in the older age group. However, for the first time, this thesis revealed that T2DM condition significantly altered the sequestration of growth factors within the healing tissue. *In vitro* evidence from the current thesis also showed that long-term expanded, hyperglycaemic-induced mesenchymal progenitor cells exhibited a decrease in the proliferative capacity. Altogether, these findings suggest that the reported *in vivo* impairment of bone repair in osseointegration studies correlated with the proliferative and the differentiative capacities of bone progenitor cells that exist within the repair sites to support osteogenesis and survival of implant.

Besides, one of the important aims in this study had been to investigate and select a suitable progenitor stem cell population, for *in vitro* analysis of the cellular biological function. Successful isolation, expansion, and characterisation of adult mesenchymal progenitor cells residing within the rat bone marrow stroma and skeletal niche demonstrated the feasibility and a practical approach of the method in generating MSCs for cell culture study. In fact, this study confirmed the great capacity of the isolated bone chips explant MSCs (BCE-MSCs), to maintain the bi-potent characteristics in long-term *in vitro* expansion culture. The findings also indicated that exposure to short- and long-term hyperglycaemic environments significantly induced both osteogenic and adipogenic potentials of MSCs, while suppressing their proliferative potential. Hence, the functional role of these MSCs is

highly dependent on different stimulatory factors present in the culture environment, which might influence their reparative role in healing processes.

On top of that, uncontrolled diabetes has long been associated with compromised osseointegration rate, which weakens implant survival and stabilisation in T2DM patients (Dowell et al. 2007; Oates et al. 2007; Gomez-Moreno et al. 2014). Hyperglycaemia increases oxidative stress levels within the diabetic tissue, and worsens by reducing or without catalase (Goth 2008; Waddington et al. 2011a). *In vivo* studies that monitored implant placed in rat mandible also identified delayed osteoblast differentiation and prolonged inflammatory responses in the T2DM model (Colombo et al. 2011). The perturbations in the healing process might also be linked with increased apoptosis and aging, mediated by advanced glycation end products (AGEs, Evans et al. 2003). Collectively, various hypotheses have been suggested to explain the mechanism of how the diabetes environment potentially influences the reparative process. However, the number of *in vitro* studies performed using MSCs populations is still relatively low; and only limited to human cells, which have been proven to demonstrate insignificant alterations in proliferative capacity and differentiation potential upon exposure to high glucose condition (Li et al. 2007; Weil et al. 2009; Cramer et al. 2010). In reviewing the literature, very few reasonable arguments were found to link the *in vivo* and *in vitro* evidence to explain in detail the possible mechanism of diabetic-induced alterations on cellular behaviour. Nonetheless, the only evidence found using MSCs to explore the delayed bone repair, as demonstrated in previous rat T2DM model, was found in streptozocin-induced model of T1DM, which suggested that diabetes reduced osteoblastic and chondrogenic capacity of MSCs, while inducing their adipogenic lineages, leading to higher nett loss of new bone formation (Stolzing et al. 2010). Moreover, in the present study, a novel combination of *in vivo* and *in vitro* analyses conducted within perspectives of T2DM revealed that the alterations of growth factors availability in the diabetic tissue might be associated with the significant delay of small proteoglycans expression and synthesis at the cellular level, which could potentially lead to overall impairment of bone healing.

Furthermore, different roles of hyperglycaemia on various types of progenitor cells have been postulated in previous studies, which include inhibition of stem cell function (Dienelt and zur Nieden 2011; Cunha et al. 2014), inducing early senescence and apoptosis through the production of reactive oxygen species (ROS) (D'Souza et al. 2009; Cramer et al. 2010) increased susceptibility to osmotic stress (Madonna et al. 2013), and decreased bone quality despite a marked elevation in matrix deposition (D'Souza et al. 2009; Abbassy et al. 2010). For the first time, this study had monitored the influence of diabetic-induced hyperglycaemia on long-term MSCs culture, to demonstrate the accumulated impact of hyperglycaemia on the proliferative potential of the cells. It further supports the rationale of using these hyperglycaemic-induced MSCs to represent the cells derived from T2DM animals. However, the analysis performed on these cells must always reflect on the fact that considerable differences do exist in the pathological progress of diabetic-induced condition between the 2D culture settings and the complex *in vivo* system.

The current study also showed that macrophages could also play an important role in regulating TGF-β_1 expression during the inflammatory phase of bone repair. Previous bone repair studies in rats indicated prolonged inflammatory responses in diabetic animal models, represented by elevated expression of TNF-α and IL-1β (Colombo et al. 2011). On comparing the classically activated macrophage (M1) and the alternatively activated macrophages (M2), data revealed that high glucose levels significantly inhibited the expression of both M1- and M2-activated macrophages markers, particularly growth factors, such as VEGF and TGF-β_1. The activation of stress-induced signalling pathways, on the other hand, was mainly activated by oxidative stress, which led to the increased production of IL-1β, TNF-α, and iNOS that might further stimulate insulin resistance in the tissues (Kaneto et al. 2005). Significantly, the present finding suggested that the macrophages involved in the prolongation of the inflammatory response observed in prior T2DM models, comprised mostly of pro-inflammatory M1-activated macrophages. Polarisation of M2 to M1-type macrophages and prolonged high levels of pro-inflammatory cells within the injury site may explain the delayed bone repair in diabetic environments, as demonstrated in the *in vivo* sample. Current evidence also showed that MSCs could secrete factors that are capable of polarising the monocytes to M2-type

activated macrophages (Ezquer et al. 2009), which is beneficial in accelerating bone repair in the affected tissue. Altogether, this study could have assisted towards enhanced understanding of the cross-talk between MSC populations and inflammatory mediators, which offer great potential and beneficial aspects for future application in regenerative therapy.

Despite the interesting findings observed within this study, there are certain limitations that need to be taken into account. First, extra caution needs to be considered in extrapolating findings from *in vitro* study to reflect the *in vivo* condition. The differences of cellular mechanisms that exist between the 2D culture and the more complex animal model system will need to be considered, prior to making any conclusion. Second, within this study, diabetic-induced long-term culture of isolated MSCs was performed due to the unsuccessful isolation of MSCs from bone chips explant of aged animal. This might further explain the absence of any report conducted using freshly isolated MSCs from aged animals, particularly the diabetic GK rats that exhibited constant hyperglycaemia from 12 weeks' old.

6.1 Future directions

Interestingly, the novel findings gathered from this study have raised more questions to deepen our comprehension on pathological and physiological perturbations in diabetic bone healing. Indeed, future studies are needed to address the mechanisms underlying the observations and outcomes herein discussed. Although the diabetic-induced bone-derived osteoprogenitor cells showed remarkable response in subsequent culture in hyperglycaemic osteogenic medium, the actual diabetic-bone cells were not been studied in this regard. Therefore, a systematic approach of *in vitro* studies, conducted using freshly isolated cells from both Wistar and T2DM animal itself may provide valuable findings to compare with the current data. It is also unclear by which mechanisms, hyperglycaemic environment may exert its impact on the osteoprogenitor cell populations, proteoglycans, growth factors, and bioavailability, which would directly influence the metabolic state and the oxidative stress levels of the cells. Thus, studies looking at systemic or local TGF-β_1 delivery on bone formation will be needed to sort between TGF-β_1's direct effects on bone cells versus the more complex MSCs reaction to a combined administration of TGF-

β_1 and biglycan/decorin. Moreover, studies designed to look at selected hyperglycaemic-induced signalling pathways in bone cells should be pursued as well, as it may further elucidate the potential therapeutic target in reversing the detrimental effects of high glucose environment on cellular damage.

6.2 Contribution of this work to the field of reparative medicine

This thesis has presented information indicating that bone healing is a complex and very controlled process, which involves a series of biological events that take place following an injury to the tissue. The original contribution of this study to the field of knowledge, particularly in reparative medicine is founded on successful identification of important cells and biomolecules that drive the changes in signalling cascade that lead to impairment of osseointegration in T2DM bone tissues. The marked alterations of TGF-β_1 expression and synthesis, obtained from both *in vivo* and *in vitro* analyses indicated an inter-dependant interactions between the bone progenitor cells, growth factors, and matrix proteoglycans, which potentially determine the subsequent bioactivity and bioavailability of each component in modulating bone repair process. Along with the current application of antioxidants, the delivery of growth factors and the demineralised bone matrix in accelerating bone-repair (Bouletreau et al. 2002; Sheweita and Khoshhal 2007; Ozdemir and Kir 2011), enhanced understanding on the identified repair mediators in this study may further assist in elucidating other potential targets for therapeutic options in promoting bone repair in T2DM, thereby improve the rate of implant survival in diabetic patients.

7.0 References

Abbas, S. et al. 2003. Tumor necrosis factor-α inhibits pre-osteoblast differentiation through its type-1 receptor. *Cytokine* 22(1-2), p.33-41.

Abbassy, M. A. et al. 2010. The effect of diabetes mellitus on rat mandibular bone formation and microarchitecture. *European Journal of Oral Sciences* 118(4), p. 364-369.

Aberg, M. et al. 2003. IGF-I has a direct proliferative effect in adult hippocampal progenitor cells. *Molecular and Cellular Neuroscience* 24(1), p. 23-40.

Abraham, N. G. et al. 2008. Bone marrow stem cell transplant into intra-bone cavity prevents type 2 diabetes: Role of heme oxygenase-adiponectin. *Journal of Autoimmunity* 30(3), p. 128-135.

Ahrens, M. et al. 1993. Expression of human BMP-2 or -4 in murine mesenchymal progenitor C3H10T1/2 cells induces differentiation into distinct mesenchymal cell lineages. *DNA and Cell Biology* 12(10), p. 871-880.

Al-Aql, Z. S. et al. 2008. Molecular mechanisms controlling bone formation during fracture healing and distraction osteogenesis. *Journal of Dental Research* 87(2), p. 107-118.

Al-Mashat, H. A. et al. 2006. Diabetes enhances mRNA levels of proapoptotic genes and caspase activity, which contribute to impaired healing. *Diabetes* 55(2), p. 487-495.

Albiero, M. et al. 2011. Defective recruitment, survival and proliferation of bone marrow-derived progenitor cells at sites of delayed diabetic wound healing in mice. *Diabetologia* 54(4), p. 945-953.

Alliston, T. et al. 2001. TGF-β-induced repression of Cbfa1 by Smad3 decreases cbfa1 and osteocalcin expression and inhibits osteoblast differentiation. *EMBO Journal* 20(9), p. 2254-2272.

Almon, R. R. et al. 2009. Gene expression analysis of hepatic roles in cause and development of diabetes in Goto-Kakizaki rats. *Journal of Endocrinology* 200, p. 331 - 346.

Al-Zube, L. et al. 2009. Recombinant human platelet-derived growth factor BB (rhPDGF-BB) and beta-tricalcium phosphate/collagen matrix enhance fracture

healing in a diabetic rat model. *Journal of Orthopaedic Research* 27(8), p. 1074-1081.

Altschul S.F., G. W., Miller W., Myers E.W. and Lipman D.J. 1990. Basic local alignment search tool. *Journal of Molecular Biology* 215, p. 403-410.

Anderson, D. M. et al. 1997. A homologue of the TNF receptor and its ligand enhance T-cell growth and dendritic-cell function. *Nature* 390(6656), p. 175-179.

Asagiri, M. and Takayanagi, H. 2007. The molecular understanding of osteoclast differentiation. *Bone* 40(2), p. 251-264.

Assoian, R. K. et al. 1987. Expression and secretion of type β transforming growth factor by activated human macrophages. *Proceedings of the National Academy of Sciences* 84(17), p. 6020-6024.

Back, S. H. et al. 2012. Endoplasmic reticulum stress in the β-cell pathogenesis of type 2 diabetes. *Experimental Diabetes Research* [online]. Available at: http://downloads.hindawi.com/journals/jdr/2012/618396.pdf [Accessed: 20 May 2012].

Bajpai, A. K. et al. 2007. 15(S)-HETE Production in human retinal microvascular endothelial cells by hypoxia: novel role for MEK1 in 15(S)-HETE–induced angiogenesis. *Investigative Ophthalmology & Visual Science* 48(11), p. 4930-4938.

Baker, S. et al. 2009. TGF-β/extracellular matrix interactions in dentin matrix: a role in regulating sequestration and protection of bioactivity. *Calcified Tissue International* 85(1), p. 66-74.

Barbu-Tudoran, L. et al. 2013. Accumulation of tissue macrophages and depletion of resident macrophages in the diabetic thymus in response to hyperglycemia-induced thymocyte apoptosis. *Journal of Diabetes and Its Complications* 27(2), p. 114-122.

Barnes, G. L. et al. 1999. Growth Factor Regulation of Fracture Repair. Journal of Bone and Mineral Research 14(11), p. 1805-1815.

Barrientos, S. et al. 2008. Perspective article: growth factors and cytokines in wound healing. *Wound Repair and Regeneration* 16(5), p. 585-601.

Barry, F. P. and Murphy, J. M. 2004. Mesenchymal stem cells: clinical applications and biological characterization. *International Journal of Biochemistry & Cell Biology* 36(4), p. 568-584.

Bastianelli, D. et al. 2014. Influence of Egr-1 in Cardiac Tissue-Derived Mesenchymal Stem Cells in Response to Glucose Variations. Biomed Research International [online] 2014, Available at: http://dx.doi.org/10.1155/2014/254793 [Accessed: 20 May 2014].

Bastide, A. et al. 2008. An upstream open reading frame within an IRES controls expression of a specific VEGF-A isoform. *Nucleic Acids Research* 36(7), p. 2434-2445.

Bastos, K. R. B. et al. 2002. Macrophages from IL-12p40-deficient mice have a bias toward the M2 activation profile. *Journal of Leukocyte Biology* 71(2), p. 271-278.

Batouli, S. et al. 2003. Comparison of stem-cell-mediated osteogenesis and dentinogenesis. *Journal of Dental Research* 82(12), p. 976-981.

Baynes, J. W. 1991. Role of oxidative stress in development of complications in diabetes. *Diabetes* 40(4), p. 405-412.

Berglundh, T. et al. 2003. *De novo* alveolar bone formation adjacent to endosseous implants. *Clinical Oral Implants Research* 14(3), p. 251-262.

Bi, Y. M. et al. 2005. Extracellular matrix proteoglycans control the fate of bone marrow stromal cells. *Journal of Biological Chemistry* 280(34), p. 30481-30489.

Bianco, P. and Robey, P. G. 2000. Marrow stromal stem cells. *Journal of Clinical Investigation* 105(12), p. 1663-1668.

Bianco, P. and Robey, P. G. 2004. Skeletal stem cells. *In Handbook of Adult Stem Cells*, R. Lanza editor. Elsevier Academic Press, San Diego, p. 415-424.

Bianco, P. et al. 1990. Expression and localization of the two small proteoglycans biglycan and decorin in developing human skeletal and non-skeletal tissues. *Journal of Histochemistry & Cytochemistry* 38(11), p. 1549-1563.

Bierhaus, A. et al. 1997. Advanced glycation end product-induced activation of NF-κB is suppressed by α-lipoic acid in cultured endothelial cells. *Diabetes* 46(9), p. 1481-1490.

Blondet, J. J. and Beilman, G. J. 2007. Glycemic control and prevention of perioperative infection. *Current Opinion in Critical Care* 13(4), p. 421-427.

Bouletreau, P. J. et al. 2002. Hypoxia and VEGF up-regulate BMP-2 mRNA and protein expression in microvascular endothelial cells: implications for fracture healing. *Plastic and Reconstructive Surgery* 109(7), p. 2384-2397.

Bouletreau, P. J. et al. 2002. The molecular biology of distraction osteogenesis. *Journal of Cranio-Maxillofacial Surgery* 30(1), p. 1-11.

Boyle, W. J. et al. 2003. Osteoclast differentiation and activation. *Nature* 423(6937), p. 337-342.

Brem, H. and Tomic-Canic, M. 2007. Cellular and molecular basis of wound healing in diabetes. *The Journal of Clinical Investigation* 117(5), p. 1219-1222.

Brem, H. et al. 2000. Healing of diabetic foot ulcers and pressure ulcers with human skin equivalent: A new paradigm in wound healing. *Archives of Surgery* 135(6), p. 627-634.

Brenta, G. 2010. Diabetes and thyroid disorders. *The British Journal of Diabetes & Vascular Disease* 10(4), p. 172-177.

Brinster, R. 2002. Germline stem cell transplantation and transgenesis. *Science* 296, p. 2174.

Brown, B. N. et al. 2012. Macrophage polarization: An opportunity for improved outcomes in biomaterials and regenerative medicine. *Biomaterials* 33(15), p. 3792-3802.

Brown, G. L. et al. 1989. Enhancement of wound healing by topical treatment with epidermal growth factor. *New England Journal of Medicine* 321(2), p. 76-79.

Brownlee, M. 2005. The pathobiology of diabetic complications: a unifying mechanism. *Diabetes* 54(6), p. 1615-1625.

Bruder, S. P. et al. 1997. Growth kinetics, self-renewal, and the osteogenic potential of purified human mesenchymal stem cells during extensive subcultivation and following cryopreservation. *Journal of Cellular Biochemistry* 64(2), p. 278-294.

Bruder, S. P. et al. 1998. Bone regeneration by implantation of purified, culture-expanded human mesenchymal stem cells. *Journal of Orthopaedic Research* 16(2), p. 155-162.

Buraschi, S. et al. 2012. Decorin protein core affects the global gene expression profile of the tumor microenvironment in a triple-negative orthotopic breast carcinoma xenograft model. *PloS One* 7(9), p. e45559.

Buse, M. G. 2006. Hexosamines, insulin resistance, and the complications of diabetes: current status. *American Journal of Physiology, Endocrinology and Metabolism* 209(1) p. E1-E8.

Byun, M. R. et al. 2013. FGF2 stimulates osteogenic differentiation through ERK induced TAZ expression. *Bone* 58, p. 72-80.

Calkhoven, C. F. et al. 2000. Translational control of C/EBPα and C/EBPβ isoform expression. *Genes and Development* 14(15), p. 1920-1932.

Capelli, C. et al. 2009. The washouts of discarded bone marrow collection bags and filters are a very abundant source of hMSCs. *Cytotherapy* 11(4), p. 403-413.

Caplan, A. I. 1997. Mesenchymal stem cells (MSCs) and their use in regeneration of skeletal tissues. *European Journal of Cell Biology* 74, p. 30-30.

Cardaropoli, G. et al. 2003. Dynamics of bone tissue formation in tooth extraction sites. *Journal of Clinical Periodontology* 30(9): 809–818.

Carragee, E. J. et al. 2011. A critical review of recombinant human bone morphogenetic protein-2 trials in spinal surgery: emerging safety concerns and lessons learned. *The Spine Journal* 11(6), p. 471-491.

Casap, N. et al. 2008. Type 2 diabetes has minimal effect on osseointegration of titanium implants in Psammomys obesus. *Clinical Oral Implants Research* 19(5), p. 458-464.

Chakraborty, D. et al. 2005. *Leishmania donovani* affects antigen presentation of macrophage by disrupting lipid rafts. *The Journal of Immunology* 175(5), p. 3214-3224.

Chan, R. W. et al. 2004. Clonogenicity of human endometrial epithelial and stromal cells. *Biology of Reproduction* 70(6), p. 1738-1750.

Chatterjee, S. et al. 2010. Alteration in marrow stromal microenvironment and apoptosis mechanisms involved in aplastic anemia: an animal model to study the possible disease pathology. *Stem cells International* [online] Available at http://dx.doi.org/10.4061/2010/932354 [Accessed: 20 June 2013].

Chen, N. X. et al. 2006. High glucose increases the expression of Cbfa1 and BMP-2 and enhances the calcification of vascular smooth muscle cells. *Nephrology Dialysis Transplantation* 21(12), p. 3435-3442.

Chen, X. et al. 2004. The small leucine-rich proteoglycan biglycan modulates BMP-4-induced osteoblast differentiation. *The FASEB Journal* 18(9), p. 948-958.

Cheng, C.F. et al. 2011. A fragment of secreted Hsp90α carries properties that enable it to accelerate effectively both acute and diabetic wound healing in mice. The *Journal of Clinical Investigation* 121(11), p. 4348-4361.

Cho, M.L. et al. 2006. Transforming growth factor-β1(TGF-β_1) down-regulates TNFα-induced RANTES production in rheumatoid synovial fibroblasts through NF-κB-mediated transcriptional repression. *Immunology Letters* 105(2), p. 159-166.

Choudhery, M. S. et al. 2012. Mesenchymal stem cells conditioned with glucose depletion augments their ability to repair -infarcted myocardium. *Journal of Cellular and Molecular Medicine* 16(19), p. 2518-2529.

Colombo, J. S. et al. 2011. Delayed osteoblast differentiation and altered inflammatory response around implants placed in incisor sockets of type 2 diabetic rats. *Clinical Oral Implants Research* 22(6), p. 578-586.

Colter, D. C. et al. 2001. Identification of a subpopulation of rapidly self-renewing and multipotential adult stem cells in colonies of human marrow stromal cells. *Proceedings of the National Academy of Sciences of the United States of America* 98(14), p. 7841-7845.

Corsi, A. et al. 2002. Phenotypic effects of biglycan deficiency are linked to collagen fibril abnormalities, are synergized by decorin deficiency, and mimic Ehlers-Danlos-like changes in bone and other connective tissues. *Journal of Bone Mineral Research* 17(7), p. 1180-1189

Cramer, C. et al. 2010. Persistent high glucose concentrations alter the regenerative potential of mesenchymal stem cells. *Stem Cells and Development* 19(12), p. 1875-1884.

Creager, M. A. et al. 2003. Diabetes and vascular disease: pathophysiology, clinical consequences, and medical therapy: Part I. *Circulation* 108(12), p. 1527-1532.

Cui, C. B. et al. 2003. Transcriptional coactivation of bone-specific transcription factor Cbfa1 by TAZ. *Molecular and Cellular Biology* 23(3), p. 1004-1013.

Cunha, J. et al. 2014. Effects of high glucose and high insulin concentrations on osteoblast function *in vitro*. *Cell and Tissue Research*, 358(1):249-56

D'Aquino, R. et al. 2009. Human mandible bone defect repair by the grafting of dental pulp stem/progenitor cells and collagen sponge biocomplexes. *European Cells and Materials* 18, p. 75-83.

D'Souza, D. R. et al. 2009. Hyperglycemia regulates Runx2 activation and cellular wound healing through the aldose reductase polyol pathway. *Journal of Biological Chemistry* 284(27), p. 17947-17955.

D'Aquino, R. et al. 2008. Dental pulp stem cells: a promising tool for bone regeneration. *Stem Cell Reviews* 4(1), p. 21-26.

Dadlani, H. et al. 2008. Smad and p38 MAP kinase-mediated signaling of proteoglycan synthesis in vascular smooth muscle. *Journal of Biological Chemistry* 283(12), p. 7844-7852.

Dalle-Donne, I. et al. 2003. Protein carbonyl groups as biomarkers of oxidative stress. *Clinica Chimica Acta* 329(1-2), p. 23-38.

Danielson, K. G. et al. 1997. Targeted disruption of decorin leads to abnormal collagen fibril morphology and skin fragility. *Journal of Cellular Biology* 136(3), p. 729-743.

Danoviz, M. and Yablonka-Reuveni, Z. 2012. Skeletal muscle satellite cells: background and methods for isolation and analysis in a primary culture system. In: DiMario, J.X. ed. *Myogenesis*. 798. Humana Press, p. 21-52.

Das, B. et al. 2009. Genetic association study of selected candidate genes (ApoB, LPL, Leptin) and telomere length in obese and hypertensive individuals. *BMC Medical Genetics* 10, p. 99.

Davies, J. and Gordon, S. 2005. Isolation and culture of murine macrophages. In: Helgason, C. and Miller, C. eds. *Basic Cell Culture Protocols*. 290. Humana Press, p. 91-103.

Davies, J. E. 2003. Understanding peri-implant endosseous healing. *Journal of Dental Education* 67(8), p. 932-949.

Davies, L. C. et al. 2010. A multipotent neural crest-derived progenitor cell population is resident within the oral mucosa lamina propria. *Stem Cells Development* 19(6), p. 819-830.

De Paula, F. J. A. et al. 2010. Novel insights into the relationship between diabetes and osteoporosis. *Diabetes/Metabolism Research and Reviews* 26(8), p. 622-630.

Deans, R. J. and Moseley, A. B. 2000. Mesenchymal stem cells: Biology and potential clinical uses. *Experimental Hematology* 28(8), p. 875-884.

Deckers, M. et al. 2002. Bone morphogenetic proteins stimulate angiogenesis through osteoblast-derived vascular endothelial growth factor A. *Endocrinology* 143(4), p. 1545-1553.

Deorosan, B. and Nauman, E. A. 2011. The role of glucose, serum, and three-dimensional cell culture on the metabolism of bone marrow-derived mesenchymal stem cells. *Stem Cells International* [online], Available at http://www.ncbi.nlm.nih.gov/pmc/articles/PMC3096318/pdf/SCI2011-429187.pdf [Accessed: 12 May 2013].

Dienelt, A. and zur Nieden, N. I. 2011. Hyperglycemia impairs skeletogenesis from embryonic stem cells by affecting osteoblast and osteoclast differentiation. *Stem Cells Development*. 20 (3), p. 465-474.

Dimitriou, R. et al. 2005. Current concepts of molecular aspects of bone healing. *Injury* 36(12), p. 1392-1404.

Ding, Y. C. et al. 2010. Mesenchymal stem-cell immunosuppressive capabilities: therapeutic implications in islet transplantation. *Transplantation* 89(3), p. 270-273.

Discher, D. E. et al. 2009. Growth Factors, matrices, and forces combine and control stem cells. Science 324(5935), p. 1673-1677.

Dominici, M. et al. 2006. Minimal criteria for defining multipotent mesenchymal stromal cells. *The International Society for Cellular Therapy position statement*. *Cytotherapy,* 8(4), p.315-317,

ISSN 1465-3249

Donath, M. Y. and Shoelson, S. E. 2011. Type 2 diabetes as an inflammatory disease. *Nature Reviews Immunology* 11(2), p. 98-107.

Dougall, W. C. 2011. Molecular Pathways: Osteoclast-dependent and osteoclast-independent roles of the RANKL/RANK/OPG pathway in tumorigenesis and metastasis. *Clinical Cancer Research*. 18(2), p. 326-35.

Dougall, W. C. et al. 1999. RANK is essential for osteoclast and lymph node development. *Genes & Development* 13(18), p. 2412-2424.

Dowell, S. et al. 2007. Implant success in people with type 2 diabetes mellitus with varying glycemic control: A pilot study. *The Journal of the American Dental Association* 138(3), p. 355-361.

Doxey, D. L. et al. 1998. Diabetes-induced impairment of macrophage cytokine release in a rat model: Potential role of serum lipids. *Life Sciences* 63(13), p. 1127-1136.

Ducy, P. et al. 1997. Osf2/Cbfa1: A transcriptional activator of osteoblast differentiation. Cell 89(5), p. 747-754.

Ebeling, P. R. et al. 1993. Short-term effects of recombinant human insulin-like growth factor I on bone turnover in normal women. *Journal of Clinical Endocrinology & Metabolism* 77(5), p. 1384-1387.

Eda, H. et al. 2011. Proinflammatory cytokines, IL-1β and TNF-α, induce expression of interleukin-34 mRNA via JNK- and p44/42 MAPK-NF-κB pathway but not p38 pathway in osteoblasts. *Rheumatology International* 31(11), p. 1525-1530.

Ehnert, S. et al. 2010. TGF- β1 as possible link between loss of bone mineral density and chronic inflammation. *PLoS One* 5(11), p. 14073.

Eizirik, D. L. et al. 2008. The Role for endoplasmic reticulum stress in diabetes mellitus. *Endocrine Reviews* 29(1), p. 42-61.

Elmarakby, A. A. et al. 2010. Inflammatory cytokines as predictive markers for early detection and progression of diabetic nephropathy. *The EPMA Journal* 1(1), p. 117-129.

Elmasri, H. et al. 2009. Fatty acid binding protein 4 is a target of VEGF and a regulator of cell proliferation in endothelial cells. *FASEB Journal* 23(11), p. 3865-3873.

Eriksen, E.F.et al. 1994. *Bone histomorphometry*. Raven press, New York, USA p. 1-12

Espinoza-Jimenez, A. et al. 2012. Alternatively activated macrophages in types 1 and 2 diabetes. *Mediators Inflammatory* 2012, p. 815953.

Evans, J. L. et al. 2002. Oxidative Stress and Stress-Activated Signaling Pathways: A Unifying Hypothesis of Type 2 Diabetes. *Endocrine Reviews* 23(5), p. 599-622

Evans, J. L. et al. 2003. Are Oxidative stress−activated signaling pathways mediators of insulin resistance and β-cell dysfunction? *Diabetes* 52(1), p. 1-8.

Eyckmans, J. et al. 2012. Adhesive and mechanical regulation of mesenchymal stem cell differentiation in human bone marrow and periosteum-derived progenitor cells. Biology Open. *1*(11), p.1058–1068.

Ezquer, F. et al. 2009. Endovenous administration of bone-marrow-derived multipotent mesenchymal stromal cells prevents renal failure in diabetic mice. *Biology of Blood and Marrow Transplant* 15(11), p. 1354-1365.

Feghali, K. and Grenier, D. 2012. Priming effect of fibronectin fragments on the macrophage inflammatory response: potential contribution to periodontitis. *Inflammation* 35(5), p. 1696-1705.

Feng, Y. F. et al. 2013. Effect of reactive oxygen species overproduction on osteogenesis of porous titanium implant in the present of diabetes mellitus. *Biomaterials* 34(9), p. 2234-2243.

Ferguson, C. et al. 1999. Does adult fracture repair recapitulate embryonic skeletal formation? *Mechanisms of Development* 87(1–2), p. 57-66.

Fernig, D. G. and Gallagher, J. T. 1994. Fibroblast growth factors and their receptors: An information network controlling tissue growth, morphogenesis and repair. *Progress in Growth Factor Research* 5(4), p. 353-377.

Ferrara, N. et al. 1998. Vascular endothelial growth factor is essential for corpus luteum angiogenesis. *Nature Medicine* 4 (3), p. 336-340.

Fiorellini, J. P. et al. 2000. A retrospective study of dental implants in diabetic patients. *International Journal Periodontics and Restorative Dentistry* 20(4), p. 366-373.

Fiorina, P. et al. 2010. The mobilization and effect of endogenous bone marrow progenitor cells in diabetic wound healing. *Cell Transplantation* 19(11), p. 1369-1381.

Flaumenhaft, R. and Rifkin, D. B. 1992. Extracellular matrix regulation of growth factor and protease activity. *Current Opinion in Cell Biology* 3(5), p. 817-823.

Forbes, J. M. et al. 2003. Role of Advanced Glycation End Products in Diabetic Nephropathy. *Journal of the American Society of Nephrology* 14(3), p. S254-S258.

Fowler, M. J. 2008. Microvascular and macrovascular complications of diabetes. *Clinical Diabetes* 26(2), p. 77-82.

Franceschi, R. T. et al. 2000. Gene therapy for bone formation: *in vitro* and *in vivo* osteogenic activity of an adenovirus expressing BMP7. *Journal of Cellular Biochemistry* 78(3), p. 476-486.

Franceschi, R. T. et al. 2004. Gene therapy approaches for bone regeneration. *Cells, Tissues, Organs* 176(1-3), p. 95-108.

Frey, H. et al. 2013. Biological interplay between proteoglycans and their innate immune receptors in inflammation. *FEBS Journal* 280(10), p. 2165-2179.

Friedenstein, A. et al. 1976. Fibroblast precursors in normal and irradiated mouse hematopoietic organs. *Experimental Hematology* 4(5):267-74.

Friedlaender, G. E. et al. 2001. Osteogenic Protein-1 (Bone Morphogenetic Protein-7) in the Treatment of Tibial Nonunions. *Journal of Bone & Joint Surgery,* 83(1) p. S151–S158

Fu, Y. et al. 2005. Adiponectin promotes adipocyte differentiation, insulin sensitivity, and lipid accumulation. *Journal of Lipid Research* 46(7), p. 1369-1379.

Fujii, H. et al. 2008. Bone formation in spontaneously diabetic Torii-newly established model of non-obese type 2 diabetes rats. *Bone* 42(2), p. 372-379.

Fujisaka, S. et al. 2009. Regulatory mechanisms for adipose tissue M1 and M2 macrophages in diet-induced obese mice. *Diabetes* 58(11), p. 2574-2582.

Galatz, L. M. et al. 2006. Characteristics of the rat supraspinatus tendon during tendon-to-bone healing after acute injury. *Journal of Orthopaedic Research* 24(3), p. 541-550.

Galiano, R. D. et al. 2004. Topical Vascular Endothelial Growth Factor Accelerates Diabetic Wound Healing through Increased Angiogenesis and by Mobilizing and Recruiting Bone Marrow-Derived Cells. *The American Journal of Pathology* 164(6), p. 1935-1947.

Gallagher, K. A. et al. 2007. Diabetic impairments in NO-mediated endothelial progenitor cell mobilization and homing are reversed by hyperoxia and SDF-1α. *The Journal of Clinical Investigation* 117(5), p. 1249-1259.

Gandhi, A. et al. 2005. The effects of local insulin delivery on diabetic fracture healing. *Bone* 37(4), p. 482-490.

Gao, Y. et al. 2009. TGF- β1 and TGF-βR1 are expressed in ameloblasts and promote MMP20 expression. *Anatomical Record* (Hoboken, N.J. : 2007) 292(6), p. 885-890.

García-Hernández, A. et al. 2012. High glucose concentrations alter the biomineralization process in human osteoblastic cells. *Bone* 50(1), p. 276-288.

Garetto, L. P. et al. 1995. Remodeling dynamics of bone supporting rigidly fixed titanium implants: a histomorphometric comparison in four species including humans. *Implant Dentistry* 4 (4), p. 235-243.

Garg A.K. (Ed.). Bone biology, harvesting, and grafting for dental implants: Rationale and clinical applications (2004). *Quintessence Publishing Co*., Chicago, U.S.A. **p.**186–191.

Gee, E. et al. 2010. p38 MAPK activity is stimulated by vascular endothelial growth factor receptor 2 activation and is essential for shear stress-induced angiogenesis. *Journal of Cellular Physiology* 222(1), p. 120-126.

Georgiou, K. R. et al. 2012. Attenuated Wnt/β-catenin signalling mediates methotrexate chemotherapy-induced bone loss and marrow adiposity in rats. *Bone* 50(6), p. 1223-1233.

Gerber, H. P. et al. 1999. VEGF couples hypertrophic cartilage remodeling, ossification and angiogenesis during endochondral bone formation. *Nature Medicine* 5(6), p. 623-628.

Giacco, F. and Brownlee, M. 2010. Oxidative stress and diabetic complications. *Circulation Research* 107(9), p. 1058-1070.

Gomez-Moreno, G. et al. 2014. Peri-implant evaluation in type 2 diabetes mellitus patients: a 3-year study. *Clinical Oral Implants Research* [online] Available at http://www.ncbi.nlm.nih.gov/pubmed/24684438 [Accessed: 20 April 2012].

Gonzalez, R. F. et al. 2009. Rat alveolar type I cells proliferate, express Oct-4, and exhibit phenotypic plasticity *in vitro*. *American Journal of Physiology-Lung Cellular and Molecular Physiology* 297(6), p.1045-55.

Goodson, W. H. and Hunt, T. K. 1979. Wound-Healing and the diabetic patient. *Surgery Gynecology & Obstetrics* 149(4), p. 600-608.

Goth, L. 2008. Catalase deficiency and type 2 diabetes. Diabetes Care 31(12), p. e93.

Goto, Y. and Kakizaki, M. 1981. The Spontaneous-diabetes rat: a model of noninsulin dependent diabetes mellitus. *Proceedings of the Japan Academy, Series B* 57(10), p. 381-384.

Govender, S. et al. 2002. Recombinant Human Bone Morphogenetic Protein-2 for Treatment of Open Tibial Fractures. *The Journal of Bone and Joint Surgery American*; 84-A(12) p. 2123-2134.

Granero-Moltó, F. et al. 2009. Regenerative effects of transplanted mesenchymal stem cells in fracture healing. *Stem Cells* 27(8), p. 1887-1898.

Graves, D. T. et al. 2011. Impact of diabetes on fracture healing. *Journal of Experimental & Clinical Medicine* 3(1), p. 3-8.

Gronthos, S. et al. 2000. Postnatal human dental pulp stem cells (DPSCs) *in vitro* and *in vivo. Proceedings of the National Academy of Sciences of the United States of America* 97(25), p. 13625-13630.

Guo, Z. et al. 2006. *In Vitro* Characteristics and *in vivo* immunosuppressive activity of compact bone-derived murine mesenchymal progenitor cells. *Stem Cells* 24(4), p. 992-1000.

Hamed, S. et al. 2010. Nitric oxide: a key factor behind the dysfunctionality of endothelial progenitor cells in diabetes mellitus type-2. *Cardiovascular Research.* 91(1), p.9-15

Harding, H. P. and Ron, D. 2002. Endoplasmic reticulum stress and the development of diabetes: a review. *Diabetes* 51(3), p. S455-S461.

Harrington, J. et al. 2014. Quantification of clonal heterogeneity of mesenchymal progenitor cells in dental pulp and bone marrow. *Connective Tissue Research* 55 (1), p. 62-67.

Harris, S. E. et al. 1994. Expression of bone morphogenetic protein messenger RNAs by normal rat and human prostate and prostate cancer cells. *Prostate* 24(4), p. 204-211.

Hasegawa, H. et al. 2008. Type 2 diabetes impairs implant osseointegration capacity in rats. *International Journal of Oral & Maxillofacial Implants* 23(2), p. 237-246.

He, H. B. et al. 2004. Diabetes causes decreased osteoclastogenesis, reduced bone formation, and enhanced apoptosis of osteoblastic cells in bacteria stimulated bone loss. *Endocrinology* 145(1), p. 447-452.

Hebert, L. F., Jr. et al. 1996. Overexpression of glutamine:fructose-6-phosphate amidotransferase in transgenic mice leads to insulin resistance. *The Journal of Clinical Investigation* 98(4), p. 930-936.

Hjelmeland, A. B. et al. 2005. Loss of smad3-mediated negative regulation of Runx2 activity leads to an alteration in cell fate determination. *Molecular and Cellular Biology* 25(21), p. 9460-9468.

Ho, V. H. and Sly, L. 2009. Derivation and characterization of murine alternatively activated (M2) macrophages. In: Reiner, N.E. ed. *Macrophages and Dendritic Cells*. Vol. 531. Humana Press, p. 173-185.

Hobot, J. A. and Newman, G. R. 1996. Immunomicroscopy: resin techniques and on-section labelling with immunocolloidal gold or immunoperoxidase--planning a protocol. *Scanning Microscopy* 10(1), p. 121-143

Hong, J. H. et al. 2005. TAZ, a transcriptional modulator of mesenchymal stem cell differentiation. *Science* 309(5737), p. 1074-1078.

Horwitz, E. et al. 2005. Clarification of the nomenclature for MSC: The International Society for Cellular Therapy position statement. *Cytotherapy* 7(5), p. 393-395.

Hotamisligil, G. S. et al. 1994. Tumor necrosis factor alpha inhibits signaling from the insulin receptor. *Proceedings of the National Academy of Sciences* 91(11), p. 4854-4858.

Hou, J. C. et al. 1993. Effects of severe diabetes and insulin on the femoral neck of the immature rat. *Journal of Orthopaedic Research* 11(2), p. 263-7

Hu, P. P. et al. 1998. Molecular mechanisms of transforming growth factor-β signaling. *Endocrine Reviews* 19(3), p. 349-363.

Huang, Q. and Sheibani, N. 2008. High Glucose Promotes Retinal Endothelial Cell Migration through Activation of Src, PI3K/Akt1/eNOS, and ERKs. *American Journal of Physiology-Lung Cellular and Molecular Physiology* 295(6), p.1647-57.

Huang, S. et al. 2012. Mesenchymal stem cells delivered in a microsphere-based engineered skin contribute to cutaneous wound healing and sweat gland repair. *Journal of Dermatological Science* 66(1), p. 29-36.

Huang, S. et al. 2012. Mesenchymal stem cells delivered in a microsphere-based engineered skin contribute to cutaneous wound healing and sweat gland repair. *Journal of Dermatological Science* 66(1), p. 29-36.

Hughes, F. J. et al. 2006. Effects of growth factors and cytokines on osteoblast differentiation. *Periodontology* 2000 41(1), p. 48-72.

Hurley, M.M., Florkiewicz, R.Z., 1996. In: Bilezikian, J.P., Raisz, L.G., Rodan, G.A. (Eds.), *Principles of Bone Biology*. Academic Press, New York, p. 627–645.

Igarashi, M. et al. 1999. Glucose or diabetes activates p38 mitogen-activated protein kinase via different pathways. *The Journal of Clinical Investigation* 103(2), p. 185-195.

Iglesias-de la Cruz, M. C. et al. 2002. Effects of high glucose and TGF- β1 on the expression of collagen IV and vascular endothelial growth factor in mouse podocytes. *Kidney International* 62(3), p. 901-913.

Ignotz, R. A. and Massagué, J. 1986. Transforming growth factor- β stimulates the expression of fibronectin and collagen and their incorporation into the extracellular matrix. *Journal of Biological Chemistry* 261(9), p. 4337-4345.

Inoguchi, T. et al. 2000. High glucose level and free fatty acid stimulate reactive oxygen species production through protein kinase C-dependent activation of NAD(P)H oxidase in cultured vascular cells. *Diabetes* 49(11), p. 1939-1945.

International Diabetes Federation. IDF Diabetes Atlas, 6th edn. Brussels, Belgium: *International Diabetes Federation, 2013* [online] Available at http://www.idf.org/diabetesatlas [Accessed: 20 December 2013].

Issad, T. and Kuo, M. 2008. O-GlcNAc modification of transcription factors, glucose sensing and glucotoxicity. *Trends in Endocrinology & Metabolism* 19(10), p. 380-389.

James, L. R. et al. 2002. Flux Through the Hexosamine Pathway Is a Determinant of Nuclear Factor κB– Dependent Promoter Activation. Diabetes 51(4), p. 1146-1156.

Jang, Y. O. et al. 2014. Effect of bone marrow-derived mesenchymal stem cells on hepatic fibrosis in a thioacetamide-induced cirrhotic rat model. *BMC Gastroenterology* 14(1), p. 198.

Janssens, K. et al. 2005. Transforming growth factor- β1 to the bone. *Endocrine Reviews* 26(6), p. 743-774.

Javed, A. et al. 2001. Runx2-C/EBP molecular interactions and functional synergism support maximal expression of osteocalcin in osteoblasts. *Molecular Biology of the Cell* 12, p. 100a-100a.

Jennings, P. E. et al. 1987. Increased Diene Conjugates in Diabetic Subjects with Microangiopathy. *Diabetic Medicine* 4(5), p. 452-456.

Jones, E. A. et al. 2002. Isolation and characterization of bone marrow multipotential mesenchymal progenitor cells. *Arthritis & Rheumatism* 46(12), p. 3349-3360.

Jones, E. and Yang, X. 2011. Mesenchymal stem cells and bone regeneration: Current status. *Injury* 42(6), p. 562-568.

Jones, P. H. and Watt, F. M. 1993. Separation of human epidermal stem-cells from transit amplifying cells on the basis of differences in integrin function and expression. *Cell* 73(4), p. 713-724.

Jun, H. S. and Yoon, J. W. 2001. The role of viruses in Type I diabetes: two distinct cellular and molecular pathogenic mechanisms of virus-induced diabetes in animals. *Diabetologia* 44(3), p. 271-285.

Jung, H. Y. et al. 2013. Relationship of tooth mortality and implant treatment in Type 2 diabetes mellitus patients in Korean adults. *Journal of Advance Prosthodontics* 5(1), p. 51-57.

Kador, P. F. 1988. The role of aldose reductase in the development of diabetic complications. *Medicinal Research Reviews* 8(3), p. 325-352.

Kaneto, H. et al. 2005. Oxidative stress, ER stress, and the JNK pathway in type 2 diabetes. *Journal of Molecular Medicine* 83(6), p. 429-439.

Kannel, W. B. and McGee, D. L. 1979. Diabetes and cardiovascular disease: The framingham study. *Journal of the American Medical Association* 241(19), p. 2035-2038.

Kanwar, M. and Kowluru, R. A. 2009. Role of glyceraldehyde 3-phosphate dehydrogenase in the development and progression of diabetic retinopathy. *Diabetes* 58(1), p. 227-234.

Kanyo, Z. F. et al. 1992. Crystallization and oligomeric structure of rat liver arginase. *Journal of Molecular Biology* 224(4), p. 1175-1177.

Karaoz, E. et al. 2009. Characterization of mesenchymal stem cells from rat bone marrow: ultrastructural properties, differentiation potential and immunophenotypic markers. *Histochemistry and Cell Biology* 132(5), p. 533-546.

Karaöz, E. et al. 2011. A comprehensive characterization study of human bone marrow mscs with an emphasis on molecular and ultrastructural properties. *Journal of Cellular Physiology* 226(5), p. 1367-1382.

Katagiri, T. and Takahashi, N. 2002. Regulatory mechanisms of osteoblast and osteoclast differentiation. *Oral Diseases* 8(3), p. 147-159.

Katz, J. et al. 1995. Cytokines and growth-factors modulate cell-growth and insulin-like growth-factor binding-protein secretion by the human salivary cell-line (hsg). *Journal of Cellular Physiology* 165(2), p. 223-227.

Katz, P. P. et al. 1991. Epidemiology and prevention of periodontal disease in individuals with diabetes. *Diabetes Care* 14(5), p. 375-385.

Kayal, R. A. et al. 2007. Diminished bone formation during diabetic fracture healing is related to the premature resorption of cartilage associated with increased osteoclast activity. *Journal of Bone and Mineral Research* 22(4), p. 560-568.

Keila, S. et al. 2001. Systemic prostaglandin E2 increases cancellous bone formation and mass in aging rats and stimulates their bone marrow osteogenic capacity *in vivo* and in vitro. *Journal of Endocrinology* 168(1), p. 131-139.

Kelly, K. and Gimble, J. 1998. 1,25-dihydroxy vitamin D3 inhibits adipocyte differentiation and gene expression in murine bone marrow stromal cell clones and primary cultures. *Endocrinology* 139(5), p. 2622-2628.

Kershaw, E. and Flier, J. 2004. Adipose tissue as an endocrine organ. *The Journal of Clinical Endocrinology & Metabolism* 89(6), p. 2548-2556.

Kharraz, Y. et al. 2013. Macrophage plasticity and the role of inflammation in skeletal muscle repair. *Mediators of Inflammation* [online] Available at www.hindawi.com/journals/mi/2013/491497/ [Accessed: 22 January 2013].

Kim, B. et al. 2013. Ascorbic acid enhances adipogenesis of 3T3-L1 murine preadipocyte through differential expression of collagens. *Lipids in Health and Disease* 12(1), p. 182.

Kim, J. and Wong, P. K. Y. 2009. Loss of ATM Impairs Proliferation of Neural Stem Cells Through Oxidative Stress-Mediated p38 MAPK Signaling. Stem Cells 27(8), p. 1987-1998.

Kim, Y. H. et al. 2006. High glucose increase cell cycle regulatory proteins level of mouse embryonic stem cells via PI3-K/Akt and MAPKs signal pathways. *Journal of Cellular Physiology* 209(1), p. 94-102.

Kini U, Nandeesh BN. 2012. Physiology of bone formation, remodelling and metabolism. In: Fogelman I, Gnanasegaran G, Van der Walls H, West C Radionuclide and hybrid bone imaging. Berlin: Springer-Verlag. p29-30.

Kitagawa, T. et al. 1998. Increased incidence of non-insulin dependent diabetes mellitus among Japanese schoolchildren correlates with an increased intake of animal protein and fat. *Clinical Pediatrics* 37(2), p. 111-115.

Koh, J. T. et al. 2008. Combinatorial gene therapy with BMP2/7 enhances cranial bone regeneration. *Journal of Dental Research* 87(9), p. 845-849.

Kolm-Litty, V. et al. 1998. High glucose-induced transforming growth factor- β1 production is mediated by the hexosamine pathway in porcine glomerular mesangial cells. *The Journal of Clinical Investigation* 101(1), p. 160-169.

Komori, T. 2002. Runx2, a multifunctional transcription factor in skeletal development. *Journal of Cellular Biochemistry* 87(1), p. 1-8.

Komori, T. et al. 1997. Targeted disruption of Cbfa1 results in a complete lack of bone formation owing to maturational arrest of osteoblasts. *Cell* 89(5), p. 755-764.

Kotsovilis, S. et al. 2006. A comprehensive and critical review of dental implant placement in diabetic animals and patients. *Clinical Oral Implants Research* 17(5), p. 587-599.

Koya, D. and King, G. L. 1998. Protein kinase C activation and the development of diabetic complications. *Diabetes* 47(6), p. 859-866.

Krebsbach, P. H. et al. 1999. Bone marrow stromal cells: Characterization and clinical application. *Critical Reviews in Oral Biology & Medicine* 10(2), p. 165-181.

Krebsbach, P. H. et al. 2000. Gene therapy-directed osteogenesis: BMP-7-transduced human fibroblasts form bone *in vivo*. *Human Gene Therapy* 11(8), p. 1201-1210.

Krebsbach, P. H. et al. 2003. Bone marrow stromal cells as a genetic platform for systemic delivery of therapeutic proteins *in vivo*: human factor IX model. *The Journal of Gene Medicine* 5(1), p. 11-17.

Kröger, H. et al. 1997. Growth Hormone, Osteoblasts, and Marrow Adipocytes: A Case Report. *Calcified Tissue International* 61(1), p. 33-35.

Kume, S. et al. 2005. Advanced Glycation End-Products Attenuate Human Mesenchymal Stem Cells and Prevent Cognate Differentiation Into Adipose Tissue, Cartilage, and Bone. *Journal of Bone and Mineral Research* 20(9), p. 1647-1658.

Kuo, Y.-R. et al. 2011. Bone marrow-derived mesenchymal stem cells enhanced diabetic wound healing through recruitment of tissue regeneration in a rat model of streptozotocin-induced diabetes. *Plastic and Reconstructive Surgery* 128(4), p. 872-880.

Kuznetsov, S. A. et al. 1997. Single-colony derived strains of human marrow stromal fibroblasts form bone after transplantation. Journal of bone and mineral research : the official journal of the *American Society for Bone and Mineral Research* 12(9), p. 1335-1347.

Kuznetsov, S. A. et al. 2004. The interplay of osteogenesis and hematopoiesis: expression of a constitutively active PTH/PTHrP receptor in osteogenic cells perturbs the establishment of hematopoiesis in bone and of skeletal stem cells in the bone marrow. *Journal of Cell Biology* 167(6), p. 1113-1122.

Kwon, D. S. et al. 2008. Treatment with bone marrow-derived stromal cells accelerates wound healing in diabetic rats. *International Wound Journal* 5(3), p. 453-463.

Laino, G. et al. 2005. A new population of human adult dental pulp stem cells: a useful source of living autologous fibrous bone tissue (LAB). *Journal of Bone and Mineral Research* 20(8), p. 1394-1402.

Laino, G. et al. 2006. In Vitro Bone Production Using Stem Cells Derived From Human Dental Pulp. *Journal of Craniofacial Surgery* 17(3), p. 511-515.

Lamberg, A. et al. 2006. Locally delivered TGF-β1 and IGF-1 enhance the fixation of titanium implants: A study in dogs. *Acta Orthopaedica* 77(5), p. 799-805.

Lamberg, A. et al. 2009. Effect of local TGF-β1 and IGF-1 release on implant fixation: comparison with hydroxyapatite coating: A paired study in dogs. *Acta Orthopaedica* 80(4), p. 499-504.

Le Blanc, K. 2006. Mesenchymal stromal cells: tissue repair and immune modulation. *Cytotherapy* 8(6), p. 559-561.

Lee, K. et al. 2011. Growth factor delivery-based tissue engineering: general approaches and a review of recent developments. *Journal of The Royal Society Interface* 8(55), p. 153-170.

Lee, M.-H. et al. 1999. Transient upregulation of CBFA1 in response to bone morphogenetic protein-2 and transforming growth factor β1 in C2C12 myogenic cells coincides with suppression of the myogenic phenotype but is not sufficient for osteoblast differentiation. *Journal of Cellular Biochemistry* 73(1), p. 114-125.

Lee, M.-H. et al. 2003. BMP-2-induced Osterix expression is mediated by Dlx5 but is independent of Runx2. *Biochemical and Biophysical Research Communications* 309(3), p. 689-694.

Lee, N. K. et al. 2007. Endocrine regulation of energy metabolism by the skeleton. *Cell* 130, p. 456 - 469.

Lee, R. H. et al. 2004. Characterization and Expression Analysis of Mesenchymal Stem Cells from Human Bone Marrow and Adipose Tissue. *Cellular Physiology and Biochemistry* 14(4-6), p. 311-324.

Levak-Frank, S. et al. 1995. Muscle-specific overexpression of lipoprotein lipase causes a severe myopathy characterized by proliferation of mitochondria and peroxisomes in transgenic mice. *The Journal of Clinical Investigation* 96(2), p. 976-986.

Li, X. L. et al. 2013. Roles of Neuronal Nitric Oxide Synthase and Inducible Nitric Oxide Synthase in Intestinal Transplantation of Rats. *Transplantation Proceedings* 45(6), p. 2497-2501.

Li, Y. P. and Stashenko, P. 1992. Proinflammatory cytokines tumor necrosis factor-alpha and IL-6, but not IL-1, down-regulate the osteocalcin gene promoter. *The Journal of Immunology* 148(3), p. 788-794.

Li, Y.-M. et al. 2007. Effects of high glucose on mesenchymal stem cell proliferation and differentiation. *Biochemical and Biophysical Research Communications* 363(1), p. 209-215.

Lieberman, J. R. et al. 2002. The Role of Growth Factors in the Repair of Bone : Biology and Clinical Applications. *Journal of Bone & Joint Surgery* 84(6), p. 1032-1044.

Lind, M. 1998. Growth factor stimulation of bone healing. Effects on osteoblasts, osteomies, and implants fixation. *Acta Orthopaedica Scandinavica Supplement*. Oct(283), p. 2-37.

Linkhart, T. A. et al. 1996. Growth factors for bone growth and repair: IGF, TGF[β] and BMP. *Bone* 19(1), p. S1-S12.

Lipscombe, L. L. et al. 2007. The Risk of Hip Fractures in Older Individuals With Diabetes. *Diabetes Care* 30(4), p. 835-841.

Liu, H. F. et al. 2012. Altered polarization, morphology, and impaired innate immunity germane to resident peritoneal macrophages in mice with long-term type 2 diabetes. *J Biomed Biotechnol* 2012, p. 867023.

Livak, K. J. and Schmittgen, T. D. 2001. Analysis of relative gene expression data using real-time quantitative PCR and the $2^{-\Delta\Delta CT}$Method. *Methods* 25(4), p. 402-408.

Löndahl, M. et al. 2010. Hyperbaric oxygen therapy facilitates healing of chronic foot ulcers in patients with diabetes. *Diabetes Care* 33(5), p. 998-1003.

Lovell-Badge, R. 2001. The future for stem cell research. *Nature* 414(6859), p. 88-91.

Lu, H. et al. 2003. Diabetes interferes with the bone formation by affecting the expression of transcription factors that regulate osteoblast differentiation. *Endocrinology* 144(1), p. 346-352.

Lyon, T. et al. 2013. Efficacy and safety of recombinant human bone morphogenetic protein-2/calcium phosphate matrix for closed tibial diaphyseal fracture. *Journal of bone and joint surgery American Volume* 95(23):2088-96.

Madonna, R. et al. 2013. Glucose metabolism, hyperosmotic stress, and reprogramming of somatic cells. *Molecular Biotechnology* 55(2), p. 169-178.

Madsen-Bouterse, S. et al. 2010. Glyceraldehyde-3-phosphate dehydrogenase in retinal microvasculature: implications for the development and progression of diabetic retinopathy. *Investigative Ophthalmology & Visual Science* 51(3), p. 1765-1772.

Magliano, D. J. et al. 2008. Glucose indices, health behaviors, and incidence of diabetes in australia: the australian diabetes, obesity and lifestyle study. *Diabetes Care* 31(2), p. 267-272.

Marcelli, C. et al. 1990. *In vivo* effects of human recombinant transforming growth factor β on bone turnover in normal mice. *Journal of Bone and Mineral Research* 5(10), p. 1087-1096.

Mareschi, K. et al. 2012. Multipotent mesenchymal stromal stem cell expansion by plating whole bone marrow at a low cellular density: a more advantageous method for clinical use. *Stem Cells International* [online] Available at http://www.hindawi.com/journals/sci/2012/920581/ [Accessed: 2 December 2013].

Marston, W. A. et al. 2003. The Efficacy and Safety of Dermagraft in Improving the Healing of Chronic Diabetic Foot Ulcers: Results of a prospective randomized trial. *Diabetes Care* 26(6), p. 1701-1705.

Maruyama, K. et al. 2007. Decreased macrophage number and activation lead to reduced lymphatic vessel formation and contribute to impaired diabetic wound healing. *The American Journal of Pathology* 170(4), p. 1178-1191.

Marx, R. E. and Garg, A. K. 1998. Bone structure, metabolism, and physiology: its impact on dental implantology. *Implant Dentistry* 7(4), p. 267-276.

Massagué, J. and Wotton, D. 2000. Transcriptional control by the TGF-β/Smad signaling system. *EMBO Journal* 19(8), p. 1745-1754.

Mayahara, H. et al. 1993. *In-vivo* stimulation of endosteal bone-formation by basic fibroblast growth-factor in rats. *Growth Factors* 9(1), p. 73-80

McClain, D. A. and Crook, E. D. 1996. Hexosamines and insulin resistance. *Diabetes* 45(8), p. 1003-1009.

McCracken, M. S. et al. 2006. Bone associated with implants in diabetic and insulin-treated rats. *Clinical Oral Implants Research* 17(5), p. 495-500.

Medina, J. et al. 2005. Evidence of angiogenesis in primary biliary cirrhosis: an immunohistochemical descriptive study. *Journal of Hepatology* 42(1), p. 124-131.

Meier, M. and King, G. L. 2000. Protein kinase C activation and its pharmacological inhibition in vascular disease. *Vascular Medicine* 5(3), p. 173-185.

Menicanin, D. et al. 2010. Identification of a common gene epxression signature associated with immature clonal mesenchymal stem cell populations derived from bone marrow and dental tissues. *Stem Cell and Development* 19, p. 1501-1510.

Merline, R. et al. 2009. The matricellular functions of small leucine-rich proteoglycans (SLRPs). *Journal of Cell Communication and Signaling* 3(3-4), p. 323-335

Meurer, S. K. et al. 2005. Identification of endoglin in rat hepatic stellate cells: new insights into transforming growth factor β receptor signaling. *Journal of Biological Chemistry* 280(4), p. 3078-3087.

Mezentsev, A. et al. 2002. Eicosanoid regulation of VEGF expression and angiogenesis in microvessel endothelial cells. *Journal of Biological Chemistry.* 277(21), p.18670-18676

Minguell, J. J. et al. 2001. Mesenchymal Stem Cells. *Experimental Biology and Medicine* 226(6), p. 507-520.

Minoura, H. et al. 2007. Mechanism by which a novel non-thiazolidinedione peroxisome proliferator-activated receptor γ agonist, FK614, ameliorates insulin resistance in Zucker fatty rats. *Diabetes, Obesity and Metabolism* 9(3), p. 369-378.

Miyama, K. et al. 1999. A BMP-inducible gene, Dlx5, regulates osteoblast differentiation and mesoderm induction. *Developmental Biology* 208(1), p. 123-133.

Mohammad, M. K. et al. 2006. Dysregulated Toll-like receptor expression and signaling in bone marrow-derived macrophages at the onset of diabetes in the non-obese diabetic mouse. *International Immunology* 18(7), p. 1101-1113.

Mohan, S. and Baylink, D. J. 1991. Bone growth factors. *Clinical Orthopaedics and Related Research* (263), p. 30-48.

Montero, A. et al. 2000. Disruption of the fibroblast growth factor-2 gene results in decreased bone mass and bone formation. *The Journal of Clinical Investigation 105(8),* p. 1085-1093.

Moreth, K. et al. 2012. Small leucine-rich proteoglycans orchestrate receptor crosstalk during inflammation. *Cell Cycle* 11(11), p. 2084-2091.

Moreth, K. et al. 2014. Biglycan-triggered TLR-2- and TLR-4-signaling exacerbates the pathophysiology of ischemic acute kidney injury. *Matrix Biology* 35(0), p. 143-151.

Morris, H. F. et al. 2000. Implant survival in patients with type 2 diabetes: placement to 36 months. *Annals of Periodontology* 5(1), p. 157-165.

Moseley, R. et al. 2004. Comparison of oxidative stress biomarker profiles between acute and chronic wound environments. *Wound Repair and Regeneration* 12(4), p. 419-429.

Mundy, G. R. et al. 1995. The effects of cytokines and growth factors on osteoblastic cells. *Bone* 17(2), p. S71-S75.

Muraglia, A. et al. 2000. Clonal mesenchymal progenitors from human bone marrow differentiate in vitro according to a hierarchical model. *Journal of Cell Science* 113(7), p. 1161-1166.

Murphy, G. et al. 1994. Regulation of Matrix Metalloproteinase Activity. *Annals of the New York Academy of Sciences* 732(1), p. 31-41.

Murray, P. J. and Wynn, T. A. 2011. Obstacles and opportunities for understanding macrophage polarization. *Journal of Leukocyte Biology* 89(4), p. 557-563.

Muschler, G. et al. 2003. Spine fusion using cell matrix composites enriched in bone marrow-derived cells. *Clinical Orthopedic Related Research* (407), p. 102-118.

Nakamura, H. et al. 2010a. Localization of Thy-1–positive cells in the perichondrium during endochondral ossification. *Journal of Histochemistry & Cytochemistry* 58(5), p. 455-462.

Nakamura, T. et al. 1995. Stimulation of endosteal bone formation by systemic injections of recombinant basic fibroblast growth factor in rats. *Endocrinology* 136(3), p. 1276-1284.

Nakamura, Y. et al. 2010b. Isolation and characterization of endosteal niche cell populations that regulate hematopoietic stem cells. *Blood* 116(9), p. 1422-1432.

Nakashima, K. et al. 2002a. The novel zinc finger-containing transcription factor osterix is required for osteoblast differentiation and bone formation. *Cell* 108(1), p. 17-29.

Nakashima, M. et al. 2002b. Induction of dental pulp stem cell differentiation into odontoblasts by electroporation-mediated gene delivery of growth/differentiation factor 11 (Gdf11). *Gene Therapy* 9, p. 814 - 818.

National Joint Registry for England, Wales, and Northern Ireland. NJR 11th annual report 2014. Hemel Hempstead: National Joint Registry, 2014. www.hqip.org.uk/assets/...2014-15/NJR-11th-Annual-Report-2014.pdf (accessed December 15, 2014)

Neuhuber, B. et al. 2008. Effects of plating density and culture time on bone marrow stromal cell characteristics. *Experimental Hematology* 36(9), p. 1176-1185.

Newman, G. R. and Hobot, J. A. 1999. Resins for combined light and electron microscopy: a half century of development. *Histochemical Journal* 31(8), p. 495-505.

Nikolovska, K. et al. 2014. A decorin-deficient matrix affects skin chondroitin/dermatan sulfate levels and keratinocyte function. *Matrix Biology* 35, p. 91-102.

Nishikawa, T. and Araki, E. 2007. Impact of mitochondrial ROS production in the pathogenesis of diabetes mellitus and its complications. *Antioxidants & Redox Signaling* 9(3), p. 343-353.

Nombela-Arrieta, C. et al. 2011. The elusive nature and function of mesenchymal stem cells. *Nature Reviews Molecular Cell Biology* 12(2), p. 126-131.

Nöth, U. et al. 2002. Multilineage mesenchymal differentiation potential of human trabecular bone-derived cells. *Journal of Orthopaedic Research* 20(5), p. 1060-1069.

Nozaki, T. and Ohura, K. 2011. Gene expression profile of dental pulp cells during differentiation into an adipocyte lineage. *Journal of Pharmacological Sciences* 115 (3), p. 354-363.

O'Connor, J. C. et al. 2007. Type 2 diabetes impairs insulin receptor substrate-2-mediated phosphatidylinositol 3-kinase activity in primary macrophages to induce a state of cytokine resistance to il-4 in association with overexpression of suppressor of cytokine signaling-3. *The Journal of Immunology* 178(11), p. 6886-6893.

Oates, T. W. et al. 2007. Glycemic control and implant stabilization in type 2 diabetes mellitus. *Laboratory Investigation* 82:1399-1405

Ohnishi, H. et al. 2012. iIdentification of mannose receptor as receptor for hepatocyte growth factor β-Chain: novel ligand-receptor pathway for enhancing macrophage phagocytosis. *Journal of Biological Chemistry* 287(16), p. 13371-13381.

Okazaki, R. 2013. Bone architecture and strength in diabetes mellitus. *Clinical Calcium* 23(7), p. 1001-1006.

Olieslagers, S. et al. 2011. TGF-β1/ALK5-induced monocyte migration involves PI3K and p38 pathways and is not negatively affected by diabetes mellitus. *Cardiovascular Research* 91(3), p. 510-518.

Olmedo, D. et al. 2003. Macrophages related to dental implant failure. *Implant Dentistry* 12(1), p. 75-80.

Oshima, H. et al. 2001. Morphogenesis and renewal of hair follicles from adult multipotent stem cells. *Cell* 104, p. 233.

Owen, C. et al. 2012. A novel Phex mutation in a new mouse model of hypophosphatemic rickets. *Journal of Cellular Biochemistry* 113(7), p. 2432-2441.

Ozdemir, M. T. and Kir, M. Ç. 2011. Repair of long bone defects with demineralized bone matrix and autogenous bone composite. *Indian Journal of Orthopaedics* 45(3), p. 226-230.

Park, F. et al. 1997. Evidence for the presence of smooth muscle α-actin within pericytes of the renal medulla. p. R1742-R1748.

Peister, A. et al. 2004. Adult stem cells from bone marrow (MSCs) isolated from different strains of inbred mice vary in surface epitopes, rates of proliferation, and differentiation potential. *Blood* 103(5), p. 1662-1668.

Pfeilschifter, J. et al. 1998. Concentration of transforming growth factor β in human bone tissue: relationship to age, menopause, bone turnover, and bone volume. *Journal Of Bone And Mineral Research* 13(4), p. 716-730.

Phinney, D. G. et al. 1999. Plastic adherent stromal cells from the bone marrow of commonly used strains of inbred mice: Variations in yield, growth, and differentiation. *Journal of Cellular Biochemistry* 72(4), p. 570-585.

Pickup, J. C. 2004. Inflammation and Activated Innate Immunity in the Pathogenesis of Type 2 Diabetes. *Diabetes Care* 27(3), p. 813-823.

Pimton, P. et al. 2011. Fibronectin-mediated upregulation of α5β1 integrin and cell adhesion during differentiation of mouse embryonic stem cells. *Cell Adhesion & Migration* 5(1), p. 73-82.

Pimton, P. et al. 2011. Fibronectin-mediated upregulation of α5β1 integrin and cell adhesion during differentiation of mouse embryonic stem cells. *Cell Adhesion & Migration* 5(1), p. 73-82.

Pittenger, M. F. et al. 1999. Multilineage Potential of Adult Human Mesenchymal Stem Cells. *Science* 284(5411), p. 143-147.

Poole, A. R. et al. 1982. The Association of a Matrix Protein with Endochondral Bone-Formation. *Journal of Cell Biology* 95(2), p. 115-115.

Poynton, A. R. and Lane, J. M. 2002. Safety profile for the clinical use of bone morphogenetic proteins in the spine. *Spine* 15(27), p. S40-48.

Prins, H.-J. et al. 2014. *In vitro* induction of alkaline phosphatase levels predicts *in vivo* bone forming capacity of human bone marrow stromal cells. *Stem Cell Research* 12(2), p. 428-440.

Prisby, R. D. et al. 2008. Altered bone mass, geometry and mechanical properties during the development and progression of type 2 diabetes in the Zucker diabetic fatty rat. *Journal of Endocrinology* 199(3), p. 379-388.

Puerta, M. et al. 2002. Effect of acute cold exposure on the expression of the adiponectin, resistin and leptin genes in rat white and brown adipose tissues. *Hormone and Metabolic Research* 34(11/12), p. 629-634.

Puleo, D. A. and Nanci, A. 1999. Understanding and controlling the bone-implant interface. *Biomaterials* 20 (23-24), p. 2311-2321.

Qu-Petersen, Z. et al. 2002. Identification of a novel population of muscle stem cells in mice: potential for muscle regeneration. *The Journal of Cell Biology* 157(5), p. 851-864.

Quarto, R. et al. 2001. Repair of large bone defects with the use of autologous bone marrow stromal cells. *New England Journal of Medicine* 344(5), p. 385-386.

Ramachandran, A. et al. 2010. Diabetes in Asia. *The Lancet* 375(9712), p. 408-418.

Rao, X. et al. 2014. The heterogenic properties of monocytes/macrophages and neutrophils in inflammatoryresponse in diabetes. *Life Sciences* 116(2):59-66

Reddy, M. A. et al. 2014. Regulation of inflammatory phenotype in macrophages by a diabetes-induced long non-coding RNA. *Diabetes* 63(12):4249-61

Reed, C. and Iozzo, R. 2002. The role of decorin in collagen fibrillogenesis and skin homeostasis. *Glycoconjugate Journal* 19(4-5), p. 249-255.

Retzepi, M. et al. 2010. Effect of diabetes and metabolic control on de novo bone formation following guided bone regeneration. *Clinical Oral Implants Research* 21(1), p. 71-79.

Rey-Giraud, F. et al. 2012. *In vitro* generation of monocyte-derived macrophages under serum-free conditions improves their tumor promoting functions. *PLoS ONE* 7(8), p. e42656.

Rinker, T. E. et al. 2014. Interactions between mesenchymal stem cells, adipocytes, and osteoblasts in a 3D tri-culture model of hyperglycemic conditions in the bone marrow microenvironment. *Integrative Biology* 6(3), p. 324-337.

Roberts, H. C. et al. 2008. Lipopolysaccharide alters decorin and biglycan synthesis in rat alveolar bone osteoblasts: consequences for bone repair during periodontal disease. *European Journal of Oral Sciences* 116(3), p. 207-216.

Robey, P. G. et al. 1987. Osteoblasts synthesize and respond to transforming growth factor-type β (TGF- β) in vitro. *The Journal of Cell Biology* 105(1), p. 457-463.

Rogowicz, A. et al. 2007. The role of matrix metalloproteinases in the development of vascular complications of diabetes mellitus--clinical implications. *Polish Archives of Internal Medicine* 117(3), p. 43-48.

Rolo, A. P. and Palmeira, C. M. 2006. Diabetes and mitochondrial function: Role of hyperglycemia and oxidative stress. *Toxicology and Applied Pharmacology* 212(2), p. 167-178.

Rosier, R. N. et al. 1998. The potential role of transforming growth factor β in fracture healing. *Clinical Orthopedic Related Research* (355), p. S294-300.

Rossetti, L. et al. 1987. Effect of chronic hyperglycemia on *in vivo* insulin secretion in partially pancreatectomized rats. *The Journal of Clinical Investigation* 80(4), p. 1037-1044.

Roughley, P. J. et al. 1993. Non-proteoglycan forms of biglycan increase with age in human articular-cartilage. *Biochemical Journal* 295, p. 421-426.

Ryoo, H. M. et al. 1997. Stage-specific expression of Dlx-5 during osteoblast differentiation: Involvement in regulation of osteocalcin gene expression. *Molecular Endocrinology* 11(11), p. 1681-1694.

Saadi, H. et al. 2007. Prevalence of diabetes mellitus and its complications in a population-based sample in Al Ain, United Arab Emirates. *Diabetes Research and Clinical Practice* 78(3), p. 369-377.

Sakai, D. et al. 2008. Bone Healing of Tooth Extraction Socket in Type 2 Diabetes. Journal of Oral Tissue Engineering 5(3), p. 134-144.

Salameh, A. et al. 1997. High D-glucose induces alterations of endothelial cell structure in a cell-culture model. *Journal of Cardiovascular Pharmacology* 30(2), p. 182-190.

Schaefer, L. 2011. Small leucine-rich proteoglycans in kidney disease. *Journal of the American Society of Nephrology* 22(7), p. 1200-1207.

Schafer, M. and Werner, S. 2008. Cancer as an overhealing wound: an old hypothesis revisited. *Nature Reviews Molecular Cell Biology* 9(8), p. 628-638.

Scherer, E. S. et al. 2012. Chronic mild hyperhomocysteinemia alters ectonucleotidase activities and gene expression of ecto-5′-nucleotidase/CD73 in rat lymphocytes. *Molecular and Cellular Biochemistry* 362(1-2), p. 187-194.

Schmidmaier, G. et al. 2003. Synergistic effect of IGF-I and TGF-β1 on fracture healing in rats: single versus combined application of IGF-I and TGF-β1. *Acta Orthopaedica Scandinavica* (74), p. 604-610.

Schmidt-Bleek, K. et al. 2012. Inflammatory phase of bone healing initiates the regenerative healing cascade. *Cell and Tissue Research* 347(3), p. 567-573.

Schmidt, A. M. et al. 1994. Cellular receptors for advanced glycation end products. Implications for induction of oxidant stress and cellular dysfunction in the pathogenesis of vascular lesions. *Arteriosclerosis, Thrombosis, and Vascular Biology* 14(10), p. 1521-1528.

Schultz, G. S. and Wysocki, A. 2009. Interactions between extracellular matrix and growth factors in wound healing. *Wound Repair and Regeneration* 17(2), p. 153-162.

Scotti, C. et al. 2010. Recapitulation of endochondral bone formation using human adult mesenchymal stem cells as a paradigm for developmental engineering. *Proceedings of the National Academy of Sciences* 107(16), p. 7251-7256.

Scutt, A. et al. 1996. Effect of age and ovariectomy on fibroblastic colony-forming unit numbers in rat bone marrow. *Calcified Tissue International* 59(4), p. 309-310.

Šedová, L. et al. 2007. Sucrose feeding during pregnancy and lactation elicits distinct metabolic response in offspring of an inbred genetic model of metabolic syndrome. *American Journal of Physiology - Endocrinology and Metabolism* 292, p. E1318-E1324.

Senanayake, S. et al. 2007. Monocyte-derived macrophages from men and women with Type 2 diabetes mellitus differ in fatty acid composition compared with non-diabetic controls. *Diabetes Research and Clinical Practice* 75(3), p. 292-300.

Seta, N. et al. 2013. Platelet-derived stromal cell-derived factor-1 is required for the transformation of circulating monocytes into multipotential cells. *PLoS One* 8(9), p. e74246.

Sharma, G.D. et al. 2003. p38 and ERK1/2 coordinate cellular migration and proliferation in epithelial wound healing: evidence of cross-talk activation between map kinase cascades. *Journal of Biological Chemistry* 278(24), p. 21989-21997.

Sharma, R. R. et al. 2014. Mesenchymal stem or stromal cells: a review of clinical applications and manufacturing practices. *Transfusion* 54(5), p. 1418-1437.

Sheweita, S. and Khoshhal, K. 2007. Calcium metabolism and oxidative stress in bone fractures: role of antioxidants. *Current Drug metabolism* 8(5), p. 519-525.

Shi, S. and Gronthos, S. 2003. Perivascular niche of postnatal mesenchymal stem cells in bone marrow and dental pulp. *Journal of Bone Mineral Research* 18, p. 696 - 704.

Shin, S.-Y. et al. 2012. The effect of peri-implant bone exposure on soft tissue healing and bone loss in two adjacent implants. *Journal Of Periodontal & Implant Science* 42(1), p. 20-24.

Shlossman, M. et al. 1990. Type 2 diabetes mellitus and periodontal disease. The *Journal of the American Dental Association* 121(4), p. 532-536.

Shyu, W. C. et al. 2006. Intracerebral peripheral blood stem cell (CD34+) implantation induces neuroplasticity by enhancing β1 integrin-mediated angiogenesis in chronic stroke rats. *The Journal of Neuroscience* 26(13), p. 3444-3453.

Silva, K. D. et al. 2001. Bone marrow stem cell and progenitor response to injury. *Wound Repair and Regeneration* 9(6), p. 495-500.

Sindrilaru, A. et al. 2011. An unrestrained proinflammatory M1 macrophage population induced by iron impairs wound healing in humans and mice. The Journal of Clinical Investigation 121(3), p. 985-997.

Singh, K. et al. 1992. Differential processing of osteopontin transcripts in rat kidney- and osteoblast-derived cell lines. *Journal of Biological Chemistry* 267(33), p. 23847-23851.

Singh, R. et al. 2001. Advanced glycation end-products: a review. *Diabetologia* 44(2), p. 129-146.

Soardo, G. et al. 2011. Oxidative stress is activated by free fatty acids in cultured human hepatocytes. *Metabolic Syndrome and Related Disorders* 9(5), p. 397-401.

Soballe, K. 1993. Hydroxyapatite ceramic coating for bone implant fixation - mechanical and histological studies in dogs. *Acta Orthopaedica Scandinavica* 255, p.1-58

Sojo, K. et al. 2005. Immunohistochemical study of vascular endothelial growth factor (VEGF) and bone morphogenetic protein-2, -4 (BMP-2, -4) on lengthened rat femurs. *Journal of Cranio-Maxillofacial Surgery* 33(4), p. 238-245.

Song, H. et al. 2005. Transfection of mesenchymal stem cells with the FGF-2 gene improves their survival under hypoxic conditions. *Molecular Cells* 19, p. 402 - 407.

Song, L. and Tuan, R. 2004. Transdifferentiation potential of human mesenchymal stem cells derived from bone marrow. *The FASEB Journal* 18(9), p. 980-982.

Sottile, V. et al. 2002. Stem cell characteristics of human trabecular bone-derived cells. *Bone* 30(5), p. 699-704.

Sparmann, G. et al. 2010. Bone marrow-derived pancreatic stellate cells in rats. *Cell Research* 20(3), p. 288-298.

Spencer, M. et al. 2010. Adipose tissue macrophages in insulin-resistant subjects are associated with collagen VI and fibrosis and demonstrate alternative activation.

American Journal of Physiolog -Endocrinology And Metabolism 299(6), p. E1016-E1027.

Srinivasan, K. and Ramarao, P. 2007. Animal models in type 2 diabetes research: an overview. *Indian Journal of Medical Research* 125 (3), p. 451-472.

Steiler, T. L. et al. 2003. Effect of hyperglycemia on signal transduction in skeletal muscle from diabetic Goto-Kakizaki rats. *Endocrinology* 144(12), p. 5259-5267.

Steinbeck, M. J. et al. 1994. NADPH-oxidase expression and in situ production of superoxide by osteoclasts actively resorbing bone. *The Journal of Cell Biology* 126(3), p. 765-772.

Stolzing, A. et al. 2006. Glucose-induced replicative senescence in mesenchymal stem cells. *Rejuvenation Research* 9(1), p. 31-35.

Stolzing, A. et al. 2010. Diabetes induced changes in rat mesenchymal stem cells. *Cells Tissues Organs* 191(6), p. 453-465.

Stolzing, A. et al. 2012. Suspension cultures of bone-marrow-derived mesenchymal stem cells: Effects of donor age and glucose level. *Stem Cells and Development* 21(14), p. 2718-2723.

Stout, R. D. 2010. Editorial: Macrophage functional phenotypes: no alternatives in dermal wound healing? *Journal of Leukocyte Biology* 87(1), p. 19-21.

Street, J. et al. 2002. Vascular endothelial growth factor stimulates bone repair by promoting angiogenesis and bone turnover. *Proceedings of the National Academy of Sciences* 99(15), p. 9656-9661.

Sunahara, K. K. and Martins, J. O. 2012. Alveolar macrophages in diabetes: friends or foes? *Journal of Leukocyte Biology* 91(6), p. 871-876.

Sung, J. H. et al. 2008. Isolation and characterization of mouse mesenchymal stem cells. *Transplantation Proceedings* 40(8), p. 2649-2654.

Suzuki, S. et al. 2005. Enamel matrix derivative gel stimulates signal transduction of BMP and TGF-β. *Journal of Dental Research* 84, p. 510 - 514.

Tadic, T. et al. 2002. Overexpression of Dlx5 in chicken calvarial cells accelerates osteoblastic differentiation. *Journal of Bone and Mineral Research* 17(6), p. 1008-1014.

Taguchi, Y. et al. 1998. Interleukin-6-type cytokines stimulate mesenchymal progenitor differentiation toward the osteoblastic lineage. *Proceedings of the Association of American Physicians* 110(6), p. 559-574.

Tang, F. R. et al. 2004. Expression of different isoforms of protein kinase C in the rat hippocampus after pilocarpine-induced status epilepticus with special reference to CA1 area and the dentate gyrus. *Hippocampus* 14(1), p. 87-98.

Tang, Y. et al. 2009. TGF- β1-induced migration of bone mesenchymal stem cells couples bone resorption with formation. *Nat Med* 15(7), p. 757-765.

Taniguchi, C. M. et al. 2006. Critical nodes in signalling pathways: insights into insulin action. *Nature Review of Molecular Cell Biol*ogy 7(2), p. 85-96.

Taniyama, Y. and Griendling, K. K. 2003. Reactive oxygen species in the vasculature. *Hypertension* 42(6), p. 1075-1081.

Tannock, L. R. 2006. Proteoglycans can mediate renal lipoprotein retention. *Diabetologia* 49(5), p. 1115-1116.

Tatarakis, N. et al. 2014. Clinical, microbiological, and salivary biomarker profiles of dental implant patients with type 2 diabetes. *Clinical Oral Implants Research* 25(7), p. 803-812.

Tesch, G. H. 2007. Role of macrophages in complications of type 2 diabetes. *Clinical and Experimental Pharmacology and Physiology* 34(10), p. 1016-1019.

Thomas, T. et al. 1999. Leptin acts on human marrow stromal cells to enhance differentiation to osteoblasts and to inhibit differentiation to adipocytes. *Endocrinology* 140(4), p. 1630-1638.

Thompson, J. et al. 2011. Renal accumulation of biglycan and lipid retention accelerates diabetic nephropathy. *American Journal of Pathology* 179(3), p. 1179-1187.

Thompson, Z. et al. 2002. A model for intramembranous ossification during fracture healing. *Journal of Orthopaedic Research* 20(5), p. 1091-1098.

Tiaka, E. K. et al. 2012. The role of hyperbaric oxygen in the treatment of diabetic foot ulcers. *Angiology* 63(4), p. 302-314.

Tian, H. et al. 2010. Novel 14S,21-dihydroxy-docosahexaenoic acid rescues wound healing and associated angiogenesis impaired by acute ethanol intoxication/exposure. *Journal of Cellular Biochemistry* 111(2), p. 266-273.

Tilg, H., et al. (2008). Gut, inflammation and osteoporosis: basic and clinical concepts. *Gut* 57(5), p. 684-694.

Tonetti, M. S. et al. 1994. Vascular adhesion molecules and initial development of inflammation in clinically healthy-human keratinized mucosa around teeth and osseointegrated implants. *Journal of Periodontal Research* 29(6), p. 386-392.

Tong, W. et al. 2007. Human embryonic stem cells undergo osteogenic differentiation in human bone marrow stromal cell microenvironments. *Journal Of Stem Cells* 2(3), p. 139-147.

Trippel, S. et al. 1996. Instructional Course Lectures, The American Academy of Orthopaedic Surgeons - Growth Factors as Therapeutic Agents p. 1272-1286.

Tropel, P. et al. 2004. Isolation and characterisation of mesenchymal stem cells from adult mouse bone marrow. *Experimental Cell Research* 295(2), p. 395-406.

Tsubone, T. et al. 2006. Effect of TGF-β inducible early gene deficiency on flexor tendon healing. *Journal of Orthopaedic Research 24*(3), p. 569-575.

Udagawa, N. et al. 2000. Osteoprotegerin Produced by Osteoblasts Is an Important Regulator in Osteoclast Development and Function. *Endocrinology* 141(9), p. 3478-3484.

Urist, M. R. 1997. Bone morphogenetic protein: The molecularization of skeletal system development. *Journal of Bone and Mineral Research* 12(3), p. 343-346.

Valero, A. M. et al. 2007. Effects of diabetes on the osseointegration of dental implants. Medicina Oral, *Patología Oral y Cirugía Bucal 12*, p. 38-43.

Vander Heiden, M. G. et al. 2001. Growth Factors Can Influence Cell Growth and Survival through Effects on Glucose Metabolism. *Molecular and Cellular Biology* 21(17), p. 5899-5912.

Veerababu, G. et al. 2000. Overexpression of glutamine: fructose-6-phosphate amidotransferase in the liver of transgenic mice results in enhanced glycogen storage, hyperlipidemia, obesity, and impaired glucose tolerance. *Diabetes* 49(12), p. 2070-2078.

Viereck, V. et al. 2002. Differential regulation of Cbfa1/Runx2 and osteocalcin gene expression by vitamin-D3, dexamethasone, and local growth factors in primary human osteoblasts. *Journal of Cellular Biochemistry* 86(2), p. 348-356.

Vogl-Willis, C. A. and Edwards, I. J. 2004. High-glucose-induced structural changes in the heparan sulfate proteoglycan, perlecan, of cultured human aortic endothelial cells. *Biochimica et Biophysica Acta (BBA)-General Subjects* 1672(1), p. 36-45.

Vonau, R. L. et al. 2001. Combination of growth factors inhibits bone ingrowth in the bone harvest chamber. *Clinical Orthopaedics and Related Research* (386),p. 243-251.

Waddington, RJ et al. 2011. Characterization of Oxidative Stress Status during Diabetic Bone Healing. *Cells Tissues Organs* 194(2-4), p. 307-312.

Waddington, R. J. et al. 2000. Reactive oxygen species: a potential role in the pathogenesis of periodontal diseases. *Oral Diseases* 6(3), p. 138-151.

Waddington, R. J. et al. 2003. Differential roles for small leucine-rich proteoglycans in bone formation. *European Cells and Materials* 6, p.12-21.

Wang, F. et al. 2010a. Type 2 diabetes mellitus impairs bone healing of dental implants in GK rats. *Diabetes Research and Clinical Practice* 88(1), p. e7-9.

Wang, L. et al. 2010b. Activation of Protein Serine/Threonine Phosphatase PP2Cα Efficiently Prevents Liver Fibrosis. *PLoS ONE* 5(12), p. e14230.

Weil, B. R. et al. 2009. High glucose concentration in cell culture medium does not acutely affect human mesenchymal stem cell growth factor production or proliferation. p. R1735-R1743.

Weinberg, E. et al. 2014. Streptozotocin-induced diabetes in rats diminishes the size of the osteoprogenitor pool in bone marrow. *Diabetes Research and Clinical Practice* 103(1), p. 35-41.

Winnall, W. R. et al. 2011. Rat resident testicular macrophages have an alternatively activated phenotype and constitutively produce interleukin-10 *in vitro*. *Journal of Leukocyte Biology* 90(1), p. 133-143.

Wong, B. R. et al. 1997. TRANCE is a novel ligand of the tumor necrosis factor receptor family that activates c-Jun N-terminal kinase in T cells. *Journal of Biological Chemistry* 272(40), p. 25190-25194.

Wu, B. et al. 2013. Lentiviral delivery of biglycan promotes proliferation and increases osteogenic potential of bone marrow-derived mesenchymal stem cells in vitro. *Journal of Molecular Histology*, p. 1-9.

Wu, Y. et al. 2007. Mesenchymal stem cells enhance wound healing through differentiation and angiogenesis. *Stem Cells* 25(10), p. 2648-2659.

Würgler-Hauri, C. C. et al. 2007. Temporal expression of 8 growth factors in tendon-to-bone healing in a rat supraspinatus model. *Journal of Shoulder and Elbow Surgery* 16(5), p. S198-S203.

Xia, P. et al. 1994. Characterization of the mechanism for the chronic activation of diacylglycerol-protein kinase C pathway in diabetes and hypergalactosemia. *Diabetes* 43(9), p. 1122-1129.

Yang, S. N. Y. et al. 2009. Growth factor-mediated hyper-elongation of glycosaminoglycan chains on biglycan requires transcription and translation. *Archives Of Physiology And Biochemistry* 115(3), p. 147-154.

Yang, S. N. Y. et al. 2010. Transforming growth factor-β regulation of proteoglycan synthesis in vascular smooth muscle: Contribution to lipid binding and accelerated atherosclerosis in diabetes. *Journal of Diabetes* 2(4), p. 233-242.

Yaturu, S. et al. 2009. Decreased bone mineral density in men with metabolic syndrome alone and with type 2 diabetes. *Medical Science Monitor* 15(1), p.5-9.

Yoon, K.-H. et al. 2006. Epidemic obesity and type 2 diabetes in Asia. *The Lancet* 368(9548), p. 1681-1688.

Young, M. et al. 2002. Biglycan knockout mice: new models for musculoskeletal diseases. *Glycoconjugation Journal* 19, p. 257-262.

Yu, M. et al. 2011. Development of mesenchymal stem cell-implant complexes by cultured cells sheet enhances osseointegration in type 2 diabetic rat model. *Bone* 49(3), p. 387-394.

Zeyda, M. et al. 2007. Human adipose tissue macrophages are of an anti-inflammatory phenotype but capable of excessive pro-inflammatory mediator production. *International Journal of Obesity* 31(9), p. 1420-1428.

Zhang, M. et al. 2002. Osteoblast-specific knockout of the insulin-like growth factor (IGF) receptor gene reveals an essential role of igf signaling in bone matrix mineralization. *Journal of Biological Chemistry* 277(46), p. 44005-44012.

Zhang, P. et al. 2010. Global healthcare expenditure on diabetes for 2010 and 2030. *Diabetes Research and Clinical Practice* 87(3), p. 293-301.

Zhang, W. et al. 2013. Klf10 inhibits IL-12p40 production in macrophage colony-stimulating factor-induced mouse bone marrow-derived macrophages. *European Journal of Immunology* 43(1), p. 258-269.

Zhang, Z. et al. 2012. Lesional Accumulation of CD163+ Macrophages/microglia in Rat Traumatic Brain Injury. *Brain Research* 1461(0), p. 102-110.

Zheng, X.F. et al. 2013. Lipopolysaccharide-Induced M2 to M1 Macrophage Transformation for IL-12p70 Production Is Blocked by *Candida albicans* Mediated Up-Regulation of EBI3 Expression. *PLoS ONE* 8(5), p. e63967.

Zhu, H. et al. 2010. A protocol for isolation and culture of mesenchymal stem cells from mouse compact bone. *Nature Protocols* 5(3), p. 550-560.

Zimmet, P. et al. 2001. Global and societal implications of the diabetes epidemic. *Nature* 414(6865), p. 782-787.

Zuk, P. et al. 2001. Multilineage cells from human adipose tissue: implications for cell-based therapies. *Tissue Engineering* 7 (2), p. 211-228.

8.0 Appendix

Work from this thesis has been presented at the following meetings:

Tissue and Cell Engineering Society (TCES) Annual Meeting and Stem Cells Symposium, Sir Martin Evans Building, School of Biosciences, Cardiff University, 2013. **Isolation and characterisation of mesenchymal stem cells from rat bone marrow and compact bone**. N. YUSOP, A.J. SLOAN, R. MOSELEY, and R. WADDINGTON**.** Abstract number 0030, 2013. *European Cells and Materials* Vol. 26. Suppl. 7, 2013 (page 95).

(http://www.ecmjournal.org/journal/supplements/vol026supp07/pdf/Vol026Supp07a095.pdf)

British Society for Oral and Dental Research (BSODR) 60th Annual Scientific Meeting and Exhibition, Bath, 2013.**Increased Biglycan Expression Alters TGF-β_1 Bioavailability During Diabetic Bone Repair.** N. YUSOP, A.J. SLOAN, R. MOSELEY, and R. WADDINGTON**.** Abstract number 0054, 2013.

(https://iadr.confex.com/iadr/bsodr13/techprogram/abstract_182220.htm)